UNIVERSIDADE ESTADUAL PAULISTA
"JÚLIO DE MESQUITA FILHO"
Câmpus de São José do Rio Preto

Maria Mariana Garcia de Oliveira

A comprehensive study of cowpea protein:

Techno-functional properties, rheological behavior, emulsification and film-forming capacity

São José do Rio Preto
2024

Maria Mariana Garcia de Oliveira

A comprehensive study of cowpea protein:

Techno-functional properties, rheological behavior, emulsification and film-forming capacity

Tese apresentada como parte dos requisitos para obtenção do título de Doutor em Engenharia e Ciência de Alimentos, junto ao Programa de Pós-Graduação em Alimentos, Nutrição e Engenharia de Alimentos, do Instituto de Biociências, Letras e Ciências Exatas da Universidade Estadual Paulista "Júlio de Mesquita Filho", Câmpus de São José do Rio Preto.

Financiadoras: CAPES e FAPESP (2020/05254–4)

Orientador: Profª. Drª. Maria Aparecida Mauro
Coorientador: Prof. Dr. Víctor Justiniano Huamaní-Meléndez

São José do Rio Preto
2024

O48c

Oliveira, Maria Mariana Garcia de

A comprehensive study of cowpea protein: Techno-functional properties, rheological behavior, emulsification and film-forming capacity / Maria Mariana Garcia de Oliveira. -- São José do Rio Preto, 2024

229 p.

Tese (doutorado) - Universidade Estadual Paulista (UNESP), Instituto de Biociências Letras e Ciências Exatas, São José do Rio Preto

Orientadora: Maria Aparecida Mauro

Coorientador: Víctor Justiniano Huamaní-Meléndez

1. Proteína vegetal. 2. Propriedades funcionais. 3. Propriedades reológicas. 4. Emulsões. 5. Filmes comestíveis. I. Título.

Sistema de geração automática de fichas catalográficas da Unesp. Dados fornecidos pelo autor(a).

Maria Mariana Garcia de Oliveira

A comprehensive study of cowpea protein:

Techno-functional properties, rheological behavior, emulsification and film-forming capacity

Tese apresentada como parte dos requisitos para obtenção do título de Doutor em Engenharia e Ciência de Alimentos, junto ao Programa de Pós-Graduação em Alimentos, Nutrição e Engenharia de Alimentos, do Instituto de Biociências, Letras e Ciências Exatas da Universidade Estadual Paulista "Júlio de Mesquita Filho", Câmpus de São José do Rio Preto.

Financiadora: CAPES e FAPESP (2020/05254–4)

Comissão Examinadora

Profª. Drª. Maria Aparecida Mauro
UNESP – Câmpus de São José do Rio Preto
Orientador

Dr. Josemar Gonçalves de Oliveira Filho
EMBRAPA – São Carolos

Prof. Dr. Vitor Augusto dos Santos Garcia
UNESP – Botucatu

Profª. Drª. Jessica Thaís do Prado Silva
UNESP – São José do Rio Preto

São José do Rio Preto
30 de agosto de 2024

Para Maria Salete e José Altair.

AGRADECIMENTOS

A Deus, minha gratidão eterna.

Aos meus pais, pelo apoio ao longo desses sete anos, que me permitiu seguir meu sonho.

À minha orientadora, Profª Drª Maria Aparecida Mauro, pela orientação, compreensão diante dos desafios que enfrentei nos últimos anos, e por tornar essa trajetória, por vezes árdua, muito mais leve.

Ao meu coorientador, Dr. Víctor Justiniano Huamaní-Meléndez, pela dedicação ao nosso trabalho e por frequentemente ter estado ao meu lado no laboratório, auxiliando-me nos experimentos.

Aos amigos que fiz durante o doutorado, Márcio, Clebê, Carol, Micael e Marcello, minha gratidão por todo o apoio, por me acolherem em seu grupo, me ouvirem e me incentivarem. Gostaria de tê-los conhecido antes.

Às minhas amigas Laís, Ana, Maísa, Taís, Fernanda e Ana E., nenhuma palavra pode expressar adequadamente a imensa gratidão que sinto por tê-las em minha vida.

Às minhas colegas de laboratório e departamento pelas conversas, cafezinhos, risadas e conselhos, Maria Fernanda e Oneide.

Às minhas alunas de iniciação científica, Ana Gabriela e Alanis. Em especial, agradeço a Ana Gabriela, que foi essencial para essa pesquisa e se tornou uma amiga querida.

À Profª. Drª. Vânia Regina Nicoletti, por disponibilizar o calorímetro diferencial de varredura, reômetro e homogeneizador.

Ao laboratório de cereais, por disponibilizar o difratômetro de raios X e o calorímetro diferencial de varredura.

Profª Drª Ana Carolina Conti, por disponibilizar o texturômetro, e à técnica Alana pelo auxílio durante as análises.

Ao Prof. Dr. Maurício Boscolo, por disponibilizar o espectrofotômetro FTIR-ATR e à aluna Lívia pelo auxílio com o equipamento.

Ao Prof. Dr. José Geraldo Nery, por disponibilizar o equipamento Zetasizer Nano ZS (FAPESP – n° Processo: 2012/24259-0) para a análise do potencial zeta e tamanho de partícula.

A todos os professores, técnicos e funcionários do Departamento de Engenharia e Tecnologia de Alimentos.

À Fundação de Amparo à Pesquisa do Estado de São Paulo (FAPESP) pelo auxílio financeiro (2020/05254–4).

O presente trabalho foi realizado com apoio da Coordenação de Aperfeiçoamento de Pessoal de Nível Superior - Brasil (CAPES), à qual agradeço.

“O sucesso nasce do querer, da determinação e persistência em se chegar a um objetivo. Mesmo não atingindo o alvo, quem busca e vence obstáculos, no mínimo fará coisas admiráveis.”

José de Alencar (n.d.)

RESUMO

O feijão-caupi (*Vigna unguiculata (L.)* Walp), uma leguminosa versátil e adaptável, nativa da África, destaca-se pelo seu alto teor de proteínas, variando entre 20 e 30%. Essa característica faz do feijão-caupi uma fonte promissora de proteína vegetal, ainda pouco explorada na indústria alimentícia. Neste estudo, a proteína concentrada do feijão-caupi (CPC) foi extraída por precipitação isoelétrica, caracterizada e avaliada quanto às suas propriedades funcionais e reológicas, sendo aplicada no desenvolvimento de emulsões e filmes comestíveis. Inicialmente, as características e propriedades do CPC tanto em pó quanto em solução foram investigadas. As globulinas foram as proteínas mais abundantes no CPC em pó, que apresentou um perfil proteico com proporção adequada de aminoácidos essenciais. O CPC, predominantemente amorfo, apresentou alta temperatura de desnaturação (131,86 °C) e na estrutura secundária de suas proteínas houve prevalência de folhas-β. Em solução, o pH representou um fator crítico sobre as propriedades tecno-funcionais do CPC, incluindo solubilidade, turbidez, formação de espuma e capacidade emulsificante, as quais melhoram em condições alcalinas. Soluções aquosas de CPC também foram analisadas quanto aos efeitos combinados de pH, concentração e temperatura sobre suas propriedades reológicas. Os resultados indicaram sensibilidade à concentração de proteína e à taxa de cisalhamento, especialmente em concentrações acima de 10%. O pH influenciou significativamente a tensão de cisalhamento e a viscosidade. O pH alcalino induziu alterações estruturais que afetaram as temperaturas de desnaturação e gelificação da proteína. O estudo também explorou a relação entre pH (3-11), concentração de óleo (2-10%) e estabilidade de emulsões, com foco na eficácia do CPC como agente emulsificante natural. O pH e a concentração de óleo impactaram significativamente a distribuição do tamanho das partículas, sendo mais uniforme em pH 9. Emulsões estabilizadas com CPC exibiram comportamento de fluido pseudoplástico, intensificado com maiores concentrações de óleo. Após tratamento térmico, emulsões em pH 7 e 9 sofreram desestabilização, enquanto em pH 11 permaneceram estáveis. Emulsões em pH 9 e 11 mostraram os maiores graus de estabilidade durante 30 dias de armazenamento. A CPC também foi avaliada como potencial matéria-prima para o desenvolvimento de filmes comestíveis. Filmes preparados em diferentes pHs (7, 9 e 11) revelaram que o pH 9 foi favorável a estruturas secundárias mais ordenadas dessas proteínas, microestrutura mais homogênea e redução da permeabilidade ao oxigênio (PO_2) no filme em relação aos outros pHs. Solubilidade, resistência à tração e deformação na ruptura não demonstraram dependência estrita do pH da solução formadora de filme. Por fim, a incorporação de emulsão nas soluções formadoras de filme

também foi investigada. A presença de emulsão melhorou a resistência à tração e o alongamento na ruptura e afetou significativamente o índice de cristalinidade relativa dos filmes, que aumentou nas formulações com 0.8 e 1% de emulsão. A formulação com 1% de emulsão apresentou a menor PO_2 e filmes sem rachaduras nas imagens de microestrutura. Filmes com mais de 0,2% de emulsão apresentaram maior opacidade, enquanto o filme controle foi mais transparente. Os resultados desta tese demonstram que o CPC possui alto potencial para aplicação como ingrediente alimentício na indústria.

Palavras–chave: Proteína vegetal, Propriedades funcionais, Propriedades reológicas, Emulsões, Filmes comestíveis

ABSTRACT

Cowpea (*Vigna unguiculata (L.)* Walp), a versatile and adaptable legume native to Africa, stands out for its high protein content, ranging between 20 and 30%. This characteristic makes cowpeas a promising source of plant protein, still underexplored in the food industry. In this study, cowpea protein concentrate (CPC) was extracted by isoelectric precipitation, characterized, and evaluated for its functional and rheological properties, being applied in the development of emulsions and edible films. Initially, the study investigated the characteristics and properties of CPC both in powder and solution forms. Globulins were the most abundant proteins in CPC powder, which showed a protein profile with an adequate proportion of essential amino acids. The predominantly amorphous CPC had a high denaturation temperature (131.86 °C), and the secondary structure of its proteins was dominated by β-sheets. In solution, pH proved to be a critical factor in the techno-functional properties of CPC, including solubility, turbidity, foaming, and emulsifying capacity, which improved under alkaline conditions. Aqueous solutions of CPC were also analyzed for the combined effects of pH, concentration, and temperature on their rheological properties. The results indicated that the rheological properties were sensitivity to protein concentration and shear rate, especially above 10%. The pH significantly influenced shear stress and viscosity. Alkaline pH induced structural changes that affected the protein's denaturation and gelation temperatures. This study also explored the relationship between pH (3-11), oil concentration (2-10%), and emulsion stability, focusing on the effectiveness of CPC as a natural emulsifying agent. pH and oil concentration significantly impacted droplet size distribution, which was more uniform at pH 9. Emulsions stabilized with CPC exhibited shear- fluid behavior, intensified with higher oil concentrations. After thermal treatment, emulsions at pH 7 and 9 became unstable, while those at pH 11 remained stable. Emulsions at pH 9 and 11 showed the highest degrees of stability over a 30-day storage period. Additionally, CPC was evaluated as a raw material for developing edible films. Films prepared at different pHs (7, 9, and 11) revealed that pH 9 was favorable to more ordered secondary structures of these proteins, more homogeneous microstructure, and reduced oxygen permeability (PO2) in the film compared to the other pHs. Solubility, tensile strength, and elongation at break did not show a strict dependence on the pH of the film-forming solution. Finally, the incorporation of emulsion into the film matrix was also investigated. The presence of emulsion improved tensile strength and elongation at break and significantly affected the relative crystallinity index of the films, which increased in the formulations with 0.8 and 1% emulsion. The formulation with 1% emulsion showed the lowest PO_2 and films without cracks

in the microstructure images. Films with more than 0.2% emulsion exhibited higher opacity, while the control film was more transparent. The results of this thesis demonstrate that CPC has high potential for application as a food ingredient in the industry.

Keywords: Plant-based protein, Functional properties, Rheological properties, Emulsions, Edible films

LIST OF FIGURES

Figure 1.1 World map focusing on the main producers of cowpea: Africa (global leader, in red) and Brazil (Latin American leader, in green).....25
Figure 1.2 Proteins' antinutritional factors and methods for their reduction 27
Figure 1.3 Protein extraction methods.....31
Figure 2.1 (a) SDS-PAGE of CPC. The first lane on the left represents the molecular mass markers; (b) CPC molar mass distribution 71
Figure 2.2 Scanning electron microscopy of CPC at magnifications of 250× (a), 500× (b), and 1000× (c) 74
Figure 2.3 XRD diffractogram profile of CPC.....75
Figure 2.4 Infrared spectra (a); composition of amide I components (b) and curve fitting spectra of amide I (c).....77
Figure 2.5 Thermogram of CPC.....79
Figure 2.6 Zeta potential (a); water solubility (b) and turbidity (c) of CPC solution at different pH 81
Figure 2.7 Foaming capacity (bars) and foam stability (points) of CPC.....83
Figure 2.8 The emulsifying capacity of CPC: (a) measurements of conductivity as a function of oil concentration for pH varying from 4 to 11 (b) oil concentration, at which the conductivity becomes zero 85
Figure 3.1 Flow curves of CPC solutions at: (a) 1% to 10%, m/m; (b) 20%, m/m. (c) Apparent viscosity as a function of the shear rate for CPC solutions (1% to 20%). Herschel-Bulkley model (dotted lines, Equation (2)); Power Law model (solid line, Equation (1)); experimental data (points). 103
Figure 3.2 Rheological behavior of CPC solutions (5%, m/m) at pH 3, 5, 7, 9 and 11: (a) Shear stress versus shear rate and fitting of the Herschel-Bulkley model (line, Equation (2)) to experimental data (points) for pH 7, 9 and 11; (b) Apparent viscosity versus shear rate and fitting of the Cross model (lines, Equation (4)) to experimental data (points) at pH 3 and 5.106
Figure 3.3 Effect of temperature on the apparent viscosity of CPC solutions (5%, m/m) at pH 7, 9 and 11: (a) Heating step, 25 – 80°C; (b) Cooling step, 80 – 5°C; and (c) Second heating step, 5 – 25°C. 110
Figure 3.4 Mechanical spectra and tan(γ) values of CPC solutions (10%, m/m) across a frequency range of 1 to 100 rad s^{-1}, for storage modulus (G') and loss modulus (G"): (a,d) pH 7; (b,e) pH 9; (c,f) pH11 112
Figure 3.5 Spectrum of the rheological behavior of CPC solution (10%, m/m) under the influence of temperature and pH: (a) Storage modulus G'; (b) Complex viscosity η*.....113
Figure 3.6 Thermogram of CPC solution (20% m/m) at pH of 7, 9, and 11. 115
Figure 4.1 Z-average diameter D_z (bars) and polydispersity index PdI (line and markers) of emulsions stabilized with CPC at different sunflower oil concentrations and pH values: (a) pH 7; (b) pH 9 and (c) pH 11 132
Figure 4.2 Droplet size distribution by volume for emulsions stabilized with CPC at different pH values and sunflower oil concentrations (a) 2%; (b) 4%; (c) 6%; (d) 8% and (e) 10% ...134
Figure 4.3 Mean diameter based on (a) surface area mean diameter ($D_{3,2}$) and (b) volume moment mean diameter ($D_{4,3}$) of emulsions stabilized with CPC at different pH levels (7 – 11) and sunflower oil concentrations (2 – 10%).....136
Figure 4.4 Flow curves and apparent viscosity of CPC-stabilized emulsions at different sunflower oil concentrations (2 – 10%) and pH levels (a, d) pH 7; (b, e) pH 9; and (c, f) pH 11. 139
Figure 4.5 Apparent viscosity curves of CPC-stabilized emulsions at different sunflower oil concentrations (2 – 10%) and pH levels (vertical) under thermal treatment (horizontal).....144

Figure 4.6 Cream layer stability (CS) of emulsions over a 30-day storage period as a function of oil content (a) pH7; (b) pH9 and (c) pH 11 146
Figure 4.7 Cream layer stability (CS) of emulsions over a 30-day storage period as a function of pH (a) 2%; (b) 4%; (c) 6%; (d) 8%; (e) 10% oil content 148
Figure 5.1 Micrographs of the smooth surface of CPC films at pH 7, pH 9 and pH 11 at magnifications of 250×, 1000× and 5000× 167
Figure 5.2 Micrographs of the rough surface of CPC films at pH 7, pH 9 and pH 11 at magnifications of 250×, 1000× and 5000× 168
Figure 5.3 Micrographs of the cross section of CPC films at pH 7, pH 9 and pH 11 at magnification of 1000× 169
Figure 5.4 XRD of (a) CPC powder and (b) CPC films at pH 7, pH 9 and pH 11 170
Figure 5.5 FTIR spectra of (a) CPC powder, (b) CPC-based films, (c) glycerol and the fitting spectra of amide I band for CPC films at pHs of 7 (d), 9 (e), and 11 (f) 173
Figure 5.6 Sorption isotherms of CPC films prepared at pH 7, 9 and 11 180
Figure 5.7 Transmittance of CPC-based films at different pHs 181
Figure 6.1 Micrographs of the smooth and rough surface of control and CPC-emulsion films prepared at different emulsion concentrations at magnifications of 250× and 1000× 201
Figure 6.2 Micrographs of the cross section of the film formed with 1% emulsion concentration at magnifications of 1000× (a) and 10000× (b) 202
Figure 6.3 XRD of (a) CPC powder, (b) control CPC films and (c) CPC-emulsion films prepared at different emulsion concentrations 203
Figure 6.4 FTIR spectra of (a) CPC powder; (b) Glycerol; (c) emulsion (0.6% protein + 4% oil) and (d) CPC films prepared at different emulsion concentrations 205
Figure 6.5 Sorption isotherms of CPC films prepared different emulsion concentrations 211
Figure 6.6 Transmittance of CPC-based films prepared at different emulsion concentrations 215

LIST OF TABLES

Table 1.1 Amino acid profile of raw cowpea 29
Table 1.2 Proximate composition of cowpea protein extracts (concentrate or isolate) on a dry basis 35
Table 1.3 Amino acid profile of cowpea protein extracts (concentrate or isolate) 37
Table 1.4 Functional properties of cowpea protein extracts (concentrate or isolate) 40
Table 1.5 Applications of cowpea protein in different food systems 52
Table 2.1 Amino acid (AA) profile of raw cowpea (RC) and CPC 73
Table 3.1 Rheological parameters of the Herschel-Bulkley model (Equation (2)) for CPC solutions (1 to 10%, m/m) and of the Power Law model (Equation (1)) for CPC solution (20%, m/m). 104
Table 3.2 Rheological parameters of the Herschel-Bulkley model (Equation (2)) for CPC solutions (5%, m/m) at pH 7, 9 and 11. 107
Table 3.3 Rheological parameters of the Cross model (Equation (4)) for CPC solutions (5%, m/m) at pH 3 and 5. 108
Table 4.1 Mean diameters D_{10} and D_{90} of droplets in emulsions stabilized with CPC at different pH levels (7 – 11) and sunflower oil concentrations (2 – 10%) 137
Table 5.1 Assignments and relative areas (%) of the amide I components of the films at the different pHs and the CPC (powder) 172
Table 5.2 Water content (%), WVP (g m^{-1} s^{-1} Pa^{-1}), and water solubility (%) of CPC films prepared at pH 7, 9 and 11 174
Table 5.3 Tensile strength (MPa) and elongation at break (%) of CPC films prepared at pH 7, 9 and 11 176
Table 5.4 GAB model parameters of the CPC films prepared at pH 7, 9 and 11 179
Table 5.5 Color parameters and visual aspect of CPC films at different pHs 182
Table 5.6 Oxygen permeability of CPC films at pHs of 7, 9 and 11 183
Table 6.1 Water content (%), WVP (g m^{-1} s^{-1} Pa^{-1}), and water solubility (%) of CPC films prepared at different emulsion concentrations 206
Table 6.2 Tensile strength (MPa) and elongation at break (%) of CPC films prepared at different emulsion concentrations 208
Table 6.3 GAB model parameters of the CPC films prepared at different emulsion concentrations 210
Table 6.4 Color parameters and opacity of CPC films prepared at different emulsion concentrations 214
Table 6.5 Oxygen permeability of CPC films prepared at different emulsion concentrations 216

SUMMARY

INTRODUCTION **18**
THESIS ORGANIZATION **20**
OBJECTIVES **20**
General objective **20**
Specifics objectives **20**
1 A REVIEW OF ADVANCES IN COWPEA PROTEIN RESEARCH AND ITS FOOD SYSTEM APPLICATION **22**
Abstract **23**
1 Introduction **24**
2 Nutritional profile and antinutritional aspects of cowpea **25**
3 Cowpea proteins **30**
3.1 Extraction methods 30
3.2 Nutritional profile and antinutritional aspects of cowpea protein 32
3.3 Amino acid profile 36
3.4 Functional properties 38
3.4.1 Zeta potential, protein solubility and surface hydrophobicity 38
3.4.2 Water and oil holding capacity and gelling properties 47
3.4.3 Emulsifying properties 48
3.4.4 Foam properties 49
3.5 Food industry uses of cowpea proteins – Applications in the food systems 51
4 Conclusions and future perspectives **54**
References **55**
2 COWPEA PROTEIN CONCENTRATE: A DETAILED ANALYSIS OF COMPOSITION, STRUCTURE, AND TECHNOLOGICAL PROPERTIES **63**
Abstract **64**
1 Introduction **65**
2 Material and methods **66**
2.1 Material 66
2.2 Methods 66
2.2.1 Cowpea protein extraction 66
2.2.2 Characterization of cowpea protein concentrate powder 67
2.2.3 Characterization of cowpea protein concentrate in aqueous solution 68
3 Results and discussion **70**
3.1 Characterization of cowpea protein concentrate powder 70

3.1.1 Molecular mass determination by SDS-PAGE 70
3.1.2 Amino acid profile 71
3.1.3 Antinutritional factors – trypsin inhibitor 73
3.1.4 Scanning electron microscopy (SEM) 74
3.1.5 X-ray diffraction (XRD) 75
3.1.6 Fourier transform infrared spectroscopy (FTIR) 76
3.1.7 Differential scanning calorimetry (DSC) 78
3.2 Characterization of cowpea protein concentrate (CPC) in aqueous medium 80
3.2.1 Water and oil holding capacity 80
3.2.2 Zeta potential (ζ), water solubility and turbidity 80
3.2.4 Foaming capacity and foam stability 83
3.2.5 Emulsifying capacity of cowpea protein concentrate (CPC) 85
4 Conclusion 87
References 87
3 EXPLORING THE RHEOLOGICAL AND THERMAL BEHAVIOR OF COWPEA PROTEIN CONCENTRATE: IMPACT OF PH AND CONCENTRATION 95
Abstract 96
1 Introduction 97
2 Material and methods 99
2.1 Material 99
2.2 Methods 99
2.2.1 Protein dispersions 99
2.2.2 Rheological behavior 99
2.2.3 Differential scanning calorimetry 102
3 Results and discussion 102
3.1 Steady-state rheological tests 102
3.1.1 Influence of protein concentration on the rheological properties of aqueous CPC dispersions 102
3.1.2 Effect of pH on flow and apparent viscosity of aqueous CPC dispersions 105
3.1.3 Effect of temperature and pH on the apparent viscosity of aqueous solutions of CPC 109
3.2 Dynamic rheological tests 110
3.2.1 Properties of aqueous solutions of CPC at different frequencies 110
3.2.2 Properties of aqueous solutions of CPC under a thermal cycle 112
3.3 Thermogram of CPC 114
4 Conclusion 116
References 117
Apendix 124

4 PROSPECTS OF COWPEA PROTEIN AS AN ALTERNATIVE AND NATURAL EMULSIFIER FOR FOOD APPLICATIONS: EFFECT OF PH AND OIL CONCENTRATION 125
Abstract 126
1 Introduction 127
2 Material and methods 128
2.1 Raw materials 128
2.2 Preparation of oil-in-water emulsions stabilized by cowpea protein 129
2.3 Droplet size and size distribution of emulsions 129
2.4 Rheological behavior 130
2.5 Stability of emulsions through gravitational method – visual assessment 131
2.6 Statistical analysis 131
3 Results and discussion 132
3.1 Emulsion droplet size 132
3.2 Emulsion rheology 138
3.2.1 Flow properties – effect of pH and oil concentration 138
3.2.2 Thermal treatment 142
3.3 Stability of emulsions through gravitational method – visual assessment 145
4 Conclusion 149
References 150
Supplementary material 154
5 MODULATING EDIBLE FILM PROPERTIES THROUGH PH: DEVELOPMENT OF A NOVEL BIOPOLYMERIC EDIBLE FILM BASED ON COWPEA PROTEIN CONCENTRATE 156
Abstract 157
1 Introduction 158
2 Materials and methods 159
2.1 Materials 159
2.2 Methods 160
2.2.1 Cowpea protein extraction 160
2.2.2 Preparation of edible films 160
2.2.3 Characterization of edible films 161
2.2.3 Statistical analysis 165
3 Results and discussion 165
3.1 Scanning electron microscopy (SEM) 165
3.2 X-ray diffraction (XRD) 169
3.3 Fourier-transform infrared (FTIR) spectroscopy 170
3.4 Water vapor permeability (WVP) and water solubility (S) 174

3.5 Mechanical properties 176
3.6 Sorption isotherm 178
3.7 Optical properties 180
3.8 Oxygen permeability (O_2P) 183
4 Conclusion 184
References 185
6 IMPROVING PROPERTIES OF COWPEA PROTEIN CONCENTRATE FILMS WITH EMULSION INCORPORATION – A COMPARATIVE STUDY 190
Abstract 191
1 Introduction 192
2 Materials and methods 193
2.1 Materials 193
2.2 Methods 194
2.2.1 Cowpea protein extraction 194
2.2.2 Preparation of oil-in-water emulsion stabilized by cowpea protein concentrate 194
2.2.3 Protein stock solution 194
2.2.4 Preparation of films incorporating emulsion 195
2.2.5 Characterization of edible films 195
2.2.6 Statistical analysis 200
3 Results and discussion 200
3.1 Scanning electron microscopy (MEV) 200
3.2 X-ray diffraction (XRD) 202
3.3 Fourier-transform infrared (FTIR) spectroscopy 204
3.4 Water vapor permeability (WVP) and water solubility (S) 206
3.5 Mechanical properties 208
3.6 Sorption isotherm 209
3.7 Optical properties 212
3.8 Oxygen permeability (O_2P) 215
4 Conclusion 217
References 218
GENERAL CONCLUSIONS 224
FUTURE PERSPECTIVES 227
REFERENCES 228

INTRODUCTION

By 2050, the global population is projected to reach approximately 9.8 billion people (United Nations, 2024). In addition to population growth, changing behaviors, beliefs, and lifestyle preferences demand the development of modern technologies that can provide high-quality and sustainable food (Ahmed et al., 2022; Aiking, 2011; Alexander et al., 2019). Addressing the challenge of feeding this growing population while minimizing environmental impacts is imperative for the food industry. One strategy for achieving more sustainable diets is to reduce excessive consumption of animal proteins while simultaneously increasing the intake of plant-based proteins.

Plant-based proteins offer a viable alternative to animal proteins, as they are low-cost and obtained from abundant resources, with sustainable cultivation systems that require less capital and energy consumption for production (Bessada et al., 2019; De Boer et al., 2014; Stone et al., 2018). Although soy is one of the primary sources of vegetable protein (Singh et al., 2008), particularly in Brazil, it is assumed that soy production will not be sufficient to meet the demand for plant-based proteins in the coming years. Therefore, the partial replacement of animal proteins by plant proteins can be driven by the diversification of protein sources, with the inclusion of legumes that are still underutilized in human nutrition.

The cowpea (*Vigna unguiculata (L.)* Walp), but also known around the world as “black-eyed peas” or “southern peas” (all used in the USA), “frijol caupí” (Spanish-speaking countries in America), “lobia” (India), “caupi” (Brazil), “caupí” and “carilla” (Spain), “niébé” (French-speaking countries in Africa) and “feijão-frade” (Portugal) (Carvalho et al., 2017), is one of the most adaptable and versatile legumes, capable of adapting to a wide range of soil types, high temperatures and drought (Carvalho et al., 2017; Ehlers & Hall, 1997). Africa is responsible for 95.3% of the world's cowpea production (FAO, 2022), while Brazil has historically been the world's third largest producer, preceded by Nigeria and Niger, and the largest producer and consumer in Latin America (Freire-Filho et al., 2023). Currently, this crop has been acquiring greater economic expression, and its cultivation is carried out by small, medium and large producers (Freire-Filho et al., 2012;2023).

Cowpeas have been the subject of research as a potential alternative source of plant-based protein. These studies have investigated the extraction of proteins and the evaluation of their properties, including solubility, water and oil retention capacity, foam formation, emulsification, as well as thermal and rheological characteristics and amino acid profiles (Ge et al., 2021; Oliveira et al., 2024; Schlangen et al., 2022; Tang et al., 2021; Vasconcelos et al., 2010). Despite the existing literature on the technological properties of cowpea protein (CP),

there is still a lack of information in the published works regarding all those properties in an integrated manner. These properties confer a broad range of applications for the proteins in question, including use in enriched products, ingredient replacement, edible films, microcapsules, and emulsions (Campbell et al., 2016; de Almeida et al., 2021; Hewage & Vithanarachchi, 2009; Pereira et al., 2009). The functionality, nutritional value and structural role of proteins are essential for their usefulness. Therefore, the present study concentrates on two main applications of cowpea protein: the stabilization of emulsions and the production of edible films.

Proteins can function as natural emulsifiers due to their amphiphilic properties, allowing them to self-aggregate and form a continuous and uniform layer around the oil droplets (Dickinson et al., 1997). The key properties of cowpea protein, including its ability to adsorb and interact with water and oil, coupled with a solubility exceeding 80%, underscore its exceptional performance as an emulsifier and stabilizer (Ge et al., 2021; Ragab et al., 2004; Tang et al., 2021; Thompson et al., 2023). To date, a single study has evaluated the emulsifying capacity of cowpea protein isolates (Thompson et al., 2023). This scarcity of research on the topic suggests that there is still a significant need for further investigation in this area.

One promising solution to the excessive use of synthetic plastics is the development of edible films. In the literature, only two studies have focused specifically on edible films based on cowpea protein (Almeida et al., 2021; Hewage & Vithanarachchi, 2009). This indicates that the potential of cowpea protein remains unexplored even though evidence of its favorable techno-functional properties. While the available literature is limited, it suggests that cowpea protein can form films with satisfactory properties. Nevertheless, the development of films with distinctive properties using this unexplored raw material may prove to be a considerable challenge.

Therefore, the objective of this thesis was to extract, characterize, and evaluate the techno-functional properties of cowpea protein with a view to its potential application in the stabilization of emulsions, and in the development of edible films. The initial step involved the extraction of cowpea protein through the application of the isoelectric precipitation technique. The resulting protein concentrate from cowpea (CPC) was then subjected to characterization and evaluation for its functionality across a range of pH values. Subsequently, the concentrate was employed in the formation of stable emulsions, which were developed at varying pH levels and oil concentrations. The emulsions were subjected to analysis in order to ascertain their droplet size and stability. Edible films based on the CPC were then obtained and characterized

at varying pH levels. Using a selected emulsion formulation, films were developed by adding different concentrations of this emulsion to the matrix, aiming to modify the film properties.

THESIS ORGANIZATION

The thesis is divided into six chapters:

Chapter 1 provides a review of the state of the art on the use of cowpea protein, focusing on extraction techniques, composition, functional properties, and potential applications. Chapters 2 to 6 present the experimental results. Chapter 2 focuses on the characterization of CPC. Chapter 3 investigates the combined effects of pH, concentration, and temperature on the rheological and thermal properties of CPC. Chapter 4 evaluates the efficacy of CPC as a stabilizing agent. Chapter 5 examines how pH alterations influence the key properties of CPC-edible films. Chapter 6 is dedicated to the incorporation of different emulsion concentrations into the film matrix, with a view to determine the impact of this component on the film's properties. To conclude, we present a general conclusion of the results obtained in this thesis, along with perspectives for future work.

OBJECTIVES

General objective

The general objective of this study is to extract and characterize cowpea protein, and to investigate its applications as both a stabilizing agent in emulsions and as base for the formation of edible films. Additionally, the study aims to evaluate the impact of incorporating these emulsions into the protein matrix of the films and analyzing how this modification affects the structural and functional properties of the resulting films.

Specifics objectives

- Extract cowpea protein (*Vigna unguiculata (L.)* Walp) using the isoelectric precipitation method and characterize it regarding its composition, physicochemical properties, and functionality at different pH levels;
- Investigate the combined effects of concentration, pH, and temperature on the rheological and thermal properties of the CPC;
- Prepare emulsions stabilized by CPC at various pH levels (3 to 11) and sunflower oil concentrations (2 to 10%), and analyze the droplet size and distribution, as well as the rheological behavior and stability of these emulsions;

- Develop CPC-based films at different pH levels and evaluate how pH values in the neutral to alkaline range influence the morphology, structural properties, optical properties, water absorption, and barrier properties of these films;
- Investigate the behavior of CPC-based films obtained at pH 9 with the addition of emulsion, evaluating how this modification affects the structure and main properties of the films.

1 A REVIEW OF ADVANCES IN COWPEA PROTEIN RESEARCH AND ITS FOOD SYSTEM APPLICATION

Maria Mariana Garcia de Oliveira[a*], Víctor Justiniano Huamaní-Meléndez[a] and Maria Aparecida Mauro[a]

[a] Department of Food Engineering and Technology, Institute of Biosciences, Humanities and Exact Sciences – São Paulo State University (UNESP), Street Cristóvão Colombo, 2265, São José do Rio Preto 15054-000, Brazil.

e-mail address: maria.mariana@unesp.br (*corresponding author)

Abstract

In response to global issues, an increasing number of people are seeking sustainable protein sources with reduced environmental impact. The proeminence of plant-based proteins is attributable to a number of factors, including environmental and health concerns, changing dietary preferences, ethical and religious considerations, and financial factors. This review addresses the viability of cowpea as an alternative protein source, with a particular focus on its potential applications within the food industry. Cowpea (*Vigna unguiculata L.* Walp) is a legume that is widely cultivated in several tropical and subtropical regions of the world. It plays an important role in the food and nutritional security of millions of people. In addition to its significance as a staple food, cowpea is also valued for its dietary properties, particularly regarding its proteins. Cowpea proteins have recently attracted considerable attention as a potential source of nutrition due to their balanced composition of essential amino acids and their functional properties, which play an important role in food technology. It is of scientific importance to be aware of and comprehend the characteristics of cowpea proteins, as this knowledge is essential for the optimal utilization of these proteins in the food industry. Furthermore, it is of considerable value to investigate the potential for novel applications and to develop more nutritious and sustainable food products. The structure of this article will adopt a logical sequence, beginning with an overview of the extraction and characterization methods of cowpea proteins. The subsequent section will examine the structural and functional properties of these proteins, followed by an analysis of current and future trends in the research and development of products derived from these proteins. Finally, the paper will present a summary of the main points discussed and an outline of potential avenues for future research in this field. This review article aims to provide a comprehensive examination of the current state of knowledge about cowpea proteins. It will highlight their functional and nutritional properties and the main scientific and technological advances in the area, ranging from extraction and characterization methods to food industry applications.

Keywords: Plant protein, Protein extraction, Nutritional properties, Functional properties

1 Introduction

The production of livestock represents a significant contributory factor to climate change, as evidenced by the degradation of pastures and arable lands, the decline of biodiversity, and other environmental consequences. Concurrently, a considerable number of individuals globally are confronted with challenges to food security as a consequence of population growth. In response to these challenges, the market has increasingly shifted towards sustainable protein sources that have a lower environmental impact (De Boer et al., 2014; Henchion et al., 2017; Sabaté et al., 2015). In this context, the use of plant-based proteins has gained prominence. In addition to environmental concerns, there are several other reasons for seeking plant-based proteins. These include health issues, changing dietary preferences, ethical and religious considerations, and financial factors. The growing demand for plant-based proteins and the pressure on conventional crop sources are driving the extraction of proteins from alternative plant-based sources (Ge et al., 2021; Locali-Pereira et al., 2022, 2024; Yu et al., 2015). These emerging sources, in conjunction with novel trends and techniques for the extraction and modification of plant protein, are aimed at alleviating the burden on the commercial production of existing animal proteins, as well as conventional plant proteins such as soy and pea.

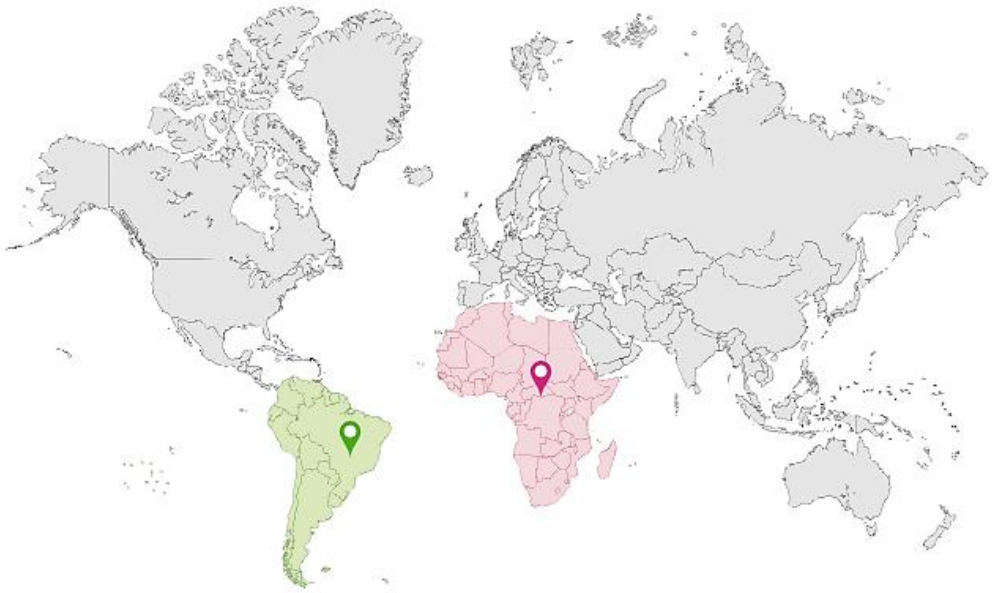
Cowpea is cultivated primarily in Africa (Figure 1.1), where it accounts for 95% of global production as well as in other tropical and subtropical regions (FAO, 2022). In Brazil, cowpea has been a highly significant food crop since the beginning of colonization. Currently, Brazil is the main producer and consumer in Latin America (Figure 1.1) (FAO, 2022; Conab, 2021; Freire-Filho & Ribeiro, 2023). Also known as black-eyed peas, string beans, and southern peas, cowpea is notable for its competitive cost and its relevance as a food source, in addition to its contribution to job and income generation (Freire-Filho et al., 2012).

Cowpea is renowned for its resilience, due to its tolerance to drought and its ability in nitrogen fixation, as well as its high nutritional density, with a protein content in dry matter ranging from 20% to 30% (Bai et al., 2020). The fractionation of cowpea flour into protein-rich fractions represents a significant opportunity to enhance its use as an ingredient in food products. In addition to its high nutritional value, cowpea protein (CP) possesses unique functional qualities (Lafarga et al., 2020; Peyrano et al., 2019; Ragab et al. 2004). Despite these advantages, cowpea protein is still underutilized in the food industry, despite its diverse potential applications.

The characteristics of cowpea proteins, including solubility, water and oil retention capacity, foaming, emulsification, and thermal properties, are significantly influenced by a

number of factors, including extraction and drying methods employed, the processing and modification conditions (pH, ionic strength, temperature), and the amino acid profiles of these proteins (Ge et al., 2021; Schlangen et al., 2022; Tang et al., 2021; Vasconcelos et al., 2010; Oliveira et al., 2024). It is therefore essential to possess a comprehensive understanding of the physicochemical and techno-functional properties of cowpea protein in response to a range of conditions, to ensure their effective application in a variety of food products and as an alternative to animal proteins.

Figure Error! No text of specified style in document..**1** World map focusing on the main producers of cowpea: Africa (global leader, in red) and Brazil (Latin American leader, in green)



Source: Author (Created with BioRender.com)

This review aims to examine the extraction, modifications (chemical and physical), physicochemical, and techno-functional properties of cowpea proteins, as well as their applications in the food industry. It is anticipated that the findings presented in this review will provide a comprehensive understanding of the potential for obtaining proteins from this plant source for use in industrial production.

2 Nutritional profile and antinutritional aspects of cowpea

The protein content in distinct cowpea cultivars can vary from 19.5% to 27.2% on a dry basis (Bai et al., 2020; Ferreira et al., 2019; Ge et al., 2021; Kewuyemi et al., 2022; Naiker et

al., 2019). Proteins play a pivotal role in these cowpea grains, as they are a pertinent source of essential amino acids, mainly leucine, phenylalanine, and lysine (Schlangen et al., 2022; Vasconcelos et al., 2010), which will be discussed further (Table 1.1). Additionally, carbohydrates constitute the predominant fraction, comprising approximately 60-65.7% (dry basis) of the overall composition and fibers also contribute to this structure, displaying disparities (5.4 – 38.5, dry basis) among the different varieties (Bai et al., 2020; Kewuyemi et al., 2022; Naiker et al., 2019). Moreover, lipids are present in relatively low quantities in cowpea grains, typically ranging from 1.2% to 5.83% on a dry basis (Ge et al., 2021; Naiker et al., 2019). Lastly, the ash content in cowpeas is approximately 3.9% on a dry basis, indicating the presence of minerals and other inorganic constituents (Bai et al., 2020; Ge et al., 2021; Kewuyemi et al., 2022).

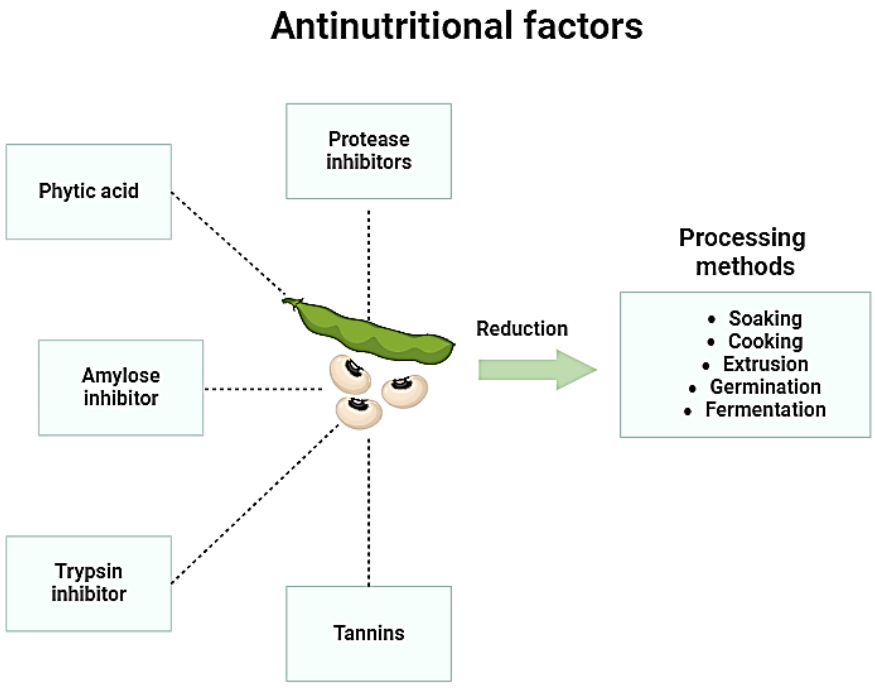
Previous studies have highlighted cowpeas as a significant dietary source of macrominerals. Among the mineral elements, potassium, phosphorus, magnesium, and calcium stand out as the most predominant, with concentrations ranging from 580 to 1450 mg/100g, 498 to 575 mg/100g, 199 to 496 mg/100g, and 71.2 to 138 mg/100g, respectively (Devi et al., 2015; Granito et al., 2005; Naiker et al., 2019).

The diversity in the chemical composition of cowpeas, encompassing proteins, carbohydrates, lipids, fibers, and ash, is observed across various cultivars, species, and environmental contexts. The significant variability observed in the intrinsic composition of unprocessed grain types can be attributed to many factors including genetic disparities, environmental influences, and agricultural methodologies, which play important roles in shaping the heterogeneous nutritional characteristics observed in cowpea. Comprehending these variances is imperative for enhancing the nutritional adequacy and utility of cowpea-derived commodities, as well as for accommodating distinct dietary requirements and preferences.

Despite being rich sources of protein, carbohydrates, vitamins, and minerals, pulses also contain various antinutritional factors (ANFs), such as protease inhibitors, phytic acid, amylose inhibitor, trypsin inhibitors, saponins, agglutinins, among others (Figure 1.2). These compounds have been demonstrated to reduce protein digestibility and hinder the availability of essential nutrients, thus falling under the classification of anti-nutritional factors (Mohanan et al., 2022). Of particular concern is the trypsin inhibitor, which reduces protein availability by impeding the digestibility of specific amino acids. To attenuate the presence of ANFs in pulses, conventional methods such as soaking, heat treatment, germination, or cooking with

water are often employed (Ramireddy & Radhakrishnan, 2021). These approaches aim to enhance the bioavailability of crucial nutrients inherent in legumes.

Figure Error! No text of specified style in document.**.2** Proteins' antinutritional factors and methods for their reduction



Source: Author (Created with BioRender.com)

The application of processing methods, such as soaking, cooking, and fermentation, has demonstrated effectiveness in reducing the levels of certain antinutrient compounds such as tannins, phytic acid, and trypsin inhibitors (Ibrahim et al., 2002). A combined approach using these techniques can be highly effective in maximizing the nutritional benefits of cowpeas. The fermentation process followed by cooking has been proven to reduce trypsin inhibitory activity and phytic acid content, promoting enhanced digestibility and nutrient absorption (Granito et al., 2005).

The study by Rivas-Vega et al. (2006) demonstrated the efficacy of extrusion processing in eliminating trypsin inhibitory activity, indicating the feasibility of this technique to enhance the nutritional quality of cowpea-based foods. The genetic diversity and distinct cultivars of cowpeas require the development of varied strategies to reduce antinutritional factors, as evidenced by the research of Frota et al. (2018) and Vasconcelos et al. (2010). Other studies (Coffigniez et al., 2019; Sreerama et al., 2012) reinforce the effectiveness of heat treatment in inactivating enzymatic inhibitors and underscore the pivotal role of soaking temperature, a

crucial variable that can be adjusted to maximize nutrient retention and minimize the presence of anti-nutrient compounds. Thus, processed flours derived from legumes, such as cowpeas, become suitable for incorporation into functional foods.

In summary, processing methods play a crucial role in reducing antinutritional factors in cowpeas, thereby enhancing their nutritional quality. However, it is essential to optimize the conditions of the treatments used to avoid undesired effects. Additionally, the importance of innovative methods, such as extrusion, which show significant promise in overcoming these challenges, is emphasized. There is also recognition of the need to consider the heterogeneity of cultivars when planning interventions, highlighting the importance of customizing processing methods according to the specific characteristics of each cultivar.

Table 1.1 presents the amino acid profile of cowpea in different forms (flour, meal, or paste). Despite the disparities observed among the published studies, a general trend seems to persist. The most abundant essential amino acids are leucine, phenylalanine, and lysine, while tryptophan is the limiting essential amino acid. Regarding non-essential amino acids, aspartic acid and glutamic acid predominate, while cysteine is found at significantly lower levels (Abu et al., 2005; Aremu, 1990; Bai et al., 2020; Martins Ferreira et al., 2022; Olivera-Castillo et al., 2007; Schlangen et al., 2022; Vasconcelos et al., 2010).

Studies investigating the amino acid content in grains of different genotypes and cultivars have identified a similar distribution pattern (Bai et al., 2020; Martins Ferreira et al., 2022; Vasconcelos et al., 2010). This pattern is characterized by the predominance of amino acids such as glutamine/glutamic acid, asparagine/aspartic acid, and phenylalanine + tyrosine, followed by a secondary prevalence of other essential amino acids such as leucine and lysine. However, it is relevant to note that the specific content of each amino acid may vary significantly among the different types of grains analyzed.

The effects of gamma irradiation (Abu et al., 2005) can also influence the amino acid composition of cowpeas. The results of gamma irradiation application at various doses, both under dry (flour) and wet (paste) conditions, demonstrated a significant reduction in the amino acids present in cowpea flour, except for tyrosine, which showed a significant increase.

The nutritional value of a protein is primarily determined by its ability to meet the human requirements for nitrogen and essential amino acids. Therefore, it is imperative to have an accurate understanding of these requirements for assessing the nutritional significance of protein in the diet. Most essential amino acids found in cowpeas, except for methionine, have been identified at levels deemed acceptable when compared to the reference standard

established by the FAO (Leser, 2013) for older age groups, including older children, adolescents, and adults.

Table Error! No text of specified style in document.**.1** Amino acid profile of raw cowpea

Amino acid composition (g 100g protein^{-1})							
Essentials							
Iso	3.8-4.0	4.1-4.3	4.6-4.8	4.0	3.2	4.0	3.5
Leu	7.0-7.6	7.6-7.8	7.2-7.3	7.9	7.0	7.1	7.3
Phe	5.0-5.5	5.2-5.3	10.5-11.1	5.9	-	5.2	3.5
Lys	6.7-7.1	7.3-7.6	6.6-6.9	7.1	6.8	6.3	6.8
Try	-	-	1.4	0.3	0.8	1.0	-
His	2.7-3.3	4.3	3.7-3.9	3.1	5.0	2.7	3.0
Val	4.9-5.0	5.1-5.4	4.2-4.4	4.8	4.1	4.6	4.2
Met	2.5-3.3	0.8-1.2	2.0-2.6	1.5	-	1.1	1.0
Thr	4.3-4.5	3.3-4.3	4.0-4.3	4.6	7.4	3.6	3.8
Non-essentials							
Asp	9.4-10.3	12.8-14.2	10.9-11.8	11.9	11.0	10.4	12.2
Glu	19.0-20.1	20.5-20.7	16.8-19.6	18.4	17.4	16.0	16.9
Ser	4.9-5.5	5.6-5.8	4.1-4.5	6.1	5.4	4.7	5.5
Gly	3.8-4.5	4.5-4.6	3.9-4.0	4.0	4.2	3.6	3.8
Arg	7.1-7.8	7.2-9.0	8.2-8.5	7.3	9.9	6.4	7.2
Ala	4.3-4.5	4.6-4.9	4.2-4.6	4.7	3.7	4.0	5.0
Pro	5.4-6.0	-	4.6-5.0	4.4	6.1	1.0	4.5
Tyr	4.3-4.5	3.2-3.6	**	0.3	-	3.1	2.9
Cys	0.5-0.6	0.5-0.6	*	0.2	-	0.9	-
Ref.	Martins et al. (2022)	Bai et al. (2020)	Vasconcelos et al. (2010)	Abu et al. (2005)	Olivera-Castillo et al. (2007)	Schlangen et al. (2022)	Aremu (1990b)

*phe+tyr; **met+cys

3 Cowpea proteins

3.1 Extraction methods

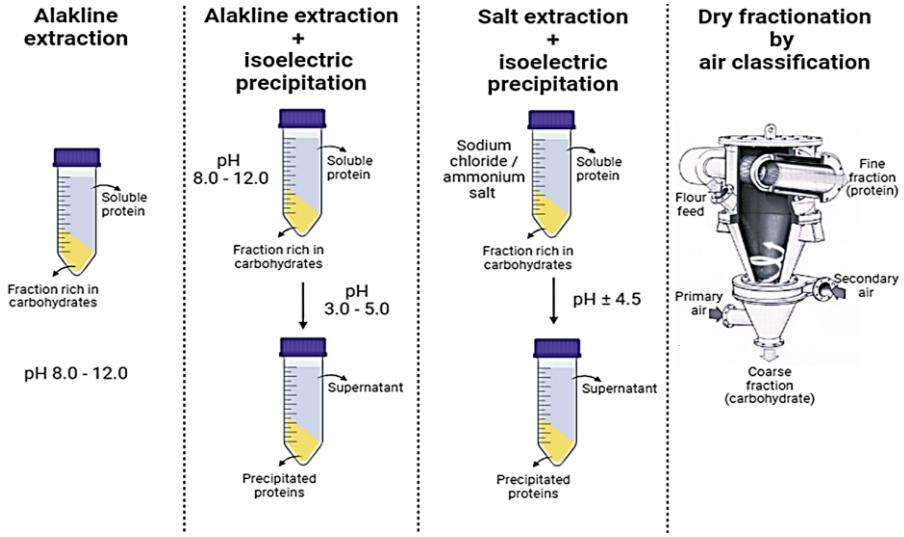
Legume proteins can be extracted using various methods, including chemical, physical, or biotechnological techniques. Among these, the chemical approach, particularly aqueous fractionation, is widely recognized as the most prevalent method. The process of legume protein extraction involves several essential stages. Firstly, the flour undergoes defatting, which entails the use of solvents such as petroleum ether, n-hexane, or n-pentane. This step aims to eliminate lipids and other lipophilic compounds that might interfere with subsequent protein extraction. Following defatting, the proteins are extracted from the defatted flour using salts, water, alcohols, or buffer solutions. Finally, the proteins are precipitated using substances such as ammonium sulfate, ethanol, methanol, acetone, or acids like hydrochloric acid or citric acid (Kumar et al., 2021; Locali-Pereira et al., 2023).

The specific extraction of protein from cowpea grains can be conducted using several techniques (Figure 1.3) (Ge et al., 2021; Lafarga et al., 2020; Moongngarm et al., 2014; Mwasaru et al., 1999a; Rudra et al., 2016; Schlangen et al., 2022). One of the most traditional approaches is isoelectric precipitation, in which protein fractions are precipitated at a pH close to their isoelectric point (pH 4.0−5.0), aiming to reduce their solubility and induce precipitation (Evans et al., 2009). This technique can be combined with an initial step of alkaline protein solubilization at a pH suitable for increasing solubility, usually between 8 and 12, before proceeding with the steps of conventional isoelectric precipitation (Table 1.2). The isoelectric precipitation technique, with or without the combination of the alkaline solubilization step, has been successful in extracting cowpea proteins. Researchers report protein extracts with up to 90% purity (Abu et al., 2005; Ge et al., 2021; Peyrano et al., 2016, 2017, 2019; Rangel et al., 2004; Tang et al., 2021).

The effects of salt extraction techniques, using ammonium sulfate (Moongngarm et al., 2014) and sodium chloride (Rudra et al., 2016), were investigated, allowing the observation of the impacts of these methods on the chemical composition of proteins. When comparing the protein content of different extraction techniques, such as isoelectric precipitation (PI), saline extraction with ammonium sulfate (ESA), and saline extraction with ammonium sulfate combined with isoelectric precipitation (ESA+PI), Moongngarm et al. (2014) observed that extraction was more efficient using only the isoelectric extraction technique (85.89%, dry basis). However, despite the higher protein content obtained by the isoelectric precipitation extraction technique, when it was combined with saline extraction, it increased the protein content of the extracted extract from 68.27% (only ESA) to 79.35% (PI + ESA). Using the same

saline extraction technique, but employing sodium chloride salt instead, Rudra et al. (2016) managed to obtain a protein extract with an even higher protein content than that observed by Moongngarm et al. (2014), reaching 89.14% (dry basis). Therefore, it is evident that combining a less conventional approach with isoelectric precipitation can lead to the attainment of protein extracts with higher protein contents. Conversely, the studies (Moongngarm et al., 2014; Rudra et al., 2016) demonstrated that, even without integrating multiple techniques, through the exclusive use of saline extraction, it was possible to achieve a protein extract with a higher and comparable content to that obtained by the conventional technique of isoelectric precipitation, by simply changing the salt used from ammonium sulfate to sodium chloride.

Figure Error! No text of specified style in document.**.3** Protein extraction methods



Source: Author – modified from Localli-Pereira et al. (2023) (Created with BioRender.com)

Unconventional strategies, such as the application of ultrasound, have also been described in the literature as methods for extracting proteins from cowpea beans (Lafarga et al., 2020; Loushigam & Shanmugam, 2023). Although the study conducted by Lafarga et al. (2020) in question did not specifically investigate the effects of ultrasound on protein extraction, another study conducted by the same researchers (Lafarga et al., 2018), but in Ganxet beans, highlights that the combination of ultrasound-assisted extraction, followed by alkalinization of the medium and precipitation at the protein's isoelectric point, may increase the efficiency of extraction and process yield. These findings are supported by Loushigam & Shanmugam (2023), who, when extracting protein from cowpea using ultrasound, concluded that, considering the processing time and extraction yield, ultrasound-assisted extraction technique demonstrated advantages in obtaining proteins. While the conventional method requires a total

extraction time of approximately 120 minutes, ultrasound-assisted extraction only requires 65 minutes. Therefore, by replacing the conventional method with ultrasound-assisted extraction, the time required for protein extraction can be halved.

Dry fractionation also offers a viable alternative to wet fractionation, providing protein-rich fractions through milling and subsequent air classification. The cowpea flour underwent air classification at three speeds (8000, 10,000, and 12,000 rpm), resulting in the separation of fine (protein-rich) and coarse (starch-rich) fractions (Schlangen et al., 2022). The findings illustrate that higher air classifier speeds enhance the enrichment of the protein-rich fine fraction by reducing the size of particles allowed to pass through the air classifier. This phenomenon theoretically enables smaller particles, such as proteins, to pass through while excluding larger particles like starch granules. However, as the protein content increases with rising air classifier speed, there is a corresponding decrease in protein yield. Theoretical protein yields in the fine fraction decreased from 55 to 46 to 44 for cowpea beans air classified at 8000, 10,000, and 12,000 rpm, respectively. Achieving a balance between protein content and yield is essential for future applications of dry fractionation in the industry (Schlangen et al., 2022).

The processing conditions of extraction techniques, such as the presence of salts, pH, air velocity, ultrasonic power, and time, among other variables, have the potential to influence the properties of cowpea protein isolates. Therefore, it is of paramount importance to assess the optimal sizing of these variables to achieve the desired outcomes.

A promising technique to be explored for optimizing the protein extraction process is the use of natural deep eutectic solvents (NADES). NADES represent an environmentally sustainable alternative for protein extraction, which has been little investigated so far (Patra et al., 2023; Zhou et al., 2022). A key feature of these solvents is their fine-tuning capability to meet specific purposes. The modification of physicochemical properties, such as polarity, pH, and viscosity, can optimize extraction efficiency by enhancing the solubility of target molecules and their interactions with NADES (Jauregi et al., 2024). Although there are few reports on their use for plant protein extraction, NADES show great potential as efficient protein extractors (Grudniewska et al., 2018; Jiao et al., 2021; Liu et al., 2017; Svigelj et al., 2017; Wahlstrom et al., 2017).

3.2 Nutritional profile and antinutritional aspects of cowpea protein

Table 1.2 summarizes the compositions of cowpea protein extracts described in studies over time. It provides the material used, the extraction method employed, and the composition

of the resulting fraction, expressed in percentage and on a dry basis of protein, carbohydrate, lipid, fiber, and ash.

The variation in the percentage of protein in the extracted fraction shows a considerable range, with values fluctuating between approximately 71.7% and 95.8% (Table 1.2). Studies that focused on concentrated proteins (Chel-Guerrero et al., 2011; Loushigam & Shanmugam, 2023; Moongngarm et al., 2014; Penchalaraju & John Don Bosco, 2022), with protein content below 90%, revealed a considerable proportion of carbohydrates in the protein fraction (10 - 18%). Studies that adopted an alkaline solution for protein solubilization, followed by isoelectric precipitation (Frota et al., 2008; Ge et al., 2021; Tang et al., 2021), showed higher protein contents, this suggests a greater efficiency in the protein extraction process, resulting in a final fraction with higher purity.

This pattern seems to be recurring for the other constituents. Protein fractions with higher protein content tend to have lower levels of lipids, fibers, and ash, which highlights the greater efficiency of the chosen method. This underscores the need to optimize extraction methods to obtain protein fractions with consistent and desirable compositions.

In addition to the methods previously discussed in *section 3.1* which can be applied prior to protein extraction from the grain, the protein extraction process itself also aims to eliminate or reduce the presence of antinutritional compounds. For this reason, the extraction and separation of proteins from plant material are fundamental steps prior to incorporating these proteins into food products.

The protein extraction process has been demonstrated to significantly reduce the levels of antinutritional compounds in cowpea protein, as evidenced by different studies (Khalid & Elhardallou, 2016; Mwasaru et al., 1999; Olivera-Castillo et al., 2007; Rangel et al., 2004). These researches employed a range of analytical techniques to assess the presence of antinutritional compounds, including phytic acid, tannins, and trypsin inhibitors, in legume seeds and their protein isolates.

A pioneering study conducted by Mwasaru et al. (1999) demonstrated the complete removal of antinutritional compounds in cowpea proteins extracted using isoelectric precipitation and micellization extraction techniques under different pHs of the extraction medium. The researchers observed a complete reduction in the levels of trypsin inhibitors, phytate, sucrose, raffinose, and stachyose in the resulting isolates. As Mwasaru et al. (1999), I. I. Khalid & Elhardallou (2016) also investigated the extraction techniques of isoelectric precipitation and micellization to obtain proteins from cowpea. However, in this study, only tannins and phytic acid were completely eliminated after the extraction process. Concomitantly,

the trypsin inhibitory activity identified in the isolates was significantly reduced (by approximately 74%) when compared to the activity found in raw cowpea flour. Furthermore, there was no statistical difference between the extraction techniques evaluated. By contrast, Rangel et al. (2004) employed purified pea vicilin as a negative control for trypsin inhibitory activity and aimed to examine the effect of heat treatment at 80 °C for 5 minutes on the reduction of this antinutrient in cowpea protein isolate. As anticipated, purified pea vicilin demonstrated the lowest levels of inhibition, while cowpea protein isolate (CPI) exhibited the highest. In response to heat treatment, a significant reduction in trypsin inhibitory activity was observed.

In general, the levels of anti-nutritional factors are strongly correlated with the parameters of the wet extraction process, including the pH of the extraction/precipitation medium, the number of washing steps, the ionic strength, and other factors. Moreover, the stability of these anti-nutritional factors against heat was a critical aspect to be evaluated. During the wet extraction process, pH variation induces protein precipitation, resulting in the separation of certain antinutrients that remain soluble during this stage (Sathya & Siddhuraju, 2015). Furthermore, adjustments in ionic strength can facilitate the breaking of electrostatic interactions between these antinutrients and proteins, which allows their separation from the protein product (Kaspchak et al., 2018; Sathya & Siddhuraju, 2015). It is important to note that some anti-nutritional factors are sensitive to heat, such as lectins and protease inhibitors, while others are more resilient, such as phytic acid, condensed tannins, saponins, and alkaloids. These methods can be employed in a strategic manner as pre- or post-processing steps to reduce the presence of antinutritional factors in protein isolates and concentrates. They can also be applied to products subjected to heat treatment before consumption (Amin et al., 2022).

Table Error! No text of specified style in document.**.2** Proximate composition of cowpea protein extracts (concentrate or isolate) on a dry basis

Ref.	Description	Extraction method	Protein (%)	Carbohydrate (%)	Fat (%)	Fibers (%)	Ash (%)
Frota et al. (2008)	Cowpea protein isolated	Alkaline solubilization and isoelectric precipitation (pH 4.5)	92.0	1.2	0.4	2.2	4.4
Ge et al. (2021)	Cowpea protein isolated	Alkaline solubilization (pH 10.0) and isoelectric precipitation (pH 4.5)	95.8	0.2	0.9	-	5.2
Chel-Guerrero et al. (2011)	Mexican cowpea protein isolate	Alkaline solubilization (pH 11.0) and isoelectric precipitation (pH 4.3)	85.3	14.5	1.2	0.7	1.2
Moongngarm et al. (2014)	Cowpea Protein Concentrate prepared by (a) isoelectric point precipitation; (b) Ammonium sulfate precipitation and (c) Ammonium sulfate + isoelectric point precipitation	Isoelectric precipitation; Ammonium sulfate precipitation and Ammonium sulfate + isoelectric precipitation	(a) 90.8 (b) 71.7 (c) 83.5	(a) 9.1 (b) 12.3 (c) 11.2	-	-	(a) 4.1 (b) 4.1 (c) 3.3
Penchalaraju et al. (2022)	Protein concentrate extracted by (a) alkaline; (b) water; (c) acid and (d) micellization precipitation	Alkaline, acid, water and salt extraction	(a) 79.5 (b) 74.4 (c) 70.8 (d) 72.9	(a) 4.9 (b) 10.0 (c) 11.6 (d) 13.8	(a) 0.1 (b) 0.6 (c) 1.2 (d) 0.2	-	(a) 6.3 (b) 8.7 (c) 5.5 (d) 6.1
Tang et al. (2021)	Cowpea protein isolate	Alkaline solubilization and isoelectric precipitation	95.4	1.5	0.6	-	2.5
Loushigam et al. (2023)	Cowpea protein concentrate	Alkaline solubilization (pH 9.0) and isoelectric precipitation (pH 4.5)	79.6	18.1	-	-	2.3

3.3 Amino acid profile

Table 1.3 presents the amino acid composition of proteins extracted from cowpeas, as documented in several studies. Amino acids are classified as either essential or non-essential and are quantified in grams of amino acid per 100 grams of protein on a dry basis.

The amino acid composition of the extracted protein fractions differs from that of cowpea flour (Table 1.1). The extraction of these proteins allows for the concentration of essential and specific amino acids, thereby enhancing their nutritional quality and making them more concentrated and rich sources of essential nutrients. This aspect is of the highest importance in order to meet the growing demands for high-quality functional foods and nutritional supplements. Despite these compositional alterations, the majority of studies indicate that this does not significantly impact the proportion of hydrophilic and hydrophobic amino acids, thus ensuring the maintenance of the nutritional and functional quality of the extracted proteins.

Amino acid composition analysis reveals a high degree of consistency among the studies investigated. A greater abundance of leucine, lysine, and phenylalanine is observed among the essential amino acids, while non-essential amino acids, such as aspartic and glutamic acid, are found in greater proportion. The data indicate that tryptophan and methionine are the primary limiting essential amino acids in this protein, while tyrosine and cystine deficiencies are observed among the non-essential amino acids. The deficiency, particularly of essential amino acids, underscores the necessity for supplementation through the ingestion of cowpea protein in conjunction with other foods that are rich in absent amino acids.

Although they exhibit a similar trend, the reported amino acid levels may vary. This variation may be attributed to differences in the processing method employed, genetic variations, environmental factors, and/or variations in seed maturation. These discrepancies between studies may influence the hydrophobic/hydrophilic amino acid ratios, which in turn may affect functional properties such as water retention capacity and gelation of the proteins. These discrepancies demonstrate the necessity for a customized methodology in the development and utilization of these proteins in diverse food applications.

Table Error! No text of specified style in document.**.3** Amino acid profile of cowpea protein extracts (concentrate or isolate)

	Amino acid composition (g 100g protein^{-1})							
				Essentials				
Iso	4.7	3.2-3.5	2.8	4.4	4.0	4.0	3.8-4.0	4.3
Leu	7.4	5.6-5.9	11.2	7.1	6.9	7.4	7.2-7.7	8.2
Phe	6.6	4.7-4.9	4.1	4.0	-	5.5	9.5-11.0*	6.5
Lys	6.8	4.9-5.2	7.4	3.9	5.1	6.3	4.6-7.3	6.8
Try	0.9	-	-	0.3	0.8	1.0	1.0-1.3	0.8
His	3.7	2.6-2.7	3.3	3.5	3.4	3.0	3.0-3.8	3.3
Val	5.0	4.4-4.6	4.4	4.6	4.8	4.6		5.3
Met	1.4	0.1-1.0	0.9	1.3	-	1.3	4.1-4.6**	1.3
Thr	5.0	1.8-2.0	3.7	2.5	4.2	3.6	3.7-4.0	3.6
				Non-essentials				
Asp	11.6	7.5-8.0	11.9	7.8	10.9	6.8	12.2-12.7	10.6
Glu	16.2	12.7-13.2	16.3	6.0	15.5	10.5	21.1-21.4	16.7
Ser	5.3	1.9-2.4	5.6	2.6	6.0	5.1	5.0-5.7	4.9
Gly	3.8	2.6-2.8	3.2	4.2	4.1	3.5	3.2-3.4	3.0
Arg	7.5	5.3-5.6	7.3	2.5	6.6	6.8	8.0-8.4	6.8
Ala	3.9	3.0-3.1	3.9	3.7	4.8	4.0	3.7-3.9	3.8
Pro	4.5	2.9-3.4	4.6	2.8	6.7	3.9	4.0-4.2	3.9
Tyr	3.9	1.7-2.7	3.1	3.2	-	3.2	-	3.4
Cys	1.8	-	-	1.8	-	0.1	-	0.2
Ref.	Rangel et al. (2004)	Horax et al. (2004)	Aremu (1990b)	Tang et al. (2021)	Olivera-Castillo et al. (2007)	Schlangen et al. (2022)	Vasconcelos et al. (2010)	Ge et al. (2021)

*phe+tyr; **met+cys

3.4 Functional properties

3.4.1 Zeta potential, protein solubility and surface hydrophobicity

Zeta potential (ζ), also known as electrokinetic potential, is an interfacial property established at the surface of a material when it comes into contact with a liquid medium. The measurements are performed at the interface of the double layer of a colloidal system, where a driving force is generated from the difference between the surface charge of the particle and the charge of the solution (Oliveira et al., 2021).

Cowpea protein exhibits a negative charge density when exposed to a pH above 3.0, with values ranging from -12 to -60 mV (Ge et al., 2021; Rudra et al., 2016). Other procedures, such as the application of ultrasound and heat, have been demonstrated to increase the magnitude of the zeta potential in colloidal systems. For instance, as demonstrated in the study conducted by Loushigam & Shanmugam (2023), ultrasonication resulted in an increase in the zeta potential of the protein from -32.9 mV to -44.2 mV at neutral pH. Additionally, the study conducted by Li et al. (2021), revealed that during the amyloid fibril formation process, there was an increase in zeta potential from 15 mV to 25 mV (pH 2) following an 8-hour heating period at 90 °C. These significant negative potentials impede the capacity of cowpea protein to generate stable suspensions and emulsions due to intermolecular repulsions (Rudra et al., 2016).

The zeta potential can be employed to identify the charge inversion point or isoelectric point (pI) of a protein. The pI is defined as the pH value at which the net charge on the particle surface is equal to zero. The pI of cowpea protein has been reported to lie within a pH range of 3 to 5 (Ge et al., 2021; Rudra et al., 2016). In this pH range, aggregation is more favored and the colloidal system is less stable.

The solubility (Table 1.4) of a protein in an aqueous medium is contingent upon the equilibrium between protein-solvent interactions (hydrophilic interactions) and protein-protein interactions (hydrophobic interactions). The greater the prevalence of protein-water interactions over protein-protein interactions, the greater the solubility.

The protein fractions exhibit a distinctive solubility profile in relation to pH, manifesting as a "U"-shaped curve. At pH values above the isoelectric point, the fractions exhibit a positive charge, while at pH values below the isoelectric point, they exhibit a negative charge. The minimum solubility is found to be closely aligned with the isoelectric point (pH 3.0–5.0), with an increase observed as the pH deviated from this range. This trend is corroborated by the positive correlation between the surface charge, as indicated by the magnitude of the zeta potential, and the protein solubility. The solubility profiles of the extracted fractions agreed with the zeta potential profiles. The solubility was considerably higher at alkaline pH values

(pH 10–12) than in acidic conditions (pH 2–3). This indicates a strong influence of the net surface charge on legume proteins on their solubility.

Although they exhibit a comparable pattern, studies that have examined protein solubility across a broad range of pH values have yielded disparate outcomes. While some studies have demonstrated that protein solubility reached levels close to 100% at extremely acidic or alkaline pHs (Khalid et al., 2012; Rangel et al., 2003), others have revealed that solubility did not even reach 50% (Chel-Guerrero et al., 2011; Moongngarm et al., 2014; Mwasaru et al., 1999b).

Protein solubility is inherently linked to the proportion of hydrophilic and hydrophobic amino acid residues in the protein structure and is significantly influenced by the presence of charged amino acid side chains. As demonstrated by the amino acid profile evaluation (Table 1.3) of cowpea proteins, lysine, aspartic acid, and glutamic acid residues are the most prevalent, representing hydrophilic amino acids. However, the proportion of hydrophobic and hydrophilic amino acids exerts a significant influence on protein solubility. Variation in this proportion of charged amino acids may be related to the composition of native proteins, the concentration process, or differences in amino acid composition between different raw materials. In all cases, amino acids with ionizable residues are responsible for electrostatic attraction or repulsion, which influences their interaction with water and, consequently, their solubilization.

Other research has investigated the impact of various techniques on the solubility of this protein, including concentration, temperature, high pressure, irradiation, and dehydration methods (Abu et al., 2006; Peyrano et al., 2016, 2017; Rudra et al., 2016). While irradiation, heat treatment, high pressure, concentration, and vacuum drying can decrease protein solubility, acylation of cowpea protein concentrate resulted in a significant increase in protein solubility compared to the untreated concentrate. Acylation at the optimal concentration results in an increase in the net negative charge of the protein, which can intensify the interaction between the protein and water, thus increasing its solubility. Conversely, the reduction in solubility observed following heat treatment and elevated concentrations can be attributed to the formation of insoluble aggregates. In contrast to freeze-dried or spray-dried samples, vacuum drying has been observed to reduce the solubility of proteins, primarily due to the formation of a crystalline structure during the drying process, which renders them more challenging to hydrate and solubilize.

Table Error! No text of specified style in document.**.4** Functional properties of cowpea protein extracts (concentrate or isolate)

Reference	Description	WHC or WAC*	OHC or OAC*	LGC (%)*	EA, EAI or EC*	ES or ESI*	FC (%)*	FS (%)*	SH*	S (%)*
Ge et al. (2021)	Protein concentrate dispersion at different pH: (a) 3.0; (b) 5.0; (c) 7.0 and (d) 9.0	WHC ($g\ g^{-1}$): (a) 4.5 (b) 1.7 (c) 3.0 (d) -	OHC ($g\ g^{-1}$): (a) 8.0 (b) 3.0 (c) 8.0 (d) 7.5	(a) 6.0 (c) 10.0 (d) 10.0	EAI ($m^2\ g^{-1}$): (a) 9.0 (b) – (c) 9.5 (d) 10.0	ESI (min): (a) 125.0 (c) 375.0 (e) 2,750	(a) 130 (b) 40 (c) 90 (d) 110	*After 2h:* (a) 90.0 (c) 82.5 (e) 37.5	(a) 2.4 (b) 4.5 (c) 2.7 (d) 2.3	(a) 45.0 (b) 15.0 (c) 82.5 (d) 97.5
Horax et al. (2004)	Protein isolate prepared from 3 cowpea varieties: (a) var 1; (b) var 2 and (c) var 3	-	-	-	-	-	-	-	(a) 548.2 (b) 387.8 (c) 572.9	-
Chel-Guerrero et al. (2011)	Protein concentrate dispersion at different pH: (a) 2.0; (b) 3.0; (c) 4.0; (d) 5.0; (e) 6.0; (f) 7.0; (g) 8.0; (h) 9.0 and (i) 10.0	WHC ($g\ g^{-1}$): 245.0	OHC ($g\ g^{-1}$): 231.0	-	EAI (%): (a, f) 50.0 (b) 45.0 (c, d, e, g, i) 43.0 (h) 40.0	ESI (%): (a, d, e) 15.0 (b, c) 5.0 (e) 45.0 (g) 65.0 (h, i) 90.0	(a) 187.5 (b, c, d) ≈37.5 (e) 43.7 (f) 50.0 (g) 125.0 (h) 150.0 (i) 175.0	*After 2h:* (a) 25.0 (b, e, f) ≈6.2 (c, d) 0.0 (g, h, i) ≈12.5	-	(a, i) ≈40.0 (b, g) ≈10.0 (c, d, f) ≈5 (h) ≈20 (e) ≈0
Mune et al. (2011)	Protein concentrate under various concentrations of acetic ((a) 0; (b) 0.25; (c) 0.50; (d) 0.75 and (e) 1.0) and succinic anhydride ((a) 0; (g) 0.25; (h) 0.50; (i) 0.75 and (j) 1.0) at neutral and isoelectric pH	-	OAC ($mL\ g^{-1}$): (a, b, e) ≈4.0 (c, d) 4.5 (f, g, i) ≈6.0 (h) 7.0	-	EAI (%): (a) 26.0 (b, c) 56.0 (d) 44.0 (e) 21.0 (f) 29.0 (g) 36.0 (h) 52.0 (i) 35.0	ESI (min): (a) 12.8 (b) 13.2 (c) 12.8 (d) 15.3 (e) 23.5 (f) 15.1 (g) 14.0 (h) 13.8 (i) 18.2	(a) 66.0 (b) 62.5 (c) 88.0 (d) 74.0 (e) 77.1 (f) 116.4 (g) 98.2 (h) 71.2 (i) 109.7	*After 1h:* (a) 26.0 (b) 8.3 (c) 5.0 (d) 2.1 (e) 1.0 (f, g, h, i) 0.0	-	(a) pH7: 38.0 pH3: 3.5 *pH7:* (b) 89.5 (c) 80.9 (d) 79.7 (e) 81.8 (f) 84.4 (g) 78.5 (h) 80.5 (i) 71.7 *pH 3.5:* (b) 7.2 (c, d) 7.3 (e) 7.4 (f) 5.3 (g) 5.0 (h, i) 4.8

Table 1.4 continued

Reference	Description	WHC or WAC*	OHC or OAC*	LGC (%)*	EA/EAI/EC*	ES/ESI*	FC (%)*	FS (%)*	SH*	S (%)*
Mune et al. (2016)	Protein concentrates from various cultivars (c1, c2, c3 and c4) subjected to different drying methods: cabinet (a), vacuum (b), and freeze (c) drying.	-	-	-	EAI (%): *c1:* (a) 55.7 (b) 53.1 (c) 55.8 *c2:* (a) 55.9 (b) 52.7 (c) 57.1 *c3:* (a) 61.5 (b) 46.0 (c) 56.0 *c4:* (a) 58.3 (b) 46.7 (c) 55.2	ESI (%): *c1:* (a) 84.4 (b) 83.3 (c) 98.4 *c2:* (a) 95.2 (b) 101.7 (c) 101.5 *c3:* (a) 61.2 (b) 15.4 (c) 100.0 *c4:* (a) 89.7 (b) 7.5 (c) 98.4	*c1:* (a) 265 (b) 193.8 (c) 213.9 *c2:* (a) 303.1 (b) 216.4 (c) 264.2 *c3:* (a) 174.4 (b) 125.3 (c) 271.1 *c4:* (a) 116.7 (b) 108.7 (c) 175.5	*After 1h:* *c1:* (a) 145.4 (b) 124.7 (c) 156.9 *c2:* (a) 109.2 (b) 132.9 (c) 205.7 *c3:* (a) 107.6 (b) 108.0 (c) 215.6 *c4:* (a) 93.3 (b) 100.0 (c) 124.5	*c1:* (a) 50.5 (b) 35.3 (c) 38.3 *c2:* (a) 37.4 (b) 21.6 (c) 22.1 *c3:* (a) 28.2 (b) 28.1 (c) 30.4 *c4:* (a) 28.6 (b) 29.6 (c) 31.1	-
Mune et al. (2016)	Protein concentrate (a) and hydrolysate (b)	-	OAC (g g^{-1}): (a) 2.1 (b) 4.3	-	EAI (%): (a) 20.0 (b) 30.0	ESI (min): (a) 15.8 (b) 14.6	(a) 66.4 (b) 90.8	(a) 60.5 (b) 38.9	-	-
Peyrano et al. (2017)	Protein concentrate dispersions at different concentrations: (a) 7.5; (b) 10.5 and (c) 15%	-	-	-	-	-	-	-	-	*pH8:* (a) 74.2 (b) 70.3 (c) 63.9 *pH10:* (a) 74.0 (b) 68.8 (c) 59.2
Schlangen et al. (2022)	Protein concentrate separated by air classification	WHC (g g^{-1}): 2.2	-	10	-	-	-	-	-	-
Tang et al. (2021)	Protein isolated	WAC (g g^{-1}): 2.8	OAC (g g^{-1}): 1.4	13	EC (%): 69.0	ES (%): 61.0	≈100	*After 1h30 min:* >10.0	-	pH3: >40.0 pHs 4-5: 20.0 pHs 7-11: 50.0

Table 1.4 continued

Reference	Description	WHC/WAC*	OHC/OAC*	LGC (%)*	EA/EAI/EC*	ES/ESI*	FC (%)*	FS (%)*	SH*	S (%)*
Peyrano et al. (2016)	Protein concentrate extracted at pH8 or 10, not treated (a) and under thermal treatment (TT) at 70 °C ((b) 5; (c) 10; (d) 30 min) and 90 °C ((e) 5; (f) 10; (g) 30 min) and high hydrostatic pressure (HHP) treatments (200 (h), 400 (i) and 600 (j) MPa)	WHC (g g^{-1}): *pH8:* (a) 1.0 (b) 1.1 (c) 1.1 (d) 1.4 (e) 1.2 (f) 1.2 (g) 1.1 (h) 1.4 (i) 1.1 (j) 0.9 *pH10:* (a) 0.9 (b) 1.3 (c) 1.4 (d) 1.5 (e) 1.1 (f) 1.1 (g) 1.5 (h) 1.2 (i) 1.5 (j) 1.7	-	*pH 8:* non-treated: 12.0 *TT:* (a) 12 (c, d) 10 (e, f, g) 14 *HHP:* (h, i) 10 (j) 12 *pH 10:* non-treated: 12.0 *TT:* (b, c, d) 12 (e, f, g) 14 *HHP:* (h, i) 10 (j) 12	-	-	-	-	*pH8:* (a) 1356 (b) 1843 (c) 1807 (d) 1548 (e) 2263 (f) 2450 (g) 2160 (h) 3401 (i) 3439 (j) 3450 *pH10:* (a) 2708 (b) 6140 (c) 6745 (d) 6764 (e) 4250 (f) 4380 (g) 4715 (h) 3172 (i) 3472 (j) 3297	*pH8:* (a) 91.5 (b) 89.9 (c) 77.1 (d) 72.2 (e) 89.9 (f) 89.6 (g) 84.7 (h) 84.9 (i) 86.9 (j) 90.6 *pH10:* (a) 93.6 (b) 90.6 (c) 88.2 (d) 91.4 (e) 93.3 (f) 93.8 (g) 96.5 (h) 87.5 (i) 86.4 (j) 92.1
Rangel et al. (2003)	Cowpea purified *Vicilins* (a) and protein concentrated (b)	-	-	-	EAI (m^2 g^{-1}): (a) 490 (b) 291	-	-	FSI (min): (a) 260 (b) 380		(a) pHs 2,3,7,11: ≈100.0 pH4: ≈ 80.0 pH5:10.0 pH6: >90.0 (b) pHs 4-6: ≤ 50.0 pHs 2,3,8 - 11: ≈100.0 pH5: 20.0; pH7: >80.0

Table 1.4 continued

Reference	Description	WHC/WAC*	OHC/OAC*	LGC (%)*	EA/EAI/EC*	ES/ESI*	FC (%)*	FS (%)*	SH*	S (%)*
Abu et al. (2006)	Proteins isolated from cowpea flours and pastes irradiated at 0 (a); 2 (b), 10 (c) and 50 (d) kGy	-	OAC (g g^{-1}): *Flours:* (a) 1.3 (b) 1.4 (c) 1.5 (d) 1.6 *Pastes:* (a) 1.2 (b) 1.3 (c) 1.4 (d) 1.5	-	EC (mL g^{-1}): *Flours:* (a) 590 (b) 638 (c) 702 (d) 787 *Pastes:* (a) 630 (b) 645 (c) 660 (d) 698	-	*Flours:* (a) 811 (b) 809 (c) 807 (d) 807 *Pastes:* (a) 807 (b) 807 (c) 807 (d) 803	-	-	*Flours:* (a) 88.9 (b) 86.2 (c) 85.6 (d) 83.5 *Pastes:* (a) 89.0 (b) 88.6 (c) 88.2 (d) 87.5
Rudra et al. (2015)	Protein isolate under different dehydration technique (a) freeze dried, (b) spray dried and (c) vacuum dried	WHC (g g^{-1}): (a) 5.1 (b) 4.6 (c) 3.2	OAC (g g^{-1}): (a) 6.3 (b) 2.5 (c) 3.2	(a) 8.0 (b) 8.0 (c) 12.0	EC (mL): (a) 7 (b) 6 (c) 5 EAI (m^2 g^{-1}): (a) 39.5 (b) 101.8 (c) 40.1	ESI (min): (a) 219366.0 (b) 3957.6 (c) 5895.0	-	-	-	(a) 58.2 (b) 58.1 (c) 50.6
Khalid et al. (2012)	Protein isolated by isoelectric (a) and micellization (b) precipitation	WAC (mL g^{-1}): (a) 2.1 (b) 2.3	OAC (mL g^{-1}) (a) 1.0 (b) 1.9	(a, b) 12.0	EC (g g^{-1}): (a) 107.4 - 160.6 (b) 106.8 - 137.7	-	-	-	-	(a) pHs 2,7-9: >90.0 pH3: 80.0 pH4: 70.0 pH5: <10.0 pH6: 60 (b) pHs 2,7- 9: >90.0 pHs 3,6: 65.0 pHs 4-5: 30.0
Lafarga et al. (2020)	Protein isolated dispersions under different pH (a) 2.0; (b) 4.0; (c) 6.0; (d) 8.0; (e) 10.0	WHC (g g^{-1}): 6.1 *(without pH correction)*	OHC (g g^{-1}): 5.8 *(without pH correction)*	-	EC (%): (a) >80.0 (b) 5.0 (c) 10.0 (d) 80.0 (e) >80.0	ES (%): (a) >90.0 (b, c) ≈40.0 (d) >70.0 (e) >90.0	(a, e) 30.0 (b, d) 20.0 (c) <10.0	-	-	-

Table 1.4 continued

Reference	Description	WHC or WAC*	OHC or OAC*	LGC (%)*	EA/EAI/EC*	ES/ESI*	FC (%)*	FS (%)*	SH*	S (%)*
Ragab et al. (2004)	Protein isolated dispersions under different pHs (a) or NaCl concentration (b)	WHC (mL g^{-1}): 2.2 *(without pH correction)*	OHC (mL g^{-1}): 1.1 *(without pH correction)*	In NaCl solution at different concentrations: 0.0 (M): - 0.5 (M): 4.0 1.0 (M): 6.0	EAI (%): 50.0 *(without pH correction)* EC (mL g^{-1}): (a) pHs 1,7: >50.0 pHs 2-3: 75.0 pHs 4-6: ≈50.0 pHs 8-9: ≈100.0 pHs 10-11: 150.0	ES (%): *After 2h:* pH2: 85.0 pH5: 65.0 pH7: 60.0 pH10: 100.0	(a) pHs 1,7: 60.0 pHs 2-3,8-9,11: ≈ 80.0 pH5: 0 pHs 4,6: <20.0 pH10: 90.0 (b) 0.4-1.6 (M): ≈50% 2.0-3.2 (M): ≈60.0 3.6-4.0 (M): ≈70.0	*After 2h:* pHs 2,5: 65.0 pH7: 75.0; pH10: 70.0	-	pH1: ≈40.0 pHs 2,8: >60.0 pHs 3,9: ≈80.0 pHs 4,5,6: <20.0 pH7: 30.0 pHs 10,11: >90.0
Mwasaru et al. (1999)	Protein isolated as a function of pH extraction (a) 8.5; (b) 9.5; (c) 10.5; (d) 11.5; (e) 12.5	WAC (mL g^{-1}): (a) 1.2 (b) 0.8 (c) 1.3 (d) 1.7 (e) 1.7 (f) 1.7	OAC (mL g^{-1}): (a) 2.0 (b) 1.7 (c) 1.3 (d) 1.7 (e) 1.7 (f) 1.7	(a, b) 6.0 (c, d, e) 10.0	EA (%): (a) ≈50.0 (b, c, d) ≈40.0 (e) 15.0	ES (%): (a) 55.0 (b) 50.0 (c) 45.0 (d) 15.0 (e) <10.0	-	-	-	*pH2:* (a) 65.0 (b) 50.0 (c) 45.0 (d) 30.0 (e) 15.0 *pH4-8:* (a, b, c, d, e) <10 *pH10:* (a) 40.0 (b) 30.0 (c) 15.0 (d, e) >10.0 *pH12:* (a) 60.0 (b) 40.0 (c) 30.0 (d) 20.0 (e) 15.0

Table 1.4 continued

Reference	Description	WHCor WAC*	OHC or OAC*	LGC (%)*	EA/EAI/EC*	ES/ESI*	FC (%)*	FS (%)*	SH*	S (%)*
Moongngarm et al. (2014)	Protein concetrate prepared by (a) isoelectric point precipitation; (b) Ammonium sulfate precipitation and (c) Ammonium sulfate + isoelectric point precipitation	WHC (g g^{-1}): (a) 1.4 (b) 0.8 (c) 1.1	OHC (g g^{-1}): (a) 5.3 (b) 2.6 (c) 3.1	(a, b, c) 14.0	EA (%): (a) 80.2 (b) 67.4 (c) 73.4	ES (%): (a) 66.9 (b) 57.4 (c) 65.0	(a) 87.7 (b) 69.9 (c) 80.9	(a) 74.0 (b) 59.1 (c) 67.4	-	pH2.5: (a) 20.0 (b) <30.0 (c) >30.0 pHs 3,6: (a, b, c) ≈15.0 pHs 4-5: ≈0.0 pHs 7-12: ≈50.0
Gunathilake et al. (2016)	Protein isolated	WHC (%): 138.1	OHC (%): 78.6	14.0	-	-	-	-	-	pH2: 57. pH4: 4.0 pH6: 8.0 pH8: 28.0 pH10: 65.0 pH12: 82.0

*WHC or WAC: water holding capacity or water absorption capacity; OHC or OAC: oil holding capacity or oil absorption capacity; LGC: least gelation concentration; EA/EAI/EC: emulsifying activity/emulsifying activity index/emulsifying capacity; ES or ESI: emulsion stability or emulsifying stability index; FC: foaming capacity; FS: foaming stability; SH: surface hydrophobicity; S: solubility.

The surface hydrophobicity of proteins can vary considerably depending on the cultivar, the application of different treatments, or the drying techniques employed (Horax et al., 2004; Mune & Sogi, 2016; Peyrano et al., 2017). Upon correlating solubility data with surface hydrophobicity, an inverse relationship between these two properties was evidenced. The study conducted by Ge et al. (2021) revealed a correlation between high protein solubility and lower surface hydrophobicity and high surface charge (zeta potential). The highest H_0 values were observed at pH 3.0, 7.0, and 9.0, while the lowest values were recorded at pH 5.0. The higher surface hydrophobicity of proteins can be attributed to the increased exposure of aromatic and aliphatic amino acid residues. On the other hand, the lower hydrophobicity values result from the tendency of proteins to aggregate when the pH approaches their isoelectric point. This phenomenon causes hydrophobic residues to be hidden within the aggregations, making them less accessible.

However, variations in surface hydrophobicity between different proteins can be attributed to natural differences in protein composition. For instance, the ratio of 11S to 7S proteins or the ratio of globulin to albumin proteins can have a significant impact on hydrophobicity. It can be observed that 11S proteins tend to exhibit greater hydrophobicity than 7S proteins, while globulins generally demonstrate higher hydrophobicity than albumins. These differences in protein composition can directly affect the interaction properties of proteins with other substances and their behavior in aqueous environments. Moreover, the hydrophilic nature of proteins, as evidenced by their lower surface hydrophobicity, indicates that a greater number of amino acids with nonpolar or hydrophobic side chains are present within the protein structure. This configuration facilitates the formation of more polarized interactions, which enhance the affinity between the protein and water. Consequently, greater solubility is achieved. Furthermore, the application of heat and pH variation during the protein extraction or pre-treatment process can induce significant changes, such as the differential occurrence of aggregation and/or dissociation, which modify the hydrophobicity profile.

The hydrophobic fraction of proteins demonstrates an inherent propensity to interact preferentially with nonpolar substances, such as oils, conferring them a competitive advantage in specific applications, such as in the formulation of emulsions. Conversely, in scenarios that demand a more efficient dispersion of proteins in an aqueous medium, those with a higher proportion of hydrophilic residues (and, consequently, lower hydrophobicity) emerge as a highly desirable characteristic. This attribute confers greater adaptability in their use in a variety of products.

3.4.2 Water and oil holding capacity and gelling properties

The mouthfeel, texture, and flavor retention of products are correlated with the water-holding capacity (WHC) and oil-holding capacity (OHC) of proteins. While a protein with high OHC is helpful for enhancing the mouthfeel and flavor retention of some food products, a protein with high WHC is advantageous for minimizing moisture loss in packaged bakery goods and preserving the freshness and moist feel of baked foods (Ge et al., 2021).

Protein precipitation and dehydration methods exert a significant influence on the WHC and OHC of cowpea proteins. In particular, freeze-drying has been shown to maintain better water and oil retention capacities compared to spray and vacuum drying methods (Rudra et al., 2016). Regarding the diverse extraction techniques (Khalid et al., 2012; Moongngarm et al., 2014), it was found that the WHC and OHC of cowpea protein obtained through isoelectric precipitation exhibited the highest retention capacity, followed by that obtained by combining extraction with ammonium sulfate and isoelectric point precipitation, while the lowest capacity was observed in the extraction using only ammonium sulfate.

Furthermore, the study by Ge et al. (2021) demonstrated the influence of pH on WHC and OHC, revealing their sensitivity to different conditions. The study compared cowpea protein isolate (CPI) with soybean protein isolate (SPI) and pea protein isolate (PPI) at different pHs. It was observed that, at pH 9, the isolates were soluble in water, demonstrating no water retention, while at pH 5, the lowest WHC and OHC were recorded. The effect of pH on OHC was more pronounced than on WHC, possibly due to the conformational change of the proteins, which exposed more hydrophobic and nonpolar groups, favoring the interaction with oil molecules. The CPI demonstrated comparable or superior performance to the SPI and the PPI at specific pH levels. This suggests that CPI may be an effective protein alternative to SPI (Ge et al., 2021).

One essential functional characteristic that greatly affects the taste and textural qualities of different food applications is the heat-induced gelation of proteins. Denaturation, aggregation, and network development are the general processes involved in the gel formation process of globular proteins (Bessada et al., 2019; Zayas, 1997). The ability of dietary proteins to gel is commonly assessed using the minimum gelation concentration (LGC). A protein with better gelation ability is indicated by a low LGC value (Ge et al., 2021).

A study by Schlangen et al. (2022) revealed that cowpea protein, separated by dry fractionation, presented a LGC of 10%. In contrast, for cowpea protein obtained by isoelectric precipitation, as observed by Gunathilake et al. (2016) and Tang et al. (2021), these values were higher, around 13-14%. The majority of studies presented in Table 1.4, which evaluated various

treatments and experimental conditions (extraction methods, extraction pHs, heat treatment, high-pressure treatment, drying methods, and pH modulation), demonstrated a larger concentration range of 6-14% (Ge et al., 2021; Moongngarm et al., 2014; Peyrano et al., 2016; Ragab et al., 2004; Rudra et al., 2016).

3.4.3 Emulsifying properties

The emulsifying properties of proteins are important for their use as food ingredients. Their effectiveness can be enhanced or reduced by various factors, including pH, ionic strength, extraction methods, and pre-treatments. Table 1.4 presents a comprehensive overview of studies that have evaluated the emulsifying properties of cowpea protein under different experimental conditions.

A study investigated the emulsifying properties of cowpea protein isolate at different pH values and the results demonstrated a strong dependence on pH for both emulsification capacity (EAI) and emulsion stability (ESI) (Ge et al., 2021). EAI values were significantly higher at pH 7.0 and 9.0 compared to pH 3.0. This increase can be attributed to the greater solubility and surface charge of the protein isolate at neutral and basic pHs, in comparison to acidic conditions. Similarly, the ESI proved to be pH-dependent, exhibiting a continuous increase as the pH rose from 3.0 to 9.0.

In a separate study, the impact of pH and NaCl concentration on the emulsification capacity of CPI was examined (Ragab et al., 2004). The emulsifying capacity of CPI was found to be minimal at pHs 4 and 5, with an increase observed outside this range, particularly at alkaline pH. This result is consistent with the findings of Ge et al. (2021). The addition of NaCl up to 0.5 M was found to improve emulsification, as it increased the solubility of the proteins, even at isoelectric pH. The emulsion stability was found to be minimal at neutral pH, with a significant decrease observed over time. In contrast, acidic and alkaline pH resulted in greater stability.

The effect of the dehydration technique for the preparation of cowpea protein isolate powder on emulsifying properties was investigated by different researchers. A comparison of the results of the studies revealed that both Rudra et al. (2016) and Mune & Sogi (2016) identified that the drying technique significantly influenced the emulsifying properties of cowpea protein. Both studies concur that freeze-drying (FD) results in higher emulsification capacity (EC/EA) and emulsion stability (ES) compared to the other drying techniques studied by the authors. Rudra et al. (2016) attributed this superiority of FD to its greater oil absorption capacity, while Mune & Sogi (2016) noted that FD promotes greater molecular flexibility of

proteins, facilitating their accommodation at the oil-water interface. Moreover, Mune & Sogi (2016) observed that there is a significant variation in the levels of EA and ES between cultivars, which is attributed to the inherent genetic differences between them.

The dependence of pH on the emulsifying properties of proteins was anticipated, given that these properties are significantly influenced by the hydrophilic-lipophilic balance, which is directly affected by pH. In addition to pH, several other parameters can impact the emulsifying properties of proteins, including protein composition, protein solubility, surface charge, and hydrophobicity. These factors determine the ability of proteins to adsorb at the oil-water interface and stabilize emulsions, thereby influencing their effectiveness in forming and maintaining emulsions.

3.4.4 Foam properties

Foaming-related properties are commonly categorized into two distinct measures: foaming capacity (FC) and foaming stability (FS). The FC is primarily influenced by the diffusion coefficients of soluble proteins towards the air-water interface, possible conformational changes, and the rearrangement of the interface. On the contrary, foam stabilization is primarily contingent upon the generation of a robust, adhesive viscoelastic film encasing each gas bubble (Bessada et al., 2019).

The study by Moongngarm et al. (2014) investigated the impact of various protein extraction methods on the FC and FS of cowpea proteins. The study revealed that isoelectric precipitation extraction (IPC-pI) yielded the highest FC and FS among the extraction methods tested. Subsequently, the ammonium sulfate extraction (CPC-AM) also showed good FC and FS to that of CPC-pI, although at a lower level. In contrast, combining the isoelectric precipitation method and ammonium sulfate (CPC-AM-pI) resulted in a lower FC and FS than CPC-pI, but higher than that found for CPC-AM. This study demonstrates that the foaming properties of proteins can be significantly influenced during the early stages of protein production, specifically during extraction.

A further aspect investigated was the influence of drying techniques on the final powdered product, with particular reference to the effects on FC and FS (Mune & Sogi, 2016). The foaming capacity of cowpea concentrate prepared by convection drying and freeze-drying was found to be superior to that of the samples obtained by vacuum drying. The researchers observed a positive correlation between the solubility of proteins prepared by freeze-drying and the FC. However, an increase in the content of disordered structure was found to decrease the FC, potentially due to a reduction in the flexibility of the proteins at the air-water interface.

Moreover, genetic variations among the different cowpea cultivars studied also influenced the foaming properties. In general, the results of the freeze-drying process followed the trend observed in the freeze-concentration process. This process was found to be the most effective in producing concentrates with high foam stability, compared to the convection and vacuum drying methods.

Physical and/or chemical pretreatments are also capable of altering the foaming properties of proteins. Succinylation and acetylation of CPCs were found to significantly enhance their foaming capacity (Mune et al., 2011). This increase was attributed to the enhanced solubility and molecular flexibility, which facilitate a more efficient migration of the protein to the air-water interface. Nevertheless, it was observed that the foam stability (FS) was higher in the untreated concentrates, suggesting that the charge density resulting from acetylation may compromise the long-term foam stability. In parallel, a physical treatment involving gamma irradiation can also modify the FC and FS of cowpea proteins (Abu et al., 2006). Irradiation at 2 kGy was found to reduce the FC in proteins extracted from cowpea flours. However, higher doses, such as 50 kGy, had a similar impact on proteins extracted from pastes. Protein denaturation and cross-linking were identified as the primary mechanisms underlying these changes. Nevertheless, irradiation up to 50 kGy did not entirely compromise the foaming properties, indicating that the material may be viable for decontamination processes without significant loss of foaming functionality.

An interesting correlation can be observed regarding the impact of pH on the foaming capacity of cowpea proteins. Ge et al. (2021) demonstrated that the lowest foam formation occurs at pH 5.0 due to the minimum protein solubility, while pH 3.0 favors better foam stability thanks to the greater surface hydrophobicity that promotes stable intermolecular interactions. In a complementary manner, Ragab et al. (2004) found that cowpea proteins do not form foam at pH 5.0, but the foaming capacity increases significantly at alkaline pH, especially at pH 10, due to the increase in charges on the protein, which weakens hydrophobic interactions and increases protein flexibility. Furthermore, the authors observed that the addition of NaCl up to 4.0 M improves the CF by increasing protein solubility.

These findings underscore the complexity and importance of carefully and appropriately selecting the extraction method, pretreatments, pH, and salinity modulation to maintain and improve the foaming properties of cowpea proteins.

3.5 Food industry uses of cowpea proteins – Applications in the food systems

Cowpea has become a legume of significant economic, social, and environmental importance. Its versatility is exemplified by its multipurpose nature, which enables it to serve both human and animal nutrition. Moreover, the utilization of cowpeas as a functional food can motivate the industry and farmers to invest in the production of this legume, thereby expanding its applications in the food industry.

The fractionation of cowpea flour into protein-rich fractions enhances its value and expands the potential applications of this commodity as an ingredient in food products. The functional properties and nutritional characteristics of cowpea protein, which have been extensively discussed throughout this review, may confer upon it increasing industrial relevance, enabling its use as a potential ingredient in various food formulations.

To date, different applications of cowpea protein in food systems have been studied (Table 1.5). These applications include the encapsulation of bioactive ingredients (Pereira et al., 2009), the emulsification of oils (Thompson et al., 2023), the manufacturing of extruded products (Dilrukshi et al., 2022), the production of meat analogs (Penchalaraju et al., 2024), the development of cereal-based products (Campbell et al., 2016; Franco-Miranda et al., 2017; Shevkani et al., 2015) and the elaboration of edible films (Hewage et al., 2009; Almeida et al., 2021).

The study developed by Pereira et al. (2009) demonstrated the potential of CPI in the microencapsulation of ascorbic acid by spray drying. The combination of maltodextrin (M) with CPI resulted in a significant improvement in the process yield, increasing from 66% to 86%. Moreover, the yield of ascorbic acid particles reached 79%, with a retention of 66% during the drying process. Scanning electron microscopy revealed that the particles exhibited a spherical and wrinkled morphology, with an average size of 8 μm. In light of the satisfactory yield and core retention rates, the authors concluded that CPI could be employed in industrial microencapsulation processes of ascorbic acid and other biomaterials using spray drying.

The enrichment of foods with vegetable proteins represents a strategy for enhancing their nutritional value and properties. In this context, the CPI has been investigated as a means of optimizing the physicochemical characteristics of foods such as breads and cakes. The impact of the addition of CPI to bakery products has been assessed in several studies (Campbell et al., 2016; Franco-Miranda et al., 2017; Shevkani et al., 2015). The objective of these studies has been to evaluate the effects of CPI on the physicochemical properties, texture profile, and sensory acceptance by consumers. Despite modifying the characteristics of the final products,

the incorporation of CPI yielded satisfactory results, with the enriched breads and cakes being well-accepted by sensory evaluation.

Table Error! No text of specified style in document.**.5** Applications of cowpea protein in different food systems

References	Application	Description
Pereira et al. (2009)	Microencapsulation of ascorbic acid	Evaluation of the use of CPI in the microencapsulation of ascorbic acid, by spray drying.
Thompson et al. (2023)	Emulsion	Effect of thermal treatments and partial hydrolysis on the emulsifying properties of CPI extracted at pH 8 and 10.
Dilrukshi et al. (2022)	Extruded snacks	Effect of extrusion process on developing novel gluten-free snacks from rice flour, cowpea and whey protein concentrate enriched with bioactive and antioxidant properties.
Franco-Miranda et al. (2017)	Mexican sweet bread	Effects of protein hydrolysates with bioactive properties in dough for a typical Mexican sweet bread on dough rheological properties, bread product physicochemical and bioactive properties, and consumer acceptance.
Campbell et al. (2016)	Bread and sponge cake	Effect of fortification of flour with CPI on the texture and sensory properties of yeast bread and sponge cake.
Shevkani et al. (2015)	Muffins	Investigate the effect of incorporation of varying levels of CPI on the pasting and muffin-making properties.
Penchalaraju et al. (2023)	Meat analogues	Replace the meat protein with pulse-based proteins and determine the suitability of the processing method for the commercialization of plant protein meat analogues.
Almeida et al. (2021)	Edible films	Effects of incorporation of CPI and cassava starch nanoparticles obtained by ultrasound on the properties of cassava starch:glycerol films.
Hewage et al. (2009)	Edible films	Effect of the concentration of the plasticizer and the pH of the medium on the mechanical and barrier properties of the cowpea protein films.

Extruded snacks with a partial addition of CPI were developed and the effects of the extrusion process on their characteristics were evaluated in comparison to a control group of snacks made only with rice flour (Dilrukshi et al., 2022). The extrusion process facilitated the

digestion of proteins and starch, increasing their bioavailability and resulting in a more complete and balanced amino acid profile in the snacks. The in vitro digestion demonstrated that the supplementation of CPI+WPC (whey protein concentrate) to rice flour reduces the glycemic response of extruded snacks, which is an important characteristic for controlling blood sugar and preventing chronic diseases such as diabetes. Considering the aforementioned results, the development of this novel ready-to-eat, gluten-free product, rich in fiber and protein, is perceived as a viable option for a healthy functional snack. Furthermore, it represents an opportunity to increase the consumption of legumes and healthy foods for people with gluten sensitivity.

Another noteworthy area of research is the development of meat analogs using CPI, which has also made advancements. In a study conducted by Penchalaraju et al. (2024), the feasibility of replacing animal protein with legume proteins, including CPI, for producing meat analogs, was evaluated. The analyzed meatballs exhibited textural properties, color, and sensory characteristics that were found to correlate positively with those of beef. The findings demonstrated that legume proteins can effectively replicate the texture, color, and organoleptic characteristics of meat, thereby establishing the feasibility of producing a range of meat analogs. These findings expand the scope of future research in this area and present promising prospects for the commercialization of meat substitutes.

Lastly, CPC has been investigated as a film-forming material for the development of edible films, particularly in light of the excessive use of synthetic plastics (Hewage et al., 2009; Almeida et al., 2021). The applications of edible films and coatings derived from food biopolymers have witnessed considerable advancement in recent years (Kumar et al., 2022). Nevertheless, cowpea protein has remained a relatively understudied area. The investigation of polysaccharides and proteins as a basis for biodegradable films is a well-established field of research, largely due to the biodegradable and renewable nature of these materials, their availability in large quantities, and also because of their sensory characteristics, and low toxicity (Kumar et al., 2022; Han, 2014). Edible films have a variety of applications, including use as standalone packaging, as a coating for food items, as active ingredient carriers, and even as a means of segregating the various ingredients of a heterogeneous foodstuff into distinct compartments (Han, 2014).

Hewage & Vithanarachchi (2009) examined films based on cowpea protein with varying pH levels (8-11) and different plasticizers (polyethylene glycol, glycerol). Based on the results of the study, the researchers identified the optimal conditions for the preparation of cowpea protein films. It is recommended that a combination of 2% glycerol and 2.5%

polyethylene glycol be used as plasticizers, while the pH of the film-forming solution should be maintained at 10. The resulting films exhibited enhancements in tensile strength, water vapor permeability, and transparency, thereby demonstrating their potential for utilization as edible food packaging materials. The second study examined the impact of cowpea protein incorporation into cassava starch films (Almeida et al., 2021). The protein demonstrated a notable influence on the mechanical properties of the films, resulting in enhanced tensile strength and modulus of elasticity while reducing elongation at break. Furthermore, an increase in protein isolate concentration in the films led to a gradual decline in water vapor permeability.

In the context of the growing global demand for nutritious foods and the search for sustainable alternatives, cowpea represents a promising and strategic option for food security. Despite the excellent nutritional and functional properties of cowpea protein, which have been extensively discussed throughout this review, it remains underutilized in the food industry. The extensive availability of this legume, coupled with the existing production technology, underscores the yet unexplored potential of fractionating cowpea into protein-rich fractions.

4 Conclusions and future perspectives

Cowpea, with its appealing nutritional profile, appears as a sustainable and promising alternative for the food industry, particularly in view of the growing demand for protein sources with reduced environmental impact.

Although still underutilized, CP has the potential to become a valuable ingredient in a variety of food products due to its techno-functional and nutritional properties. The final properties of the protein are significantly influenced by the extraction, drying and modification methods employed, including variables such as pH, ionic strength and temperature. These modifications in the characteristics of cowpea protein offer a wide range of opportunities for its application in various food products.

CP is distinguished by its gelling properties, rendering it an optimal choice for incorporation into gel products, meat products, and meat analogues. Moreover, CP is particularly suited to use in ice cream, cakes, meringues, and emulsified products due to its high foaming and emulsifying capacity. CPI's high water and oil retention capacity makes it ideal for products such as breads, cakes, muffins and sausages, where hydration and fat content are critical parameters. Its low viscosity represents a significant advantage in several operations in the context of engineering, as well as in the areas of food science and technology. In addition to the operational benefits, this distinctive quality offers considerable advantages in the efficient incorporation of this protein into beverages, edible/biodegradable films with the potential to

replace conventional plastics, as well as coatings that require even distribution over foods and surfaces. Consumer preferences are evolving in a manner that favors the expansion of sustainable plant-based proteins, thereby creating opportunities for cowpea consumption to extend beyond its traditional geographic boundaries.

The review emphasizes the necessity for an in-depth comprehension of the physicochemical and techno-functional properties of CP to optimize its utilization in the food industry and develop more nutritious and sustainable products. Conventional CP extraction techniques have the potential for improvements and optimizations, with particular emphasis on the use of natural deep eutectic solvents (NADES), which are emerging as a sustainable alternative for protein extraction, offering advantages such as low cost, biodegradability, and non-toxicity. Furthermore, it is indispensable to pursue further research on the structure, bioactivity, and digestibility of CP, thereby supplementing the topics covered in this review. It is anticipated that this review will serve as a foundation for future research endeavors aimed at expanding the knowledge base on cowpea protein and its potential applications.

References

Abu, J. O., Muller, K., Duodu, K. G., & Minnaar, A. (2005). Functional properties of cowpea (*Vigna unguiculata* L. Walp) flours and pastes as affected by γ-irradiation. *Food Chemistry*, *93*(1), 103–111. https://doi.org/10.1016/j.foodchem.2004.09.010

Abu, J. O., Müller, K., Duodu, K. G., & Minnaar, A. (2006). Gamma irradiation of cowpea (*Vigna unguiculata* L. Walp) flours and pastes: Effects on functional, thermal and molecular properties of isolated proteins. *Food Chemistry*, *95*(1), 138–147. https://doi.org/10.1016/j.foodchem.2004.12.040

Almeida, F. C., de Souza, C. O., Philadelpho, B. O., França Lemos, P. V., Cardoso, L. G., Santana, J. S., Alves da Silva, J. B., Cruz Correia, P. R., Camilloto, G. P., de Souza Ferreira, E., & Druzian, J. I. (2021). Combined effect of cassava starch nanoparticles and protein isolate in properties of starch-based nanocomposite films. *Journal of Applied Polymer Science*, *138*(18). https://doi.org/10.1002/app.50008

Amin, A., Petersen, I. L., Malmberg, C., & Orlien, V. (2022). Perspective on the Effect of Protein Extraction Method on the Antinutritional Factor (ANF) Content in Seeds. In *ACS Food Science and Technology* (Vol. 2, Issue 4, pp. 604–612). American Chemical Society. https://doi.org/10.1021/acsfoodscitech.1c00464

Aremu, C. Y. (1990). Proximate and Amino Acid Composition of Cowpea (*Vigna unguiculata*, Walp) Protein Concentrate Prepared by Isoelectric Point Precipitation. *Food Chemistry*, *37*(1), 61-68.

Bai, Z., Huang, X., Meng, J., Kan, L., & Nie, S. (2020). A comparative study on nutritive peculiarities of 24 Chinese cowpea cultivars. *Food and Chemical Toxicology*, *146*, 111841. https://doi.org/10.1016/j.fct.2020.111841

Bessada, S. M. F., Barreira, J. C. M., & Oliveira, M. B. P. P. (2019). Pulses and food security: Dietary protein, digestibility, bioactive and functional properties. *Trends in Food Science and Technology*, *93*, 53–68. https://doi.org/10.1016/j.tifs.2019.08.022

Campbell, L., Euston, S. R., & Ahmed, M. A. (2016). Effect of addition of thermally modified cowpea protein on sensory acceptability and textural properties of wheat bread and sponge cake. *Food Chemistry*, *194*, 1230–1237. https://doi.org/10.1016/J.FOODCHEM.2015.09.002

Chel-Guerrero, L., Maldonado-Hoil, M., Burgos-Pérez, A., Castellanos-Ruelas, A., & Betancur-Ancona, D. (2011). Functional and some nutritional properties of an isoelectric protein isolate from Mexican cowpea (*Vigna unguiculata*) seeds. *Journal of Food & Nutrition Research*, *50*(4).

Coffigniez, F., Briffaz, A., Mestres, C., Akissoé, L., Bohuon, P., & El Maâtaoui, M. (2019). Impact of soaking process on the microstructure of cowpea seeds in relation to solid losses and water absorption. *Food Research International*, *119*, 268–275. https://doi.org/10.1016/j.foodres.2019.02.010

Conab – Companhia Nacional de Abastecimento. Feijão. (2021). Acompanhamento da Safra Brasileira [de] Grãos: Safra 2020/2021: Quarto Levantamento, v. 8, n. 4, p. 41-52. Available at: https://www.conab.gov.br/info-agro/safras/graos/boletim-da-safra-de-graos?start=20. Accessed on: June 20, 2024.

De Boer, J., Schösler, H., & Aiking, H. (2014). "Meatless days" or "less but better"? Exploring strategies to adapt Western meat consumption to health and sustainability challenges. *Appetite*, *76*, 120–128. https://doi.org/10.1016/j.appet.2014.02.002

Devi, C. B., Kushwaha, A., & Kumar, A. (2015). Sprouting characteristics and associated changes in nutritional composition of cowpea (*Vigna unguiculata*). *Journal of Food Science and Technology*, *52*(10), 6821–6827. https://doi.org/10.1007/s13197-015-1832-1

Dilrukshi, H. N., Torrico, D. D., Brennan, M. A., & Brennan, C. S. (2022). Effects of extrusion processing on the bioactive constituents, in vitro digestibility, amino acid composition, and antioxidant potential of novel gluten-free extruded snacks fortified with cowpea and whey protein concentrate. *Food chemistry*, *389*, 133107. https://doi.org/10.1111/ijfs.15462

Evans, D. R. H., Romero, J. K., & Westoby, M. (2009). Chapter 9 - Concentration of Proteins and Removal of Solutes. In *Methods in Enzymology*. Academic Press Inc. https://doi.org/10.1016/S0076-6879(09)63009-3

FAO – Food and Agriculture Organization. Production quantities of Cow peas dry by country. Available at: <http://faostat.fao.org/>. Accessed on: June 21, 2024.

Ferreira, L. M. M., Mendes-Ferreira, A., Benevides, C. M. J., Melo, D., Costa, A. S. G., Mendes-Faia, A., & Oliveira, M. B. P. P. (2019). Effect of controlled microbial fermentation on nutritional and functional characteristics of cowpea bean flours. *Foods*, *8*(11). https://doi.org/10.3390/foods8110530

Franco-Miranda, H., Chel-Guerrero, L., Gallegos-Tintoré, S., Castellanos-Ruelas, A., & Betancur-Ancona, D. (2017). Physicochemical, rheological, bioactive and consumer acceptance analyses of concha-type Mexican sweet bread containing Lima bean or cowpea hydrolysates. *LWT*, *80*, 250–256. https://doi.org/10.1016/j.lwt.2017.02.034

Freire Filho, F. R., Ribeiro, V. Q., Freire Filho, F. R., & Ribeiro, V. Q. (2023). Feijão-Caupi na Embrapa Meio-Norte: melhoramento, cultivares lançadas, genealogias e base genética. EMBRAPA. Available at: http://www.alice.cnptia.embrapa.br/alice/handle/doc/1156685. Accessed on: January 20, 2024.

Freire-Filho, F. R., Ribeiro, V. Q., Rocha, M. D. M., Silva, K. J. D., Nogueira, M. D. S., & Rodrigues, E. V. (2012). Production, breeding and potential of cowpea crop in Brazil. EMBRAPA. Available at: http://www.infoteca.cnptia.embrapa.br/infoteca/handle/doc/953612. Accessed on: January 20, 2024.

Frota, K. D. M. G., Lopes, L. A. R., Silva, I. C. V., & Arêas, J. A. G. (2018). Molecular profile, purity and presence of trypsin inhibitors in cowpea protein isolates. *Revista Caatinga*, *31*(1), 202–208. https://doi.org/10.1590/1983-21252018v31n123rc

Frota, K. D. M. G., Soares, R. A. M., & Arêas, J. A. G. (2008). Composição química do feijão caupi (*Vigna unguiculata L*. Walp), cultivar BRS-Milênio. *Food Science and Technology*, *28*, 470-476.

Ge, J., Sun, C. X., Mata, A., Corke, H., Gan, R. Y., & Fang, Y. (2021). Physicochemical and pH-dependent functional properties of proteins isolated from eight traditional Chinese beans. *Food Hydrocolloids*, *112*. https://doi.org/10.1016/j.foodhyd.2020.106288

Granito, M., Torres, A., Frias, J., Guerra, M., & Vidal-Valverde, C. (2005). Influence of fermentation on the nutritional value of two varieties of Vigna sinensis. *European Food Research and Technology*, *220*(2), 176–181. https://doi.org/10.1007/s00217-004-1011-5

Grudniewska, A., de Melo, E. M., Chan, A., Gniłka, R., Boratynski, F., & Matharu, A. S. (2018). Enhanced protein extraction from oilseed cakes using glycerol–choline chloride deep eutectic solvents: a biorefinery approach. *ACS sustainable chemistry & engineering*, *6*(11), 15791-15800.

Gunathilake, K. G. T., Wansapala, M. A. J., & Herath, H. M. T. (2016). Comparison of nutritional and functional properties of mung bean (*Vigna radiate*) and cowpea (*Vigna unguiculata*) protein isolates processed by isoelectric precipitation. *International Journal of Innovative Research in Technology, 3*(2), 139-148.

Han, J. H. (2014). Edible Films and Coatings: A Review. In *Innovations in Food Packaging: Second Edition* (pp. 213–255). Elsevier Ltd. https://doi.org/10.1016/B978-0-12-394601-0.00009-6

Henchion, M., Hayes, M., Mullen, A. M., Fenelon, M., & Tiwari, B. (2017). Future protein supply and demand: Strategies and factors influencing a sustainable equilibrium. *Foods*, *6*(7), 1–21. https://doi.org/10.3390/foods6070053

Hewage, S., & Vithanarachchi, S. M. (2009). Preparation and characterization of biodegradable polymer films from cowpea (*Vigna unguiculata*) protein isolate. *Journal of the National Science Foundation of Sri Lanka, 37(1)*, 53-57.

Horax, R., Hettiarachchy, N. S., Chen, P., & Jalaluddin, M. (2004). Preparation and characterization of protein isolate from cowpea (*Vigna unguiculata L*. Walp.). *Journal of Food Science*, *69*(2), fct114-fct118.

Ibrahim, S. S., Habiba, R. A., Shatta, A. A., & Embaby, H. E. (2002). Effect of soaking, germination, cooking and fermentation on antinutritional factors in cowpeas. *Nahrung - Food*, *46*(2), 92–95. https://doi.org/10.1002/1521-3803(20020301)46:2<92:AID-FOOD92>3.0.CO;2-P

Jauregi, P., Esnal-Yeregi, L., & Labidi, J. (2024). Natural deep eutectic solvents (NADES) for the extraction of bioactives: emerging opportunities in biorefinery applications. *PeerJ Analytical Chemistry*, *6*, e32.

JIAO, X. B., WANG, G. Y., LI, J. H., WANG, X. Y., MENG, G. Q., & CUI, J. D. (2021). A comparative study of methods for extracting protein from sesame residue. *Biotechnology Bulletin*, *37*(4), 273.

Kaspchak, E., Mafra, L. I., & Mafra, M. R. (2018). Effect of heating and ionic strength on the interaction of bovine serum albumin and the antinutrients tannic and phytic acids, and its influence on in vitro protein digestibility. *Food Chemistry*, *252*, 1–8. https://doi.org/10.1016/j.foodchem.2018.01.089

Kewuyemi, Y. O., Kesa, H., & Adebo, O. A. (2022). Biochemical properties, nutritional quality, colour profile and techno-functional properties of whole grain sourdough and malted cowpea and quinoa flours. *International Journal of Food Science and Technology*, *57*(3), 1527–1543. https://doi.org/10.1111/ijfs.15512

Khalid, I. I., & Elhardallou, S. B. (2016). Factors That Compromise the Nutritional Value of Cowpea Fluor and Its Protein Isolates. *Food and Nutrition Sciences*, *07*(02), 112–121. https://doi.org/10.4236/fns.2016.72013

Khalid, I. I., Elhardallou, S. B., & Elkhalifa, E. A. (2012). Composition and functional properties of cowpea (*Vigna ungiculata L.* Walp) flour and protein isolates. *Academic Journals Inc.*, *7*(3), 113-122. https://10.3923/ajft.2012.113.122

Kumar, L., Ramakanth, D., Akhila, K., Gaikwad, K. K. (2022). Edible films and coatings for food packaging applications: a review. *Environmental Chemistry Letters, 20*(1), 875-900. https://doi.org/10.1007/s10311-021-01339-z

Kumar, M., Tomar, M., Potkule, J., Verma, R., Punia, S., Mahapatra, A., Belwal, T., Dahuja, A., Joshi, S., Berwal, M. K., Satankar, V., Bhoite, A. G., Amarowicz, R., Kaur, C., & Kennedy, J. F. (2021). Advances in the plant protein extraction: Mechanism and recommendations. *Food Hydrocolloids*, *115*, 106595. https://doi.org/10.1016/J.FOODHYD.2021.106595

Lafarga, T., Álvarez, C., Bobo, G., & Aguiló-Aguayo, I. (2018). Characterization of functional properties of proteins from Ganxet beans (Phaseolus vulgaris L. var. Ganxet) isolated using an ultrasound-assisted methodology. *LWT*, *98*, 106–112. https://doi.org/10.1016/J.LWT.2018.08.033

Lafarga, T., Álvarez, C., Villaró, S., Bobo, G., & Aguiló-Aguayo, I. (2020). Potential of pulse-derived proteins for developing novel vegan edible foams and emulsions. *International Journal of Food Science and Technology*, *55*(2), 475–481. https://doi.org/10.1111/ijfs.14286

Leser, S. (2013). The 2013 FAO report on dietary protein quality evaluation in human nutrition: Recommendations and implications. *Nutrition Bulletin*, *38*(4), 421-428.

Li, T., Wang, L., Zhang, X., Geng, H., Xue, W., & Chen, Z. (2021). Assembly behavior, structural characterization and rheological properties of legume proteins based amyloid fibrils. *Food Hydrocolloids*, *111*. https://doi.org/10.1016/j.foodhyd.2020.106396

Liu, R. L., Yu, P., Ge, X. L., Bai, X. F., Li, X. Q., & Fu, Q. (2017). Establishment of an aqueous PEG 200-based deep eutectic solvent extraction and enrichment method for pumpkin (Cucurbita moschata) seed protein. *Food Analytical Methods*, *10*, 1669-1680.

Locali-Pereira, A. R., Boire, A., Berton-Carabin, C., Taboga, S. R., Solé-Jamault, V., & Nicoletti, V. R. (2023). Pigeon Pea, An Emerging Source of Plant-Based Proteins. *ACS Food Science and Technology*, *3*(11), 1777–1799. https://doi.org/10.1021/acsfoodscitech.3c00268

Locali-Pereira, A. R., Caruso, Í. P., Rabesona, H., Laurent, S., Meynier, A., Kermarrec, A., Birault, L., Geairon, A., Le Gall, S., Thoulouze, L., Solé-Jamault, V., Berton-Carabin, C., Boire, A., & Nicoletti, V. R. (2024). Pre-treatment effects on the composition and functionalities of pigeon pea seed ingredients. *Food Hydrocolloids*, *152*, 109923. https://doi.org/10.1016/j.foodhyd.2024.109923

Locali-Pereira, A. R., Kubo, M. T. K., Fuzetti, C. G., & Nicoletti, V. R. (2022). Functional Properties of Physically Pretreated Kidney Bean and Mung Bean Flours and Their Performance in Microencapsulation of a Carotenoid-Rich Oil. *Frontiers in Sustainable Food Systems*, *6*. https://doi.org/10.3389/fsufs.2022.845566

Loushigam, G., & Shanmugam, A. (2023). Modifications to functional and biological properties of proteins of cowpea pulse crop by ultrasound-assisted extraction. *Ultrasonics Sonochemistry*, *97*. https://doi.org/10.1016/j.ultsonch.2023.106448

Martins Ferreira, W., Rodrigues Lima, G., Cabral Macedo, D., Freire Júnior, M., & Pimentel, C. (2022). Cowpea: A low-cost quality protein source for food safety in marginal areas for agriculture. *Saudi Journal of Biological Sciences*, *29*(12). https://doi.org/10.1016/j.sjbs.2022.103431

Mohanan, A., Harrison, K., Cooper, D. M. L., Nickerson, M. T., & Ghosh, S. (2022). Conversion of Pulse Protein Foam-Templated Oleogels into Oleofoams for Improved Baking Application. *Foods*, *11*(18). https://doi.org/10.3390/foods11182887

Moongngarm, A., Sasanam, S., Pinsiri, W., Inthasoi, P., Janto, S., & Pengchai, J. (2014). Functional properties of protein concentrate from black cowpea and its application. *American Journal of Applied Sciences*, *11*(10), 1811–1818. https://doi.org/10.3844/ofsp.9483

Mune Mune, M. A., Minka, S. R., & Mbome, I. L. (2011). Functional properties of acetylated and succinylated cowpea protein concentrate and effect of enzymatic hydrolysis on solubility. *International Journal of Food Sciences and Nutrition*, *62*(4), 310–317. https://doi.org/10.3109/09637486.2010.538670

Mune, M. A. M., & Sogi, D. S. (2016). Emulsifying and Foaming Properties of Protein Concentrates Prepared from Cowpea and Bambara Bean Using Different Drying Methods. *International Journal of Food Properties*, *19*(2), 371–384. https://doi.org/10.1080/10942912.2015.1023399

Mwasaru, M. A., Muhammad, K., Bakar, J., & Man, Y. B. C. (1999a). Effects of isolation technique and conditions on the extractability, physicochemical and functional properties of

pigeonpea (*Cajanus cajan*) and cowpea (*Vigna unguiculata*) protein isolates. I. Physicochemical properties. *Food Chemistry*, *67*(4), 435-443.

Mwasaru, M. A., Muhammad, K., Bakar, J., & Man, Y. B. C. (1999b). Effects of isolation technique and conditions on the extractability, physicochemical and functional properties of pigeonpea (*Cajanus cajan*) and cowpea (*Vigna unguiculata*) protein isolates. II. Functional properties. *Food Chemistry*, *67*, 445 – 452.

Naiker, T. S., Gerrano, A., & Mellem, J. (2019). Physicochemical properties of flour produced from different cowpea (*Vigna unguiculata*) cultivars of Southern African origin. *Journal of Food Science and Technology*, *56*(3), 1541–1550. https://doi.org/10.1007/s13197-019-03649-1

Oliveira, M. M. G., Fessori, A. G. B. W., Huamaní-Meléndez, V. J., & Mauro, M. A. (2024). Exploring the rheological and thermal behavior of cowpea protein concentrate: Impact of pH and concentration. *Colloids and Surfaces A: Physicochemical and Engineering Aspects*, *694*, 134106. https://doi.org/10.1016/j.colsurfa.2024.134106

Oliveira, M. M., Silva, K. S., & Mauro, M. A. (2021). Evaluation of Interactions Between Carboxymethylcellulose and Soy Protein Isolate and their Effects on the Preparation and Characterization of Composite Edible Films. *Food Biophysics*, *16*, 214–228. https://doi.org/10.1007/s11483-020-09659-3

Olivera-Castillo, L., Pereira-Pacheco, F., Polanco-Lugo, E., Olvera-Novoa, M., Rivas-Burgos, J., & Grant, G. (2007). Composition and bioactive factor content of cowpea (*Vigna unguiculata* L. Walp) raw meal and protein concentrate. *Journal of the Science of Food and Agriculture*, *87*(1), 112–119. https://doi.org/10.1002/jsfa.2684

Patra, A., Prasath, V. A., & Pandiselvam, R. (2023). Deep eutectic solvent: An emerging trend for extraction of plant proteins. *Journal of Molecular Liquids*, 122887.

Penchalaraju, M., & John Don Bosco, S. (2022). Legume protein concentrates from green gram, cowpea, and horse gram. *Journal of Food Processing and Preservation*, *46*(4), e16477. https://doi.org/10.1111/jfpp.16477

Penchalaraju, M., Poshadri, A., Swaroopa, G., Nikkam, I. T., & John Don Bosco, S. (2024). Leveraging Indian pulse proteins for plant-based mock meat III: physicochemical characterization, FTIR spectra and texture profile analysis of meat analogues. *International Journal of Food Science and Technology*, *59*(1), 649–660. https://doi.org/10.1111/ijfs.16828

Pereira, H. V. R., Saraiva, K. P., Carvalho, L. M. J., Andrade, L. R., Pedrosa, C., & Pierucci, A. P. T. R. (2009). Legumes seeds protein isolates in the production of ascorbic acid microparticles. *Food Research International*, *42*(1), 115–121. https://doi.org/10.1016/j.foodres.2008.10.008

Peyrano, F., de Lamballerie, M., Avanza, M. V., & Speroni, F. (2017). Calorimetric Study of Cowpea Protein Isolates. Effect of Calcium and High Hydrostatic Pressure. *Food Biophysics*, *12*(3), 374–382. https://doi.org/10.1007/s11483-017-9493-4

Peyrano, F., de Lamballerie, M., Speroni, F., & Avanza, M. V. (2019). Rheological characterization of thermal gelation of cowpea protein isolates: Effect of processing conditions. *LWT*, *109*, 406–414. https://doi.org/10.1016/j.lwt.2019.04.048

Peyrano, F., Speroni, F., & Avanza, M. V. (2016). Physicochemical and functional properties of cowpea protein isolates treated with temperature or high hydrostatic pressure. *Innovative Food Science and Emerging Technologies*, *33*, 38–46. https://doi.org/10.1016/j.ifset.2015.10.014

Ragab, D. D. M., Babiker, E. E., & Eltinay, A. H. (2004). Fractionation, solubility and functional properties of cowpea (*Vigna unguiculata*) proteins as affected by pH and/or salt concentration. *Food Chemistry*, *84*(2), 207–212. https://doi.org/10.1016/S0308-8146(03)00203-6

Ramireddy, L., & Radhakrishnan, M. (2021). Cold plasma applications on pulse processing. *Pulse Foods: Processing, Quality and Nutraceutical Applications*, 295–307. https://doi.org/10.1016/B978-0-12-818184-3.00012-X

Rangel, A., Domont, G. B., Pedrosa, C., & Ferreira, S. T. (2003). Functional properties of purified vicilins from cowpea (*Vigna unguiculata*) and pea (*Pisum sativum*) and cowpea protein isolate. *Journal of Agricultural and Food Chemistry*, *51*(19), 5792–5797. https://doi.org/10.1021/jf0340052

Rangel, A., Saraiva, K., Schwengber, P., Narciso, M. S., Domont, G. B., Ferreira, S. T., & Pedrosa, C. (2004). Biological evaluation of a protein isolate from cowpea (*Vigna unguiculata*) seeds. *Food Chemistry*, *87*(4), 491–499. https://doi.org/10.1016/j.foodchem.2003.12.023

Rivas-Vega, M. E., Goytortúa-Bores, E., Ezquerra-Brauer, J. M., Salazar-García, M. G., Cruz-Suárez, L. E., Nolasco, H., & Civera-Cerecedo, R. (2006). Nutritional value of cowpea (*Vigna unguiculata* L. Walp) meals as ingredients in diets for Pacific white shrimp (*Litopenaeus vannamei* Boone). *Food Chemistry*, *97*(1), 41–49. https://doi.org/10.1016/j.foodchem.2005.03.021

Rudra, S. G., Sethi, S., Jha, S. K., & Kumar, R. (2016). Physico-chemical and functional properties of cowpea protein isolate as affected by the dehydration technique. *Legume Research*, *39*(3), 370–378. https://doi.org/10.18805/lr.v0iOF.9441

Sabaté, J., Sranacharoenpong, K., Harwatt, H., Wien, M., & Soret, S. (2015). The environmental cost of protein food choices. *Public Health Nutrition*, *18*(11), 2067–2073. https://doi.org/10.1017/S1368980014002377

Sathya, A., & Siddhuraju, P. (2015). Effect of processing methods on compositional evaluation of underutilized legume, Parkia roxburghii G. Don (*yongchak*) seeds. *Journal of Food Science and Technology*, *52*(10), 6157–6169. https://doi.org/10.1007/s13197-015-1732-4

Schlangen, M., Taghian Dinani, S., Schutyser, M. A. I., & van der Goot, A. J. (2022). Dry fractionation to produce functional fractions from mung bean, yellow pea and cowpea flour. *Innovative Food Science and Emerging Technologies*, *78*, 103018. https://doi.org/10.1016/j.ifset.2022.103018

Shevkani, K., Kaur, A., Kumar, S., & Singh, N. (2015). Cowpea protein isolates: Functional properties and application in gluten-free rice muffins. *LWT - Food Science and Technology*, *63*(2), 927–933. https://doi.org/10.1016/J.LWT.2015.04.058

Sreerama, Y. N., Sashikala, V. B., Pratape, V. M., & Singh, V. (2012). Nutrients and antinutrients in cowpea and horse gram flours in comparison to chickpea flour: Evaluation of

their flour functionality. *Food Chemistry*, *131*(2), 462–468. https://doi.org/10.1016/j.foodchem.2011.09.008

Svigelj, R., Bortolomeazzi, R., Dossi, N., Giacomino, A., Bontempelli, G., & Toniolo, R. (2017). An effective gluten extraction method exploiting pure choline chloride-based deep eutectic solvents (ChCl-DESs). *Food Analytical Methods*, *10*, 4079-4085.

Tang, X., Shen, Y., Zhang, Y., Schilling, M. W., & Li, Y. (2021). Parallel comparison of functional and physicochemical properties of common pulse proteins. *LWT*, *146*, 111594. https://doi.org/10.1016/j.lwt.2021.111594

Thompson, C. M. B., Acevedo, B. A., Añón, M. C., & Avanza, M. V. (2023). Emulsifying Capacity of Cowpea Protein Isolates. Effect of Thermal and Hydrolytic Treatment. *Plant Foods for Human Nutrition*, *78*(2), 366–374. https://doi.org/10.1007/s11130-023-01072-8

Vasconcelos, I. M., Maia, F. M. M., Farias, D. F., Campello, C. C., Carvalho, A. F. U., de Azevedo Moreira, R., & de Oliveira, J. T. A. (2010). Protein fractions, amino acid composition and antinutritional constituents of high-yielding cowpea cultivars. *Journal of Food Composition and Analysis*, *23*(1), 54–60. https://doi.org/10.1016/j.jfca.2009.05.008

Wahlström, R., Rommi, K., Willberg-Keyriläinen, P., Ercili-Cura, D., Holopainen-Mantila, U., Hiltunen, J., ... & Kuutti, L. (2017). High yield protein extraction from Brewer's spent grain with novel carboxylate salt-urea aqueous deep eutectic solvents. *ChemistrySelect*, *2*(29), 9355-9363.

Yu, L., Yang, W., Sun, J., Zhang, C., Bi, J., & Yang, Q. (2015). Preparation, characterization and physicochemical properties of the phosphate modified peanut protein obtained from *Arachin Conarachin* L. *Food Chemistry*, *170*, 169–179. https://doi.org/10.1016/j.foodchem.2014.08.047

Zayas, J. F. (1997). Functionality of Proteins in Food. In *Functionality of Proteins in Food*. Springer Berlin Heidelberg. https://doi.org/10.1007/978-3-642-59116-7

Zhou, Y., Wu, W., Zhang, N., Soladoye, O. P., Zhang, Y., & Fu, Y. (2022). Deep eutectic solvents as new media for green extraction of food proteins: Opportunity and challenges. *Food Research International*, *161*, 111842.

2 COWPEA PROTEIN CONCENTRATE: A DETAILED ANALYSIS OF COMPOSITION, STRUCTURE, AND TECHNOLOGICAL PROPERTIES

Maria Mariana Garcia de Oliveira[a], Ana Gabriela Baroni Wicher Fessori[a], Víctor Justiniano Huamaní-Meléndez[a], Maria Aparecida Mauro[a]

[a] Department of Food Engineering and Technology, Institute of Biosciences, Humanities and Exact Sciences – São Paulo State University (UNESP), Street Cristóvão Colombo, 2265, São José do Rio Preto 15054-000, Brazil.

e-mail address: maria.mariana@unesp.br (corresponding author)

Abstract

Cowpea represents an alternative protein source still underutilized, whose potential needs to be exploited due to its high nutritional quality and ability to grow on poor soils and survive in regions with low levels of rainfall. This study broadens our understanding of cowpeas and identifies potential avenues for further research and development of unconventional protein sources. The cowpea protein concentrate (CPC) exhibited a diverse size distribution with intense bands around 50 kDa, corresponding to globulins, especially vicilins. Furthermore, the protein profile of cowpea exhibited an adequate proportion of essential amino acids. Scanning electron microscopy revealed an irregular and porous structure in the CPC, resulting from the sublimation of ice crystals during freeze-drying. X-ray diffraction analysis indicated a predominantly amorphous structure, as evidenced by a low relative crystallinity index of 40.83%, which is particularly indicative of a β-sheet structure. Infrared spectroscopy analysis confirmed the prevalence of a secondary β-sheet structure in CPC, which characterizes the 7S protein fraction. Differential scanning calorimetry analysis revealed a high denaturation temperature at 131.86 °C, indicating that the cowpea protein can withstand more severe thermal treatments. The CPC in solution demonstrated that pH plays a crucial role in its techno-functional properties, including solubility, turbidity, foaming, and emulsifying capacity. At pH levels between 3 and 5, mostly physical instability was observed, contrasting with more alkaline pH conditions.

Keywords: Pulse crop, Plant-based proteins, Alternative protein, Techno-functional properties, pH

1 Introduction

Globally, there has been a growing interest in diversifying protein sources, not only to reduce the environmental footprint often associated with animal-derived proteins but also to meet the demand of the increasing number of people adopting vegan, vegetarian, and flexitarian diets (Rosenfeld et al., 2020; Spendrup & Hovmalm, 2022). In the search for a healthy and environmentally sustainable food system, Food Science and Engineering have driven research into non-conventional protein sources, including legume grains (Ragab et al., 2004; Shen et al., 2022).

Among these sources, cowpea (Vigna unguiculata (L.) Walp) stands out as an underexplored plant-based protein, with the African continent accounting for 95.3% of global cowpea production (Faostat, 2022). Despite its predominance in African production, cowpea exhibits a unique adaptability to diverse environmental conditions and stands out not only for its cost-effective but also for containing an average of 20 to 30% protein on a dry weight basis (Carvalho et al., 2012; Frota et al., 2018). Protein products, such as cowpea protein, are gaining popularity as food additives in various regions worldwide. However, the successful incorporation of plant proteins into food products primarily depends on their favorable properties (Oliveira et al., 2024; Peyrano et al., 2017; 2016; Ragab et al., 2004; Shevkani et al., 2015a).

Studies on cowpea protein have highlighted several desirable properties including solubility, viscosity, water and oil holding capacity, foaming and emulsifying capacity, and gelation. Ragab and colleagues (2004) observed high solubility of cowpea protein at alkaline pH, while slightly acidic pH and high salt concentration resulted in lower emulsifying capacity, emulsion activity, and stability, as well as reduced foam formation and stability. A research group investigating the thermal, functional, and gel properties of cowpea protein isolates identified the sensitivity of these properties to factors such as extraction technique, salt presence, pH, temperature, pressure, and protein concentration (Peyrano et al., 2017). When assessing the amino acid composition, the protein derived from this legume stands out for its abundance of essential amino acids, primarily leucine (Horax et al., 2004; Tang et al., 2021). These properties favor the application of this protein in enriched products, ingredient substitution, edible films, microcapsules, and emulsions (Campbell; Euston; Ahmed, 2016; Pereira et al., 2009; Almeida et al., 2021; Hewage & Vithanarachchi, 2009).

Despite existing studies on the technological properties of cowpea protein (CP), there is still a lack of information in the literature regarding the comprehensive exploration of its chemical composition, molecular structure, and techno-functional properties in an integrated

manner. This investigation aims to fill this knowledge gap, providing a solid foundation for the effective utilization of CP. Throughout this article, each aspect of CP, from its molecular size to its techno-functional responses under different pH conditions, will be addressed in detail. The integration of these aspects is intended to provide a complete understanding of CP and its practical implications. Consequently, it is anticipated that this contribution will advance research in plant proteins, with a special focus on cowpea.

2 Material and methods

2.1 Material

The subject of this study was cowpea protein concentrate (CPC) that was found to contain 78.63 ± 0.90% protein, 10.34% carbohydrates, 6.73 ± 0.04% moisture, 3.38 ± 0.03% ash, and 0.93 ± 0.03% lipids representing its primary compositional components. For the preparation of solutions containing CPC, distilled water was used for dilution, along with analytical-grade reagents such as sodium hydroxide (40%, m/m) and hydrochloric acid (50%, m/m) (Synth, Labsynth, Diadema, Brazil) for the pH adjustment of the samples, and sunflower oil (Liza, São Paulo, Brazil).

2.2 Methods

2.2.1 Cowpea protein extraction

Cowpea protein extraction was performed using the isoelectric precipitation method, as described by Moser, Ferreira, and Nicoletti (2019), with some modifications. Cowpea grains were washed, macerated for at least 12 hours under refrigeration (4 °C), and then ground in a blender with distilled water at a 1:3 (w/w) ratio for 3 minutes. The pH of the mixture was adjusted to 8 with a concentrated NaOH solution. The suspension was stirred in a mechanical stirrer (MA 039, Marconi, Brazil) for 45 minutes at room temperature (25 °C). The solution was then centrifuged (Hitachi, CR22N, Japan) at 10,000×g for 20 minutes, and the supernatant was collected. A second extraction was performed on the precipitate under the same conditions. The supernatants from both extractions were combined, and the pH was adjusted to 4.5 with 0.1 M HCl. To separate the precipitated protein, a further centrifugation step was carried out. The supernatant was discarded, and the precipitate was redispersed in distilled water and the pH adjusted to 7. The extract was then packed, frozen, and lyophilized (JJ Científica, São Carlos, Brazil).

2.2.2 Characterization of cowpea protein concentrate powder

2.2.2.1 Molecular mass determination by SDS-PAGE

Molecular mass distribution analysis in CPC was performed using the SDS-PAGE method, following the protocol of Brunelle and Green (2014) with specific modifications. Ten milligrams of protein were diluted in 1 mL of Milli-Q water and mixed with a buffer (1:4 ratio), consisting of 10% glycerol, 5% β-mercaptoethanol, 2.3% SDS, and 0.0625 M Tris-HCl (pH=6.8). The solution was boiled for 10 min, applied to a 10% SDS-polyacrylamide gel (1 mm thickness), and subjected to electrophoresis at 120 V. The gel was stained with Coomassie Brilliant Blue, and quantification was performed using Precision Plus Protein Standards as a reference. Images were processed with GIMP v. 2.10 software and analyzed with ImageJ v. 1.53n. Peak and area were determined using Fityk v. 1.3 software.

2.2.2.2 Amino acid profile

The amino acid quantification of the raw cowpea as cowpea flour, and the CPC, was determined by high-performance liquid chromatography using the methodologies described by White et al. (1986) and Hagen et al. (1989). Tryptophan content was assessed via spectrophotometry, following the procedure outlined by Spies (1967). A total of 18 amino acids were determined, comprising 9 essential amino acids (phenylalanine, histidine, leucine, isoleucine, lysine, methionine, threonine, valine, and tryptophan) and 9 non-essential amino acids (aspartic acid, glutamic acid, alanine, arginine, cysteine, glycine, proline, serine, and tyrosine).

2.2.2.3 Trypsin inhibitor

The trypsin inhibitor activity, expressed in trypsin inhibitor units (TIU), was determined in the raw cowpea as cowpea flour, and in the CPC, according to the official method proposed by the AOCS Official Method Ba 12a-2020 (2021). One TIU represents an arbitrary unit of trypsin defined as a 0.01 increase in absorbance units at 410 nm/10 mL of the reactive mixture under assay conditions. The trypsin inhibitor is expressed as the number of trypsin inhibitor units inhibited per mg of sample.

2.2.2.4 Scanning electron microscopy (SEM)

Samples of CPC were stored at room temperature in desiccators containing silica for 5 days. Prior to analysis, the samples were fixed on aluminum stubs with carbon tape and then coated with a thin layer of gold under vacuum for 3 min. The images were analyzed using a

scanning electron microscope with a dual-beam operating with secondary electrons (SE) (FESEM, Helios NanoLab 600i FIB Workstation, FEI, Hillsboro, Oregon, USA).

2.2.2.5 Wide angle x-ray scattering (WAXS)

The analysis of Wide-Angle X-Ray Scattering (WAXS) of CPC was performed using a benchtop diffractometer (Rigaku, RINT 2000, Japan). The equipment operated at a voltage of 50 kV and a current of 30 mA, using Cu radiation, λ = 1.542 Å, and K line. Diffractograms were obtained between angles (2θ) of 5° to 60° at a scanning speed of 2° min^{-1}.

2.2.2.6 Fourier transform infrared spectroscopy (FTIR)

Infrared analyses of CPC were carried out using a Fourier Transform Infrared Spectrometer (FTIR), PerkinElmer (Spectrum Two, Waltham, MA), with attenuated total reflectance (ATR) accessory and a diamond crystal. Spectra for each sample were recorded from 400 to 4000 cm−1 with 32 scans at 4 cm-1 resolution (Cui et al., 2020). For this analysis, the samples were stored in desiccators with silica gel for 7 days at room temperature.

2.2.2.7 Differential scanning calorimetry (DSC)

A differential scanning calorimeter Perkin Elmer (DSC 8000, PerkinElmer Corp, Shelton, CT, USA) was used to investigate the thermal properties of CPC. Indium was used as a standard for temperature and heat flow calibration, while an empty pan served as a reference for the analysis. The samples, after being weighed and hermetically sealed in aluminum pans, were cooled from 25 to -50 °C at a rate of 10 °C min−1, maintained at this temperature for 1 min, and then heated to 10 °C min-1 from -80 to 250 °C (Fan & Roos, 2016). The scans were conducted in duplicate and the data were collected using Perkin Elmer Pyris software, version 10.0 (Perkin Elmer Inc., Shelton, CT, USA).

2.2.3 Characterization of cowpea protein concentrate in aqueous solution

2.2.3.1 Oil and water holding capacity

As proposed by Ragab et al. (2004), 1 g of CPC was added to 10 g of distilled water or sunflower oil, homogenized, and centrifuged at 2,200 × g for 30 min (CR22N, Hitachi, Japan). The supernatant was removed, and the remaining mass was recorded. Water and oil holding capacity was calculated and expressed as grams of retained water or oil per 1 g of protein sample.

2.2.3.2 Zeta potential (ζ)

The electrical charge of aqueous solutions of CPC (0.6% m/m) was quantified in a pH range of 3 to 11 by measuring the electrophoretic mobility (Oliveira et al., 2021) with the detection of light scattering of mobility on the Malvern Zetamaster equipment (Zetasizer Nano – ZS, Malvern, United Kingdom).

2.2.3.3 Water solubility

The CPC was solubilized in water and the pH was adjusted in the range of 3 to 11, after which the solutions were vortexed and centrifuged (5,000 × g, 15 min, 25 °C). The protein content in the supernatant was determined according to the Bradford methodology (Bradford, 1976), and the protein solubility was calculated as the ratio between the protein content in the supernatant and the protein content in the initial mass of the sample.

2.2.3.4 Turbidity of cowpea protein concentrate in aqueous media

The turbidity analysis of proteins as a function of pH was studied based on the methodology proposed by Omura et al. (2021). CPC (0.5%, m/m) was dispersed in distilled water and kept under magnetic stirring for 4 hours at room temperature. The pH of the mixtures was adjusted in a range from 3 to 11 and the absorbance of the samples was measured at 600 nm using a UV-Vis spectrophotometer (Thermo Scientific, GENESYS 10S UV-VIS, EUA) with distilled water as the blank. Next, absorbance values were expressed as turbidity using Equation (1).

$$T = \frac{2.303 \times abs}{l} \qquad (1)$$

where T is the turbidity and *l* is the optical path corresponding to the width of the cuvette.

2.2.3.5 Foaming capacity and foam stability

The foaming capacity and foam stability of CPC were evaluated as a function of pH according to the methodology proposed by Ragab et al. (2004). Aqueous solutions containing CPC (2%, m/v) at pH levels ranging from 3 to 11 were prepared and homogenized using an ultra-turrax homogenizer (T18 basic, IKA, Brazil) at 300 rpm for 5 min. Subsequently, the foam was transferred to a graduated cylinder and the foam volume was measured at 30 seconds. The

calculated volume increase was expressed as the percentage foam capacity. To determine foam stability, the decrease in foam volume over time was measured after 30 min (Liu et al., 2021).

2.2.3.6 Emulsifying capacity

The methodology employed was that described by Karaca et al. (2011) and Stone et al. (2015), with certain modifications. Aqueous solutions containing 0.6% of the CPC were prepared at pH levels ranging from 3 to 11. Aliquots of 2 g of the aforementioned solution were placed in 50 mL Falcon tubes. Sunflower oil, ranging from 4 to 21 g, was added to each tube. The contents of the tubes were homogenized using an ultra-turrax (T18 basic, IKA, Brazil) at 4,000 rpm, gradually increasing the speed to 7,000 rpm. Homogenization lasted for 3 min. Subsequently, the conductivities of the emulsions were measured using a conductivity meter (Mettler, SevenCompact S230-Basic), with the conductivity recorded in μS cm-1. The emulsion capacity was determined at the inversion point, defined as the point at which an oil-in-water emulsion transitions into a water-in-oil emulsion, and was expressed as g of oil homogenized per g of protein prior to the inversion. Readings were taken in triplicate.

3 Results and discussion

3.1 Characterization of cowpea protein concentrate powder

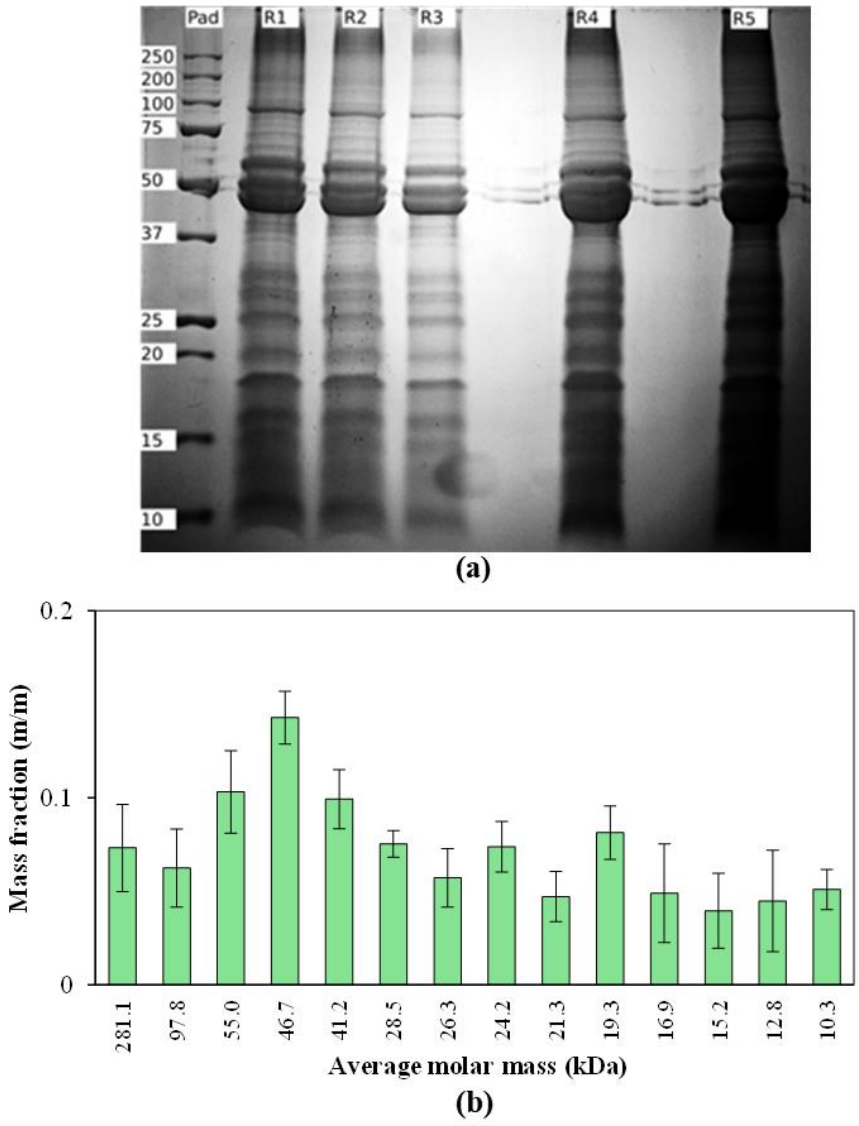
3.1.1 Molecular mass determination by SDS-PAGE

Figure 2.1 (a, b) depicts the electrophoretogram and molecular weights (kilodaltons – kD) of the CPC. It is noted that the CPC exhibits a broad size distribution. The largest group of proteins present in the storage tissues of legume cotyledons are the globulins. Indeed, in cowpea, the majority of the seed protein is found in the globulin fractions, followed by the albumin fractions (Murray et al., 1983; Freitas et al., 2004).

The most intense bands are close to the size of 50 kDa (Figure 2.1.a), a finding that is corroborated by the molar size distribution graph, which indicates a greater density of proteins with sizes between 41.2 – 55 kDa, with the largest fraction being constituted by 46.7 kDa proteins (Figure 2.1b). These bands correspond to polypeptides belonging to the 7S globulin fraction, which is also referred to as vicilin and is sometimes named phaseolin (Makeri et al., 2017). The strong band is consistent with the findings reported by Jafari et al. (2016) and Rui et al. (2015) for white bean proteins, as well as with a molecular weight distribution within the range of 43 to 53 kDa for winged bean seed and common bean (Makeri et al., 2017; Romero et al., 1975; Freitas et al., 2004).

Furthermore, molecular weights with less intense but prominent bands were also identified near 100 and 30 kDa. Previous studies have attributed the molecular weights of 91 – 105 kDa and near 30 kDa to the major albumin polypeptides (Peyrano et al., 2016; Vasconcelos et al., 2010; Murray et al., 1983).

Figure Error! No text of specified style in document.**.4 (**a) SDS-PAGE of CPC. The first lane on the left represents the molecular mass markers; (b) CPC molar mass distribution



Source: elaborated by the author.

3.1.2 Amino acid profile

The nutritional value of proteins is essentially based on the presence and quantity of essential amino acids they provide, and their quality is determined by the adequate proportion

of these essential amino acids in relation to the body's needs. Thus, proteins that contain all essential amino acids in suitable proportions are considered “complete proteins” and are highly valued in the diet because they provide the nutrients necessary for growth, repair, and maintenance of the body.

Table 2.1 compares the amino acid composition, divided into two categories: essential and non-essential, in 100 grams of raw cowpea (seed flour) and CPC. A substantial increase in both essential and non-essential amino acids is observed in CPC compared to raw cowpea, which positively contributes to the nutritional value of the protein concentrate. The proportions of essential amino acids relative to total amino acids in the grain in CPC were 38.78% and 39.85%, respectively. In addition, the ratio of essential/non-essential amino acids in the grain increased from 63.34% to 66.25%. However, both ratios show a small increase in the protein concentrate profile compared to its original matrix, which suggests that the extraction process does not greatly affect the amino acid composition.

Both samples exhibited similar amino acid profiles, with higher concentrations, particularly of leucine, phenylalanine, and lysine (essential), and aspartic acid, glutamic acid, and arginine (non-essential), while tryptophan, methionine, and cysteine are present in lower concentrations. Even though tryptophan and methionine levels are the lowest found, they are not considered limiting amino acids. On the contrary, all essential amino acids are present in adequate proportions, in both raw cowpea and CPC, according to the Food and Agriculture Organization (Leser, 2013) recommended scoring pattern, for older age groups, including older children, adolescents, and adults (Table 2.1).

Amino acids can be categorized into several classes based on the interaction of their side chains with water. Amino acids with aliphatic (Ala, Ile, Leu, Met, Pro, and Val) and aromatic (Phe, Trp, and Tyr) side chains are hydrophobic and therefore have limited solubility in water. On the other hand, polar (hydrophilic) amino acids are highly soluble in water and can be either charged, such as Arg, Asp, Glu, His, and Lys, or uncharged, such as Ser, Thr, Asn, Gln, and Cys (Damodaran et al., 2008). Due to the subtle differences observed in the ratio of essential to non-essential amino acids in the protein concentrate compared to raw cowpea, there will also be no significant impact on the ratio of total hydrophilic to hydrophobic amino acids. The proportion of hydrophilic amino acids fraction was 59% in the raw cowpea and 58% in the CPC, while the hydrophobic fraction of amino acids corresponded to 41% and 42% in the raw cowpea and CPC, respectively.

Beyond its nutritional relevance, the amino acid composition reflects the profiles of protein side chains and plays an important role in influencing the physicochemical and

functional behavior of these macromolecules (Tang et al., 2021; Brishti et al., 2017), topics that will be explored throughout this article.

Table Error! No text of specified style in document.**.6** Amino acid (AA) profile of raw cowpea (RC) and CPC

Amino acids	**Raw cowpea (g AA · 100g $^{-1}$ RC)**	**CPC (g AA · 100g $^{-1}$ CPC)**	**FAO recommendation* (2011)**
	Essentials		
Isoleucine (Ils)	0.97	3.19	0.30
Leucine (Leu)	1.78	6.07	0.61
Phenylalanine (Phe)	1.36	4.50	0.41
Lysine (Lys)	1.58	4.95	0.48
Tryptophan (Trp)	0.16	0.56	0.07
Histidine (His)	0.72	2.29	0.16
Valine (Val)	1.11	3.68	0.40
Methionine (Met)	0.28	1.12	0.23
Threonine (Thr)	0.87	2.60	0.25
	Non-essentials		
Aspartic Acid (Asp)	2.81	8.88	-
Glutamic acid (Glu)	4.19	13.44	-
Serine (Ser)	1.21	3.99	-
Glycine (Gly)	0.94	2.63	-
Arginine (Arg)	1.86	5.43	-
Alanine (Ala)	0.97	2.96	-
Proline (Pro)	0.94	3.02	-
Tyrosine (Tyr)	0.78	2.72	-
Cystine (Cys)	0.24	0.64	-

*Older child, adolescents, and adults

3.1.3 Antinutritional factors – trypsin inhibitor

The presence of antinutritional compounds, such as trypsin inhibitor, represents one of the main underlying causes of low bioavailability of proteins and micronutrients in legumes.

This antinutrient can form complexes with key proteins and essential minerals, resulting in their decreased absorption by the body (Yadav et al., 2019). Therefore, the removal of these antinutrients is of utmost importance to optimize the availability of essential nutrients. Conventional processing methods, including dehulling, soaking, and heat treatments, have been demonstrated to be effective in reducing the levels of antinutrients (Locali-Pereira et al., 2024).

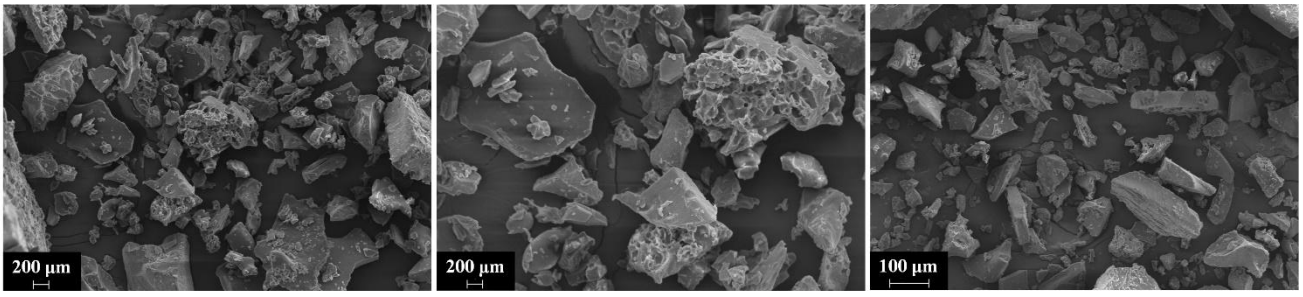
The trypsin inhibitor is expressed as the number of trypsin inhibitor units (TIU) inhibited per milligram of protein. The TIU was 73.22 TIU/mg of protein for raw beans (grain flour) and 22.89 TIU/mg of protein for the CPC. The combination of soaking and subsequent protein extraction through isoelectric precipitation resulted in a reduction of TIU by over 68%. This finding was also corroborated by Locali-Pereira et al. (2024), who identified a significant positive effect in the combination of seed soaking and protein fractionation method to attenuate the activity of trypsin inhibitors in protein concentrates of pigeon pea, achieving a reduction of approximately 79%.

3.1.4 Scanning electron microscopy (SEM)

Figure 2.2 depicts scanning electron microscopy (SEM) of CPC at magnifications of 250, 500, and 1000 ×.

The morphological structure of freeze-dried CPC is composed of particles of irregular shape and size, with a porous appearance in certain areas. Previous studies have described the appearance of powders dried using the freeze-drying technique as glassy, with an irregular structure resembling broken glass or a flake-like structure and the presence of pores (Möller et al., 2021; Wang et al., 2020; Wu et al., 2021).

Figure Error! No text of specified style in document.**.5** Scanning electron microscopy of CPC at magnifications of 250× (a), 500× (b), and 1000× (c)



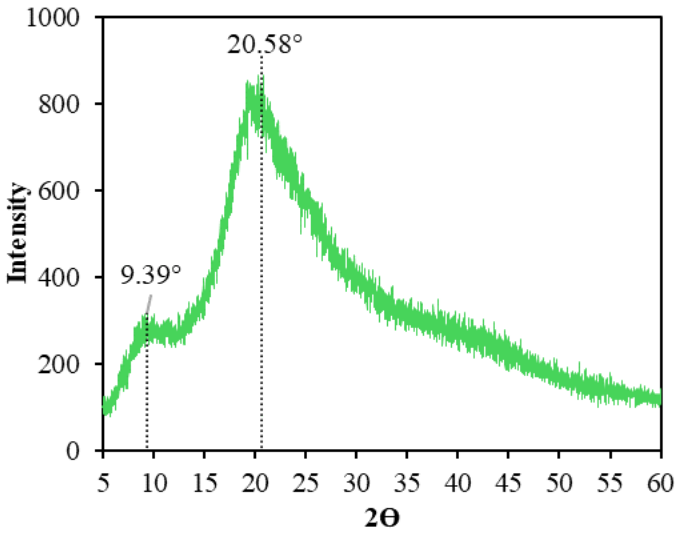
Source: elaborated by the author.

The application of low temperatures during the freeze-drying process coupled with the lack of resistance to break the frozen droplets formed or the changes undergone on the surface during drying may explain the formation of flake-like structures (Park et al., 2022; Wu et al., 2021). The porous structure observed in freeze-dried materials results from the sublimation of ice crystals formed during the freezing stage of the CPC. The porous structure formed determines the permeability and resistance to the flow of water vapor through the dry product. The larger the pore radius of the dry porous product, the lower the resistance to the flow of water vapor, thus facilitating the drying rate during the sublimation stage of the freeze-drying process (Assegehegn et al., 2020).

3.1.5 X-ray diffraction (XRD)

The XRD pattern of CPC is shown in Figure 2.3. The diffractogram displays two peaks of low definition, a shoulder at 2θ=9.39° and a peak of greater intensity at 2θ=20.58° (Figure 2d). The profile obtained for the raw material is characteristic of structures with a low degree of crystallinity. The peaks in the protein X-ray reflection pattern with 2θ angle of approximately 10° and 20° correspond to the α-helix and β-sheet structure, respectively (Oliveira et al., 2021; Chen et al., 2013), this indicates that the β-sheet structure is more prevalent than the α-helix in CPC.

Figure Error! No text of specified style in document.**.6** XRD diffractogram profile of CPC



Source: elaborated by the author.

The amorphous structure of the CPC is confirmed by the low degree of its calculated crystallinity, using the relative crystallinity index (RCI), which yielded a value of 40.83%. A protein with a more amorphous structure generally hydrates and solubilizes more easily than one with a more crystalline structure (Rudra et al., 2016). Solubility is a key property that impacts various other functional characteristics of proteins, a subject that will be further discussed.

The low protein crystallinity is attributed to the freeze-drying process, in which molecular motion is restricted as dehydration proceeds above a certain protein concentration level, and the system begins to behave as an amorphous solid (Phan-Xuan et al., 2020). This is evidenced by the micrographs of freeze-dried CPC, which exhibit a ribbon/flake structure, indicating that the proteins were dried without undergoing thermal denaturation. In contrast, drying methods that employ higher temperatures and pressures tend to promote an increased crystallization of structures.

3.1.6 Fourier transform infrared spectroscopy (FTIR)

Regarding the FTIR spectrum, some bands stand out and provide information about the molecular composition of the CPC (Figure 2.4).

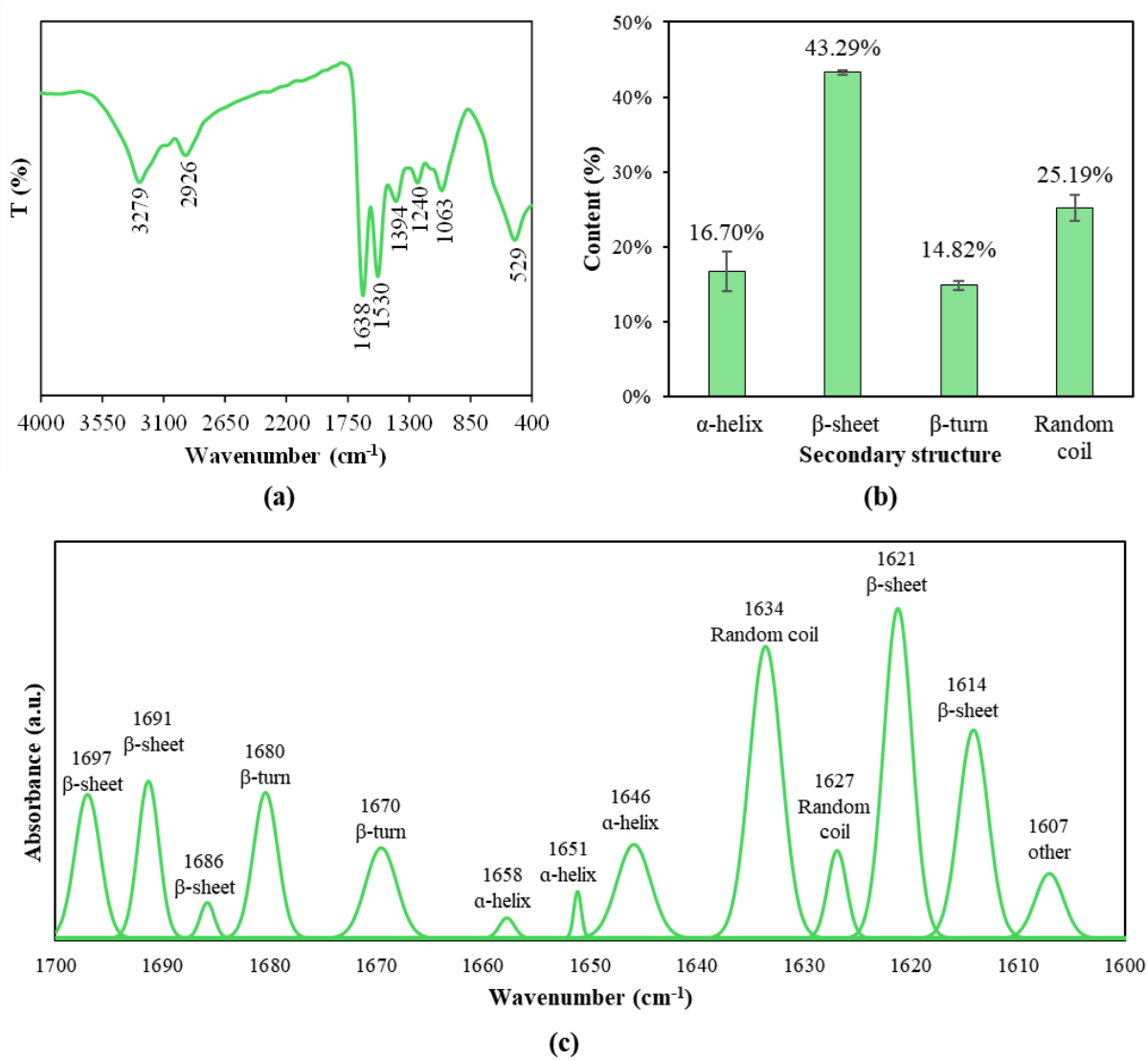
The band at 3279 cm^{-1} is attributed to the amide A band, which can be correlated with the stretching mode of the N-H bond (Stuart, 1997; Rozenberg & Shoham, 2007). The band at 2926 cm^{-1} indicates the asymmetrical C-H stretching absorption from aliphatic compounds corresponding to the CH2 group (Stuart, 1997). The 1638, 1530, and 1240 cm^{-1} bands are attributed to the amide I (C=O stretching), amide II (N-H bending), and amide III (C-N stretching vibration/N-H bending vibration) bands, respectively (Garrido et al., 2016). Additionally, bands within the range of 996 cm^{-1} to 1150 cm^{-1}, which encompass the band at 1063 cm^{-1}, highlighted in the spectrum, are indicative of C-O bonds (Garrido et al., 2016; Sanches et al., 2021).

Quantitative information regarding secondary structures was obtained by applying the second derivative and subsequent Gaussian band-deconvolution (R^2=0.980) to the amide I region (1700 - 1600 cm^{-1}), allowing us to evaluate the contribution of protein secondary structure. The secondary structure of proteins arises from hydrogen bonding, with β-sheet and β-turn predominating. In the α-helix, a single polypeptide chain forms a right-handed helix, stabilized by hydrogen bonds between peptide groups. The β-sheet, also stabilized by hydrogen bonds, exhibits a flattened zigzag structure and can be twisted, resembling β-turn structures.

Regions lacking secondary structures are termed “random coils”, although they are not truly random, only irregular structures (Clark et al., 2019).

Even though the absorption band of the amide I from the polypeptide backbone occurs in the same spectral region as that of amino acid side chains, the latter have been found to contribute relatively little when measured in D_2O, in comparison to the absorption of the amide I band (Stuart, 1997).

Figure Error! No text of specified style in document.**.7** Infrared spectra (a); composition of amide I components (b) and curve fitting spectra of amide I (c)



Source: elaborated by the author.

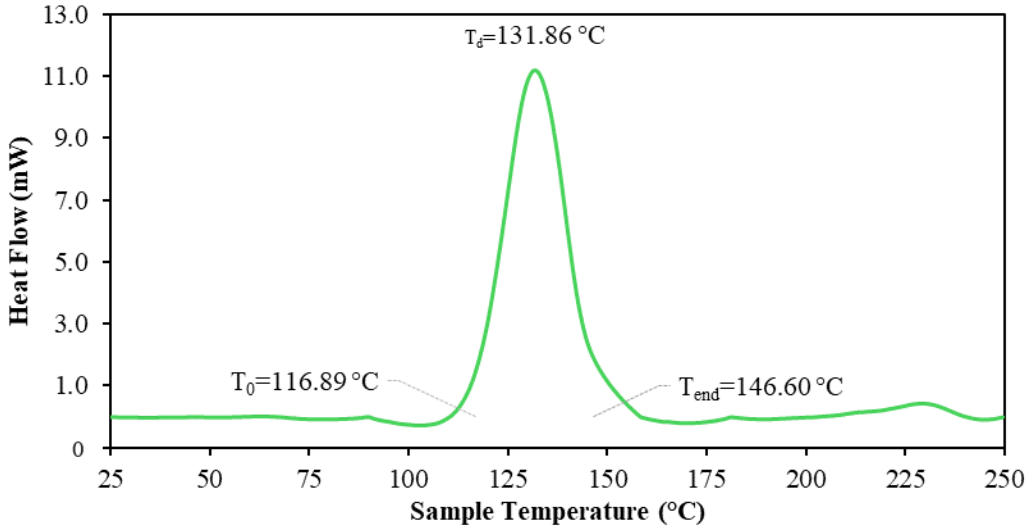
The wavelength assignments to the structural components of the amide I were as follows: β-sheet 1700-1685 cm^{-1}, β-turn 1684-1664 cm^{-1}, α-helix 1663-1643 cm^{-1}, random coil 1642-1627 cm^{-1}, and β-sheet 1626-1610 $cm^{-1.}$ The peak transitions were assigned according to Zhao et al. (2021). The percentages of secondary structure conformations obtained from the deconvolution analysis are shown in Figure 2.4 (b,c) and are as follows: 43.29% β-sheet, 25.19% random coil, 16.70% α-helix, and 14.82% β-turn. In agreement with the X-ray pattern, the data obtained from the FTIR analysis revealed that the predominant secondary structure in the CPC was the β-sheet. The β-sheet and α-helix structures are well-known for their high stability due to their extensive involvement in hydrogen bonding (Clark et al., 2019). In line with the X-ray pattern, which shows a more intense peak corresponding to the β-sheet structure, the data obtained from the FTIR analysis also revealed that the predominant secondary structure in the CPC is the β-sheet. The 7S protein fraction is characterized by a high content of β-sheet structures, suggesting that this configuration contributes to a more crystalline structure (Chen et al., 2013; Carbonaro& Nuraca, 2010; Lawrence et al., 1994).

Studies on concentrated and isolated cowpea proteins consistently indicate a prevalent β-structure in their secondary composition (Gómez et al., 2021; Mune & Sogi, 2016). Nevertheless, the distribution of the secondary structure components in cowpea proteins varies according to studies. Factors such as thermal processing, heating, water content, extraction pH, and pulse variety contribute to structural variations. Dehydrated proteins by lyophilization showcase distinct properties compared to their soluble counterparts, often experiencing a decline in α-helix content while β-sheet increases (Phan-Xuan et al., 2020). These authors demonstrated that dehydration induces structural shifts of protein molecules, which undergo deformation to continuously fill the spaces formed as freeze-drying proceeds. However, heating conditions can disrupt the secondary structure of proteins by affecting disulfide and hydrogen linkages, resulting in the reorganization of protein secondary structure. Moreover, acidic conditions can decrease the content of α-helix and random coil, while extremely alkaline conditions can lead to a decrease in the content of α-helix and β-sheet (Gómez et al., 2021; Mune & Sogi, 2016; Shevkani et al., 2015b).

3.1.7 Differential scanning calorimetry (DSC)

The thermal properties of the CPC were evaluated using differential scanning calorimetry analysis, aiming to observe the effect of the thermal process conditions on the protein. The average thermal parameters of the CPC (T_{onset}, $T_{d,}$ and T_{end}) are shown in the thermogram in Figure 2.5.

Figure Error! No text of specified style in document.**.8** Thermogram of CPC



Source: elaborated by the author.

CPC denaturation is marked by an endothermic peak at 131.86 °C, starting at 116.89 °C. The Td of a protein is generally independent of concentration when in solution, where this temperature, in most cases, is below 100 °C. However, at low water contents, Td increases, and the endothermic peaks are shifted to temperatures close to 120 °C (Kitabatake et al., 1989). Tang et al. (2021) and Ricci et al. (2018) recorded the occurrence of thermal denaturation in proteins isolated from cowpea and various legumes at temperatures above 140 °C. A higher denaturation temperature indicates greater thermal stability of the protein, which may be influenced by its structure, conformation, and cross-links through disulfide bonds (Shevkani et al., 2015b).

The enthalpy change (ΔH) reflects the extension of the ordered structure of the globulins, as the transition from the native state to the denatured state occurs. The significantly higher enthalpy (223.76 J/g) associated with this peak than that reported by other researchers (Tang et al., 2021) suggests a more intense thermal transition. Analogous to the present study, Penchalaraju et al. (2024), also found high values of ΔH when investigating the properties of protein concentrates from legumes, including cowpea. Horse gram protein concentrate exhibited the highest enthalpy (287.73 J/g), followed by the green gram protein concentrate (249.27 J/g) and the cowpea protein concentrate (237.07 J/g). Arntfield & Murray (1981) observed a correlation between Td and ΔH values and the different treatments that the protein had undergone before analysis. For instance, if a greater fraction of the protein was not denatured during the preparation process, a high Td and a high ΔH would be anticipated.

Moreover, discrepancies in enthalpy values can be attributed to the combination of both, endothermic and exothermic processes. The former includes the disruption of hydrogen bonds, whereas the latter encompasses protein aggregation and disruption of hydrophobic interactions, whose contributions will concomitantly influence the overall ΔH value (Arntfield & Murray, 1981).

3.2 Characterization of cowpea protein concentrate (CPC) in aqueous medium

3.2.1 Water and oil holding capacity

CPC had a water and oil holding capacity of 1.37 ± 0.08 g/g CPC and 1.72 ± 0.04 g/g CPC, respectively. These values are within the range reported in the literature consulted, where, for water holding, values are established between 1.06 and 2.27 g/g concentrate and for oil from 0.95 to 1.80 g/g concentrate (Khalid et al., 2012; Peyrano et al., 2016; Ragab et al., 2004; Kinsella, 1979). Factors such as protein and fiber content may account for differences in the swelling capacity of these proteins, as well as being related to greater or lesser availability of polar amino acids for interacting with water. In oil-water systems, the protein diffuses to the interface, where it functions as a surfactant reducing the surface tension (Kinsella, 1979). The fat absorption mechanism is elucidated in detail by Kinsella (1979) based on the physical properties of proteins, which depend on innumerable factors. These include the median conditions (pH, temperature, ion effects), denaturation grade, the native conformation of the protein, and its flexibility. Conversely, several authors have related the oil absorption capacity not only to the distinct conformational characteristics of the proteins but also to their nonpolar side chains (Ragab et al., 2004).

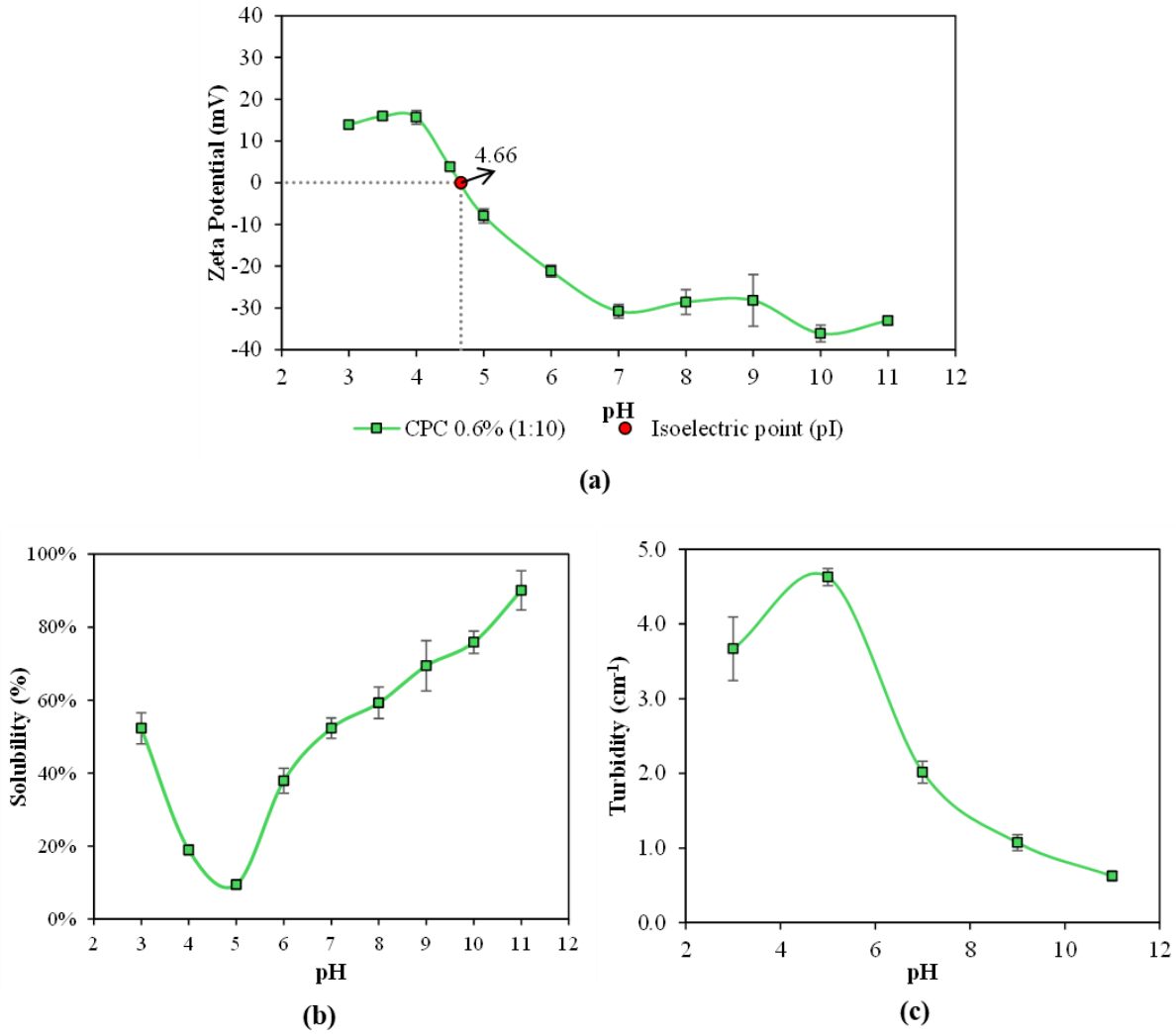
A relevant observation that can be made regarding these results is that CPC has demonstrated a slightly higher affinity for oil than for water, which may be advantageous for applications in oil-rich food formulations. This superior affinity for the oil phase may have been reinforced by the presence of hydrophobic regions with a significant portion of nonpolar amino acid residues, mainly those with high hydrophobicity (Zimmerman et al., 1968), including Leucine, Isoleucine, Valine, and Phenylalanine (Table 1), which would enhance interactions with oil molecules.

3.2.2 Zeta potential (ζ), water solubility and turbidity

The effect of pH on the electrokinetic potential of aqueous CPC solutions at a concentration of 0.6% (m/m) and dilution in a ratio of 1:10 is shown in Figure 2.6a.

The point indicated in Figure 6a corresponds to the charge reversal pH or isoelectric point (pI) of the cowpea protein, where the net charge on the particle surface is zero. At this point, the protein aggregation is more favored, and the colloidal system is less stable. As the pH is shifted to more alkaline regions away from the pI, the concentration of negative charges in the medium increases, resulting in higher zeta potential values in modulus than those at pH values below the pI. The isoelectric point of cowpea protein isolate has been reported to lie within the pH range of 3.4 to 6.0 (Rudra et al., 2016; Chel-Guerrero et al., 2011). The value obtained in the present study is consistent with the previously reported range for cowpea and also aligns with the range established for other plant proteins, including those from soybean (≈4.5), chickpea (≈3.7), and pea (≈4.3) (Moser et al., 2019; Omura et al., 2021; Oliveira et al., 2021).

Figure Error! No text of specified style in document..**9** Zeta potential (a); water solubility (b) and turbidity (c) of CPC solution at different pH



Source: elaborated by the author.

The zeta potential measurement can be employed to characterize the stability of a solution, with the magnitude of the zeta potential and the charge sign serving as indicators of the prevailing surface charge. The greater the magnitude of the zeta potential, the more charged the particles are, and the greater the electrostatic repulsive force. Consequently, the greater the stability, since the probability of the particles resisting aggregation increases.

A low magnitude of zeta potential indicates that the attractive forces may outweigh the repulsive forces, and the mixture will likely form clumps. In general, zeta potential values from ±30 to ±40 mV are considered to represent suspensions with a moderate degree of stability (Prakash et al., 2014). The region between pHs 3 and 5 exhibited values ranging from approximately -8 to 16 mV, which, according to the literature, represents a region of physical instability. In contrast, from pH 7 onwards, the measurements were close to -30 mV, indicating that the particles behave more stably in this pH range and have less tendency to agglomerate.

Figure 2.6 also illustrates the results obtained for the solubility of CPC, demonstrating the dependence of the solubility on the pH of the solution (Figure 2.6b). As the alkalinity of the medium increased, the solubility of CPC exhibited a progressive rise, from 38% at pH 6 to 90% at pH 11. At more acidic pH values, the solubility exhibited a sudden decline, dropping from pH 3 to pH 4 and 5. While the solubility at pH 3 was greater than 50%, the solubilities at pH 4 and 5 were the lowest observed within the entire pH range evaluated, with values of approximately 18% and 9%, respectively.

Studies that have jointly addressed the solubility and the study of the charges of these protein solutions, have reported that the solubility of proteins depends on their surface charge, which is correlated with the pH (Freitas et al., 2017; Moser et al., 2019). The low solubility of the protein at pH in the range of 3 to 5 is due to its proximity to the isoelectric point of the protein (≈4.7). In this vicinity, proteins tend to aggregate, and protein-water interaction is minimal, resulting in low protein solubility and an increased tendency to precipitate. As pH moves away from this point, protein solubility increases due to an increase in the net charges of the solution resulting from protein unfolding, which favors electrostatic repulsion and improves protein-water interactions (Liu et al., 2021; Freitas et al., 2017). This behavior is clearly identified when correlating the solubility profile (Figure 2.6b) and the zeta potential (Figure 2.6a).

Turbidity measurements (Figure 2.6c) are useful for indicating the colloidal state of the dispersed particles. In general, high values of this index indicate low protein solubility values. As the turbidity increases the amount of soluble protein in the medium decreases, and the number of protein aggregates formed rises.

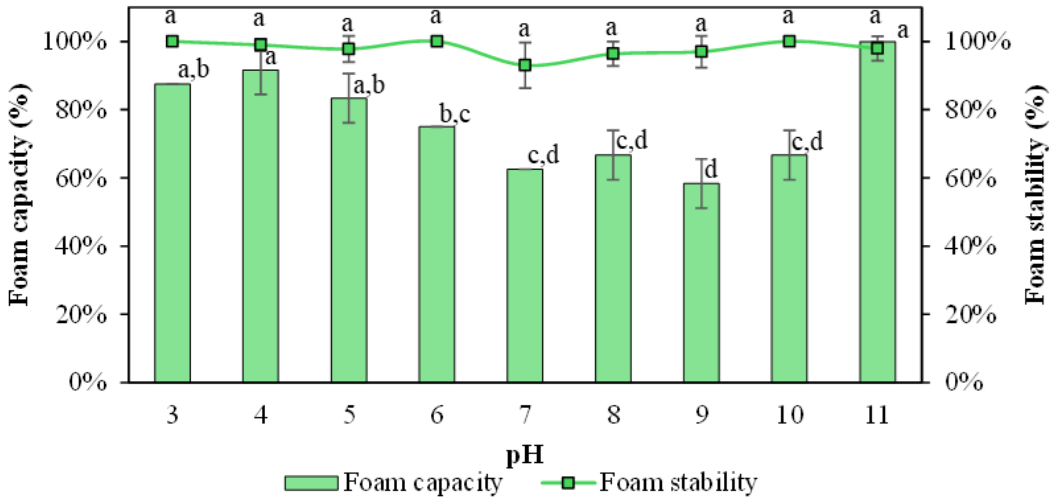
The highest turbidity is found at pH 5, which corresponds to the lowest solubility. At this pH, aggregation is favored, and the colloidal system is less stable since this pH is located in the region close to the average pI of the CPC (≈4.7, Figure 2.6a). The decrease in electrostatic repulsion around the isoelectric point (pI) led to hydrophobic interactions between non-polar amino acids, stimulating the formation of protein self-aggregates. As these aggregates grow, their solubility progressively decreases, untimely leading to precipitation (Omura et al., 2021). At pH values below or above 5, the decrease in turbidity is directly correlated to the increase in protein solubility.

From the relationship between solubility, ζ-potential, and turbidity, it can be concluded that the protein becomes more soluble as the pH moves away from the pI, especially at alkaline conditions, because protein-water interactions are favored at these pH levels, leading to lower turbidity values due to less precipitated matter (Omura et al., 2021; Mauri & Anon, 2006).

3.2.4 Foaming capacity and foam stability

Figure 2.7 provides data on the foaming capacity and foam stability as a function of the pH studied.

Figure Error! No text of specified style in document.**.10** Foaming capacity (bars) and foam stability (points) of CPC



Source: elaborated by the author.

It is possible to observe that at pH 3, 4, and 5, the foaming capacity of CPC was high, reaching 87.5% at pH 3, 91.7% at pH 4, and 83.3% at pH 5. These results demonstrate a good

foaming capacity in the vicinity of the isoelectric point, which is generally not expected (Damodaran et al., 2008). However, as documented by the same authors, a comparable behavior has been previously observed in albumin. The protein exhibited a diminished foaming capacity across the pH range of 6 to 10, with values oscillating between 58 to 75%. Conversely, the highest foaming capacity was observed at pH 11, reaching approximately 100%. The statistical analysis indicates that the foaming capacities at pH 3, 4, 5, and 11 are statistically equivalent and significantly higher than at pH 7, 8, 9, and 10, which are also similar to each other. The foaming capacity and stability of cowpeas have been previously reported by Mune & Sogi (2016) to be generally satisfactory. However, a comparison between the values derived from disparate methodologies reveals inconsistencies. Variables such as dispersion concentration, foaming equipment, rotor speed, foaming time, and protein content influence the results, as well as the extraction and drying processes of the proteins, which may also impact the outcomes (Mune & Sogi, 2016; Lee et al., 2020).

The results also demonstrate that the foam formed from CPC was markedly stable after 30 minutes of rest. Although the reduction in foam formation under specific pH conditions, the stability remained at nearly 100%, indicating that the CPC is capable of forming stable foams for over 30 minutes.

Both solubility and charge density affect the structural properties of proteins, which directly influence the foaming capacity. The partial unfolding of a protein affects its molecular rearrangement at the air-water interface, which can favor the formation of foam and its stability, as they are capable of further reducing surface tension (Aluko & Yada, 1997; Mune & Sogi, 2016).

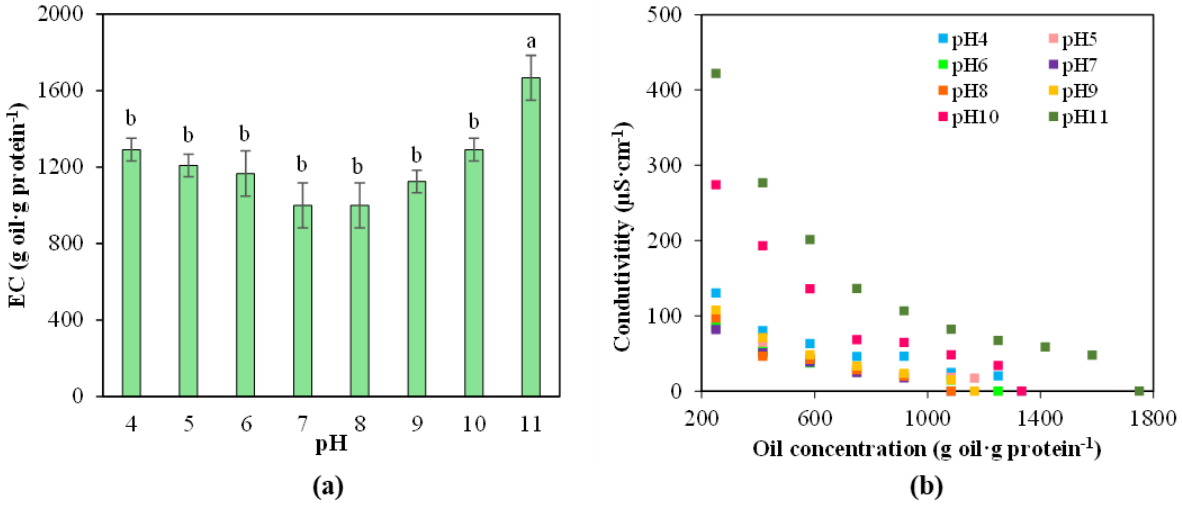
A correlation between the foaming capacity (Figure 2.7), solubility, and charge density (Figure 6 (a,b)) of the cowpea protein data reveals a protein with high solubility at most pH values studied and with an excellent ability to form foam, particularly at pH 11. At lower charge densities, such as those observed at pHs 3 – 5, protein-protein interactions are favored, promoting the formation of robust interfacial membranes and facilitating the foaming capacity (Aluko et al., 2009). At the same time, a high charge density present at pH values above 6 (Figure 6a) results in the weakening of hydrophobic interactions, thereby increasing the flexibility of proteins. This phenomenon enables proteins to unfold partially at the water/air interface, enhancing their capacity to encapsulate air particles, which contributes to a substantial increase in foam formation (Aluko & Yada, 1995; Ragab et al., 2004; Rangel et al., 2003).

3.2.5 Emulsifying capacity of cowpea protein concentrate (CPC)

The emulsifying capacity (EC) of the CPC was determined by potentiometry, in which the breaking or inversion point of the emulsion was identified by measuring the electrical conductivity. This point indicates that the oil becomes the continuous phase, as it is a component that presents conduction resistance.

This phenomenon is evident upon analysis of the curves in Figure 2.8a, wherein the conductivity approaches zero as the oil concentration increases. In addition to the expected variation concerning oil concentration, pH also exerts an influence. One particular note are pHs 10 and 11, which stand out among the curves, starting with significantly higher conductivities and decreasing more markedly with the addition of oil, while the other pH values show a less pronounced reduction in conductivity.

Figure Error! No text of specified style in document.**.11** The emulsifying capacity of CPC: (a) measurements of conductivity as a function of oil concentration for pH varying from 4 to 11 (b) oil concentration, at which the conductivity becomes zero



Source: elaborated by the author.

The EC values were found to be high, ranging from 1000 to 1666.67 g of oil per gram of protein. In a similar determination, Karaca and collaborators (2011) employed the potentiometry method to ascertain the emulsifying capacity of proteins extracted from chickpeas, broad beans, lentils, and peas by isoelectric precipitation, found values of approximately 477 to 520 (g oil/g protein) at pH 7. However, it is important to acknowledge

that the EC value is dependent upon the methodology employed in each study and is markedly influenced by various factors, including emulsion volume, emulsifying speed, oil type, protein concentration, and equipment utilized to prepare the emulsions (Pearce & Kinsella, 1978).

Although a tendency for EC values to increase as they move away from the neutral zone was observed, as shown in Figure 8b, this increase was only statistically significant at pH 11. In contrast, no statistically significant difference was observed at the other pH conditions. Despite CPC having a greater capacity to retain oil than water, the emulsifying capacity of a protein is not solely dependent on this ability.

The EC is associated with the solubility, surface charge, and molecular structure of the protein, as well as with protein-protein, protein-oil, and protein-water interactions (Gouvêa et al., 2023). The solubility, turbidity, and zeta potential data indicate that pH 11 represents a condition of greater negative charge density and protein solubility. Under these conditions, the protein dissociates and unfolds, exposing more hydrophobic groups on its surface and altering its conformational structure. This favors protein-water interaction and contributes to faster protein adsorption at the water-oil interface, consequently enhancing the EC (Shen et al., 2023). The surface hydrophobicity of the protein is also a significant factor to be considered. Proteins with a highly hydrophobic surface will interact more extensively with oil or fat, to the formation of stronger protein films that tend to become superior emulsifiers and enhance emulsifying capacity (Brishti et al., 2017).

As has been observed for other protein sources (Ragab et al., 2004; Shen et al., 2023; Ngui et al., 2021), the EC also exhibits lower values at pHs close to neutrality and higher values at extreme pHs. The findings of the study conducted by Shen et al. (2022) demonstrated that when isolated pea protein was subjected to pH 9, its capacity to adsorb at the interface was significantly enhanced, resulting in a higher emulsifying capacity than at pH 3, 5, and 7. This can be attributed to the existence of a flexible and soft conformation in PPI after treatment at pH 9, which promotes interfacial rearrangement and an increase in EC. Additionally, it was observed that an alkaline pH enhanced the capacity for emulsion formation in both, bambara and cowpea beans (Ngui et al., 2021; Ragab et al, 2004). The EC of a protein is intrinsically linked to the hydrophilic-lipophilic balance, which, in turn, depends on the pH (Ragab et al., 2004). Furthermore, an appropriate combination of solubility, hydrophobicity, and molecular flexibility contributes substantially to the high emulsifying capacity of globular proteins (Ngui et al., 2021).

4 Conclusion

This research explores the challenges and complexities of cowpea protein concentrate (CPC) and allows us to correlate molecular structure, chemical composition, and techno-functional properties. SDS-PAGE analysis of CPC reveals a diverse size distribution, with the presence of intense bands around 50 kDa, whose bands are characteristic of 7S globulins (vicilins). X-ray diffraction and FTIR analyses indicate an amorphous structure with a certain degree of crystallinity. The peak found at $2\theta=20.58°$ is primarily attributed to the predominant secondary structure, β-sheet, which contributes to an ordered and stable structure. The elevated denaturation temperature indicates enhanced thermal stability, which is likely attributable to the protein structure.

All essential amino acids present in cowpea beans are in adequate proportions, according to the recommendations set forth by the FAO for older age groups. Ratios between essential and non-essential amino acids in CPC remained consistent with the extraction yield. Furthermore, the study also demonstrates that conventional processing methods effectively reduce the levels of trypsin inhibitors, as evidenced by the significant decrease observed after soaking and protein extraction.

CPC demonstrates a pronounced affinity for oil than water, offering potential advantages for oil-rich food formulations. The impact of pH on CPC's electrokinetic potential, solubility, and turbidity is considerable. Conditions at the vicinity of the isoelectric point induce aggregation, reduce solubility, and increase turbidity, whereas extreme alkalinity enhances stability. The emulsifying and foaming capacities of CPC are high and pH-dependent. At pH 11, a noteworthy increase can be attributed to protein unfolding, which exposes hydrophobic residues and improves protein-water interaction.

The research underscores the relevance of CPC in the food and nutrition sectors and facilitates its use in various product formulations and nutritional enhancements. With its promising attributes and emerging recognition, CPC is positioned to overcome nutritional challenges and meet consumer demand for sustainable protein sources.

References

Almeida, F. C., de Souza, C. O., Philadelpho, B. O., Franca Lemos, P. V., Cardoso, L. G., Santana, J. S., ... & Druzian, J. I. (2021). Combined effect of cassava starch nanoparticles and protein isolate in properties of starch-based nanocomposite films. *Journal of Applied Polymer Science*, *138*(18), 50008. https://doi.org/10.1002/app.50008

Aluko, R. E., & Yada, R. Y. (1995). Structure-function relationships of cowpea (*Vigna unguiculata*) globulin isolate: influence of pH and NaCl on physicochemical and functional properties. *Food Chemistry, 53,* 259-265.

Aluko, R. E., & Yada, R. Y. (1997). Some physicochemical and functional properties of cowpea (*Vigna unguiculata*) isoelectric protein isolate as a function of pH and salt concentration. *International Journal of Food Sciences and Nutrition, 48(1),* 31-39.

Aluko, R. E., Mofolasayo, O. A., & Watts, B. M. (2009). Emulsifying and foaming properties of commercial yellow pea (*Pisum sativum* L.) seed flours. *Journal of Agricultural and Food Chemistry, 57(20),* 9793–9800. https://doi.org/10.1021/jf902199x

AOCS. Assaying trypsin inhibitor activity. Method Ba 12a-2020. First approval, 2020. Official methods and recommended practices of the AOCS. Urbana, IL: American Oil Chemists' Society; 2021.

Arntfield, S. D., & Murray, E. D. (1981). The influence of processing parameters on food protein functionality I. Differential scanning calorimetry as an indicator of protein denaturation. *Canadian Institute of Food Science and Technology Journal, 14(4),* 289-294.

Assegehegn, G., Brito-de la Fuente, E., Franco, J. M., & Gallegos, C. (2020). An Experimental-Based Approach to Construct the Process Design Space of a Freeze-Drying Process: An Effective Tool to Design an Optimum and Robust Freeze-Drying Process for Pharmaceuticals. *Journal of Pharmaceutical Sciences, 109(1),* 785–796. https://doi.org/10.1016/j.xphs.2019.07.001

Bradford, M. M. (1976). A rapid and sensitive method for the quantitation of microgram quantities of protein utilizing the principle of protein-dye binding. *Analytical Biochemistry, 72*(1–2), 248–254. https://doi.org/10.1016/0003-2697(76)90527-3

Brishti, F. H., Zarei, M., & Muhammad, K. (2017). Evaluation of the functional properties of mung bean protein isolate for development of textured vegetable protein Improving Bioavailability of Antihypertensive Bioactive Peptides Derived from Actinopyga lecanora. *International Food Research Journal, 24(4),* 1595-1605.

Brunelle, J. L.; & Green, R.. (2014). One-dimensional SDS-Polyacrylamide Gel Electrophoresis (1D SDS-PAGE). In: *Methods in Enzymology*. Elsevier, p. 151–159.

Campbell, L., Euston, S. R., & Ahmed, M. A. (2016). Effect of addition of thermally modified cowpea protein on sensory acceptability and textural properties of wheat bread and sponge cake. *Food Chemistry, 194,* 1230-1237. https://doi.org/10.1016/j.foodchem.2015.09.002

Carbonaro, M., & Nucara, A. (2010). Secondary structure of food proteins by Fourier transform spectroscopy in the mid-infrared region. *Amino acids, 38,* 679-690.

Carvalho, A. F. U., de Sousa, N. M., Farias, D. F., da Rocha-Bezerra, L. C. B., da Silva, R. M. P., Viana, M. P., Gouveia, S. T., Sampaio, S. S., de Sousa, M. B., de Lima, G. P. G., de Morais, S. M., Barros, C. C., & Filho, F. R. F. (2012). Nutritional ranking of 30 Brazilian genotypes of cowpeas including determination of antioxidant capacity and vitamins. *Journal of Food Composition and Analysis, 26(1–2),* 81–88. https://doi.org/10.1016/j.jfca.2012.01.005

Chel-Guerrero, L., Maldonado-Hoil, M., Burgos-Pérez, A., Castellanos-Ruelas, A. & Betancur–Ancona, D. (2011). Functional and some nutritional properties of an isoelectric protein isolate from Mexican cowpea (*Vigna unguiculata*) seeds. *Journal of Food and Nutrition Research, 50(4)*, 210–220.

Chen, J., Chen, X., Zhu, Q., Chen, F., Zhao, X., Ao, Q. (2013). Determination of the domain structure of the 7S and 11S globulins from soy proteins by XRD and FTIR. *Journal of the Science of Food and Agriculture, 93*, 1687-1691.

Clark, D. P., Pazdernik, N. J., & McGehee, M. R. (2019). Protein Structure and Function. In *Molecular Biology* (pp. 445–483). Elsevier. https://doi.org/10.1016/B978-0-12-813288-3.00014-8

Cui, L., Bandillo, N., Wang, Y., Ohm, J. B., Chen, B., & Rao, J. (2020). Functionality and structure of yellow pea protein isolate as affected by cultivars and extraction pH. *Food Hydrocolloids, 108*. https://doi.org/10.1016/j.foodhyd.2020.106008

Damodaran, S., & Parkin, K. L. (Eds.). (2008). *Fennema's food chemistry* (Fourth edition). CRC Press,Taylor & Francis Group.

Fan, F. & Roos, Y. H. (2016). Structural relaxations of amorphous lactose and lactose-whey protein mixtures. *Journal of Food Engineering, 179*, 106-115.

Faostat. Production quantities of Cow peas dry by country. Disponível em: <http://faostat.fao.org/>. Accessed January 30, 2024.

Freitas, M. L. F., Albano, K. M., & Telis, V. R. N. (2017). Characterization of biopolymers and soy protein isolate-high-methoxyl pectin complex. *Polimeros, 27(1)*, 62–67. https://doi.org/10.1590/0104-1428.2404

Freitas, R. L., Teixeira, A. R., & Ferreira, R. B. (2004). Characterization of the Proteins from Vigna unguiculata Seeds. *Journal of Agricultural and Food Chemistry, 52(6)*, 1682–1687. https://doi.org/10.1021/jf0300588

Frota, K. D. M. G., Lopes, L. A. R., Silva, I. C. V., & Arêas, J. A. G. (2018). Molecular profile, purity and presence of trypsin inhibitors in cowpea protein isolates. *Revista Caatinga, 31(1)*, 202–208. https://doi.org/10.1590/1983-21252018v31n123rc

Garrido, T., Etxabide, A., Guerrero, P., & De La Caba, K. (2016). Characterization of agar/soy protein biocomposite films: Effect of agar on the extruded pellets and compression moulded films. *Carbohydrate Polymers, 151*, 408–416. https://doi.org/10.1016/J.CARBPOL.2016.05.089.

Gómez, A., Gay, C., Tironi, V., & Avanza, M. V. (2021). Structural and antioxidant properties of cowpea protein hydrolysates. *Food Bioscience, 41*. https://doi.org/10.1016/j.fbio.2021.101074

Gouvêa, L., Caldeira, R., de Lima Azevedo, T., Galdeano, M. C., Felberg, I., Lima, J. R., & Grassi Mellinger, C. (2023). Physical and techno-functional properties of a common bean protein concentrate compared to commercial legume ingredients for the plant-based market. *Food Hydrocolloids, 137*. https://doi.org/10.1016/j.foodhyd.2022.108351

Hagen, S. R., Frost, B., & Augustin, J. (1989). Precolumn phenylisothiocyanate derivatization and liquid chromatography of amino acids in food. *Journal of the Association of Official Analytical Chemists*, *72*(6), 912-916. https://doi.org/10.1093/JAOAC/72.6.912

Hewage, S., & Vithanarachchi, S. M. (2009). Biodegradable polymer films from cowpea protein isolate Preparation and characterization of biodegradable polymer films from cowpea (*Vigna unguiculata*) protein isolate. *Journal of the National Science Foundation of Sri Lanka, 37(1),* 53-57.

Horax, R., Hettiarachchy, N. S., Chen, P., & Jalaluddin, M. (2004). Preparation and characterization of protein isolate from cowpea (*Vigna unguiculata L*. Walp.). *Journal of Food Science, 69(2)*. https://doi.org/10.1111/j.1365-2621.2004.tb15500.x

Jafari, M., Rajabzadeh, A. R., Tabtabaei, S., Marsolais, F., & Legge, R. L. (2016). Physicochemical characterization of a navy bean (Phaseolus vulgaris) protein fraction produced using a solvent-free method. *Food Chemistry*, *208*, 35-41. https://doi.org/10.1016/j.foodchem.2016.03.102

Karaca, A. C., Low, N., & Nickerson, M. (2011). Emulsifying properties of chickpea, faba bean, lentil and pea proteins produced by isoelectric precipitation and salt extraction. *Food Research International, 44(9),* 2742–2750. https://doi.org/10.1016/j.foodres.2011.06.012

Khalid, I. I., Elhardallou, S. B., & Elkhalifa, E. A. (2012). Composition and functional properties of cowpea (*Vigna ungiculata L*. Walp) flour and protein isolates. *American Journal of Food Technology, 7(3),* 113-122.

Kinsella, J. E. (1979). Functional properties of soy proteins. *Journal of the American Oil Chemists' Society*, *56(3),* 242-258.

Kitabatake, N., Tahara, M., & Doi, E. (1989). Denaturation temperature of soy protein under low moisture conditions. *Agricultural and Biological Chemistry*, *53*(4), 1201-1202.

Lawrence, M. C., Izard, T., Beuchat, M., Blagrove, R. J., & Colman, P. M. (1994). Structure of phaseolin at 2· 2 Å resolution: implications for a common vicilin/legumin structure and the genetic engineering of seed storage proteins. *Journal of Molecular Biology*, *238*(5), 748-776.

Lee, H. W., Lu, Y., Zhang, Y., Fu, C., & Huang, D. (2021). Physicochemical and functional properties of red lentil protein isolates from three origins at different pH. *Food Chemistry*, *358*, 129749. https://doi.org/10.1016/j.foodchem.2021.129749

Leser, S. (2013). The 2013 FAO report on dietary protein quality evaluation in human nutrition: Recommendations and implications. *Nutrition Bulletin, 38*(4), 421-428.

Liu, F. F., Li, Y. Q., Wang, C. Y., Zhao, X. Z., Liang, Y., He, J. X., & Mo, H. Z. (2021). Impact of pH on the physicochemical and rheological properties of mung bean (*Vigna radiata L*.) protein. *Process Biochemistry*, *111*, 274-284. https://doi.org/10.1016/j.procbio.2021.10.008

Locali-Pereira, A.R., Caruso, Í.Putinhon., Rabesona, H., Laurent, S., Meynier, A., Kermarrec, A., Birault, L., Geairon, A., Le Gall, S., Thoulouze, L., Solé-Jamault, Vé., Berton-Carabin, C., Boire, A., Nicoletti, V. R., Pre-treatment effects on the composition and functionalities of pigeon pea seed ingredients, *Food Hydrocolloids* (2024), doi: https://doi.org/10.1016/j.foodhyd.2024.109923

Makeri, M. U., Mohamed, S. A., Karim, R., Ramakrishnan, Y., & Muhammad, K. (2017). Fractionation, physicochemical, and structural characterization of winged bean seed protein fractions with reference to soybean. *International Journal of Food Properties*, *20*, 2220-2236.

Möller, A. C., van der Padt, A., & van der Goot, A. J. (2021). From raw material to mildly refined ingredient – Linking structure to composition to understand fractionation processes. *Journal of Food Engineering*, *291*. https://doi.org/10.1016/j.jfoodeng.2020.110321

Moser, P., Ferreira, S., & Nicoletti, V. R. (2019). Buriti oil microencapsulation in chickpea protein-pectin matrix as affected by spray drying parameters. *Food and Bioproducts Processing*, *117*, 183–193. https://doi.org/10.1016/j.fbp.2019.07.009

Mune, M. A. M., & Sogi, D. S. (2016). Emulsifying and Foaming Properties of Protein Concentrates Prepared from Cowpea and Bambara Bean Using Different Drying Methods. *International Journal of Food Properties*, *19(2)*, 371–384. https://doi.org/10.1080/10942912.2015.1023399

Murray, D. R., MacKenzie, K. F., Vairnhos, F., Peoples, M. B., Atkins, C. A., Pate, J. S. Electrophoretic studies of the seed proteins of cowpea, *Vigna unguiculata* (L.) Walp. (1983). *Zeitschrift für Pflanzenphysiologie*, *109*, 363-370.

Ngui, S. P., Nyobe, C. E., Bakwo Bassogog, C. B., Nchuaji Tang, E., Minka, S. R., & Mune Mune, M. A. (2021). Influence of pH and temperature on the physicochemical and functional properties of Bambara bean protein isolate. *Heliyon*, *7(8)*. https://doi.org/10.1016/j.heliyon.2021.e07824

Oliveira, M. M. G., Fessori, A. G. B. W., Huamaní-Meléndez, V. J., & Mauro, M. A. (2024). Exploring the rheological and thermal behavior of cowpea protein concentrate: Impact of pH and concentration. *Colloids and Surfaces A: Physicochemical and Engineering Aspects*, *694*, 134106. https://doi.org/10.1016/j.colsurfa.2024.134106

Oliveira, M. M. G., Silva, K. S., & Mauro, M. A. (2021). Evaluation of interactions between carboxymethylcellulose and soy protein isolate and their effects on the preparation and characterization of composite edible films. *Food Biophysics*, *16(2)*, 214-228. https://doi.org/10.1007/s11483-020-09659-3

Omura, M. H., de Oliveira, A. P. H., Soares, L. de S., Coimbra, J. S. dos R., de Barros, F. A. R., Vidigal, M. C. T. R., Baracat-Pereira, M. C., & de Oliveira, E. B. (2021). Effects of protein concentration during ultrasonic processing on physicochemical properties and techno-functionality of plant food proteins. *Food Hydrocolloids*, *113*. https://doi.org/10.1016/j.foodhyd.2020.106457

Park, J., Do, S., Lee, M., Ha, S., & Lee, K. G. (2022). Preparation of turmeric powder with various extraction and drying methods. *Chemical and Biological Technologies in Agriculture*, *9(1)*. https://doi.org/10.1186/s40538-022-00307-1

Pearce, K. N., & Kinsella, J. E. (1978). Emulsifying properties of proteins: evaluation of a turbidimetric technique. *Journal of agricultural and food chemistry*, *26(3)*, 716-723.

Penchalaraju, M., Poshadri, A., Swaroopa, G., Nikkam, I. T., & John Don Bosco, S. (2024). Leveraging Indian pulse proteins for plant-based mock meat III: physicochemical

characterisation, FTIR spectra and texture profile analysis of meat analogues. *International Journal of Food Science & Technology*, *59*(1), 649-660. https://doi.org/10.1111/ijfs.16828

Pereira, H. V. R., Saraiva, K. P., Carvalho, L. M. J., Andrade, L. R., Pedrosa, C., & Pierucci, A. P. T. R. (2009). Legumes seeds protein isolates in the production of ascorbic acid microparticles. *Food Research International*, *42*(1), 115-121.

Peyrano, F., de Lamballerie, M., Avanza, M. V., & Speroni, F. (2017). Calorimetric Study of Cowpea Protein Isolates. Effect of Calcium and High Hydrostatic Pressure. *Food Biophysics, 12(3)*, 374–382. https://doi.org/10.1007/s11483-017-9493-4

Peyrano, F., Speroni, F., & Avanza, M. V. (2016). Physicochemical and functional properties of cowpea protein isolates treated with temperature or high hydrostatic pressure. *Innovative Food Science and Emerging Technologies, 33*, 38–46. https://doi.org/10.1016/j.ifset.2015.10.014

Phan-Xuan, T., Bogdanova, E., Millqvist Fureby, A., Fransson, J., Terry, A. E., & Kocherbitov, V. (2020). Hydration-induced structural changes in the solid state of protein: A SAXS/WAXS study on lysozyme. *Molecular pharmaceutics*, *17*(9), 3246-3258. https://doi.org/10.1021/acs.molpharmaceut.0c00351

Prakash, S., Mishra, R., Malviya, R., & Sharma, K. (2014). Measurement Techniques and Pharmaceutical Applications of Zeta Potential: A Review. *Journal of Chronotherapy and Drug Delivery, 2*, 33–40. http://www.chronotherapyjournal.net

Ragab, D. D. M., Babiker, E. E., & Eltinay, A. H. (2004). Fractionation, solubility and functional properties of cowpea (*Vigna unguiculata*) proteins as affected by pH and/or salt concentration. *Food Chemistry, 84(2)*, 207–212. https://doi.org/10.1016/S0308-8146(03)00203-6

Rangel, A., Domont, G. B., Pedrosa, C., & Ferreira, S. T. (2003). Functional properties of purified vicilins from cowpea (*Vigna unguiculata*) and pea (*Pisum sativum*) and cowpea protein isolate. *Journal of Agricultural and Food Chemistry, 51(19)*, 5792–5797. https://doi.org/10.1021/jf0340052

Ricci, L., Umiltà, E., Righetti, M. C., Messina, T., Zurlini, C., Montanari, A., Bronco, S., & Bertoldo, M. (2018). On the thermal behavior of protein isolated from different legumes investigated by DSC and TGA. *Journal of the Science of Food and Agriculture, 98(14)*, 5368–5377. https://doi.org/10.1002/jsfa.9078

Romero, J., Sun, S. M. M., McLeester, R. C., Bliss, F. A., & Hall, T. C. (1975). Heritable variation in a polypeptide subunit of the major storage protein of the bean, Phaseolus vulgaris L. *Plant Physiology*, *56*(6), 776-779.

Rosenfeld, D. L., Rothgerber, H., & Janet Tomiyama, A. (2020). From mostly vegetarian to fully vegetarian: Meat avoidance and the expression of social identity. *Food Quality and Preferenc*e, *85*. https://doi.org/10.1016/j.foodqual.2020.103963

Rozenberg, M., Shoham, G. (2007). FTIR spectra of solid poly-L-lysine in the stretching NH mode range. *Biophysical Chemistry*, *125*, 166–171. https://doi.org/10.1016/j.bpc.2006.07.008

Rudra, S. G., Sethi, S., Jha, S. K., & Kumar, R. (2016). Physico-chemical and functional properties of cowpea protein isolate as affected by the dehydration technique. *Legume Research, 39(3)*, 370–378. https://doi.org/10.18805/lr.v0iOF.9441

Rui, X., Wen, D., Li, W., Chen, X., Jiang, M., & Dong, M. (2015). Enrichment of ACE inhibitory peptides in navy bean (*Phaseolus vulgaris*) using lactic acid bacteria. *Food & Function*, *6*(2), 622-629.

Sadat, A., & Joye, I. J. (2020). Peak fitting applied to fourier transform infrared and raman spectroscopic analysis of proteins. *Applied Sciences (Switzerland)*, *10*(17). https://doi.org/10.3390/app10175918

Sanches, M. A., Camelo-Silva, C., Tussolini, L., Tussolini, M., Zambiazi, R. C., & Becker Pertuzatti, P. (2021). Development, characterization and optimization of biopolymers films based on starch and flour from jabuticaba (*Myrciaria cauliflora*) peel. *Food Chemistry, 343*. https://doi.org/10.1016/j.foodchem.2020.128430

Shen, Q., Dai, H., Wen, L., Zheng, W., Li, B., Dai, J., Li, B., & Chen, Y. (2023). Effects of pH-shifting treatments on the emulsifying properties of rice protein isolates: Quantitative analysis of interfacial protein layer. *Food Research International, 164*. https://doi.org/10.1016/j.foodres.2022.112306

Shen, Y., Babu, K. S., Amamcharla, J., & Li, Y. (2022). Emulsifying properties of pea protein/guar gum conjugates and mayonnaise application. *International Journal of Food Science and Technology, 57(7)*, 3955–3966. https://doi.org/10.1111/ijfs.15564

Shevkani, K., Kaur, A., Kumar, S., & Singh, N. (2015a). Cowpea protein isolates: Functional properties and application in gluten-free rice muffins. *LWT, 63(2)*, 927–933. https://doi.org/10.1016/j.lwt.2015.04.058

Shevkani, K., Singh, N., Kaur, A., & Rana, J. C. (2015b). Structural and functional characterization of kidney bean and field pea protein isolates: A comparative study. *Food Hydrocolloids, 43*, 679–689. https://doi.org/10.1016/j.foodhyd.2014.07.024

Spendrup, S., & Hovmalm, H. P. (2022). Consumer attitudes and beliefs towards plant-based food in different degrees of processing – The case of Sweden. *Food Quality and Preference, 102*. https://doi.org/10.1016/j.foodqual.2022.104673

Spies, J. R. Determination of tryptophan in protein. *Analytical Chemistry*, v. 39, n. 9, p. 1412-1415, 1967.

Stone, A. K., Karalash, A., Tyler, R. T., Warkentin, T. D., & Nickerson, M. T. (2015). Functional attributes of pea protein isolates prepared using different extraction methods and cultivars. *Food Research International, 76(P1)*, 31–38. https://doi.org/10.1016/j.foodres.2014.11.017

Stuart, B. H. (1997). *Biological applications of infrared spectroscopy*. John Wiley & Sons.

Tang, X., Shen, Y., Zhang, Y., Schilling, M. W., & Li, Y. (2021). Parallel comparison of functional and physicochemical properties of common pulse proteins. *LWT, 146*. https://doi.org/10.1016/j.lwt.2021.111594

Vasconcelos, I. M., Maia, F. M. M., Farias, D. F., Campello, C. C., Carvalho, A. F. U., de Azevedo Moreira, R., & de Oliveira, J. T. A. (2010). Protein fractions, amino acid composition and antinutritional constituents of high-yielding cowpea cultivars. *Journal of Food Composition and Analysis, 23(1),* 54–60. https://doi.org/10.1016/j.jfca.2009.05.008

Wang, H., Tong, X., Yuan, Y., Peng, X., Zhang, Q., Zhang, S., Xie, C., Zhang, X., Yan, S., Xu, J., Jiang, L., Qi, B., & Li, Y. (2020). Effect of Spray-Drying and Freeze-Drying on the Properties of Soybean Hydrolysates. *Journal of Chemistry*, 2020. https://doi.org/10.1155/2020/9201457

White, J. A., Hart, R. J., & Fry, J. C. (1986). An evaluation of the Waters Pico-Tag system for the amino-acid analysis of food materials. *The Journal of Automatic Chemistry*, *8*(4), 170.

Wu, G., Hui, X., Liang, J., Liu, H., Chen, H., Gong, X., Brennan, M. A., Zeng, X. A., Guo, X., & Brennan, C. S. (2021). Combination of rehydrated whey protein isolate aqueous solution with blackcurrant concentrate and the formation of encapsulates via spray-drying and freeze-drying: Alterations to the functional properties of protein and their anticancer properties. *Food Chemistry, 355*. https://doi.org/10.1016/j.foodchem.2021.129620

Yadav, N., Kaur, D., Malaviya, R., Saini, P., & Anjum, S. (2019). Enhancement in mineral bioavailability of extruded pulses with reduced antinutrients. British Food Journal, 121(11), 2967-2978. https://doi.org/10.1108/BFJ-04-2019-0236

Zhao, J., Cui, J. K., Chen, R. X., Tang, Z. Z., Tan, Z. L., Jiang, L. Y., & Liu, F. (2021). Real-time in-situ quantification of protein secondary structures in aqueous solution based on ATR-FTIR subtraction spectrum. Biochemical Engineering Journal, 176, 108225.

Zimmerman, J. M., Eliezer, N., & Simha, R. (1968). The characterization of amino acid sequences in proteins by statistical methods. *Journal of theoretical biology*, *21*(2), 170-201. https://doi.org/10.1016/0022-5193(68)90069-6

3 EXPLORING THE RHEOLOGICAL AND THERMAL BEHAVIOR OF COWPEA PROTEIN CONCENTRATE: IMPACT OF PH AND CONCENTRATION

Maria Mariana Garcia de Oliveira[a], Ana Gabriela Baroni Wicher Fessori[a], Víctor Justiniano Huamaní-Meléndez[a] and Maria Aparecida Mauro[a]

[a] Department of Food Engineering and Technology, Institute of Biosciences, Humanities and Exact Sciences – São Paulo State University (UNESP), Street Cristóvão Colombo, 2265, São José do Rio Preto 15054-000, Brazil.

e-mail address: maria.mariana@unesp.br (corresponding author)

Article published in the journal
Colloids and Surfaces A: Physicochemical and Engineering Aspects
(DOI: doi.org/10.1016/j.colsurfa.2024.134106)
Rights to use the article as part of the Thesis in Appendix A.

Abstract

This study confronts challenges from global population growth, focusing on protein supply strains and the environmental impact of traditional animal sources. Delving into unexplored territory, this study investigates the combined effects of pH, concentration, and temperature on the rheological and thermal properties of cowpea protein concentrate (CPC). Steady-state and oscillatory rheological tests, along with differential scanning calorimetric analysis, were conducted to unveil the behavior of CPC solutions. The results revealed sensitivity to protein concentration and shear rate, especially at higher concentrations (>10%), and pH emerged as a critical factor, significantly influencing shear stress and viscosity. The elastic and viscous components of alkaline CPC solutions exhibit weak gel behavior, influenced by both pH and frequency. Temperature-induced changes in viscosity and gelation highlight the interaction between thermal conditions and protein structures. The thermal cycle helps explain changes in molecular interactions induced by temperature, with pH playing a role in influencing gelatinization and denaturation. The denaturation temperature (T_d) in the thermograms corresponds to vicilin fractions and emphasizes the prominence of denaturation and gelation at neutral pH, where T_d was pH 7 > pH 9 > pH 11. Alkaline pH induced significant structural changes, resulting in a gelation onset temperature below the denaturation onset temperature. This study provides a deeper understanding into the rheological and thermal properties of CPC solutions, emphasizing the roles of concentration, pH, and temperature, useful for various steps of industrial processing, before and after thermal gelation. These findings are important for promoting the use of cowpea proteins in the food industry in response to the evolving needs of a growing global population.

Keywords: Rheology; Differential Scanning Calorimetry; Apparent Viscosity; Protein Denaturation; Plant Protein

1 Introduction

Projections conducted by the United Nations (2022) indicate that the world population could reach >11 billion people by the year 2100. The growing increase in population presents significant challenges to food security and sustainability, inevitably resulting in a lack of protein supply, primarily from animal sources. Protein production becomes a concern due to the intensive land and resource requirements of traditional animal sources, impacting biodiversity, natural resource depletion, climate change, and high production, maintenance, and market costs (De Boer, Schösler & Aiking, 2014; Van-Zanten, Mollenhorst, Klootwijk, Middelaar & Boer, 2016; Henchion et al., 2017; González-Pérez &Arellano, 2009; Sabaté, Sranacharoenpong, Harwatt, Wien & Soret, 2015).

Moreover, the increasing popularity of vegan, vegetarian, and flexitarian diets (Spendrup & Hovmalm, 2022; Rosenfeld, Rothgerber, & Tomiyama, 2020) has made them attractive targets for the food industry. In this context, proteins obtained from plants, cereals, and legumes offer an alternative, either to be included in or to substitute for human diets and food systems. Proteins with technologically useful functional properties, such as solubility and the ability to form emulsions, foams, or gels, are being researched, and protein isolates and concentrates from various legumes meet these requirements (Shen et al., 2022; Aluko, Mofolasayo & Watts, 2009; Ragab, Babiker & Eltinay, 2004).

In this context, plant-based proteins, including those obtained from legumes such as cowpea (*Vigna unguiculata* (L.) Walp), have stood out due to their functional properties and composition (Ragab et al., 2004; Aluko & Yada, 1995). Predominantly cultivated in Africa, a continent responsible for 95% of the global production, cowpea is highly adaptable and nutritious, with a notable protein content of 20%–30% on a dry basis (Frota, Soares & Arêas, 2008; Frota, Lopes, Silva & Arêas, 2018; Carvalho et al., 2012; Appiah, Asibuo & Kumah, 2011). Despite being underutilized in the food industry, cowpea protein holds vast application potential. The large globulin fraction (vicilin) of cowpea protein confers specific functional properties such as foaming capacity, emulsifying activity (Rangel et al., 2003), thermal stability and hydrophobicity, making it a valuable ingredient for food development applications (Zhang, Gao, Yang, 2009). Due to its properties and functionalities, this protein plays an important role as a raw material, ingredient, and/or food additive in studies replacing wheat flour in baked products such as biscuits (Moongngarm et al., 2014). Cowpea protein also has the advantage of being rich in lysine, which is the limiting amino acid for most cereals (Horax et al., 2004; Rangel et al., 2003, Saio et al., 1978). In addition, cowpea protein contributes to the production of microparticles capable of protecting and releasing specific components (Pereira et al., 2009)

and the development of biodegradable films with the potential to replace conventional plastics (Hewage; Vithanarachchi, 2009). Moreover, recent studies have highlighted its excellent antioxidant properties and functional improvements after thermal treatment (Gómez, Gay, Tironi & Avanza, 2023; Almeida et al., 2022; Thompson, Acevedo, Añón & Avanza, 2023). Recently, a new research frontier, modified surface materials via mussel-inspired chemistry, has shown potential for obtaining self-healing materials (Jiang et al., 2019), such as hydrogels designed based on food residues (Liu et al., 2019) or plant proteins (Xiao et al., 2023). Rheology has been widely employed as a fundamental tool to investigate and understand the behavior of these materials under different processing conditions, particularly concerning their mechanical performance, including tensile strength and deformation, as well as the characterization of the rheological parameters G′ (storage modulus) and G″ (loss modulus). The importance of rheology-extends beyond analysis, encompassing process optimization and quality assurance, as it allows observing how gel properties are sensitive to factors such as concentration, temperature, pH and pressure (Sosa et al., 2023, Chen et al., 2022; Peyrano, De Lamballerie, Avanza & Speroni, 2019; Peyrano, Speroni & Avanza, 2016).

Based on scientific evidence, it has been shown that protein solutions undergo behavioral transitions under different processing conditions, exhibiting both viscous and elastic behavior. In addition, proteins are highly sensitive to pH. However, to the best of our knowledge, the effect of pH, simultaneously with other process variables, on the physical and rheological properties of the cowpea protein solutions, particularly for industrial food applications, has not been reported.

Therefore, understanding the behavior of cowpea protein under different processing conditions, is essential to optimize its industrial use at all stages of the process. This study aims to gain an in-depth understanding of the combined effects of concentration, pH, and temperature on rheological and thermal properties and explain them in terms of structural changes and intermolecular interactions. The evaluation of viscosity, elasticity, and flow patterns in protein solutions and gels is fundamental to elucidate these transformations and provide valuable information and clarification on how these factors affect the properties of cowpea protein concentrate (CPC) solutions, during processing.

2 Material and methods

2.1 Material

As the object of the study, CPC extracted through the isoelectric precipitation method (Moser, Ferreira & Nicoletti, 2019) and lyophilized by the JJ Científica Co. (São Carlos, São Paulo, Brazil) was used. The protein concentrate contained in its composition 78.63% ± 0.90% of proteins, 10.34% of carbohydrates, 6.73% ± 0.04% of moisture, 3.38% ± 0.03% of ash, and 0.93% ± 0.03% of lipids. The CPC sample is composed of protein fractions with molecular weights ranging from 10 kDa to 280, with the predominance of polypeptides in the 41 to 55 kDa size range. For the preparation of solutions containing CPC, distilled water was used for dilution, as well as analytical-grade reagents such as sodium hydroxide (40%, m/m) and hydrochloric acid (50%, m/m) for the pH correction of the samples.

2.2 Methods

2.2.1 Protein dispersions

Aqueous dispersions of CPC with a protein content of 1%, 2%, 3%, 4%, 5%, 10%, and 20% (m/m) were prepared at room temperature (25 °C) and were mixed for 5 min with a homogenizer ultra-turrax (T18 basic, IKA, Brazil). Following the same preparation method, an aqueous solution containing 5% CPC was prepared at different pH values (3, 5, 7, 9, and 11).

2.2.2 Rheological behavior

The rheological behavior of aqueous solutions of CPC and the effects of protein concentration (1%–20%; m/m), pH (3–11), and temperature on this behavior were evaluated. Rheological characterization was performed through steady-state and oscillatory tests using an AR-2000EX rotational rheometer (TA Instruments, New Castle, DE, USA) equipped with a Peltier system for temperature control during measurements. The concentric cylinder geometry was used to determine the shear stress curves as a function of the shear rate. To assess the influence of temperature on rheological properties, the cone and plate geometry (steel cone with a 61 mm diameter and 52 μm gap) were selected due to their better temperature control capabilities, as they have a smaller contact area and require a smaller sample quantity to conduct the test.

2.2.2.1 Steady-state tests—effect of protein concentration, pH, and temperature

Shear stress versus shear rate curves were obtained for samples varying their CPC concentrations from 1% to 20%. Based on these results, stress versus shear rate curves were then determined for the samples at different pH values (3–11), this time keeping the CPC content constant at 5%. Evaluations were performed over a range of 0.1–158 s^{-1} at 25 °C. The data were fitted to the power law and Herschel–Bulkley models (Rao, 2007; Bird, 1987), Equations (1) and (2), respectively, and the goodness of fit was assessed based on the coefficient of determination (R^2).

$$\tau = K\dot{\gamma}^n \quad (1)$$

$$\tau = \tau_0 + K\dot{\gamma}^n \quad (2)$$

in which τ (Pa) is the shear stress, $\dot{\gamma}$ (s^{-1}) is the shear rate, K (Pa s) is the consistency index, and n is the behavior index and τ_0 is the yield stress.

Viscosity is not a property of non-Newtonian fluids, which vary with shear rate. Therefore, an apparent viscosity η_a (Pa s) is usually calculated from Equation (3) (Rao, 2007).

$$\eta_a = \frac{\tau}{\dot{\gamma}} \quad (3)$$

The behavior of acid solutions was explained by the Cross model (Cross, 1965), which describes the dependence of the apparent viscosity, η_a (Pa s), on the shear rate, $\dot{\gamma}$ (s^{-1}), according to Equation (4).

$$\eta_a = \eta_\infty + \frac{\eta_0 - \eta_\infty}{1+(\alpha\dot{\gamma})^m} \quad (4)$$

where, m is the Cross exponent, η_a is the apparent viscosity (Pa s), η_0 and η_∞ are the zero-shear rate viscosity and the infinite-shear rate viscosity (Pa s), respectively, and α is the Cross time constant, related to the relaxation time (s).

To assess the impact of temperature on rheological properties, temperature ramp analyses were performed while keeping the protein concentration at 5% (m/m). A shear rate of

100 s^{-1} was applied with a heating rate of 2 °C min^{-1}. The test comprised three stages: initially, a heating stage from 25 °C to 80 °C, followed by a cooling stage down to 5 °C, and finally, reheating the sample to 25 °C.

2.2.2.2 Dynamic tests—frequency sweeps and thermal cycle

Due to equipment limitations, the oscillatory tests were performed with aqueous solutions containing 10% CPC. This decision was based on the observed similarity in rheological behavior between the 5% and 10% solutions, as evidenced by the statistical equivalence in the consistency index (K) and *n* parameters, as discussed in the Results and Discussion section. To determine the region of linear viscoelastic behavior (LVR), oscillatory stress sweeps were performed at a frequency of 0.1 rad s^{-1} with strain values ranging from 0.0001% to 1.0%. Frequency sweeps were then performed at a constant strain of 0.1% within the LVR range to obtain the mechanical spectra: storage modulus (G′) and loss modulus (G″). All dynamic tests were conducted at a temperature of 25 °C.

The thermal cycle consisted of a heating stage from 25 °C to 90 °C at a heating rate of 2 °C min^{-1}, followed by an isothermal step of 20 min at 90 °C and a cooling stage to 40 °C at 2 °C min^{-1}. The thermal cycle was conducted at 0.1% strain and 0.1 rad s^{-1}.

From the storage (G′) and loss (G″) moduli, it is possible to calculate the complex viscosity, η* (Equation (5)), where G* is the dynamic complex modulus, and the phase angle tangent (Equation (6)) (Winter, 2009; Khanna, 1991). Molecules can undergo two types of motion: elastic displacement and viscous flow, the occurrences of which depend on frequency. Complex viscosity considers both the viscous and elastic aspects of a material's behavior, measured at an oscillating frequency. Equation (5) shows the dependence of complex viscosity on frequency (ω) (Khanna, 1991).

$$\eta^* = \frac{\sqrt{G'^2 + G''^2}}{\omega} = \frac{G^*}{\omega} \quad (5)$$

$$\tan(\delta) = \frac{G''}{G'} \quad (6)$$

2.2.3 Differential scanning calorimetry

A differential scanning calorimeter (Pyris 1, Perkin Elmer, Norwalk, CT, USA) was used to study, in duplicate, the thermal properties of aqueous solutions of concentrated cowpea protein prepared as described in Section 2.2.1, at a concentration of 20% (m/m) and pH levels of 7, 9, and 11. Indium was used as a standard for temperature and heat flow calibration, and an empty pan was used as a reference for the analysis. Hermetically sealed aluminum pans were prepared, containing approximately 9–10 mg of each sample. The samples were heated at a rate of 10 °C min^{-1} from 25 °C to 100 °C.

3 Results and discussion

3.1 Steady-state rheological tests

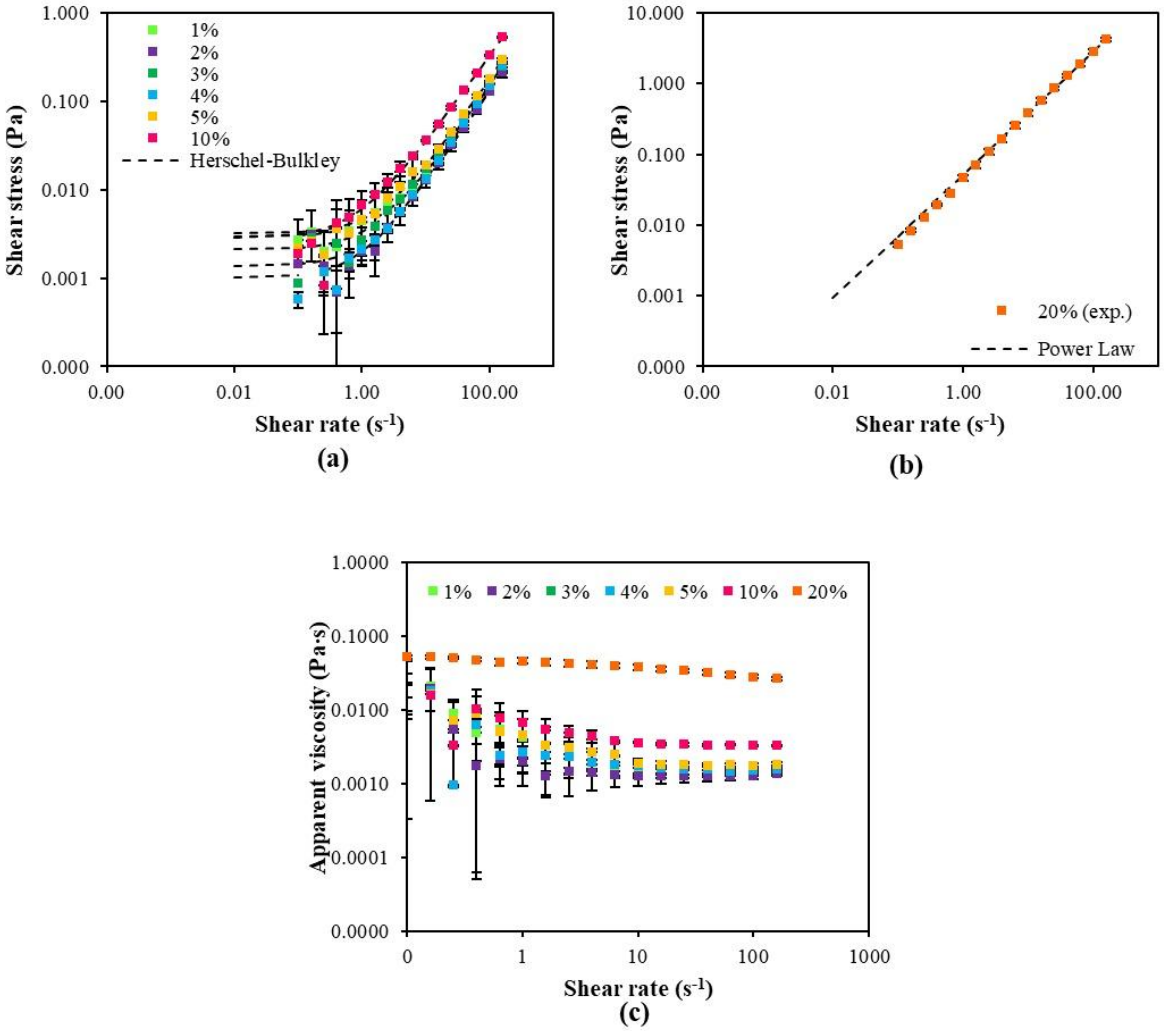
3.1.1 Influence of protein concentration on the rheological properties of aqueous CPC dispersions

The effect of shear rate and concentration (1%–20%, m/m) of solutions of CPC on shear stress and viscosity is shown in Figs. 1(a, b, c).

Notably, these solutions were intentionally maintained at the natural pH of the mixture, which varied within a range of 7.0 (1%)–6.5 (20%) without any pH adjustment. The significance of pH will be explored in subsequent sections. From the flow curves, different behaviors were observed. Solutions with lower protein concentrations (1%–5%, m/m) show similar rheological behavior, with some increase in shear stress as protein concentration increases, especially at higher shear rates. Higher concentrations (10% and 20%) show a more pronounced increase in shear stress at higher shear rates. Examining the data for the highest protein concentration (20%), it is evident that the fluid reaches >10 times higher shear stresses as the shear rate increases. This could be explained by an increase in intra- or intermolecular entanglements, which may initially provide a high shear resistance, leading to a more pronounced shear thinning behavior (Huang, Zeng, Xiong & Huang, 2016). Therefore, the concentration of the medium above a critical value can change the tendency of diluted solutions and lead to a far higher flow resistance (Huamaní-Meléndez, Mauro & Darros-Barbosa, 2021).

Since the flow curves of CPC solutions at 1%–10% concentration show yield stress, the Herschel–Bulkley model (Equation (2)) was used. By contrast, at 20% concentration, the power law model (Equation (1)) was applied. Their parameters are shown in Table 3.1.

Figure Error! No text of specified style in document.**.12** Flow curves of CPC solutions at: (a) 1% to 10%, m/m; (b) 20%, m/m. (c) Apparent viscosity as a function of the shear rate for CPC solutions (1% to 20%). Herschel-Bulkley model (dotted lines, Equation (2)); Power Law model (solid line, Equation (1)); experimental data (points).



Source: elaborated by the author.

The consistency index (K), which describes the resistance of the material to deformation at a given shear stress, showed statistically similar values among samples with CPC concentrations ranging from 1% to 10%. Conversely, the sample containing 20% protein concentrate showed significantly higher values. Correlating Figure 3.1c with the K index values, it is evident that there is a relationship between fluid viscosity and concentration. The higher the fluid viscosity is, the higher the magnitude of K is, resulting in a greater resistance to deformation.

Table Error! No text of specified style in document.**.7** Rheological parameters of the Herschel-Bulkley model (Equation (2)) for CPC solutions (1 to 10%, m/m) and of the Power Law model (Equation (1)) for CPC solution (20%, m/m).

CPC concentration (%)	$\tau_0 \times 10^3$ (Pa)	$K \times 10^3$ (Pa s^n)	n (-)	R^2
1	0.95 ± 0.02^{a}	1.03 ± 0.03^{a}	1.05 ± 0.01^{ab}	0.999
2	1.38 ± 0.08^{a}	0.96 ± 0.04^{a}	1.07 ± 0.01^{ab}	0.999
3	3.20 ± 1.63^{a}	1.18 ± 0.16^{a}	1.06 ± 0.02^{ab}	0.999
4	1.28 ± 0.90^{a}	0.95 ± 0.05^{a}	1.10 ± 0.01^{b}	0.999
5	4.29 ± 2.71^{a}	1.33 ± 0.02^{a}	1.06 ± 0.01^{ab}	0.999
10	4.16 ± 1.40^{b}	3.10 ± 0.09^{a}	1.01 ± 0.01^{a}	0.999
20	-	51.46 ± 4.77^{b}	0.87 ± 0.01^{c}	0.999

The results are expressed as the mean ± standard deviation. Means with the same lowercase letter in the same column did not differ significantly at $p \leq 0.05$ according to Tukey's test.

Through the apparent viscosity (Figure 3.1c), it is also possible to observe that, for shear rates <10 s^{-1}, there was a slight decrease in viscosity with increasing shear rate. In these regions, the flow occurs through layers of more organized particles, minimizing contact between them and resulting in shear thinning. Therefore, at low shear rates (<10 s^{-1}), for concentrations up to 10%, the protein solutions behaved as pseudoplastic fluids, whereas above this critical rate value, the viscosity remained unchanged, regardless of changes in the shear rate, resembling Newtonian fluids (Huang et al., 2016; Zarei & Aalaie, 2020; Wei, Lin & Liu, 2019). The 20% CPC curve is an exception to this behavior, as it shows a continuous decrease in apparent viscosity over the entire range of shear rates evaluated. Beliciu and Moraro (2011) observed a similar pattern, although more pronounced, for soy protein, where the viscosity decreased with increasing shear rates for solutions with concentrations >7.5%. A possible explanation for the decrease in viscosity of concentrated solutions is that chain entanglement is reduced and the three-dimensional macromolecule has a better orientation during flow (Varesano, Aluigi, Vineis & Tonin, 2008). In this scenario, protein molecules deform and elongate in the direction of flow, leading to a reduction in apparent viscosity due to heightened shear stress (Malhotra & Coupland, 2004; Taherian et al., 2011; Saricaoglu, 2020).

In summary, shear stress and viscosities increased with increasing concentration. This increase was accentuated for the 20% concentration solution, suggesting that macromolecular chains overlap and become entangled in concentrated media. Shear rates up to 10 s^{-1} caused a decrease in viscosity from 1% to 10% solutions, after which it was almost constant. By contrast, at 20%, it decreased over the entire shear rate range, probably due to a better alignment of the molecules.

One of the innovative aspects of CPC dispersions lies in their low viscosity, which represents an advantage in various operations in the context of food engineering, science, and technology. In addition to the operational benefits, this unique characteristic provides advantages in terms of the efficient incorporation of proteins into products such as liquid foods (Liu et al. 2021), allows the formulation of film-forming solutions and coatings that are evenly distributed over food and surfaces (Hewage; Vithanarachchi, 2009), and enables the production of smaller-sized particles in emulsions and particulate systems (Thompson et al., 2023; Pereira et al., 2009).

3.1.2 Effect of pH on flow and apparent viscosity of aqueous CPC dispersions

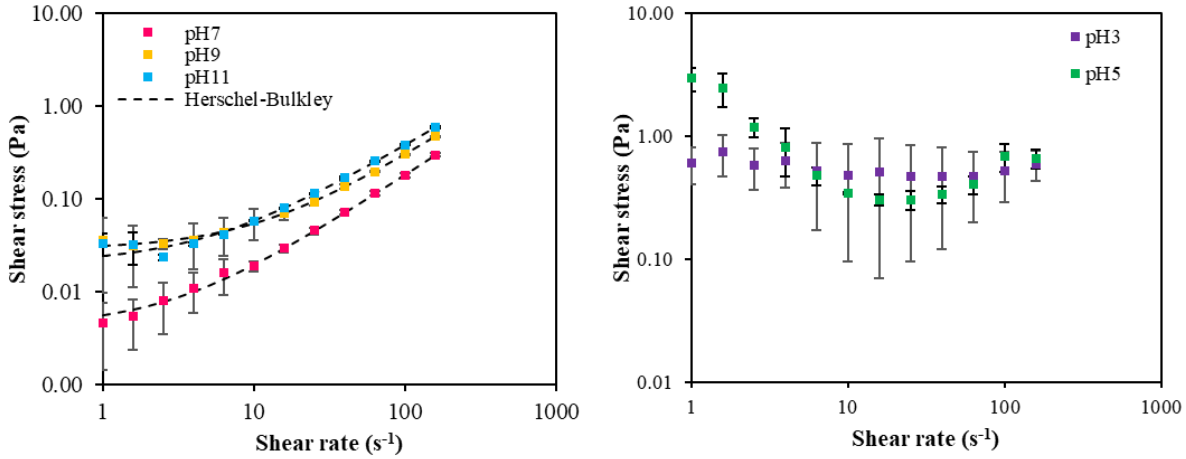
With an interest in exploring the use of diluted solutions, and based on the results of previous assays, it was found that these solutions exhibit similar behaviors. Therefore, the concentration of 5% CPC was selected to continue the rheological tests.

The behavior of CPC dispersions (5%, m/m) over a pH range from 3 to 11 was evaluated and is shown in Figs. 2(a, b) on a logarithmic scale to facilitate the visualization of the pH effect. Conversely, the error bars have an asymmetric appearance due to the scale.

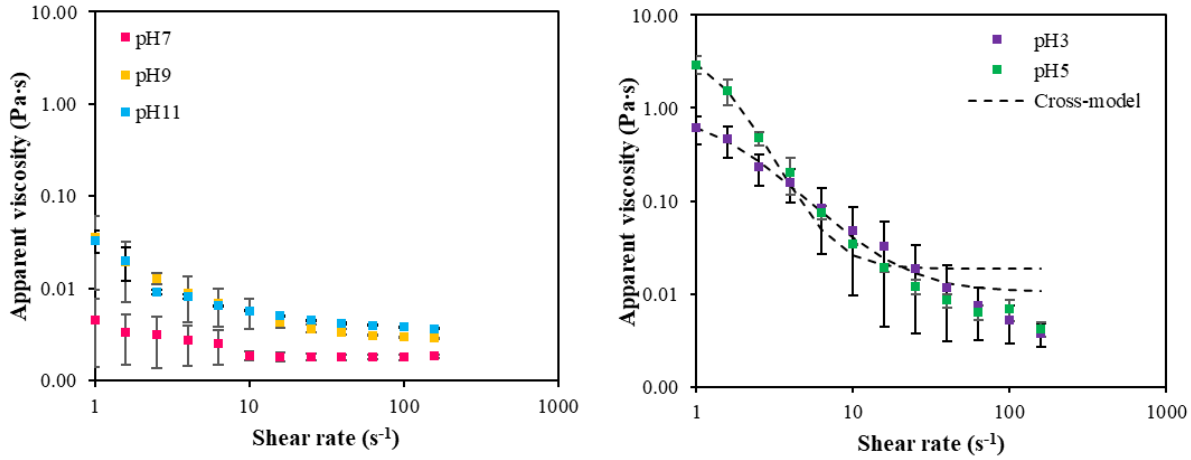
As with concentration, pH altered the rheological properties of the CPC dispersions. At neutral (pH 7) and alkaline (pH 9 and 11) conditions, the Herschel–Bulkley model was used to fit the experimental data and determine the yield stress. The fitting parameters are shown in Table 3.2, and, except for an initial yield stress (Table 3.2), *n* remained statistically unchanged and close to 1, regardless of the condition of the medium. Increasing the pH affected the viscosity of the fluid, with a notable increase particularly evident when comparing pH 7 with pH 9 and 11, as confirmed in Figure 3.2b. However, starting at 10 s^{-1}, apparent viscosity was almost independent of the shear rate, and the solution resembled a Newtonian fluid (Huang et al., 2016).

The CPC solutions prepared at pH of 3 and 5 exhibited a distinct variation in shear stress and viscosity with shear rate. Throughout the range analyzed, pH 3 maintained a narrow stress range of 0.5–0.7 Pa, with a slight increase toward the end of the process. Conversely, pH 5 showed a decrease in stress with increasing shear rate up to a critical rate of approximately 20 s^{-1}, after which the stress started to increase again. Hence, the utilization of the Herschel–Bulkley model, which was previously satisfactorily fitted to experimental data for pH of 7–11, became a less representative choice.

Figure Error! No text of specified style in document.**.13** Rheological behavior of CPC solutions (5%, m/m) at pH 3, 5, 7, 9 and 11: (a) Shear stress versus shear rate and fitting of the Herschel-Bulkley model (line, Equation (2)) to experimental data (points) for pH 7, 9 and 11; (b) Apparent viscosity versus shear rate and fitting of the Cross model (lines, Equation (4)) to experimental data (points) at pH 3 and 5.



(a)



(b)

Source: elaborated by the author.

The apparent viscosity behavior of pH 3 and 5 (Figure 3.2b) suggests three regions that characterize shear-induced rearrangements in the conformation of the molecular chains (Rao, 2007). At this pH range, proteins adopt a more compact and globular conformation due to proximity to the isoelectric point, resulting in the formation of larger particles in clusters (Jaramillo et al., 2011), which aggregates remain due to hydrophobic attraction between molecules (Ge et al., 2021; Rudra et al., 2016). With the application of low shear, molecules

begin to untangle, leading to a reduction in viscosity as shear increases, until they reach a state of maximum disentanglement, and no rearrangements occur (Rao, 2007). This rheological behavior can be accurately described by the Cross model ($R^2 > 0.99$), which states that at low shear rates, the fluid exhibits Newtonian properties with constant η_0; then, in a shear thinning range of shear rates, the dispersion viscosity decreases according to the power law relationship; and finally, the shear rate is sufficiently high that the polymer chains do not undergo considerable rearrangement, where η_∞ is a constant (Rao, 2007).

Other studies on the rheological evaluation of suspensions of different plant proteins, such as mung bean (Liu et al., 2021) and hazelnut (Gul et al., 2023) have also investigated the shear thinning behavior at pH 3 – 5. The formers (Liu et al., 2021), using a concentration of 250mg/ml, found apparent viscosities in the range of 0.0103–41.6520 Pa·s) at pH 5.0, which were higher than those at pH 3.0 (0.0078–14.6520 Pa·s), as observed in our study. These values were higher than those found for CPC, probably due to the lower concentration of CPC (5 %, m/m). In addition, in contrast to our results, the Hershel-Bulkley model was able to describe the shear thinning behavior of the mung bean protein. Gul et al. (2023), evaluating a 4% (m/v) suspension of hazelnut protein, found the lowest solubility between pH 3 and 4, with the maximum shear stress at these values, in a range between 3 and 8. The shear stress values were comparable to our values; however, the behavior of the flow curves was well described by the Ostwald-de-Waele model. Despite the different models, these studies explain the rheological behavior near the isoelectric point not only based on the disruption of molecular interactions between the proteins with increasing shear rate but also by the alignment of the major axes of the molecules in the direction of the applied flow, which may include dissociation of weakly associated structures such as dimers and oligomers into monomers (Damodaran & Parkin, 2008).

Table Error! No text of specified style in document.**.8** Rheological parameters of the Herschel-Bulkley model (Equation (2)) for CPC solutions (5%, m/m) at pH 7, 9 and 11.

pH	$\tau_0 \times 10^3$ (Pa)	$K \times 10^3$ (Pa s^n)	n (-)	R^2
7	4.29 ± 2.71^{ab}	1.33 ± 0.02^{b}	1.06 ± 0.01^{a}	0.999
9	2.33 ± 0.67^{b}	2.40 ± 0.05^{ab}	1.03 ± 0.03^{a}	0.999
11	2.04 ± 0.42^{a}	4.06 ± 0.04^{a}	0.97 ± 0.02^{a}	0.999

The results are expressed as the mean ± standard deviation. Means with the same lowercase letter in the same column did not differ significantly at $p \leq 0.05$ according to Tukey's test.

The parameters obtained by fitting the Cross model to the experimental data at pH 3 and 5 are shown in Table 3.3. Although the viscosity values at a zero-shear rate, η_0, experienced a decrease with increasing acidification of the medium, pH significantly affected only the values of the constant *m*, which characterizes the behavior of the material in terms of the deformation rate.

Table Error! No text of specified style in document.**.9** Rheological parameters of the Cross model (Equation (4)) for CPC solutions (5%, m/m) at pH 3 and 5.

pH	$\eta_0 \times 10^1$ (Pa s)	$\eta_\infty \times 10^3$ (Pa s)	α (s)	*m*	R^2
3	9.37 ± 3.81[a]	4.53 ± 0.07[a]	0.68 ± 0.04[a]	1.78 ± 0.17[a]	0.991
5	29.49 ± 6.46[a]	4.18 ± 0.51[a]	0.61 ± 0.02[a]	0.90 ± 0.00[b]	0.999

The results are expressed as the mean ± standard deviation. Means with the same lowercase letter in the same column did not differ significantly at $p \leq 0.05$ according to Tukey's test.

It should also be emphasized that the apparent viscosity at acidic pH was higher than those determined at pH 7, 9, and 11 for a considerable part of the process (Figure 3.2b). pH 5 lies in a region extremely close to the isoelectric point of the legume proteins, which is usually between pH 4 and pH 6 (Mwasaru, Muhammad, Bakar & Man, 1999a, 1999b; Ragab et al., 2004; Moongngarm et al., 2014; Gunathilake, Wansapala & Herath, 2016), and in this vicinity, the proteins exhibit low solubility and a tendency to aggregate and precipitate, resulting in higher viscosity. In this case, a pH close to the isoelectric point of the protein showed greater shear resistance compared with other pH values in the CPC solution (Figure 3.2a). Yadav, Shire & Kalonia (2011) attribute the dominance of attractive interactions to the self-associating behavior of proteins at their isoelectric point, which results in increased resistance to flow, leading to a high solution viscosity. As the pH of the solution moves away from the isoelectric point to higher values, an increase in negative charges occurs (Oliveira et al., 2020), and a decrease in viscosity is expected, which happened up to pH 7. Conversely, as pH increased from neutral to alkaline conditions, viscosities increased, although they were lower than under acidic conditions (pH 3 and 5) due to the proximity of the isoelectric point. Extreme pH values promote a certain degree of denaturation of the protein, which changes the conformational structure, exposing more active sites for interactions (Mauri & Añón, 2006), increasing solubility and interchain electrostatic repulsion (Liu et al., 2021). Krstonošić et al. (2020) also observed higher viscosities of the pea and soy protein aqueous solutions at pH 9.0 than at their natural pH, which was attributed to the higher solubility of these proteins at the higher pH. In turn, Mohanan, Nickerson & Ghosh (2020) have related repulsive interactions to the increase

in viscosity of pea and fava bean protein solutions with increasing pH. The same trend of increasing viscosity with pH was found by Peng et al. (2020) for mildly fractionated soy protein.

Another distinctive feature of this study is the deeper understanding of the rheology of cowpea solutions at high pH ranges, which has been little explored in the scientific literature. It is an important process variable as it has the potential to significantly alter the product properties. The results obtained provide relevant information for understanding the rheological properties of these solutions in the food industry and highlight the potential of CPC as a substitute for other plant protein sources in the formulation and structuring of new materials.

3.1.3 Effect of temperature and pH on the apparent viscosity of aqueous solutions of CPC

The apparent viscosity as a function of temperature of CPC solutions (5%, m/m) at different pH levels (7–11) was evaluated and its experimental data are presented in Figs. 3(a, b, c). The assays at pH 3 and 5 could not be conducted due to the rapid sedimentation of the protein, preventing repeatability.

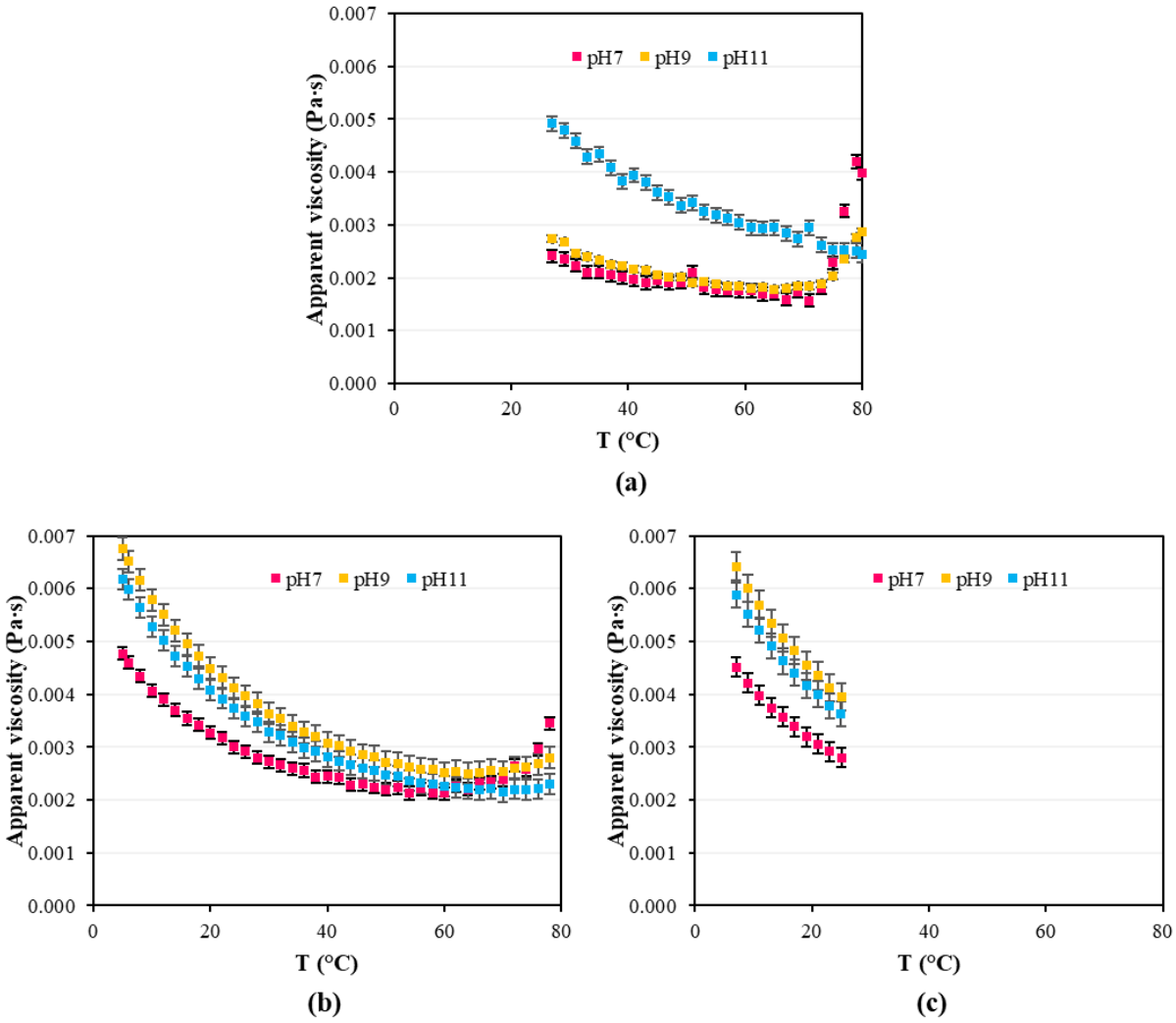
At pH 11, there was a continuous decrease in viscosity throughout the initial heating stage. By contrast, the apparent viscosity of pH levels 7 and 9 decreased until approximately 70 °C, followed by a sudden increase up to 90 °C (Figure 3.3a). The decrease in apparent viscosity occurs due to the reduction in the medium's viscosity with increasing temperature and, primarily, because of the prevalence of Brownian motion at high temperatures (Berli, Deiber & Añón, 1999; Meng & Ma, 2001). The abrupt increase in apparent viscosity of the pH 7 and 9 samples in regions >70 °C may be related to the onset of globulin denaturation, which will be discussed in more detail in the identification of the denaturation temperature (section 3.3).

The cooling stage from 80 °C–5 °C was characterized by an increase in viscosity as the systems were cooled, with a more pronounced increase observed in the more alkaline pH levels (Figure 3.3b). The cooling stage is followed by a brief reheating stage (Figure 3.3c) to return to room temperature (5 °C–25 °C). During the last stage, the viscosity of the samples starts to decrease again, and after returning to room temperature, it is evident that the final viscosity diverges from the initial viscosity as the medium becomes more alkaline. The lower final viscosity after the brief heating treatment observed at pH 11 may indicate that proteins have undergone partial hydrolysis of peptide bonds in an alkaline medium, leading to irreversible denaturation (Damodaran & Parkin, 2008).

In summary, the effects of the temperature cycle on the viscosity of the solutions are accentuated by the acidic or alkaline pH. In the former, there is particle sedimentation, whereas

in the latter, the molecular structure changes; the more the alkalinity, the more irreversible the changes.

Figure Error! No text of specified style in document.**.14** Effect of temperature on the apparent viscosity of CPC solutions (5%, m/m) at pH 7, 9 and 11: (a) Heating step, 25 – 80°C; (b) Cooling step, 80 – 5°C; and (c) Second heating step, 5 – 25°C.



Source: elaborated by the author.

3.2 Dynamic rheological tests

3.2.1 Properties of aqueous solutions of CPC at different frequencies

The LVR of solutions of CPC (10% m/m) under different deformation conditions and pH levels (pH 3–11) was assessed, as oscillatory tests must be conducted in the linear viscoelastic region. pH 3 and 5 did not exhibit a linear region within the deformation range. Under these conditions, rapid phase separation is expected to occur due to protein precipitation near the isoelectric point of cowpea protein (between 4 and 6), which depends on the cowpea

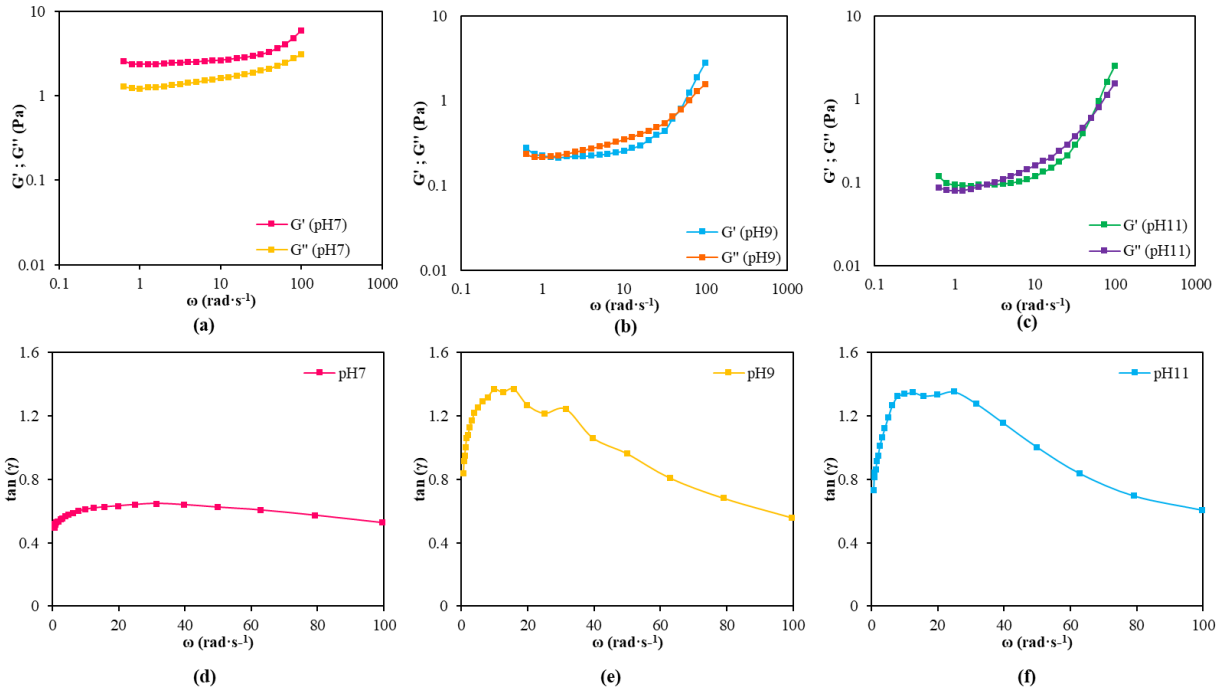
variety and the pH of protein extraction as it affects the solubility of the protein fractions (Mwasaru et al., 1999a~~,~~, 1999b). For the remaining pH values, the linearity was maintained up to approximately 0.1% deformation, which was considered a safe value for the oscillatory testing.

Figure 4 shows the effect of pH on the rheological behavior of CPC solutions (10%) across a frequency range of 1–100 rad s^{-1}, highlighting the linear region for pH 7 (a), pH 9 (b), and pH 11 (c).

As the medium alkalinity increased, the values of the elastic (storage modulus, G′) and viscous (loss modulus, G″) components decreased. Although most studies performed this analysis after thermal gelation, which made the order of the moduli not comparable to our values, this trend has been observed with other proteins containing vicilin fractions, such as pigeon pea (Sosa et al., 2023), pea (Tanger et al., 2022) and soybean (Renkema et al., 2002). The pigeon pea protein isolates (concentration of 10%, m/m) showed a slight decrease in the moduli, from pH 6.3 to pH 8.3, which was explained by a strong repulsion between the molecules, reducing the aggregation rate and forming a homogeneous gel network. Tanger et al. (2022), who studied pea protein in dispersions with a concentration of 15% at pH from 3 to 9, obtained the lowest solubility and the highest G' and gel stiffness at pH 4.5. Conversely, the lowest G’ values were found at pH 9, in a pattern similar to that observed in our study. The decrease in modulus value with increasing pH can be attributed to protein unfolding, which increases solubility and electrostatic repulsion between chains (Liu et al., 2021). Under alkaline conditions the net charge increases, weakening hydrophobic interactions (Rangel et al., 2003; Ragab et al., 2004), which reduces the ability of proteins to form a cohesive network under these conditions and leads to a decrease in the G' and G" moduli (Renkema et al., 2002).

At pH 7 (Figure 3.4a), the elastic behavior predominated over the viscous behavior and showed less frequency dependence than the alkaline dispersions (Figs. 4b and c). In this case, unlike the other pH levels, the G′ values remained higher than the G″ values throughout the process, suggesting that there were no significant changes in the microstructure but rather the formation of a more continuous and structured protein network. The small magnitude difference between the values of G′ and G″ and their similar pattern increasing their dependence on frequency means that a smaller percentage of the stored energy is recovered, and, thus, the structure of the studied solutions can be considered a weak gel, falling between the structure of true gels and concentrated solutions (Rao, 2007; Zhao et al., 2020).

Figure Error! No text of specified style in document.**.15** Mechanical spectra and tan(γ) values of CPC solutions (10%, m/m) across a frequency range of 1 to 100 rad s^{-1}, for storage modulus (G') and loss modulus (G"): (a,d) pH 7; (b,e) pH 9; (c,f) pH11



Source: elaborated by the author.

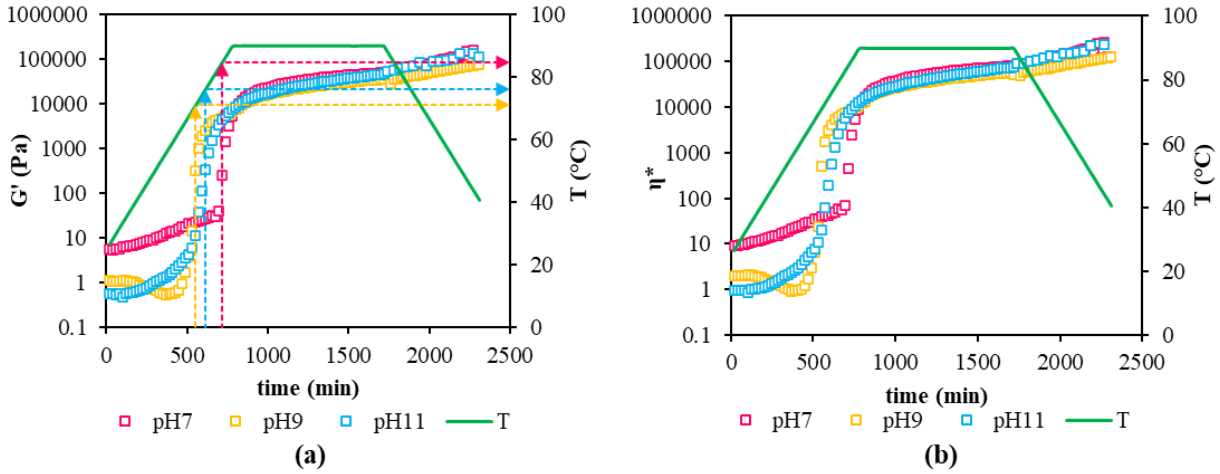
At lower frequencies (<10 rad s^{-1}), the initial values recorded for pH 9 and 11 exhibited an overlap of their respective G′ and G″ (Figs. 4b and c). The evolution of frequency altered the behavior of these solutions, and G″ became more pronounced, suggesting a behavior closer to that of a liquid. Furthermore, for the alkaline solutions at a frequency close to 100 rad s^{-1}, G′ becomes greater than G″ due to the rearrangement of the solution's microstructure components, and thus, the elastic response prevails. This can also be observed by tan(γ) values >1 until 50 rad s^{-1} for alkaline solutions (Figure 3.4d–3.4f).

3.2.2 Properties of aqueous solutions of CPC under a thermal cycle

The ability of proteins to form gels upon heating is generally considered an important functional property. In general, gelation is preceded by the denaturation of proteins, and if G′ < G″, the onset temperature of heat-induced gelation can be determined from the crossover of the moduli (Tang, 2008). However, the thermal gelation of globular proteins is a complex process involving denaturation, dissociation–association, and aggregation and is influenced by many parameters, including the type of protein, its composition, and concentration, environmental

parameters such as the presence of salts and pH, and gelation conditions such as temperature and time (Renkema et al., 2000). Consequently, for some protein dispersions, G′ may be higher than G″ but still liquid, making it difficult to determine the gelation temperature (T_{gel}) (Speroni, Jung & Lamballerie, 2010). In these cases, another criterion other than the crossover can be used, based on a significant increase in the G′ modulus (>0.5 Pa min^{-1}) (Renkema et al., 2000). Therefore, this criterion was used in the present study, and G′ is represented as a function of time in the thermal cycle in Figure 3.5a. At milder temperatures, G′ increased slowly, reaching values <10–30 Pa, before abrupt changes at 68 °C for pH 9, 71 °C for pH 11, and 83 °C for pH 7. These temperatures mark the onset of gelation for the CPC solutions.

Figure Error! No text of specified style in document.**.16** Spectrum of the rheological behavior of CPC solution (10%, m/m) under the influence of temperature and pH: (a) Storage modulus G'; (b) Complex viscosity η*.



Source: elaborated by the author.

As shown in Figure 3.5, pH influences the gelatinization temperature of cowpea protein. The variation in gelatinization temperature is mainly due to changes in the secondary structure of the proteins because of pH variation, making pH shifting a convenient approach to modify the structural and textural properties of proteins (Li et al., 2020; Min et al., 2023).

The storage (G′) and loss (G″) moduli were used to calculate G* (Equation (6)) and hence η* (Equation (5)) during the thermal cycle tests. G* was practically equal to G′ since the storage modulus was always greater than the loss modulus. The rheological behavior of the CPC during the thermal cycle is represented by η* as a function of time in Figure 3.5b.

At milder temperatures, the viscosity values were lower, especially in the alkaline medium. η* followed a behavior similar to that of G′ and G*, increasing steadily up to the gelation temperature, when an abrupt increase was observed, and then another step of steady increase occurred until the start of the cooling step, when the rate increased again. Although the initial values were different, all viscosities tended to converge after gelation. Viscosity typically changes progressively with temperature; however, when a thermal transition occurs, viscosity changes abruptly due to changes in the molecular structure and interactions of protein molecules (Liu et al., 2009; Peyrano et al., 2016). Identifying these changes enables the quantification and characterization of the stability of protein macromolecules in solution. The difference in viscosity at each pH is related to changes in protein structure as the pH changes. Under more alkaline conditions, proteins have greater solubility than at neutral pH, and if less aggregation is expected due to charge repulsion, more reactive sites will be available to allow interaction between proteins to form an ordered network, which could explain the lower initial gelation temperatures than at neutral pH. Furthermore, proteins have heterogeneous charge distributions that form charged patches, and surface patch-binding interactions are based on the tendency of polyions to bind oppositely charged patches, allowing attraction to overcome repulsion between similarly charged patches (Pathak et al., 2017). Nevertheless, after the thermal transition, the viscosity values were close regardless of pH.

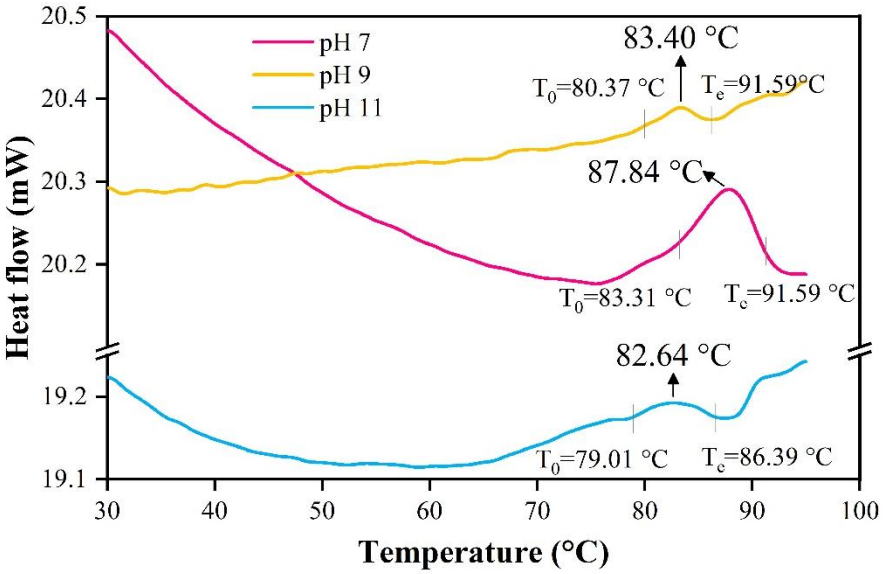
3.3 Thermogram of CPC

The stability of proteins in relation to temperature is generally determined by differential scanning calorimetry (DSC), in which an endothermic peak can be observed due to the alteration in the higher-order structure of the protein.

As shown in Figure 3.6, in the protein solution with pH 7, the endothermic peak at pH 7, T_d=87.84 °C, is significantly larger than the peaks observed in the solutions at pH 9 and 11. Interesting, the onset gelation temperature (82.9 °C, Figure 3.5a) preceded T_d. In studies with cowpea protein at a pH close to neutrality, endothermic peaks were observed at temperatures around 80 °C (Okechukwu, Rao, 1997; Peyrano, De Lamballerie, Avanza & Speroni, 2017; Peyrano et al., 2019), which is lower than the peak of 87.84 °C found in this study. These differences may be related to the cultivar used, or even to the heating rate and protein concentration, since the cited authors used heating rates of 5 and 1 °C min^{-1} and protein concentrations of 50% and 7.5%–10.5%, respectively. Conversely, under the same conditions (10 °C min^{-1} and 20% protein), other studies found denaturation values close to those found in the present study (Wright & Boulter, 1980; Horax, Hettiarachchy, Chen & Jalaluddin, 2004).

This temperature is attributed to the denaturation of the 7S vicilin fractions (Tang, 2008). It is known that the main proteins present in cowpeas are globulins, consisting of two high-molecular-weight proteins called legumin and vicilin (11S and 7S, respectively), with the 7S fraction predominating (De Souza et al., 2018). It is also observed that the peak is asymmetric, covering a wide temperature range. This phenomenon occurs due to the overlap of multiple denaturation peaks in the same range, which is characteristic of proteins extracted from seeds (Peyrano et al., 2017).

Figure Error! No text of specified style in document.**.17** Thermogram of CPC solution (20% m/m) at pH of 7, 9, and 11.



Source: elaborated by the author.

In the protein solution at pH 9, it is still possible to observe an endothermic peak at 83.4 °C that is broad and asymmetric, suggesting that fractions not affected by pH undergo denaturation due to temperature. Thus, some of the protein fractions were denatured by the alkali, resulting in an endothermic peak of lower enthalpy than that observed at pH 7. In addition, the onset gelation temperature was 68 °C, showing that gel formation preceded protein denaturation. This behavior was also observed at pH 11, where most of the protein fractions have lost their structural organization, resulting in a small and poorly defined peak at T_d = 82.64 °C from fractions still resistant to high pH that have not been degraded. The onset gelation temperature was 71 °C, which was lower than the denaturation onset temperature. The gelation ability attributed to vicilin has also been related to the predominance of the 7S fraction over the

11S fraction, although there is no consensus on the mechanism of legumin and vicilin gel formation (Gravel & Doyen, 2023; Ren, Xia, Gunes & Ahrné, 2024).

Peyrano et al. (2019) studied the gelation of concentrated solutions of cowpea proteins extracted at pH 8 and pH 10 and observed the gelation onset temperature before the denaturation onset temperature in the later solution. This behavior can be related to gelation inducers such as pressure, pH, and chemical and enzymatic agents (Rao, 2007; Camp, Messens, Clément & Huyghebaert, 1997).

The investigation into cowpea protein stability under temperature-induced denaturation and gelation reveals that, at pH 7, the denaturation peak exceeds those observed at pH 9 and 11, suggesting that alkaline media reduces the denaturation temperature. At a more alkaline environment (pH 11), the presence of a small peak at T_d indicates diverse protein responses, highlighting the intricate alterations induced by pH in the structure and behavior of cowpea protein. The protein fraction related to vicilin provides specific properties to the cowpea protein as a plant-based ingredient.

4 Conclusion

Unraveling the intricate mechanisms of plant proteins requires immersion in the complex interactions governed by concentration, pH, and temperature. In addition to elucidating some of the rheological and thermal nuances of CPC, this study offers new perspectives for food production for a growing world population that is increasingly demanding quality and sustainability in future foods. Rheological analysis of CPC solutions showed significant sensitivity to protein concentration and shear rate, especially at higher concentrations, resulting in far higher flow resistance than at concentrations <10%. The apparent viscosity showed a shear thinning behavior at low shear rates (<10 s^{-1}) for solutions up to 10% concentration, whereas above this critical rate, the viscosity was invariant, similar to Newtonian fluids; at 20% concentration, a shear thinning behavior was observed in all ranges of shear rates. pH played a critical role, with acidic conditions near the isoelectric point significantly affecting shear stress, viscosity, and elastic behavior, whereas neutral and alkaline conditions maintained consistent behavior. During the thermal cycle, molecular interactions and protein structures were altered, leading to progressive changes in viscosity. Remarkably, pH changes also affected viscosity and elastic properties, suggesting that protein structure changes due to pH fluctuations contributed to these variations.

Thermal cycle and DSC analysis revealed temperature-induced changes in molecular interactions and the role of pH in influencing gelation and denaturation temperatures. Distinct

patterns were found under different pH and temperature conditions. Alkaline pH induced significant structural changes, resulting in different thermal transition patterns. Denaturation and gelation onset temperatures at alkaline pH were lower than those at neutral pH. Gelation started before the onset of denaturation at pH 9 and 11. At neutral pH, T_d corresponded to the 7S vicilin fraction, and denaturation was more pronounced than at alkaline pH.

In conclusion, this study provides in-depth insights into how protein concentration, pH, and temperature affect the molecular interactions and the rheological and thermal properties of CPC solutions. These findings are crucial to guide the application of these proteins in the food and industrial sectors and provide valuable information for the development of plant-based products.

References

Almeida, T. S., Da Cruz Souza, C. A., De Cerqueira E Silva, M. B., Batista, F. P. R., Ferreira, E. S., Santos, A. L. S., Silva, L. N., Melo, C. R., Bani, C., Bianconi, M. L., Cardoso, J. C., De Albuquerque-Júnior, R. L. C., De Melo Barbosa, R., Pereira, M. M., Souto, E. B., Soares, C. M. F., & Severino, P. (2022). Extraction and characterization of β-viginin protein hydrolysates from cowpea flour as a new manufacturing active ingredient. *Technologies*, *10*(4), 89. https://doi.org/10.3390/technologies10040089

Aluko, R. E., & Yada, R. Y. (1995). Structure-function relationships of cowpea (*Vigna unguiculata*) globulin isolate: Influence of pH and NaCl on physicochemical and functional properties. *Food Chemistry*, *53*(3), 259–265. https://doi.org/10.1016/0308-8146(95)93931-G

Aluko, R. E., Mofolasayo, O. A., & Watts, B. M. (2009). Emulsifying and foaming properties of commercial yellow pea (*pisum sativum* L.) seed flours. *Journal of Agricultural and Food Chemistry*, *57*(20), 9793–9800. https://doi.org/10.1021/jf902199x

Appiah, F., Asibuo, J. Y., & Kumah, P. (2011). Physicochemical and functional properties of bean flours of three cowpea (*Vigna unguiculata* L. Walp) varieties in Ghana. *African Journal of Food Science*, *5*(2), 100-104.

Beliciu, C. M., & Moraru, C. I. (2011). The effect of protein concentration and heat treatment temperature on micellar casein–soy protein mixtures. *Food Hydrocolloids*, *25*(6), 1448–1460. https://doi.org/10.1016/j.foodhyd.2011.01.011

Berli, C. L. A., Deiber, J. A., & Añón, M. C. (1999). Heat-induced phenomena in soy protein suspensions. Rheometric data and theoretical interpretation. *Journal of Agricultural and Food Chemistry*, *47*(3), 893–900. https://doi.org/10.1021/jf9806053

Bird, R. B. (Ed.). (1987). *Dynamics of polymeric liquids* (2nd ed). Wiley.

Camp, J. V., Messens, W., Clément, J., Huyghebaert. (1996). Influence of pH and sodium chloride on the high pressure-induced gel formation of a whey protein concentrate. *Food Chemistry, 60(3),* 417-424.

Carvalho, A. F. U., De Sousa, N. M., Farias, D. F., Da Rocha-Bezerra, L. C. B., Da Silva, R. M. P., Viana, M. P., Gouveia, S. T., Sampaio, S. S., De Sousa, M. B., De Lima, G. P. G., De Morais, S. M., Barros, C. C., & Filho, F. R. F. (2012). Nutritional ranking of 30 Brazilian genotypes of cowpeas including determination of antioxidant capacity and vitamins. *Journal of Food Composition and Analysis*, *26*(1–2), 81–88. https://doi.org/10.1016/j.jfca.2012.01.005

Chen, D., & Campanella, O. H. (2022). Limited enzymatic hydrolysis induced pea protein gelation at low protein concentration with less heat requirement. *Food Hydrocolloids*, *128*, 107547. https://doi.org/10.1016/j.foodhyd.2022.107547

Cross, M. M. (1965). Rheology of non-Newtonian fluids: A new flow equation for pseudoplastic systems. *Journal of Colloid Science*, *20*(5), 417–437. https://doi.org/10.1016/0095-8522(65)90022-X

Damodaran, S., & Parkin, K. L. (Eds.). (2008). *Fennema's food chemistry* (Fourth edition). CRC Press,Taylor & Francis Group.

De Boer, J., Schösler, H., & Aiking, H. (2014). "Meatless days" or "less but better"? Exploring strategies to adapt Western meat consumption to health and sustainability challenges. *Appetite*, *76*, 120–128. https://doi.org/10.1016/j.appet.2014.02.002

De Souza Ferreira, E., Capraro, J., Sessa, F., Magni, C., Demonte, A., Consonni, A., Augusto Neves, V., Maffud Cilli, E., Duranti, M., & Scarafoni, A. (2018). New molecular features of cowpea bean (*Vigna unguiculata* L. Walp) β-vignin. *Bioscience, Biotechnology, and Biochemistry*, *82*(2), 285–291. https://doi.org/10.1080/09168451.2017.1419855

Frota, K. D. M. G., Lopes, L. A. R., Silva, I. C. V., & Arêas, J. A. G. (2018). Molecular profile, purity and presence of trypsin inhibitors in cowpea protein isolates. *Revista Caatinga*, *31*, 202–208. https://doi.org/10.1590/1983-21252018v31n123rc

Frota, K. D. M. G., Soares, R. A. M., & Arêas, J. A. G. (2008). Composição química do feijão caupi (*Vigna unguiculata* L. Walp), cultivar BRS-Milênio. *Ciência e Tecnologia de Alimentos*, *28*(2), 470–476. https://doi.org/10.1590/S0101-20612008000200031

Ge, J.; Sun, C. X.; Mata, A.; Corke, H.; Gan, R. Y.; Fang, Y. (2021). Physicochemical and PH-Dependent Functional Properties of Proteins Isolated from Eight Traditional Chinese Beans. *Food Hydrocolloids*, *112*. https://doi.org/10.1016/j.foodhyd.2020.106288.

Gómez, A., Gay, C., Tironi, V., & Avanza, M. V. (2021). Structural and antioxidant properties of cowpea protein hydrolysates. *Food Bioscience*, *41*, 101074. https://doi.org/10.1016/j.fbio.2021.101074

González-Pérez, S., & Arellano, J. B. (2009). Vegetable protein isolates. In: *Handbook of hydrocolloids*. Woodhead Publishing, 2009, 383-419.

Gravel, A., & Doyen, A. (2023). Pulse globulins 11s and 7s: Origins, purification methods, and techno-functional properties. *Journal of Agricultural and Food Chemistry*, *71*(6), 2704–2717. https://doi.org/10.1021/acs.jafc.2c07507

Gul, O., Gul, L. B., Baskıncı, T., Parlak, M. E., & Saricaoglu, F. T. (2023). Influence of pH and ionic strength on the bulk and interfacial rheology and technofunctional properties of hazelnut

meal protein isolate. *Food Research International, 169,* 112906. https://doi.org/10.1016/j.foodres.2023.112906

Gunathilake, K. G. T., Wansapala, M. A. J., & Herath, H. M. T (2016). Comparison of nutritional and functional properties of mung bean (*Vigna radiate*) and cowpea (*Vigna unguiculata*) protein isolates processed by isoelectric precipitation. *International Journal of Innovative Research in Technology*, 3, 139-148.

Henchion, M., Hayes, M., Mullen, A. M., Fenelon, M., Tiwari, B. (2017). Future Protein Supply and Demand: Strategies and Factors Influencing a Sustainable Equilibrium. *Foods, 6 (n. 56)*. https://doi.org/10.3390/foods6070053

Hewage, S., & Vithanarachchi, S. M. (2009). Preparation and characterization of biodegradable polymer films from cowpea (*Vigna Unguiculata*) protein isolate. *Journal of the National Science Foundation of Sri Lanka*, *37*(1), 53. https://doi.org/10.4038/jnsfsr.v37i1.457

Horax, R., Hettiarachchy, N. S., Chen, P., & Jalaluddin, M. (2004). Preparation and characterization of protein isolate from cowpea (*Vigna unguiculata* L. Walp.). *Journal of Food Science*, *69*(2). https://doi.org/10.1111/j.1365- 2621.2004.tb15500.x

Huamaní-Meléndez, V. J., Mauro, M. A., & Darros-Barbosa, R. (2021). Physicochemical and rheological properties of aqueous Tara gum solutions. *Food Hydrocolloids*, *111*, 106195. https://doi.org/10.1016/j.foodhyd.2020.106195

Huang, J., Zeng, S., Xiong, S., Huang, Q. (2016). Steady, dynamic, and creep-recovery rheological properties of myofibrillar protein from grass carp muscle. *Food Hydrocolloids, 61,* 48–56. http://dx.doi.org/10.1016/j.foodhyd.2016.04.043

Jaramillo, D. P., Roberts, R. F., & Coupland, J. N. (2011). Effect of pH on the properties of soy protein–pectin complexes. *Food Research International*, *44*(4), 911-916. https://doi.org/10.1016/j.foodres.2011.01.057

Jiang, X., Wang, W., Bai, L., Yang, L., Chen, H., Yang, H., ... & Cheng, Z. (2019). Microwave-assisted reversible coordination-mediated polymerization for self-healing hybrid materials: RGO@ PDA simultaneous as catalyst and nanocomposites in one-pot. *Macromolecular Materials and Engineering*, *304*(12), 1900477. https://doi.org/10.1002/mame.201900477

Khanna, Y. P. (1991). Dynamic melt rheology. I: Re-examining dynamic viscosity in relationship to the steady shear flow viscosity. *Polymer Engineering & Science*, *31*(6), 440–444. https://doi.org/10.1002/pen.760310610

Krstonošić, V. S., Kalić, M. D., Dapčević-Hadnađev, T. R., Lončarević, I. S., & Hadnađev, M. S. (2020). Physico-chemical characterization of protein stabilized oil-in-water emulsions. *Colloids and Surfaces A: Physicochemical and Engineering Aspects*, *602*, 125045. https://doi.org/10.1016/j.colsurfa.2020.125045

Li, J., Wu, M., Wang, Y., Li, K., Du, J., Bai, Y. (2020). Effect of pH-shifting treatment on structural and heat induced gel properties of peanut protein isolate. *Food Chemistry, 325*. https://doi.org/10.1016/j.foodchem.2020.126921

Liu, C., Vailhe, C., Samuel, N., & Min, Q. (2009). A simple and reproducible approach to characterize protein stability using rheology. *International Journal of Pharmaceutics*, *374*(1–2), 1–4. https://doi.org/10.1016/j.ijpharm.2009.03.030

Liu, F. F., Li, Y. Q., Wang, C. Y., Zhao, X. Z., Liang, Y., He, J. X., & Mo, H. Z. (2021). Impact of pH on the physicochemical and rheological properties of mung bean (*Vigna radiata* L.) protein. *Process Biochemistry*, *111*, 274-284.

Liu, S., Rao, Z., Wu, R., Sun, Z., Yuan, Z., Bai, L., ... & Chen, H. (2019). Fabrication of microcapsules by the combination of biomass porous carbon and polydopamine for dual self-healing hydrogels. *Journal of Agricultural and Food Chemistry*, *67*(4), 1061-1071. https://doi.org/10.1021/acs.jafc.8b06241

Malhotra, A., & Coupland, J. N. (2004). The effect of surfactants on the solubility, zeta potential, and viscosity of soy protein isolates. *Food Hydrocolloids*, *18*(1), 101–108. https://doi.org/10.1016/S0268-005X(03)00047-X

Mauri, A. N., & Añón, M. C. (2006). Effect of solution pH on solubility and some structural properties of soybean protein isolate films. *Journal of the Science of Food and Agriculture*, *86*(7), 1064–1072. https://doi.org/10.1002/jsfa.2457

Meng, G.-T., & Ma, C.-Y. (2001). Flow property of globulin from red bean (*Phaseolus angularis*). *Food Research International*, *34*(5), 401–407. https://doi.org/10.1016/S0963-9969(00)00184-8

Min, C., Zhang, C., Pu, H., Li, H., Ma, W., Kuang, J., Huang, J., & Xiong, Y. L. (2023). pH - shifting alters textural, thermal, and microstructural properties of mung bean starch–flaxseed protein composite gels. *Journal of Texture Studies*, *54*(2), 323–333. https://doi.org/10.1111/jtxs.12743

Mohanan, A., Nickerson, M. T., & Ghosh, S. (2020). Utilization of pulse protein-xanthan gum complexes for foam stabilization: The effect of protein concentrate and isolate at various pH. *Food Chemistry*, *316*, 126282. https://doi.org/10.1016/j.foodchem.2020.126282

Moongngarm, A., Sasanam, S., Pinsiri, W., Inthasoi, P., Janto, S., & Pengchai, J. (2014). Functional properties of protein concentrate from black cowpea and its application. *American Journal of Applied Sciences*, *11*(10), 1811–1818. https://doi.org/10.3844/ofsp.9483

Moser, P., Ferreira, S., & Nicoletti, V. R. (2019). Buriti oil microencapsulation in chickpea protein-pectin matrix as affected by spray drying parameters. *Food and Bioproducts Processing*, *117*, 183–193. https://doi.org/10.1016/j.fbp.2019.07.009

Mwasaru, M. A., Muhammad, K., Bakar, J., & Man, Y. B. C. (1999). Effects of isolation technique and conditions on the extractability, physicochemical and functional properties of pigeonpea (*Cajanus cajan*) and cowpea (*Vigna unguiculata*) protein isolates. I. Physicochemical properties. *Food Chemistry*, *67*(4), 435–443. https://doi.org/10.1016/S0308-8146(99)00150-8

Mwasaru, M. A., Muhammad, K., Bakar, J., & Man, Y. B. C. (1999). Effects of isolation technique and conditions on the extractability, physicochemical and functional properties of pigeonpea (*Cajanus cajan*) and cowpea (*Vigna unguiculata*) protein isolates. II. Functional properties. *Food Chemistry*, *67*(4), 445–452. https://doi.org/10.1016/S0308-8146(99)00151-X

Okechukwu, P. E., & Rao, M. A. (1997). Calorimetric and rheological behavior of cowpea protein plus starch (Cowpea and corn) gels. *Food Hydrocolloids*, *11*(3), 339–345. https://doi.org/10.1016/S0268-005X(97)80064-1

Oliveira, M. M. G., Souza, K. S., & Mauro, M. A. (2021). Evaluation of interactions between carboxymethylcellulose and soy protein isolate and their effects on the preparation and characterization of composite edible films. *Food Biophysics*, *16*(2), 214-228. https://doi.org/10.1007/s11483-020-09659-3

Pathak, J., Priyadarshini, E., Rawat, K., & Bohidar, H. B. (2017). Complex coacervation in charge complementary biopolymers: Electrostatic versus surface patch binding. *Advances in Colloid and Interface Science*, *250*, 40–53. https://doi.org/10.1016/j.cis.2017.10.006

Peng, Y., Kersten, N., Kyriakopoulou, K., & van der Goot, A. J. (2020). Functional properties of mildly fractionated soy protein as influenced by the processing pH. *Journal of Food Engineering*, *275*, 109875. https://doi.org/10.1016/j.jfoodeng.2019.109875

Pereira, H. V. R., Saraiva, K. P., Carvalho, L. M. J., Andrade, L. R., Pedrosa, C., & Pierucci, A. P. T. R. (2009). Legumes seeds protein isolates in the production of ascorbic acid microparticles. *Food Research International*, *42*(1), 115–121. https://doi.org/10.1016/j.foodres.2008.10.008

Peyrano, F., De Lamballerie, M., Avanza, M. V., & Speroni, F. (2017). Calorimetric study of cowpea protein isolates. Effect of calcium and high hydrostatic pressure. *Food Biophysics*, *12*(3), 374–382. https://doi.org/10.1007/s11483-017-9493-4

Peyrano, F., De Lamballerie, M., Avanza, M. V., & Speroni, F. (2019). Rheological characterization of the thermal gelation of cowpea protein isolates: Effect of pretreatments with high hydrostatic pressure or calcium addition. *LWT*, *115*, 108472. https://doi.org/10.1016/j.lwt.2019.108472

Peyrano, F., Speroni, F., & Avanza, M. V. (2016). Physicochemical and functional properties of cowpea protein isolates treated with temperature or high hydrostatic pressure. *Innovative Food Science & Emerging Technologies*, *33*, 38–46. https://doi.org/10.1016/j.ifset.2015.10.014

Ragab, D. M., Babiker, E. E., & Eltinay, A. H. (2004). Fractionation, solubility and functional properties of cowpea (*Vigna unguiculata*) proteins as affected by pH and/or salt concentration. *Food Chemistry*, *84*(2), 207–212. https://doi.org/10.1016/S0308-8146(03)00203-6

Rangel, A.; Saraiva, K.; Schwengber, P.; Narciso, M. S.; Domont, G. B.; Ferreira, S. T.; Pedrosa, C. (2004). Biological Evaluation of a Protein Isolate from Cowpea (*Vigna Unguiculata*) Seeds. *Food Chemistry, 87 (4),* 491–499. https://doi.org/10.1016/j.foodchem.2003.12.023.

Rao, M. A. (2007). *Rheology of fluid and semisolid foods: principles and applications*. Springer Science & Business Media.

Ren, W., Xia, W., Gunes, D. Z., Ahrné, L. (2024). Heat-induced gels from pea protein soluble colloidal aggregates: Effect of calcium addition or pH adjustment on gelation behavior and rheological properties. *Food Hydrocolloids, 147.* https://doi.org/10.1016/j.foodhyd.2023.109417

Renkema, J. M. S., Lakemond, C. M. M., de Jongh, H. H. J., Gruppen, H., Ton van Vliet. (2000). The effect of pH on heat denaturation and gel forming properties of soy proteins. *Journal of Biotechnology, 79*, 223–230. https://doi.org/10.1016/S0168-1656(00)00239-X

Renkema, J. M., Gruppen, H., & Van Vliet, T. (2002). Influence of pH and ionic strength on heat-induced formation and rheological properties of soy protein gels in relation to denaturation and their protein compositions. *Journal of Agricultural and Food Chemistry, 50*(21), 6064-6071. https://doi.org/10.1021/jf020061b

Rosenfeld, D. L., Rothgerber, H., & Janet Tomiyama, A. (2020). From mostly vegetarian to fully vegetarian: Meat avoidance and the expression of social identity. *Food Quality and Preference*, *85*, 103963. https://doi.org/10.1016/j.foodqual.2020.103963

Rudra, S. G.; Sethi, S.; Jha, S. K.; Kumar, R. (2016). Physico-Chemical and Functional Properties of Cowpea Protein Isolate as Affected by the Dehydration Technique. *Legume Research, 39*(3), 370–378. https://doi.org/10.18805/lr.v0iOF.9441.

Sabaté, J., Sranacharoenpong, K., Harwatt, H., Wien, M., & Soret, S. (2015). The environmental cost of protein food choices. *Public Health Nutrition, 18*(11), 2067–2073. https://doi.org/10.1017/S1368980014002377

Saricaoglu, F. T. (2020). Application of high-pressure homogenization (Hph) to modify functional, structural and rheological properties of lentil (*Lens culinaris*) proteins. *International Journal of Biological Macromolecules*, *144*, 760–769. https://doi.org/10.1016/j.ijbiomac.2019.11.034

Shen, Q., Xiong, T., Zheng, W., Luo, Y., Peng, W., Dai, J., Song, R., Li, Y., Liu, S., Li, B., & Chen, Y. (2022). The effects of thermal treatment on emulsifying properties of soy protein isolates: Interfacial rheology and quantitative proteomic analysis. *Food Research International, 157*, 111326. https://doi.org/10.1016/j.foodres.2022.111326

Sosa, E. I. F., Chaves, M. G., Peyrano, F., Quiroga, A. V., & Avanza, M. V. (2023). Thermal Gelation of Proteins from Cajanus cajan Influenced by pH and Ionic Strength. *Plant Foods for Human Nutrition*, *78*(3), 574-583. https://doi.org/10.1007/s11130-023-01086-2

Spendrup, S., & Hovmalm, H. P. (2022). Consumer attitudes and beliefs towards plant-based food in different degrees of processing – The case of Sweden. *Food Quality and Preference*, *102*, 104673. https://doi.org/10.1016/j.foodqual.2022.104673

Speroni, F., Jung, S., De Lamballerie, M. (2010). Effects of Calcium and Pressure Treatment on Thermal Gelation of Soybean Protein. *Journal of Food Science, 75(1),* 30–38. https://doi.org/10.1111/j.1750-3841.2009.01390.x

Taherian, A. R., Mondor, M., Labranche, J., Drolet, H., Ippersiel, D., & Lamarche, F. (2011). Comparative study of functional properties of commercial and membrane processed yellow pea protein isolates. *Food Research International*, *44*(8), 2505–2514. https://doi.org/10.1016/j.foodres.2011.01.030

Tang, C.-H. (2008). Thermal denaturation and gelation of vicilin-rich protein isolates from three Phaseolus legumes: A comparative study. *LWT - Food Science and Technology, 41*(8), 1380–1388. https://doi.org/10.1016/j.lwt.2007.08.025

Tanger, C., Müller, M., Andlinger, D., & Kulozik, U. (2022). Influence of pH and ionic strength on the thermal gelation behaviour of pea protein. *Food Hydrocolloids*, *123*, 106903. https://doi.org/10.1016/j.foodhyd.2021.106903

Thompson, C. M. B., Acevedo, B. A., Añón, M. C., & Avanza, M. V. (2023). Emulsifying capacity of cowpea protein isolates. Effect of thermal and hydrolytic treatment. *Plant Foods for Human Nutrition*, *78*(2), 366–374. https://doi.org/10.1007/s11130-023-01072-8

Van Zanten, H. H. E., Mollenhorst, H., Klootwijk, C. W., Van Middelaar, C. E., & De Boer, I. J. M. (2016). Global food supply: Land use efficiency of livestock systems. *The International Journal of Life Cycle Assessment*, *21*(5), 747–758. https://doi.org/10.1007/s11367-015-0944-1

Varesano, A., Aluigi, A., Vineis, C., & Tonin, C. (2008). Study on the shear viscosity behavior of keratin/PEO blends for nanofibre electrospinning. *Journal of Polymer Science Part B: Polymer Physics*, *46*(12), 1193–1201. https://doi.org/10.1002/polb.21452

Wei, M., Lin, K., & Liu, H. (2019). Experimental investigation on hysteretic behavior of a shear thickening fluid damper. *Structural Control and Health Monitoring*, *26*(9). https://doi.org/10.1002/stc.2389

Winter, H. H. (2009). Three views of viscoelasticity for Cox–Merz materials. *Rheologica Acta*, *48*(3), 241–243. https://doi.org/10.1007/s00397-008-0329-5

World population prospects—Population division—United nations. Obtido 23 de novembro de 2023, de https://population.un.org/wpp/

Wright, D. J., & Boulter, D. (1980). Differential scanning calorimetric study of meals and constituents of some food grain Legumes. *Journal of the Science of Food and Agriculture*, *31*(12), 1231–1241. https://doi.org/10.1002/jsfa.2740311203

Xiao, L., Hou, Y., Xue, Z., Bai, L., Wang, W., Chen, H., ... & Wei, D. (2023). Soy protein isolate/genipin-based nanoparticles for the stabilization of Pickering emulsion to design self-healing guar gum-based hydrogels. *Biomacromolecules*, *24*(5), 2087-2099. https://doi.org/10.1021/acs.biomac.2c01507

Yadav, S., Shire, S. J., & Kalonia, D. S. (2011). Viscosity analysis of high concentration bovine serum albumin aqueous solutions. *Pharmaceutical research*, *28*, 1973-1983. https://doi.org/10.1016/j.colsurfa.2020.125045

Zarei, M., & Aalaie, J. (2020). Application of shear thickening fluids in material development. *Journal of Materials Research and Technology*, *9*(5), 10411–10433. https://doi.org/10.1016/j.jmrt.2020.07.049

Zhao, X., Xing, T., Xu, X., & Zhou, G. (2020). Influence of extreme alkaline pH induced unfolding and aggregation on PSE-like chicken protein edible film formation. *Food Chemistry*, *319*, 126574. https://doi.org/10.1016/j.foodchem.2020.126574

Apendix

Publishing rights

ELSEVIER

Rights and Access

Exploring the Rheological and Thermal Behavior of Cowpea Protein Concentrate: Impact of pH and Concentration

Corresponding author	Dr Maria Mariana Garcia de Oliveira
E-mail address	maria.mariana@unesp.br
Journal	Colloids and Surfaces A: Physicochemical and Engineering Aspects
Article number	134106
Our reference	COLSUA_134106
PII	S0927-7757(24)00967-1

Order Confirmation

Thank you for taking the time to complete the Rights and Access form.

Order number	OACSRCOLSUA1341060
Order date	29 April 2024
Research Funders	State of Sao Paulo Research Foundation Grant numbers: 2020/05254-4, 2021/08321-7 Coordination of Higher Education Personnel Improvement Grant numbers: 88887.499675/2020-00 National Council for Scientific and Technological Development Grant numbers: 2021/2022-3320
Publishing Option	Subscription
Publishing Agreement	• I am one author signing on behalf of all co-authors of the manuscript I may post the accepted manuscript in my institutional repository and make this public after an embargo period. To ensure the sustainability of peer-reviewed research in journal publications, I may not share the final article publicly, for example on ResearchGate or Academia.edu. Further details on Elsevier Sharing Policy here. Based on information provided the embargo period/end date is 24 months.

All content on this website: Copyright © 2024 Elsevier B.V., its licensors, and contributors. All rights are reserved, including those for text and data mining, AI training, and similar technologies.

4 PROSPECTS OF COWPEA PROTEIN AS AN ALTERNATIVE AND NATURAL EMULSIFIER FOR FOOD APPLICATIONS: EFFECT OF PH AND OIL CONCENTRATION

Maria Mariana Garcia de Oliveira[a], Ana Gabriela Baroni Wicher Fessori[a], Víctor Justiniano Huamaní-Meléndez[a], Maria Aparecida Mauro[a]

[a] Department of Food Engineering and Technology, Institute of Biosciences, Humanities and Exact Sciences – São Paulo State University (UNESP), Street Cristóvão Colombo, 2265, São José do Rio Preto 15054-000, Brazil.

e-mail address: maria.mariana@unesp.br (corresponding author)

Manuscript submitted to the International Journal of Biological Macromolecules

ISSN: 0141-8130

Abstract

Recognizing the increasing need to expand the knowledge base regarding novel sources of more sustainable proteins, this study investigates the relationship between pH (3-11), oil concentration (2-10%), and emulsion stability, with particular emphasis on the effectiveness of cowpea protein concentrate (CPC) as a natural emulsifier. The pH and oil concentration significantly impact particle size distribution, which was notably more uniform at pH9. Rheological analysis of CPC-stabilized emulsions reveals a transition from shear thinning to thickening flow behavior at higher shear rates. At pH7, viscosity decreases with increasing oil concentration; at pH 9 and 11 this effect is less pronounced. Following thermal treatment, the original emulsion viscosity at pH 7 and 9 is modified. This is not observed at pH11, and the minimal thermal effect was attributed to the already unfolded protein chains. At pH 3 and 5, phase separation occurs within 24 hours. Emulsions at pH9 and 11 exhibited the highest degrees of stability over a 30-day storage period. The lowest, at pH7, was correlated with increased particle mobility. In the majority of cases at neutral and alkaline pH, CPC proved to be an effective emulsifying agent, demonstrating its potential for extending stability by preventing coalescence and sedimentation.

Keywords: Plant protein; Emulsifying agent; Particle size distribution; Rheological behavior; Thermal effects

1 Introduction

Traditionally, a kinetically stable emulsion can be achieved by increasing the oil content in its composition. The high oil concentration contributes to the tight packing of dispersed droplets, resulting in good resistance to external forces [1]. Despite the benefits of high stability and the ability to carry nutrients, the drawbacks of high oil emulsions also manifest themselves in foods. Advances in food science have led to significant changes in the formulation of low-fat products, particularly in light of consumer preferences [2–4], but such emulsions may also pose obstacles to their integration into some food systems. In addition to the increasing demand for low-fat foods, there is an equally significant need for products and systems that require lower oil concentrations and low viscosity. This demand is particularly evident in applications involving the incorporation of emulsions into films and packaging [5–7], the formulation of salad dressings [8], and the production of microcapsules [9].

Due to the high proportion of aqueous phase, low-fat emulsions are more thermodynamically unstable systems in the absence of an appropriate emulsifying agent. These emulsions tend to decompose rapidly and separate into multiple phases. An effective emulsifier is characterized by a proper balance between polar and non-polar groups, which ensures optimal surface activity and water solubility [10]. Therefore, meeting the ideal requirements to enhance the formation and stability of a low oil-to-water ratio system is challenging. The use of various biopolymers as emulsifier agents for emulsions has received considerable attention from researchers in this field. The primary challenge in synthesizing these emulsions lies in identifying an effective bio-derived polymer that contributes to emulsion formation while ensuring product stability.

Proteins can act as natural emulsifiers due to their amphiphilic properties, allowing them to self-aggregate and form a continuous and uniform layer around the oil droplets [11]. A quest for alternative protein sources in the food industry is propelled not only by the nutritional value and functionality of proteins but also by the urgent need to promote sustainable practices in the face of rapid population growth and environmental challenges [12,13]. All of these factors underscore the importance of transitioning to more sustainable and resource-efficient protein sources.

Despite soy being one of the primary sources of plant-based protein, its use has been controversial. Concerns primarily revolve around allergenicity, genetic modifications, and production restrictions, particularly in European countries [14]. As an alternative, plant proteins from other sources have been explored. In this context, cowpea (*Vigna unguiculata*) comes up

as a promising candidate. Native to Africa and thriving in tropical and subtropical climates [15], cowpea is recognized for its versatility and nutritional value. With an average protein content ranging from 17 to 27% in its composition [16], cowpea protein represents a viable alternative to soy and other conventional sources. Studies have reported satisfactory properties such as solubility, water holding capacity, gelation, emulsification, and foaming capacity [17–20]. Moreover, key properties of cowpea protein, including its ability to absorb and interact with water and oil, coupled with a solubility exceeding 80%, underscore its exceptional performance as an emulsifier and stabilizer [17,19–21]. These attributes make it a compelling option for applications in emulsified foods and formulations.

To date, only one study has addressed the evaluation of the emulsifying capacity of cowpea protein isolates [21]. In this study, researchers investigated the modifications caused by the effects of thermal treatments (70 and 90 °C) and partial hydrolysis by digestion with alcalase on the emulsifying properties of cowpea protein isolates extracted at pH 8 and 10. The thermal treatments did not promote the improvement of the emulsion stability of the cowpea protein isolates; however, the protein concentration proved to be an important factor for both particle size and emulsion stability. Increasing the concentration of proteins available for formulation resulted in improvements in emulsifying properties.

This study introduces new topics not yet studied, aiming to obtain emulsions stabilized by cowpea protein concentrate (CPC) under different pH conditions of the medium. In summary, this research proposes a more sustainable and cost-effective method to successfully prepare low-oil emulsions stabilized by CPC, employing the variation of medium pH as a simple and effective strategy to modify the properties of the system. In this study, the protein extracted from cowpea beans is applied to stabilize the emulsion, without synthetic emulsifiers or dual combination with another biopolymer. The aim of using it in isolation is to assess whether this new protein source, specifically without the assistance of other biopolymers or synthetic emulsifiers, plays a satisfactory role.

2 Material and methods

2.1 Raw materials

Cowpea protein concentrate (CPC), with a protein content of 79%, and type 1 sunflower oil (Liza, Brazil) were used to prepare the emulsions. Additionally, analytical grade reagents, including sodium hydroxide and hydrochloric acid (Synth, Brazil), were employed for pH adjustment.

2.2 Preparation of oil-in-water emulsions stabilized by cowpea protein

Oil-in-water emulsions were prepared with a fixed protein concentration of 0.6% (m/m) and oil concentrations ranging from 2 to 10%, relative to the total emulsion mass, within a pH range of 3 to 11. The samples underwent an initial homogenization step using an ultra-turrax (T18 basic, IKA, Brazil) at 10,000 rpm for 5 minutes, followed by re-homogenization using a high-pressure homogenizer (APV, SPX FLOW, Lab Series model 2000, United Kingdom), with 300 bar in the first homogenization stage and 30 bar in the second stage. The emulsions were stored under refrigeration (4 °C).

2.3 Droplet size and size distribution of emulsions

The measurement of droplet size and evaluation of size distribution of emulsions were conducted using the Malvern Zetamaster equipment (Zetasizer Nano – ZS, Malvern, United Kingdom). The Zetasizer software was employed for data collection.

Emulsions were prepared as described in *section 2.2* for a pH range of 3 to 11 and oil concentrations ranging from 2 to 10%. The samples were diluted in distilled water at a ratio of 1:100 to take the measurements of the z-average diameter (D_z), the polydispersity [22] and the droplet size distribution [23]. The droplet size of the emulsions was also represented as the mean surface area (Equation 1) or Sauter Mean Diameter ($D_{3,2}$) and as the mean volume moment (Equation 2) or De Brouckere Mean Diameter ($D_{4,3}$) [24].

$$D_{3,2} = \frac{\sum n_i \cdot d_i^3}{\sum n_i \cdot d_i^2} \quad (1)$$

$$D_{4,3} = \frac{\sum n_i \cdot d_i^4}{\sum n_i \cdot d_i^3} \quad (2)$$

in which D is the diameter of each droplet, and n is the total number of droplets evaluated.

In addition, diameters were characterized based on the maximum droplet size for a specific percentage volume of the sample, indicated by $D_V(10)$ and $D_V(90)$, corresponding to 10 and 90% of the cumulative relative frequency of the distribution curve, respectively [24].

2.4 Rheological behavior

The rheological behavior of cowpea protein-stabilized emulsions was investigated concerning temperature, oil concentration, and pH variations. Due to the pronounced instability observed during the experiments with samples obtained at pH 3 and 5, rheological tests were performed only on emulsions prepared at pH 7, 9, and 11. The flow study encompassed the formulations with all five different oil concentrations (2, 4, 6, 8, and 10%). To evaluate the impact of temperature on the rheological properties, formulations with 2, 6, and 10% concentration of oil phase that represent the minimum, average, and maximum oil levels, respectively, were selected. Rheological analysis was performed using an AR-2000EX rotational rheometer (TA Instruments, New Castle, DE, USA) equipped with a Peltier system for temperature regulation. Shear stress curves were determined using a concentric cylinder geometry, while the influence of temperature was assessed using cone and plate geometry (steel cone, 61 mm diameter, 52 μm gap) due to its superior temperature control and reduced sample requirements.

Shear stress versus shear rate curves were generated over a range of 0.1–158 s^{-1}, at 25 °C. The experimental data were fitted to the Power model [25], represented by Equation (3). The quality of the fit was determined by evaluating the coefficient of determination (R^2). The apparent viscosity (Pa s) was also calculated as follows Equation (4) [25].

$$\tau = K\,\dot{\gamma}^{\,n} \qquad (3)$$

$$\eta_a = \frac{\tau}{\dot{\gamma}} \qquad (4)$$

in which τ (Pa) is the shear stress, $\dot{\gamma}$ (s^{-1}) is the shear rate, K (Pa s) is the consistency index and n is the behavior index.

To investigate the effect of temperature on the rheological properties of the emulsions, a shear rate of 100 s^{-1} was applied with a temperature increase rate of 2 °C min^{-1}. The experiment consisted of three stages: heating from 25 °C to 80 °C, followed by cooling down to 5 °C, and finally reheating of the sample back to 25 °C.

2.5 Stability of emulsions through gravitational method – visual assessment

To assess the stability of the emulsions, samples were prepared at pH 3, 5, 7, 8, 9, and 11, as previously described in *section 2.1*. Following preparation, approximately 10 g of each emulsion was transferred to labeled test tubes. The initial height of each emulsion was measured, and the tubes were placed in a climate chamber at 4 ºC. Over 30 days, the stability of the emulsions was monitored daily by measuring the heights of the interfaces between the different phases formed, including the serum, the intermediate emulsion, and the cream layer. The creaming index (%CI) was calculated based on the height measurements, as described by Equation 5. This index indicates complete phase separation in an emulsion, distinguishing a transparent phase without droplets (serum) and another phase rich in droplets (cream) [26].

For samples that did not exhibit complete phase separation (cream and serum), the cream layer stability (CS) was evaluated according to the methodology proposed by Karaca et al. [27]. This entailed measuring the thickness of the cream phase, located at the top of the tube, and the turbid, optically opaque layer immediately below the cream, which maintains a similar appearance to the original emulsion. The CS (%) was determined by Equation 6, considering the reduction of the turbid layer (H_{turbid}) relative to the total height of the emulsion (H_{total}).

$$CI\ (\%) = \frac{H_s}{H_{total}} \quad (5)$$

$$CS\ (\%) = \frac{H_{turbid}}{H_{total}} \quad (6)$$

in which H_s represents the serum height; H_{total} denotes the total height of the emulsion, and H_{turbid} is the turbid layer height.

2.6 Statistical analysis

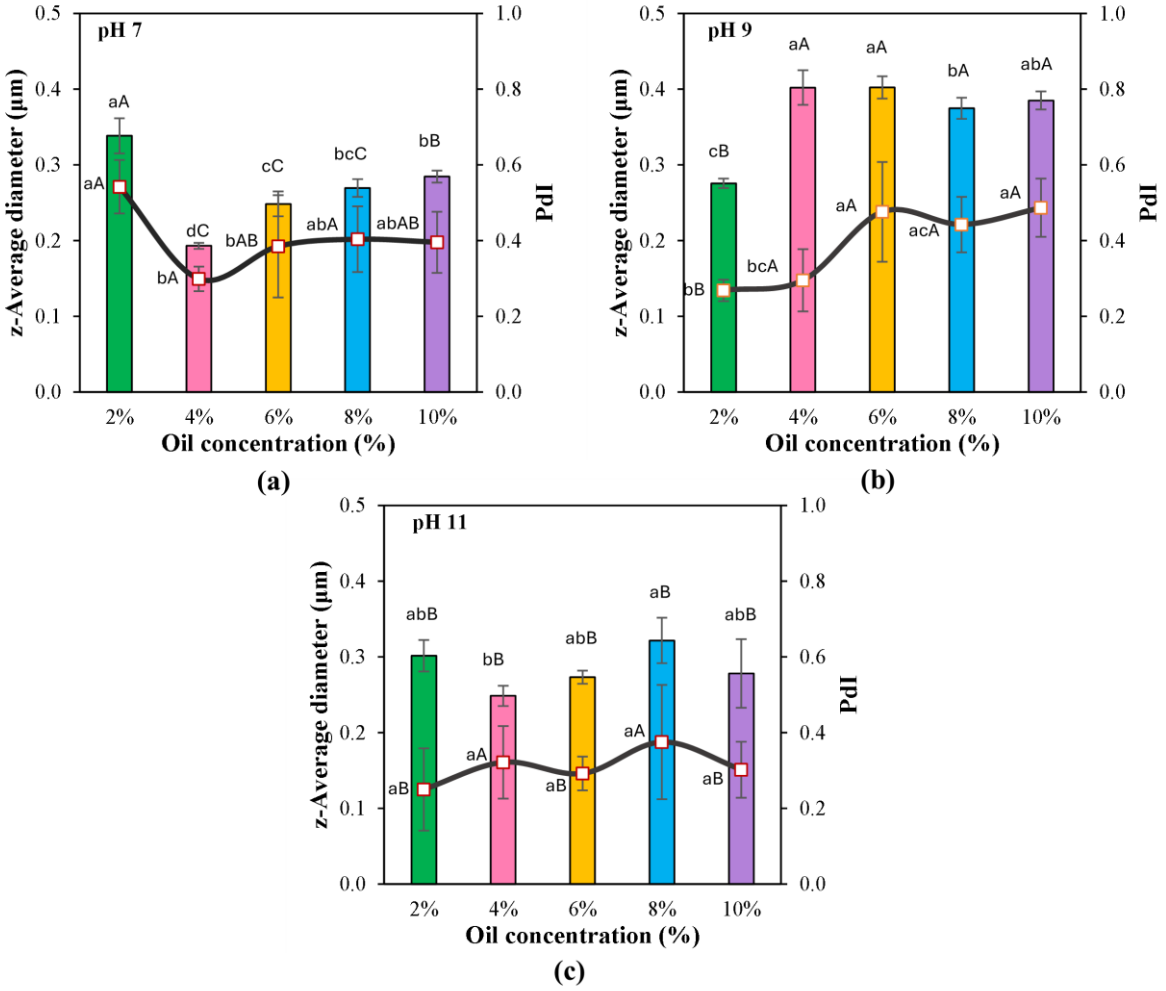
The data are expressed as means ± standard deviation. Statistical analysis was performed using one-way analysis of variance (ANOVA) followed by Tukey's test at a 5% significance level. Specifically, for the mean diameters $D_{3,2}$ and $D_{4,3}$, Duncan's test was applied at a 5% significance level to identify significant differences.

3 Results and discussion

3.1 Emulsion droplet size

The z-average diameter (D_z) of the droplets and the polydispersity index (PdI) from emulsions stabilized with CPC at different pH (7 – 11) and sunflower oil content (2 – 10%) are represented in Figure 4.1. The experiments with the emulsions prepared at pH 3 and 5 were not considered due to the presence of large-sized droplets and sedimentation, along with a high polydispersity in the size distribution, which rendered the results unreliable.

Figure Error! No text of specified style in document.**.18** Z-average diameter D_z (bars) and polydispersity index PdI (line and markers) of emulsions stabilized with CPC at different sunflower oil concentrations and pH values: (a) pH 7; (b) pH 9 and (c) pH 11



Source: elaborated by the author. Means with the same lowercase letter for the same pH did not differ significantly at $p \leq 0.05$ according to Tukey's test. Means with the same capital letter for the same concentration at different pH did not differ significantly at $p \leq 0.05$ according to Tukey's test.

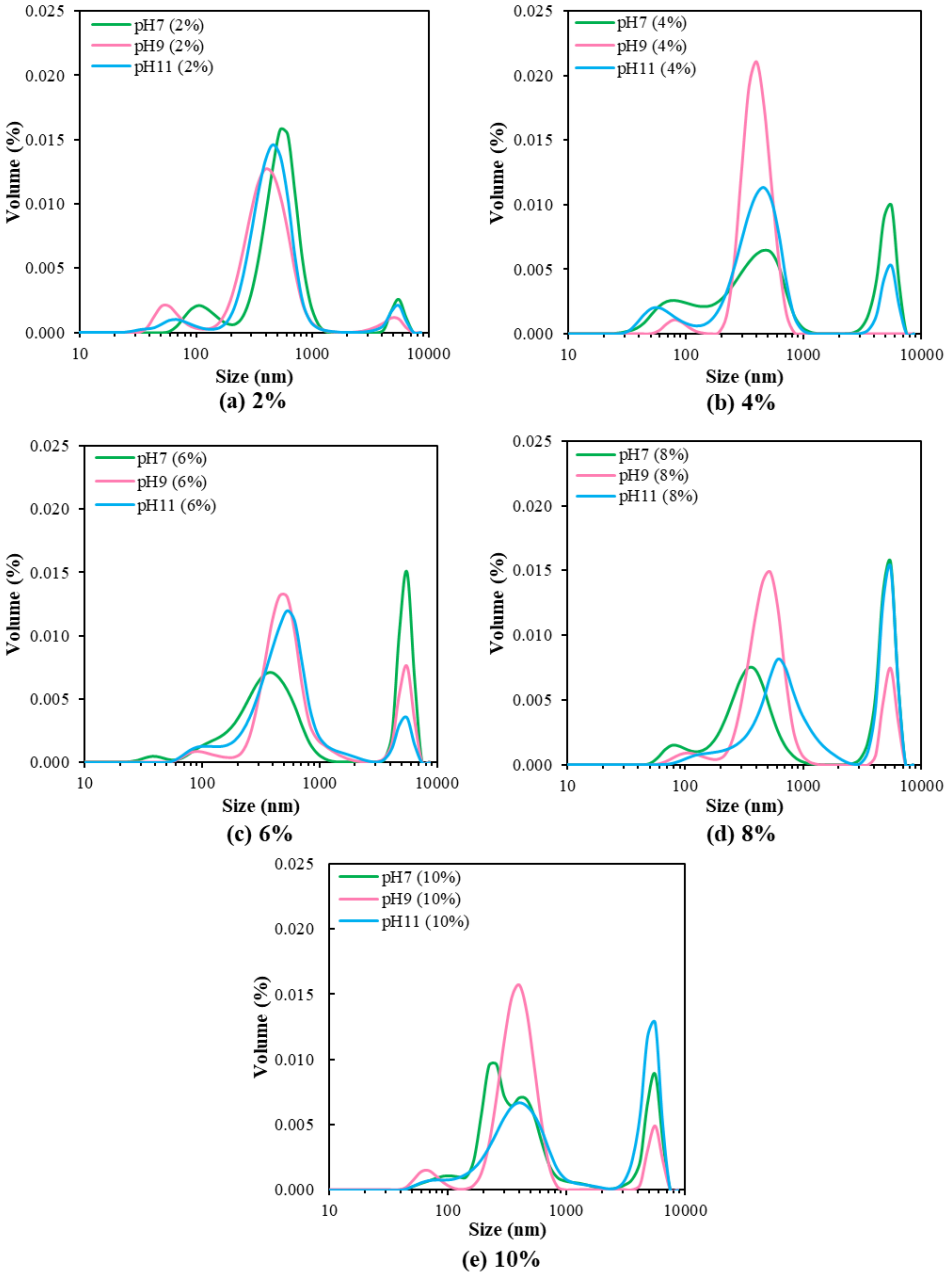
The D_z values provided a measure of the average size of all droplets, calculated from the intensity weighted distribution as result of the dynamic light scattering technique. The mean D_z values ranged from 0.19 to 0.40 μm, reflecting the complexity of the emulsion systems studied, influenced by both, pH and oil concentration. At equivalent oil concentrations, the pH 9 emulsion exhibited larger droplet sizes than the pH 7 and 11 emulsions, except at 2% oil concentration. For emulsions with identical pH values, the size differences between the emulsions were small at pH 11. At pH 9, only the 2% oil concentration demonstrated a more pronounced difference, while at pH 7, this behavior was observed for the 2% and 4% oil concentrations.

The polydispersibility (PdI), which describes the width or spread of the droplet size distribution, presented mean values ranging from 0.25 to 0.54. PdI values followed a trend quite similar to that of D_z (Figure 4.1), with no significant differences at pH 11, but with more pronounced differences at 2% and 4% oil concentrations at pH 7 and 9. Colloidal particles with PdI values close to zero suggest a narrow distribution of droplet sizes, indicating a monodisperse system where the droplets are relatively uniform in size. Conversely, a PdI value exceeding 0.1 signifies a more extensive range of droplet sizes, indicative of a polydisperse system [28]. It is, in fact, typical of a food system for particles to exhibit variation in size. In the current study, a polydisperse system is observed, underscoring the importance of obtaining information concerning the droplet size distribution in the emulsions, as will be discussed subsequently.

Figure 4.2 shows representative particle size distribution profiles based on volume, of the emulsion prepared at pH 7, 9, and 11 with oil concentration varying from 2 to 10%. All curves exhibited a multimodal or bimodal behavior, indicating high heterogeneity in the droplet size in the samples, which can be attributed to the aggregation of proteins and the flocculation of oil droplets [29]. With the increase in oil concentration from 2% to 10%, there was a general rise in the presence of larger droplets and a reduction in the volume of smaller droplets distributed in the emulsions. Tabilo-Munizaga and collaborators [29] also observed that as the proportion of oil increased, while the proportion of protein remained constant, there was an increase in both droplet size and PdI. This led them to conclude that, with a larger amount of oil phase relative to the available protein, the latter may be insufficient to completely cover the oil droplet surface. This imbalance could lead the smaller droplets to coalesce into larger ones, resulting in a broader dispersion of droplet sizes. In their study of emulsions of orange essential oil (6% by mass), Francisco and collaborators [30] observed a comparable pattern when varying the concentration of pea and soy protein in a range of 0.6% to 6.0%. At low protein

concentration (0.6% by mass), a broad size distribution of oil droplets was observed. The increase in protein concentration from 0.6% to 1.2% resulted in a shift towards a bimodal distribution, with a more pronounced peak in a smaller range of droplet sizes. This indicated the presence of smaller droplets and a more uniform distribution as the protein concentration increased in relation to the oil concentration; however, above this concentration, the protein was sufficient to maintain the droplet diameter independent of the protein concentration.

Figure Error! No text of specified style in document.**.19** Droplet size distribution by volume for emulsions stabilized with CPC at different pH values and sunflower oil concentrations (a) 2%; (b) 4%; (c) 6%; (d) 8% and (e) 10%



Source: elaborated by the author.

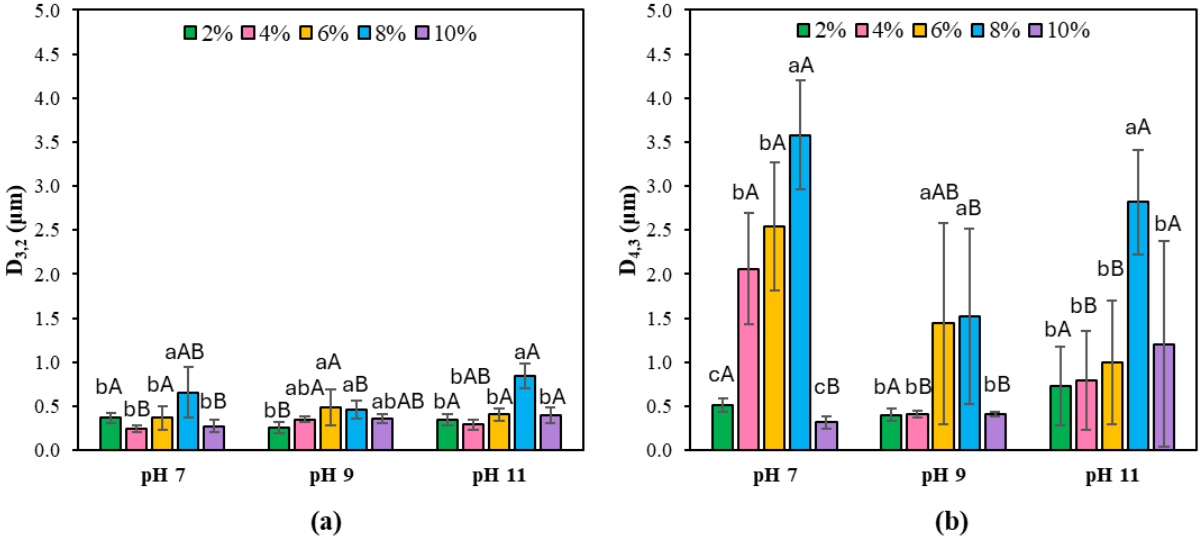
It is observed that pH 9 was the condition in which, except for the 2% oil concentration, the emulsions showed a higher volume distribution of smaller droplets, which could characterize more homogeneous emulsions with smaller droplet sizes. Additionally, for the 4% oil concentration, a less polydisperse distribution was observed in the emulsions at this pH, where the samples exhibited a prominent peak near 400 nm and a smaller one in smaller droplets (80 nm). In this context, most of the proteins are probably involved in stabilizing the droplets, which reduces aggregation. However, at pH 9, the results observed for D_z reflect the prominent peak of the distribution, which in most concentrations, was around 400 nm. Compared to the other pH values, pH 9 appeared to be the condition that led to larger D_z. The absence of information about smaller or larger droplets makes it difficult to evaluate the potential for coalescence or flocculation of droplets.

Therefore, to facilitate the analysis of droplet size distribution data, it was assessed through the statistical parameters $D_{3,2}$ and $D_{4,3}$ (Figure 4.3). The Sauter diameter is more sensitive to the presence of fine droplets in the size distribution, characterized by small and spherical droplets, since it is an average diameter based on specific surface per unit volume [24]. The smaller the $D_{3,2}$, the greater the specific area for protein adsorption. In contrast, the De Brouckere diameter is more sensitive to the presence of large droplets in the size distribution [23] and is therefore a good indicator of droplet aggregation, as it reflects the size of the droplets that constitute most of the sample volume. The results support this information; the volume-weighted mean diameter ($D_{4,3}$) ranged from 0.32 to 2.88 μm, while the surface-weighted mean diameter $D_{3,2}$ showed values approximately 80% smaller (0.24 to 0.77 μm). Hence, the parameter $D_{4,3}$ demonstrates higher sensitivity to the rise in oil concentration within the emulsions. An increase in the oil volumetric fraction relative to protein may result in a gradual rise in $D_{4,3}$, due to a reduction in the available protein covering oil droplets, which subsequently diminishes their capacity to prevent droplet aggregation and coalescence within the emulsion. In addition, an increase in the volumetric fraction of the oil increases the packing fraction, which may increase the collision frequency and thus the size of the aggregates [31]. The ratio of the protein to oil concentrations in emulsions has been associated with a reduction in droplet size and the achievement of more uniform droplets [32]. At lower oil concentrations, more dissolved protein is available in the medium, facilitating the formation of a thicker adsorption layer, which directly influences the stabilization of emulsion droplets during the emulsification process and the high-speed shearing of oil molecules [33]. However, not all treatments follow

the trend of higher protein availability leading to smaller droplet sizes. It appears that both insufficient and excessive protein availability resulted in larger emulsion droplet sizes, whereas at appropriate concentrations, a finer emulsion could be obtained.

In this context, in addition to the sunflower oil/protein ratio, pH also played a significant role. As the pH value increases, the protein molecules become increasingly negatively charged, which results in enhanced electrostatic repulsion between the charges of the amino acids within the same protein molecule, thereby facilitating protein unfolding [34]. At the same time, repulsion can increase the protein adsorption at the oil/water interface, promoting the formation of more homogeneous and smaller droplets. Additionally, variations in the molecular structure of proteins affect their surface properties and consequently determine whether or not the protein acts as an effective surfactant. Krstonošić et al. [33] observed that increasing the pH value from 7 to 9 resulted in a decrease in the average droplet diameters of pea and potato protein-stabilized emulsions, whereas for emulsions containing whey and soy proteins, this decrease was not significant.

Figure Error! No text of specified style in document.**.20** Mean diameter based on (a) surface area mean diameter ($D_{3,2}$) and (b) volume moment mean diameter ($D_{4,3}$) of emulsions stabilized with CPC at different pH levels (7 – 11) and sunflower oil concentrations (2 – 10%)



Source: elaborated by the author. Means with the same lowercase letter for the same pH did not differ significantly at $p \leq 0.05$ according to Dunkan's test. Means with the same capital letter for the same concentration at different pH did not differ significantly at $p \leq 0.05$ according to Dunkan's test.

A noteworthy variability in $D_{4,3}$ values concerning pH is observed, and no discernible pattern emerges. Conversely, for a given pH, as the oil concentration increases from 2% to 8%, the average droplet size tends to increase and then decrease at an oil concentration of 10%.

Specifically at pH 9, there appears to be greater homogeneity in droplet sizes regardless of the tested oil concentrations, indicating potentially higher droplet stability. The data for $D_{3,2}$ also indicate that there is no evident correlation between average droplet size and pH. Furthermore, a discernible trend concerning oil concentration dependence aligns with the behavior observed for $D_{4,3}$.

The primary distinction between the $D_{4,3}$ and the $D_{3,2}$ is the larger size of the former, particularly at oil concentrations of 4, 6, and 8%, which is to be expected when the sample contains a high concentration of fine droplets [23, 24]. Furthermore, it is noteworthy that, in general, the 8% oil concentration consistently yielded the largest droplet size, regardless of pH. Additionally, pH 9 yielded smaller average droplet sizes than the other pH values.

In the case of volume-weighted droplet size distributions, the diameter is determined based on the maximum droplet size for a given percentage volume of the sample [24]. The diameters $D_V(10)$ and $D_V(90)$, which correspond to 10% and 90% respectively, of the relative cumulative volume in the droplet size distribution curve, are presented in Table 4.1. The results of the size distribution (Figure 4.2) are corroborated by the $D_V(10)$ and $D_V(90)$, which highlight the distinction between the two distributions, thereby indicating that the system exhibits high polydispersity. This is not solely dependent on the oil concentration but also on the pH.

Table Error! No text of specified style in document.**.10** Mean diameters D_{10} and D_{90} of droplets in emulsions stabilized with CPC at different pH levels (7 – 11) and sunflower oil concentrations (2 – 10%)

%	$D_V(10)$ (µm)			$D_V(90)$ (µm)		
oil	**pH 7**	**pH 9**	**pH 11**	**pH 7**	**pH 9**	**pH 11**
2	$0.16 \pm 0.04^{ab,A}$	$0.15 \pm 0.08^{b,A}$	$0.24 \pm 0.03^{a,A}$	$0.75 \pm 0.12^{c,A}$	$0.61 \pm 0.12^{a,A}$	$0.63 \pm 0.07^{b,A}$
4	$0.08 \pm 0.01^{b,B}$	$0.26 \pm 0.02^{ab,A}$	$0.08 \pm 0.02^{b,B}$	$5.58 \pm 0.31^{b,A}$	$0.54 \pm 0.07^{a,B}$	$0.59 \pm 0.05^{b,B}$
6	$0.17 \pm 0.05^{a,B}$	$0.33 \pm 0.09^{a,A}$	$0.21 \pm 0.02^{a,B}$	$5.98 \pm 0.24^{a,A}$	$0.63 \pm 0.05^{a,B}$	$0.71 \pm 0.07^{b,B}$
8	$0.23 \pm 0.09^{a,A}$	$0.30 \pm 0.05^{a,A}$	$0.30 \pm 0.09^{a,A}$	$6.15 \pm 0.06^{a,A}$	$0.65 \pm 0.05^{a,C}$	$5.93 \pm 0.15^{a,B}$
10	$0.15 \pm 0.03^{ab,B}$	$0.15 \pm 0.08^{ab,AB}$	$0.30 \pm 0.10^{a,A}$	$0.44 \pm 0.14^{c,B}$	$0.56 \pm 0.05^{a,B}$	$5.90 \pm 0.26^{a,A}$

Means with the same lowercase letter for the same pH did not differ significantly at $p \leq 0.05$ according to Tukey's test. Means with the same capital letter for the same concentration at different pH did not differ significantly at $p \leq 0.05$ according to Tukey's test.

Consequently, it is reasonable to infer that 80% of the total volume is associated with droplets with average diameters ranging from 0.08 µm to 5.98 µm, 0.15 µm to 0.65 µm, and 0.08 µm to 5.93 µm for pHs 7, 9, and 11, respectively. These measurements also mirrored the distinctive characteristics observed at pH 9. Under this pH condition, 90% of the volume occupied by the droplets corresponded to droplets smaller than 0.65 µm, while for pHs 7 and

11, depending on the oil concentration, droplet sizes could be up to approximately 10 times larger. The more uniform distribution observed at pH 9 is corroborated by the greater similarity in the values of $D_V(10)$ and $D_V(90)$ for this pH.

In summary, the analysis of emulsion droplet size distribution revealed the impact of oil concentration, protein content, and pH on emulsions. These factors exert significant influence on both droplet size and distribution. It is noteworthy that as oil concentration increases, there is a general tendency for droplet sizes to become larger until a critical concentration (8%), at which point droplet size decreases. However, this trend was not uniform across all pH levels. pH 9 appeared to be a critical parameter, displaying more consistent droplet sizes and potentially enhanced stability, especially at lower oil concentrations. Furthermore, the polydispersity index and distribution pattern highlighted the diversity in droplet sizes within the emulsions. Selecting the statistical parameters $D_{3,2}$ and $D_{4,3}$ facilitated a more comprehensive understanding of the distribution profile, corroborated by the cumulative volume distributions $D_V(10)$ and $D_V(90)$.

3.2 Emulsion rheology

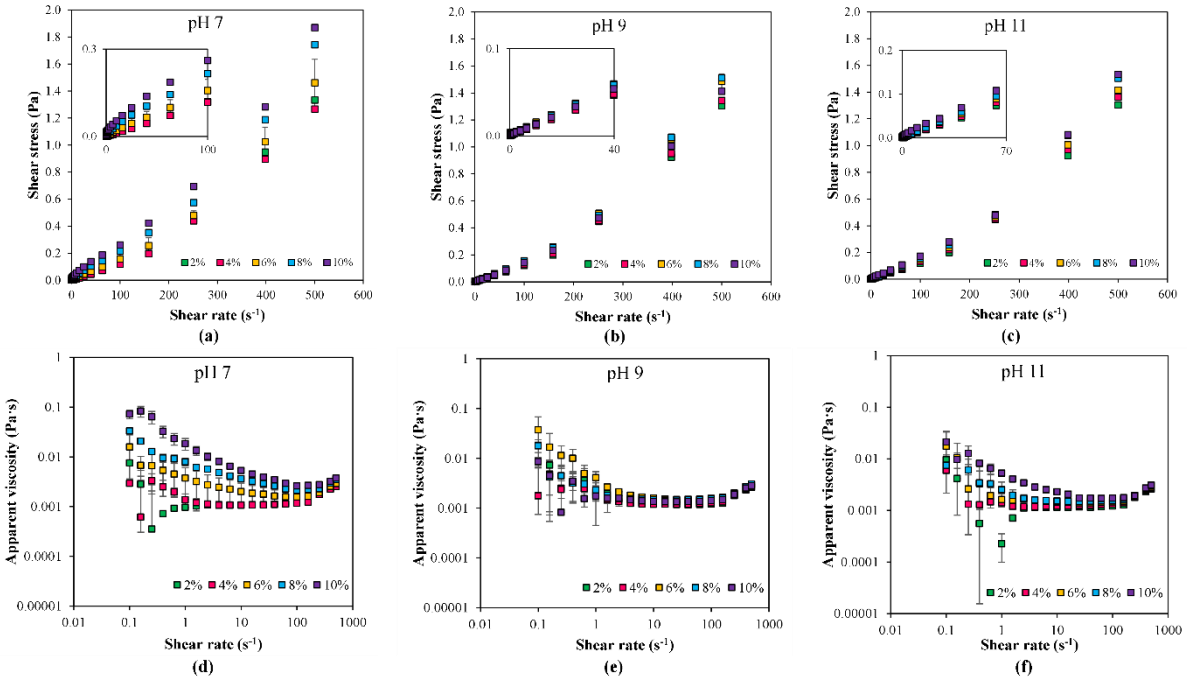
3.2.1 Flow properties – effect of pH and oil concentration

Figure 4.4 (a, b, c) depicts the flow curves and demonstrates the effect of shear rate on the shear stress value of emulsions stabilized by cowpea protein at different pH values (7, 9, and 11) and oil contents (2 – 10%). As anticipated, the oil content significantly impacted the rheological response of the O/W emulsions to shear forces. With increasing oil phase content (from 2 to 10%), the emulsions featuring higher oil concentrations exhibited a more pronounced evolution in shear stress. This trend is particularly evident when examining the curves for emulsions prepared at pH 7 (Figure 4.4a). Conversely, an increase in pH from 7 to 9 or 11 resulted in a reduction of the discrepancy between the stress induced by varying oil concentrations, which became less pronounced (Figures 4.4b and 4.4c).

A detailed examination of the experimental data reveals that a specific frequency value is associated with a transition in the rheologic behavior, as observed in practically all formulations. As illustrated in the accompanying zooms, an increase in shear stress is observed in the initial frequency range as the shear rate rises, exhibiting a slight convex curvature towards the shear stress axis. This behavior corresponds to shear thinning fluid. As the frequency is increased, a discernible shift in curvature is observed in the full graphic, resulting in a concave shape in the direction of the stress axis, which indicates that the fluid exhibits shear-thickening behavior.

Regarding the apparent viscosities depicted in Figures 4.4d, 4.4e, and 4.4f, it is possible to discern more clearly the regime transitions. At a pH of 7, the viscosity behavior undergoes a shift at a frequency of approximately 100 s^{-1}, from which it exhibits the characteristics of a shear-thickening fluid for oil concentrations ranging from 4% to 10%. Nevertheless, at frequencies below 1 s^{-1}, the viscosity of the emulsion with 2% oil concentration exhibited a sudden decline and a subsequent increase, accompanied by significant deviations from the mean values. At pH 9, the inflection point exhibited a range of values, from 16 to 40 s^{-1}, with a general trend of increasing values with decreasing concentration. At pH 11, the inflection point is observed between 10 and 63 s^{-1} for the 4% to 10% range, while the 2% oil sample exhibited a behavior similar to that observed at pH 7. For pH 9 and pH 11, the emulsions display shear-thickening behavior that extends beyond the identified inflection point. However, inconsistencies and discrepancies were noted at frequencies of 1 s^{-1} or lower for both pH levels. The presence of discrepancies or deviations at extremely low frequencies ($\leq$ 1 s^{-1}) at all pH levels indicates that measurements within this range may be constrained, particularly for low oil concentrations. The observed viscosity behavior at varying pH levels and oil concentrations highlights the complexity of rheological transitions in emulsions as a function of shear rate, reflecting changes in the internal structure and dynamics of the emulsions.

Figure Error! No text of specified style in document**..21** Flow curves and apparent viscosity of CPC-stabilized emulsions at different sunflower oil concentrations (2 – 10%) and pH levels (a, d) pH 7; (b, e) pH 9; and (c, f) pH 11.



Source: elaborated by the author.

The viscosity-shear rate dependence in dispersions or suspensions has been the subject of several theories [35-38]. However, the challenge of predicting the behavior of such fluids has persisted due to the numerous factors influencing their rheological properties [38]. As previously observed by Wagner and Brady [37], modifications in the microstructure of a colloidal dispersion are associated with the transitions to shear thinning and shear thickening. Ozel and colleagues [35], in their study of fumed silica particles dispersed in colloidal suspensions, observed the occurrence of shear thickening/thinning flow behavior, which they attributed to the microstructure of particles in continuous media, associated changes in cluster sizes, and the interaction forces among particle-particle and particle-polymer interactions. However, emulsions have particularities. As McClements [26] reports, the flocculation or coalescence of oil droplets in an emulsion has a significant impact on their stability and rheological properties, potentially leading to a range of behaviors as a function of shear rate.

Krstonošić et al. [33] studied emulsions stabilized by four different protein sources (soy, potato, pea, and whey), and the dispersed phase concentration was increased from 5% to 30% oil. Their results for lower oil content show behavior strictly of pseudoplastic fluid for all proteins tested, while at 30% oil content it closely resembles Newtonian fluids. As aforementioned, the explanation is not straightforward due to the numerous factors that influence the outcome. These include the structure of the droplets and the surfaces available for protein adsorption, the attraction and aggregation of the droplets under the applied stress, as

well as the properties of the oil phase, such as density, viscosity, and surface tension [33,39]. Bellalta et al. [39] examined emulsions with high oil content (50%, 55%, and 60%), and found that emulsions with lower oil content exhibited Newtonian behavior, whereas those containing 60% oil displayed shear-thinning behavior. As the oil content increased, the droplets became closer, causing the oil droplets to pack together, and intensifying inter-particle interactions. The degree of thixotropy of the emulsions increased with an increase in the oil content, and their time-dependent viscosity behavior was successfully described by a kinetic model.

The preceding explanation indicates that the apparent viscosity of emulsions may also be influenced by their oil content, as depicted in Figure 4. In general, the high oil content resulted in higher resistance to shear stress, which is attributed to the tight packing of dispersed droplets [1]. This is evidenced at pH 7 (Figures 4.4a, 4.4d) and at pH 11 (Figures 4.4c, 4.4f). Nevertheless, at pH 9, this trend was not evident at the highest concentrations (6% to 10%). In this range, the maximum stress resistance at the lowest frequency was observed at 6% oil content.

Regarding pH, as evidenced by the droplet size distribution results (Figure 2), there is a tendency for droplet diameter reduction and a more homogeneous size distribution in emulsions at alkaline pH values. This may explain the pH effect on variation in viscous properties. The enhancement of protein solubility at pH levels distant from the isoelectric point (pI) enables its rapid association with the oil-water interface. At the same time, the rise in net charge promotes the electrostatic repulsion of the oil droplets coated with proteins, hindering coalescence [40]. The repulsion is particularly intense at pH values significantly above or below the protein pI, preventing their aggregation. Conversely, pH in the vicinity of the pI can result in the formation of larger droplet sizes, which may contribute to an increase in emulsion viscosity. This is attributable to a reduction in the net charge, which renders an electrostatic repulsion insufficient to overcome van der Waals attraction, leading to flocculation [41]. Consequently, at pH values closer to the pI, the viscosity of the emulsion may increase as a consequence of a greater degree of attraction between the droplets [42].

In the present study, emulsions at pH 7 exhibit a heightened propensity for coalescence or flocculation, which can be attributed to the diminished electrostatic repulsion of protein [34]. This fact can increase viscosities, as aggregates retain part of the continuous phase within their structures, thereby promoting viscosity enhancement [26, 42]. In contrast, at alkaline pH values (9 and 11) the emulsions exhibited lower viscosities, which may indicate a reduction in droplet coalescence and flocculation [43].

The steady reduction in viscosity with increasing shear rate is observed at all pH values, characteristic of pseudoplastic fluids, which is more frequent than dilatant fluid behavior [26]. As posited by the author, at intermediate shear rates, droplets become aligned in the flow, forming two-dimensional sheets comprising droplets enabling relatively easy sliding over each other, which lowers their viscosity; however, at higher shear rates, disruption of these sheets occurs, resulting in increased viscosity. Moreover, shear thickening may also occur when the shear stress applied to an emulsion causes the dispersed phase to flocculate as a result of an increase in the frequency of collisions between the droplets [26].

The most pronounced reduction in apparent viscosity with increasing shear rates in the range of 0.1 to 100 s^{-1} occurs at pH 7 (Figure 4.4 d), indicating pseudoplastic behavior. Conversely, the steady reduction at pH 9 and 11 is less evident, as the protein is in its most soluble form at more alkaline pH values, with its chains more extended and possibly even partially denatured [44]. Moreover, pH appears to be the primary factor influencing the observed variations, while shear rate exerts a minor effect on viscosity, especially in the intermediate shear rate range of approximately 0.1 to 100 s^{-1}. Based on this, in this range, the apparent viscosity of emulsions reaches approximately constant values, approaching a Newtonian fluid behavior particularly for pH 9 in all concentrations, and pH 11 except at 10% oil concentration. Finally, at shear rates above this intermediate range, for all formulations, there is a clear increase in emulsion viscosity with increasing shear, which is characteristic of dilatant fluids.

3.2.2 Thermal treatment

The heating and cooling tests (25 °C to 80 °C, 80 °C to 5 °C, and 5 °C to 25 °C) were conducted on a limited set of formulations, focusing on extreme oil concentrations (2% and 10%) and an intermediate concentration (6%).

The relationship between the apparent viscosity of the emulsions and the temperature was evaluated, and the corresponding experimental data are shown in Figure 4.6 (a, b, c). Emulsions exhibited an initial apparent viscosity of approximately 0.001 Pa s at all pH values, with exception of those prepared at pH 7 with an oil concentration of 10%, which exhibited a notably higher apparent viscosity (approximately 0.003 Pa s) at the onset of the heating process.

During the initial heating phase, the emulsions exhibited distinct behaviors, which were influenced by the pH of the continuous phase and the amount of oil present. At pH 7, the apparent viscosity did not exhibit distinct changes until reaching 45 °C. A gradual increase in apparent viscosity was observed from 45 °C for concentrations of 6% and 10% oil. In contrast,

at a 2% oil concentration, this increase commenced at a later temperature, 50 °C. The viscosity values demonstrated a tendency towards stabilization at approximately 55 °C for the 10% oil concentration and 65 °C for the 2% and 6% concentrations. For pH 9, the apparent viscosities of the emulsions exhibited slight variations, suggesting a tendency towards an increase, although they remained within a narrow range of values. In contrast, at the most alkaline conditions (pH 11), the apparent viscosity demonstrated a proclivity towards a reduction in value with increasing temperature, although the variation also remained within a narrow range of values.

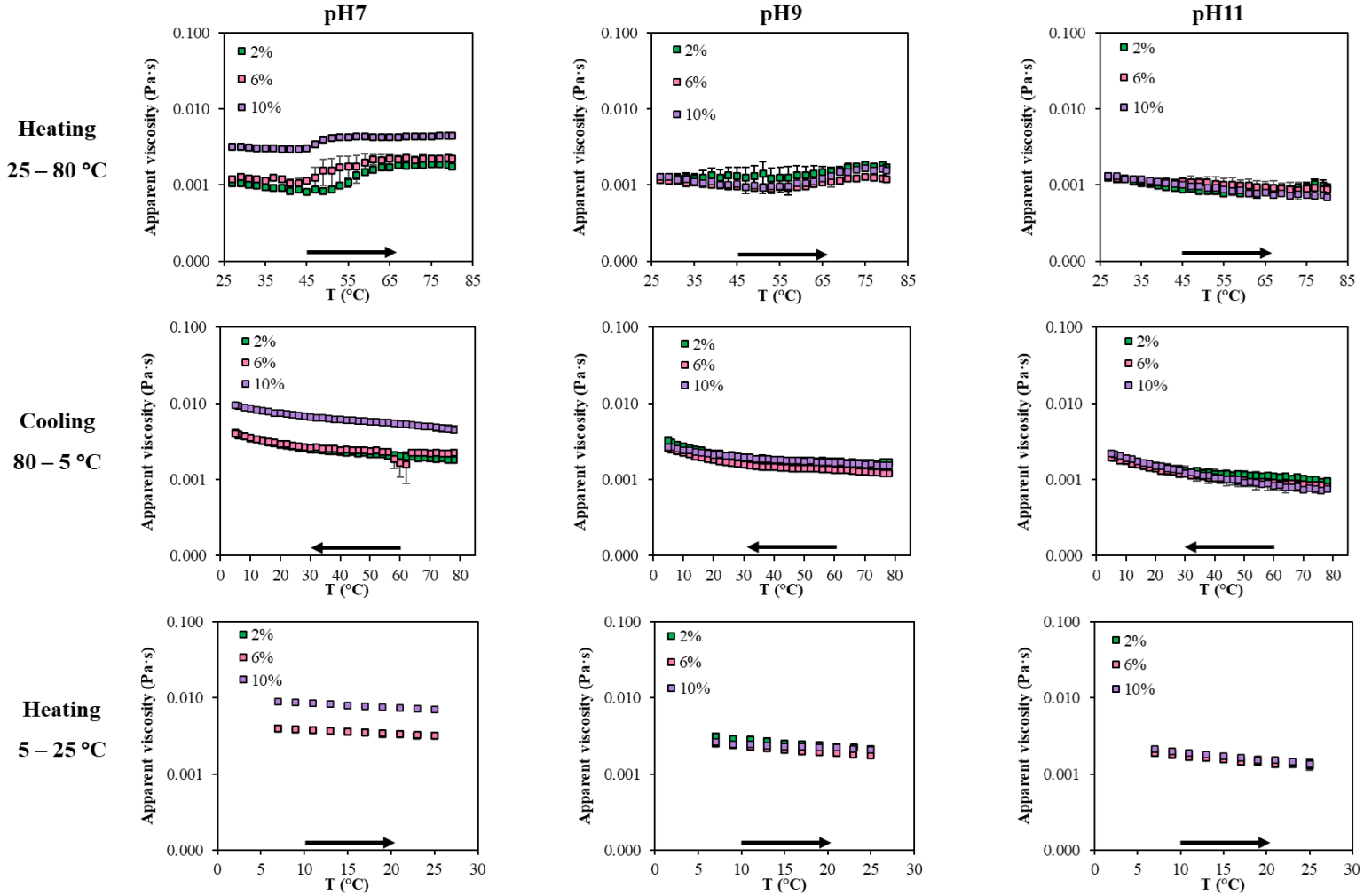
The change in apparent viscosity behavior observed during the heating can be attributed to several underlying factors, including interactions between the dispersed oil droplets and the continuous phase which subsequently led to alterations in the emulsion microstructure. As temperature rises, the mobility of molecules within the emulsion increases, which may facilitate interactions between the dispersed oil droplets and the continuous phase [45,46]. This can lead to an increased entanglement of the emulsion components, and, at even higher temperatures, the thermal energy may surpass intermolecular forces, leading to the formation of larger aggregates or structural rearrangements that contribute to an increase in viscosity. This effect is particularly pronounced in systems with higher dispersed phase concentration, where the available space for droplet movement is significantly limited and the droplets are in close proximity, which facilitates protein aggregation and droplet flocculation [46,47].

The observed rise in viscosity during heating may also be related to heat-induced gelation and denaturation, either adsorbed or non-adsorbed protein. Oliveira et al. [44] determined the denaturation temperatures of CPC in aqueous solution across a range of pH values, yielding 87.84 °C at pH 7, 83.40 °C at pH 9, and 82.64 °C at pH 11, all of which are above 80 °C. However, the denaturation temperature of proteins in the emulsion, compared to that in the aqueous solution, may shift to a lower value, as proteins adsorbed at the water-oil interface are more susceptible to thermal denaturation [46,48].

During the cooling stage (80 – 5 °C), an increase in viscosity was observed as the system cooled down, particularly at neutral pH. Following cooling, a brief heating stage ensues to restore the temperature to the initial room temperature (5 – 25 °C). During this phase, the viscosity of the samples decreases, with the expectation of returning to the initial levels before the thermal process. However, for pHs 7 and 9, this does not occur; the final viscosity is higher than the initial, indicating an irreversible process. Additionally, the difference between the final and initial viscosity is more pronounced for emulsions at neutral pH than at pH 9.

The hypotheses that emulsions are destabilized due to accelerated coalescence and protein denaturation, both caused by heat, are thus confirmed for pHs 7 and 9, which exhibited irreversible behavior under the influence of temperature. The greatest apparent viscosity variation was observed in emulsions at pH 7 with a 10% oil concentration, suggesting that the protein-coated droplets are in close proximity and exhibit reduced electrostatic repulsion. At pH 9, smaller variations were observed, including 10% oil concentrations, which may be attributed to the higher electrostatic repulsion of the charged protein surface on the droplets compared to pH 7. In contrast, pH 11 demonstrated reduced susceptibility to undergo thermal action in comparison to other conditions. At pH 11, despite fluctuations in viscosity, the heat was insufficient to destabilize the emulsion, maintaining its stability. It is anticipated that, with increasing temperature, protein unfolding will occur, leading to a reduction in viscosity. However, in this pH condition, the protein is already in its most soluble form, with extended chains and exposed groups, resulting in lower sensitivity to changes in molecular interactions induced by heating [44].

Figure Error! No text of specified style in document..**22** Apparent viscosity curves of CPC-stabilized emulsions at different sunflower oil concentrations (2 – 10%) and pH levels (vertical) under thermal treatment (horizontal)



Source: elaborated by the author.

3.3 Stability of emulsions through gravitational method – visual assessment

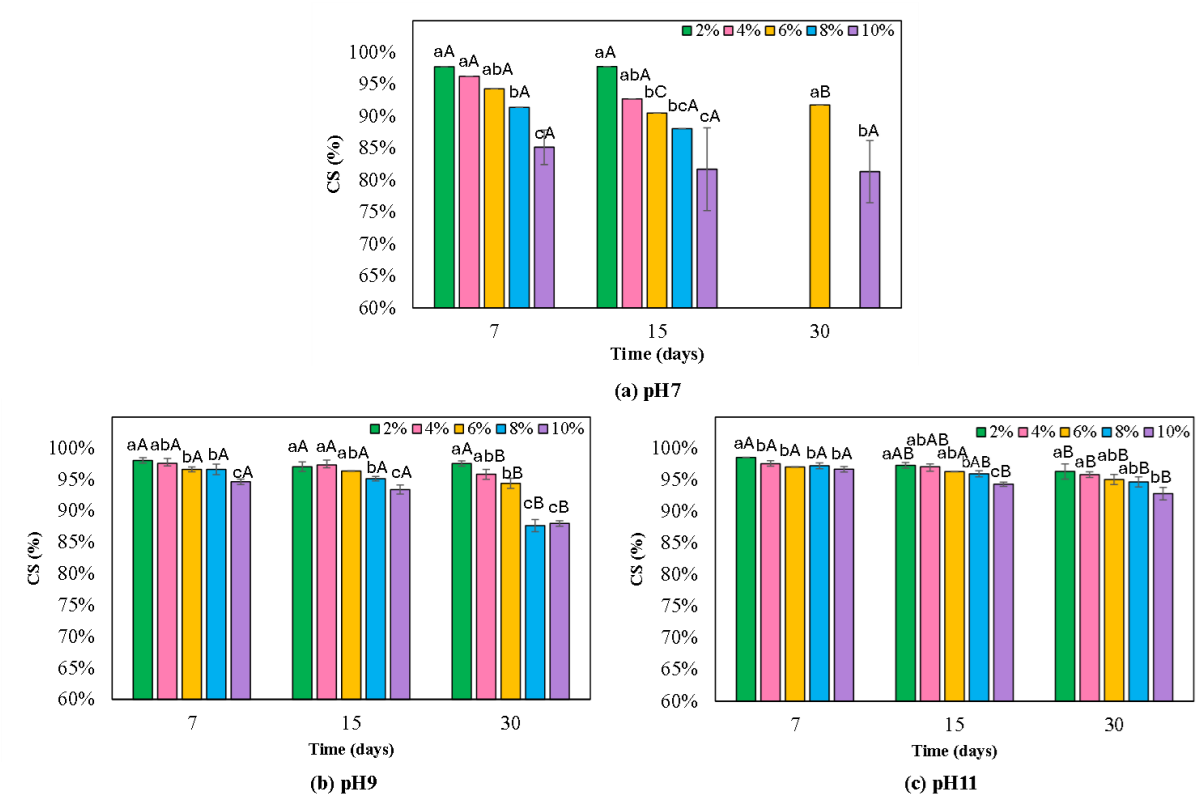
Emulsions were prepared at pH 3, 5, 7, 9, and 11, with a fixed concentration of CPC at 0.6% and oil concentrations varying from 2 to 10% relative to the total mass of the solution. These emulsions were stored at 4 °C and evaluated visually over 30 days to determine whether phase separation occurred. Initially, upon passage through the high-pressure homogenizer (300 bar) and subsequent transferred to test tubes, the emulsions displayed a uniform appearance devoid of any discernible phase separation.

Following a 24-hour refrigerated storage period at 4 °C, all formulations prepared at pH 3 and 5 (from 2 to 10% oil) exhibited a visible phase separation into serum and cream, as anticipated based on prior experience in emulsion preparation for droplet size analysis (*section 3.1*). This separation is illustrated in Supplementary Material – Figure S1. These results highlight the complexity involved in forming emulsions stabilized by proteins near their pI, typically between 3.4 – 6.0 for cowpea protein [17,49]. As the pH approaches the pI, the overall charge of the protein approaches zero, resulting in minimal electrostatic repulsion between proteins [34]. Consequently, protein-coated droplets will come closer together, increasing the risk of coalescence.

The remaining pH values (7, 9, and 11) were continuously monitored. Although complete phase separation (serum and cream) did not occur, after two days of storage, the appearance of a cream layer on the surface of the tubes was observed, while a layer similar to the original emulsion remained just below (Supplementary Material – Figure S2). The cream layer exhibited a subtle demarcation line between it and the less oil-concentrated emulsion, which was almost imperceptible, especially in the early days. During the initial stages of formation, the surface layer did not exceed an average thickness of 0.5 cm, representing less than 4% of the total volume of the emulsion stored in the test tube.

The evolution of the cream layer over the 30-day storage period was monitored and its stability was evaluated based on the data collected. The cream layer stability (CS) from the 7th to the 30th day of storage is presented in Figure 4.7 as a function of oil content while Figure 4.8 depicts CS as a function of pH. The data for pHs 3 and 5 are not represented in the graph due to the occurrence of phase separation. Emulsions containing 2%, 4%, and 8% oil, prepared at pH 7, also displayed phase separation after 21 days (2%) and 28 days (4% and 8%) of storage (Supplementary Material – Figure S3). Consequently, these measurements are also omitted from Figures 4.7 and 4.8.

Figure Error! No text of specified style in document..**23** Cream layer stability (CS) of emulsions over a 30-day storage period as a function of oil content (a) pH7; (b) pH9 and (c) pH 11



Source: elaborated by the author. Means with the same lowercase letter for the same day did not differ significantly at $p \leq 0.05$ according to Tukey's test. Means with the same capital letter for the same concentration at different day did not differ significantly at $p \leq 0.05$ according to Tukey's test.

Figure 4.7 demonstrates that the CS declines as the oil concentration increases, and this effect is more pronounced as the storage period progresses. The behavior of the cream layer during storage is influenced by a number of factors, including the interactions between oil droplets and proteins within the emulsion. The decline in stability over time can be attributed to the upward movement of protein-coated oil droplets towards the surface, where they aggregate to form the cream layer. This migration occurs as gravitational forces overpower the stabilizing forces within the emulsion, such as electrostatic repulsion between droplets [47].

The observation of a thicker cream layer in emulsions with higher oil concentrations lends support to this explanation, as a larger quantity of oil facilitates the migration and accumulation of droplets at the surface. This phenomenon is particularly noticeable in emulsions containing 10% oil, which develop a thicker cream layer over the storage time, demonstrating the lowest stability.

The pH 11 condition stands out for its capacity to maintain emulsion stability above 90% even after 30 days of storage, indicating a reduced propensity for phase separation and cream layer formation. In contrast, pH 7 exhibits stability below 85%, and complete phase separation is observed for some conditions, suggesting greater droplet mobility and, consequently, faster cream layer formation. In pH values distant from the pI and when the droplet charge is sufficiently high, there is a greater electrostatic repulsion between protein molecules, impairing aggregation and increasing emulsion stability. Additionally, attractive intermolecular interactions between adsorbed proteins may occur due to their hydrophobic nature, which can be strong enough to overcome electrostatic repulsion and promote flocculation [50,51]. The process of droplet flocculation typically results in an accelerated cream formation of cream in emulsions, which in turn reduces the stability of the emulsion [52].

The evolution of the cream layer can be correlated with the droplet size of the emulsions (*section 3.1*). Emulsions prepared at pH values that demonstrate a higher propensity for phase separation, such as pH 7, exhibit a more polydisperse droplet size distribution than those prepared at more stable pH, such as pH 9 and pH 11. The increased mobility of droplets at pH values that favor phase separation may facilitate a faster coalescence of oil droplets, resulting in distinct droplet size distributions and thus contributing to the quicker formation of the cream layer. Conversely, in more stable pH conditions, such as pH 9 and 11, the formation of the cream layer is delayed.

Furthermore, protein solubility can contribute to the increased formation of the cream phase. In their study of the emulsifying and physicochemical properties of protein isolates derived from chickpeas, fava beans, lentils, and peas, Karaca et al. [27] observed that the rate of cream formation increased rapidly at low levels of isolate solubility and exhibited a gradual decline as isolate solubility increased. The solubility of cowpea protein at pH 7 was reported to be approximately 30%, while at pH 9 and 11, it was found to be approximately 85% and 95%, respectively [19].

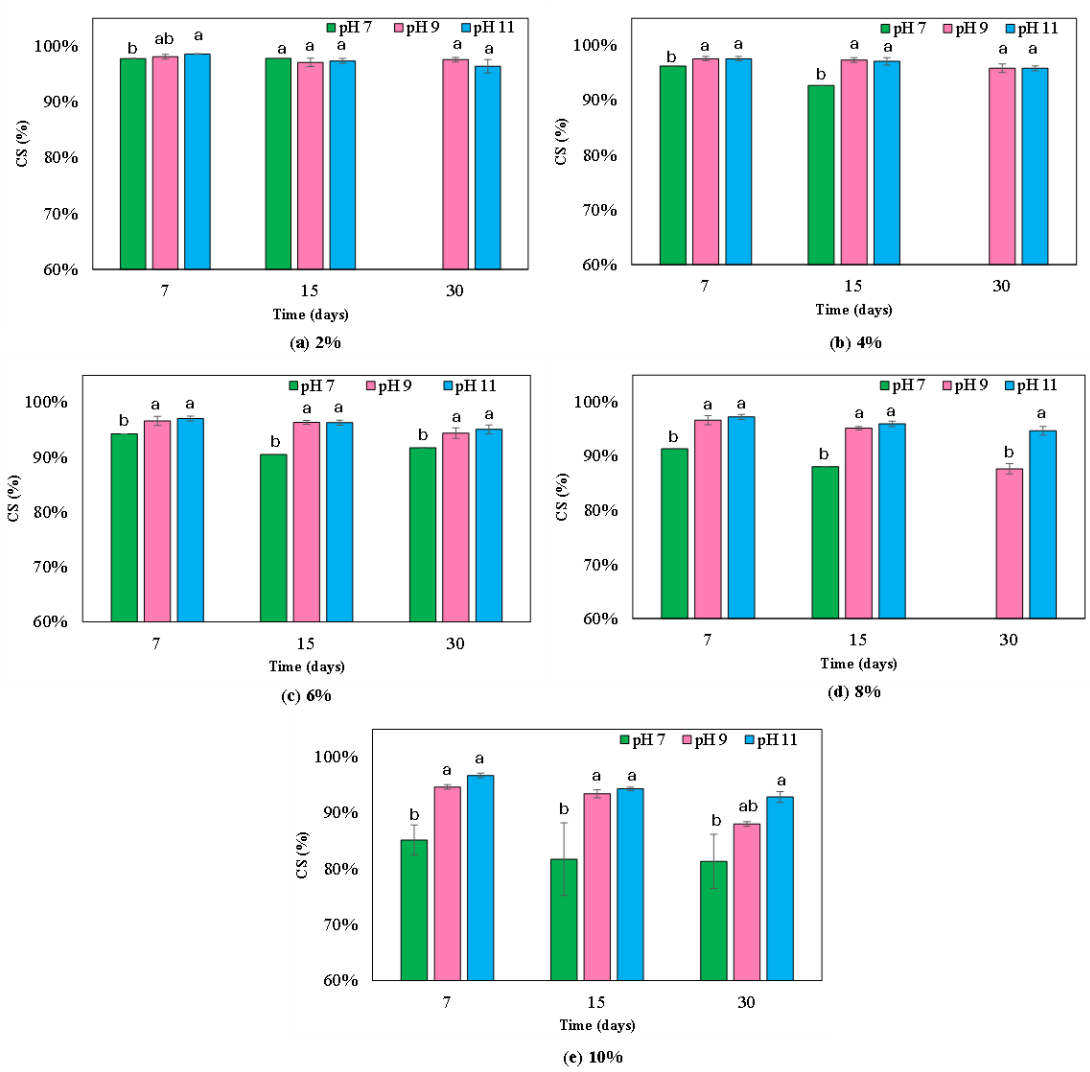
The creaming index (CI) was calculated for the assays that exhibited phase separation. At pH 5, CI values ranged from 42.2 ± 1.5% to 39.0% ± 0.5%, for the highest and lowest oil concentrations, respectively. For pH 3, emulsions with 2% oil recorded an average CI of 19.0 ± 0.2%, while for emulsions with 10% oil, the CI was 68.2 ± 2.9%. At pH 7, phase separation occurred only after a storage period exceeding 20 days, with a CI of 30.7 ± 1.9% for samples containing 2% oil, 24.3 ± 5.6% for 4% oil, and 23.9 ± 2.7% for 8% oil.

Although some formulations at pH 7 exhibited phase separation indicating the formation of distinct serum and cream layers after 30 days (2%, 4%, and 8% concentrations,

Supplementary Material – Figure S3), it is noteworthy that CPC exhibited the capacity to maintain the stability of these emulsions for over 20 days. This observation suggests that, even under conditions where phase separation is favored, the protein presence plays a crucial role in stabilizing the emulsions, providing their stability for a certain period.

The impact of pH on the formation of the cream layer can be more effectively discerned for each oil concentration, as illustrated in Figure 4.8. This graphical representation underscores the diminished stability of emulsions at pH 7 and the analogous characteristics at pH 9 and 11, with a marginal advantage observed for the highest pH at 8% and 10% concentration after 30 days.

Figure Error! No text of specified style in document.**.24** Cream layer stability (CS) of emulsions over a 30-day storage period as a function of pH (a) 2%; (b) 4%; (c) 6%; (d) 8%; (e) 10% oil content



Source: elaborated by the author. Means with the same lowercase letter for the same day did not differ significantly at $p \leq 0.05$ according to Tukey's test.

In summary, the ability of CPC to maintain emulsion stability can be attributed to its emulsifying and stabilizing properties, which are contingent upon the pH conditions and concentrations in complex relationship between a multitude of variables, including electrostatic interactions, shape and conformation of proteins, and concentration of each component in the solution. These variables, in turn, determine the size of droplets, solution viscosity, and mobility of droplets that ultimately will influence the emulsifying and stability performance of the emulsions. CPC has demonstrated efficacy in alkaline conditions, both pH 9 and pH 11.

4 Conclusion

The pH and oil concentration were identified as determinants that influence the droplet size distribution in emulsions. The results demonstrated a broader distribution of droplet sizes, which was explained by the parameters $D_{3,2}$ and $D_{4,3}$ and the cumulative volume distributions $D_V(10)$ and $D_V(90)$. The droplet size distribution at pH 9 was observed to exhibit greater homogeneity in comparison to those at pH 7 and 11.

The rheological analysis of CPC-stabilized emulsions exhibits a complex behavior, showing a shift from shear-thinning to thickening at higher shear rates. At pH 7, viscosity decreases as oil concentration increases, while at pH 9 and 11, this effect is less pronounced. Under thermal treatment, results revealed changes in viscosity throughout the heating and cooling processes, with these variations attributed to modifications in the emulsion's microstructure and intermolecular interactions. The pH exerted a considerable influence on the viscosity changes that occurred during the heating phase. Emulsions at pH 11 demonstrated enhanced stability and resistance to temperature-induced alterations.

The stability of the emulsion and its capacity to maintain a stable cream layer were also affected by variations in pH and oil concentration within the formulation. Emulsions prepared at pH 7 demonstrated a heightened tendency for phase separation and cream layer formation, suggesting a correlation between particle mobility and emulsion stability. Conversely, emulsions prepared at pH 9 and 11 demonstrated enhanced cream layer stability, exhibiting a practically comparable stability profile.

Overall, the study presents a comprehensive analysis of the complex interaction between pH, oil concentration, and emulsion stability. The results demonstrate that concentrated cowpea protein has the ability to stabilize emulsions, even in conditions suited to phase separation. This reinforces its potential as a highly effective emulsifying agent.

References

[1] Z. Song, Y. Yang, F. Chen, J. Fan, B. Wang, X. Bian, Y. Xu, B. Liu, Y. Fu, Y. Shi, X. Zhang, N. Zhang, Effects of Concentration of Soybean Protein Isolate and Maltose and Oil Phase Volume Fraction on Freeze–Thaw Stability of Pickering Emulsion, Foods 11 (2022). https://doi.org/10.3390/foods11244018.

[2] A.E. Blok, D.P. Bolhuis, L.N. Arnaudov, K.P. Velikov, M. Stieger, Influence of thickeners (microfibrillated cellulose, starch, xanthan gum) on rheological, tribological and sensory properties of low-fat mayonnaises, Food Hydrocoll 136 (2023) 108242. https://doi.org/10.1016/J.FOODHYD.2022.108242.

[3] Y. Gao, D. Lin, H. Peng, R. Zhang, B. Zhang, X. Yang, Low oil Pickering emulsion gels stabilized by bacterial cellulose nanofiber/soybean protein isolate: An excellent fat replacer for ice cream, Int J Biol Macromol 247 (2023) 125623. https://doi.org/10.1016/J.IJBIOMAC.2023.125623.

[4] Y.A.R. Heikal, A.A. Hassan, A.A. Abou-Arab, F.M. Abu-Salem, D.E.S.H. Azab, Nano formulated soy proteins as a fat replacer in low fat mayonnaise formula, Journal of the Saudi Society of Agricultural Sciences 22 (2023) 469–479. https://doi.org/10.1016/J.JSSAS.2023.04.006.

[5] I. Dammak, P.J. do Amaral Sobral, Formulation and Stability Characterization of Rutin-Loaded Oil-in-Water Emulsions, Food Bioproc Tech 10 (2017) 926–939. https://doi.org/10.1007/s11947-017-1876-5.

[6] I. Dammak, P.J. do A. Sobral, Active gelatin films incorporated with eugenol nanoemulsions: effect of emulsifier type on films properties, Int J Food Sci Technol 54 (2019) 2725–2735. https://doi.org/10.1111/ijfs.14183.

[7] I. Dammak, R.V. Lourenço, P.J. do A. Sobral, Active gelatin films incorporated with Pickering emulsions encapsulating hesperidin: Preparation and physicochemical characterization, J Food Eng 240 (2019) 9–20. https://doi.org/10.1016/j.jfoodeng.2018.07.002.

[8] Z. Ma, J.I. Boye, J. Fortin, B.K. Simpson, S.O. Prasher, Rheological, physical stability, microstructural and sensory properties of salad dressings supplemented with raw and thermally treated lentil flours, J Food Eng 116 (2013) 862–872. https://doi.org/10.1016/j.jfoodeng.2013.01.024.

[9] H.V.R. Pereira, K.P. Saraiva, L.M.J. Carvalho, L.R. Andrade, C. Pedrosa, A.P.T.R. Pierucci, Legumes seeds protein isolates in the production of ascorbic acid microparticles, Food Research International 42 (2009) 115–121. https://doi.org/10.1016/j.foodres.2008.10.008.

[10] R. Mozuraityte, E. Kotsoni, J. Cropotova, T. Rustad, Low-fat (<50%) oil-in-water emulsions, Omega-3 Delivery Systems: Production, Physical Characterization and Oxidative Stability (2021) 241–254. https://doi.org/10.1016/B978-0-12-821391-9.00010-7.

[11] E. Dickinson, M. Golding, M.J.W. Povey, Creaming and Flocculation of Oil-in-Water Emulsions Containing Sodium Caseinate, 1997.

[12] J. De Boer, H. Schösler, H. Aiking, “Meatless days” or “less but better”? Exploring strategies to adapt Western meat consumption to health and sustainability challenges, Appetite 76 (2014) 120–128. https://doi.org/10.1016/j.appet.2014.02.002.

[13] H.H.E. van Zanten, H. Mollenhorst, C.W. Klootwijk, C.E. van Middelaar, I.J.M. de Boer, Global food supply: land use efficiency of livestock systems, International Journal of Life Cycle Assessment 21 (2016) 747–758. https://doi.org/10.1007/s11367-015-0944-1.

[14] European Commission: Report from the Commission to the Council and the European Parliament on the Development of Plant Proteins in the European Union - COM. 2018:757:. final. 2018.

[15] FAOSTAT. Production quantities of Cowpeas dried by country. Available at: <http://faostat.fao.org/>. Accessed on: April 27th. 2024.

[16] Z. Bai, X. Huang, J. Meng, L. Kan, S. Nie, A comparative study on nutritive peculiarities of 24 Chinese cowpea cultivars, Food and Chemical Toxicology 146 (2020). https://doi.org/10.1016/j.fct.2020.111841.

[17] J. Ge, C.X. Sun, A. Mata, H. Corke, R.Y. Gan, Y. Fang, Physicochemical and pH-dependent functional properties of proteins isolated from eight traditional Chinese beans, Food Hydrocoll 112 (2021). https://doi.org/10.1016/j.foodhyd.2020.106288.

[18] T. Lafarga, C. Álvarez, S. Villaró, G. Bobo, I. Aguiló-Aguayo, Potential of pulse-derived proteins for developing novel vegan edible foams and emulsions, Int J Food Sci Technol 55 (2020) 475–481. https://doi.org/10.1111/ijfs.14286.

[19] D.D.M. Ragab, E.E. Babiker, A.H. Eltinay, Fractionation, solubility and functional properties of cowpea (*Vigna unguiculata*) proteins as affected by pH and/or salt concentration, Food Chem 84 (2004) 207–212. https://doi.org/10.1016/S0308-8146(03)00203-6.

[20] X. Tang, Y. Shen, Y. Zhang, M.W. Schilling, Y. Li, Parallel comparison of functional and physicochemical properties of common pulse proteins, LWT 146 (2021). https://doi.org/10.1016/j.lwt.2021.111594.

[21] C.M.B. Thompson, B.A. Acevedo, M.C. Añón, M. V. Avanza, Emulsifying Capacity of Cowpea Protein Isolates. Effect of Thermal and Hydrolytic Treatment, Plant Foods for Human Nutrition 78 (2023) 366–374. https://doi.org/10.1007/s11130-023-01072-8.

[22] J.C. Thomas, The determination of log normal particle size distributions by dynamic light scattering, J Colloid Interface Sci 117 (1987) 187–192. https://doi.org/10.1016/0021-9797(87)90182-2.

[23] T.C. Polachini, A.C.K. Sato, R.L. Cunha, J. Telis-Romero, Density and rheology of acid suspensions of peanut waste in different conditions: An engineering basis for bioethanol production, Powder Technol 294 (2016) 168–176. https://doi.org/10.1016/j.powtec.2016.02.022.

[24] E. Drioli, L. Giorno, Encyclopedia of Membranes, 2016.

[25] M.A. Rao, Flow and Functional Models for Rheological Properties of Fluid Foods, 2007.

[26] D.J. McClements, Food emulsions: principles, practices, and techniques, 2016.

[27] A.C. Karaca, N. Low, M. Nickerson, Emulsifying properties of chickpea, faba bean, lentil and pea proteins produced by isoelectric precipitation and salt extraction, Food Research International 44 (2011) 2742–2750. https://doi.org/10.1016/j.foodres.2011.06.012.

[28] N. Raval, R. Maheshwari, D. Kalyane, S.R. Youngren-Ortiz, M.B. Chougule, R.K. Tekade, Importance of physicochemical characterization of nanoparticles in pharmaceutical product development, in: Basic Fundamentals of Drug Delivery, Elsevier, 2018: pp. 369–400. https://doi.org/10.1016/B978-0-12-817909-3.00010-8.

[29] G. Tabilo-Munizaga, R. Villalobos-Carvajal, C. Herrera-Lavados, L. Moreno-Osorio, M. Jarpa-Parra, M. Pérez-Won, Physicochemical properties of high-pressure treated lentil protein-based nanoemulsions, LWT 101 (2019) 590–598. https://doi.org/10.1016/J.LWT.2018.11.070.

[30] C.R.L. Francisco, F.D. de Oliveira Júnior, G. Marin, I.D. Alvim, M.D. Hubinger, Plant proteins at low concentrations as natural emulsifiers for an effective orange essential oil microencapsulation by spray drying, Colloids Surf A Physicochem Eng Asp 607 (2020) 125470. https://doi.org/10.1016/J.COLSURFA.2020.125470.

[31] Q. Guo, T.H. Mu, Emulsifying properties of sweet potato protein: Effect of protein concentration and oil volume fraction, Food Hydrocoll 25 (2011) 98–106. https://doi.org/10.1016/j.foodhyd.2010.05.011.

[32] N. Bojanić, S. Vidosavljević, A. Fišteš, Z. Šereš, E. Fodor, N. Maravić, Emulsion stabilising capacity of sunflower meal depending on fraction protein content and particle size, Int J Food Sci Technol 59 (2024) 333–342. https://doi.org/10.1111/ijfs.16814.

[33] V.S. Krstonošić, M.D. Kalić, T.R. Dapčević-Hadnađev, I.S. Lončarević, M.S. Hadnađev, Physico-chemical characterization of protein stabilized oil-in-water emulsions, Colloids Surf A Physicochem Eng Asp 602 (2020) 125045. https://doi.org/10.1016/J.COLSURFA.2020.125045.

[34] M.M. Garcia De Oliveira, K. De Souza Silva, M.A. Mauro, Evaluation of Interactions Between Carboxymethylcellulose and Soy Protein Isolate and their Effects on the Preparation and Characterization of Composite Edible Films, (2021). https://doi.org/10.1007/s11483-020-09659-3.

[35] B. G., Ozel, A. Orum, M. Yildiz, & Y. Z. Menceloglu, Experimental study on the rheology of anisotropic, flocculated and low volume fraction colloids, Korea-Aust Rheol J 26 (2014) 105-116. https://doi.org/10.1007/s13367-014-0011-7

[36] C. D. Cwalina, & N. J. Wagner, Material properties of the shear-thickened state in concentrated near hard-sphere colloidal dispersions, J Rheol 58 4 (2014) 949-967.

[37] N. J. Wagner, J. F. Brady, Shear thickening in colloidal dispersions, Phys Today 62 10 (2009) 27–32. https://doi.org/10.1063/1.3248476

[38] J. F. Brady, & G. Bossis, The rheology of concentrated suspensions of spheres in simple shear flow by numerical simulation, J Fluid Mech 155 (1985) 105-129.

[39] P. Bellalta, E. Troncoso, R.N. Zúñiga, J.M. Aguilera, Rheological and microstructural characterization of WPI-stabilized O/W emulsions exhibiting time-dependent flow behavior, LWT 46 (2012) 375–381. https://doi.org/10.1016/j.lwt.2011.12.017.

[40] K. Östbring, M. Matos, A. Marefati, C. Ahlström, G. Gutiérrez, The effect of pH and storage temperature on the stability of emulsions stabilized by rapeseed proteins, Foods 10 (2021). https://doi.org/10.3390/foods10071657.

[41] C.E. Gumus, E.A. Decker, D.J. McClements, Formation and Stability of ω-3 Oil Emulsion-Based Delivery Systems Using Plant Proteins as Emulsifiers: Lentil, Pea, and Faba Bean Proteins, Food Biophys 12 (2017) 186–197. https://doi.org/10.1007/s11483-017-9475-6.

[42] Y. Zhu, H. Gao, W. Liu, L. Zou, D.J. McClements, A review of the rheological properties of dilute and concentrated food emulsions, J Texture Stud 51 (2020) 45–55. https://doi.org/10.1111/jtxs.12444.

[43] X. Zhang, B. Qi, F. Xie, M. Hu, Y. Sun, L. Han, L. Li, S. Zhang, Y. Li, Emulsion stability and dilatational rheological properties of soy/whey protein isolate complexes at the oil-water interface: Influence of pH, Food Hydrocoll 113 (2021). https://doi.org/10.1016/j.foodhyd.2020.106391.

[44] M.M.G. de Oliveira, A.G.B.W. Fessori, V.J. Huamaní-Meléndez, M.A. Mauro, Exploring the rheological and thermal behavior of cowpea protein concentrate: Impact of pH and concentration, Colloids Surf A Physicochem Eng Asp 694 (2024). https://doi.org/10.1016/j.colsurfa.2024.134106.

[45] E. Domian, D. Mańko-Jurkowska, A. Górska, Heat-induced gelation, rheology and stability of oil-in-water emulsions prepared with patatin-rich potato protein, Food and Bioproducts Processing 139 (2023) 144–156. https://doi.org/10.1016/j.fbp.2023.03.008.

[46] E. Domian, D. Mańko-Jurkowska, The effect of homogenization and heat treatment on gelation of whey proteins in emulsions, J Food Eng 319 (2022). https://doi.org/10.1016/j.jfoodeng.2021.110915.

[47] D.J. Mcclements, The rheology of emulsion-based food products, 2003.

[48] D.J. McClements, Protein-stabilized emulsions, Curr Opin Colloid Interface Sci 9 (2004) 305–313. https://doi.org/10.1016/j.cocis.2004.09.003.

[49] S.G. Rudra, S. Sethi, S.K. Jha, R. Kumar, Physico-chemical and functional properties of cowpea protein isolate as affected by the dehydration technique, Legume Research 39 (2016) 370–378. https://doi.org/10.18805/lr.v0iOF.9441.

[50] C.C. Berton-Carabin, L. Sagis, K. Schroën, Formation, Structure, and Functionality of Interfacial Layers in Food Emulsions, 24 (2018). https://doi.org/10.1146/annurev-food-030117.

[51] K. Muijlwijk, I. Colijn, H. Harsono, T. Krebs, C. Berton-Carabin, K. Schroën, Coalescence of protein-stabilised emulsions studied with microfluidics, Food Hydrocoll 70 (2017) 96–104. https://doi.org/10.1016/j.foodhyd.2017.03.031.

[52] E. Dickinson, Milk protein interfacial layers and the relationship to emulsion stability and rheology.

Supplementary material

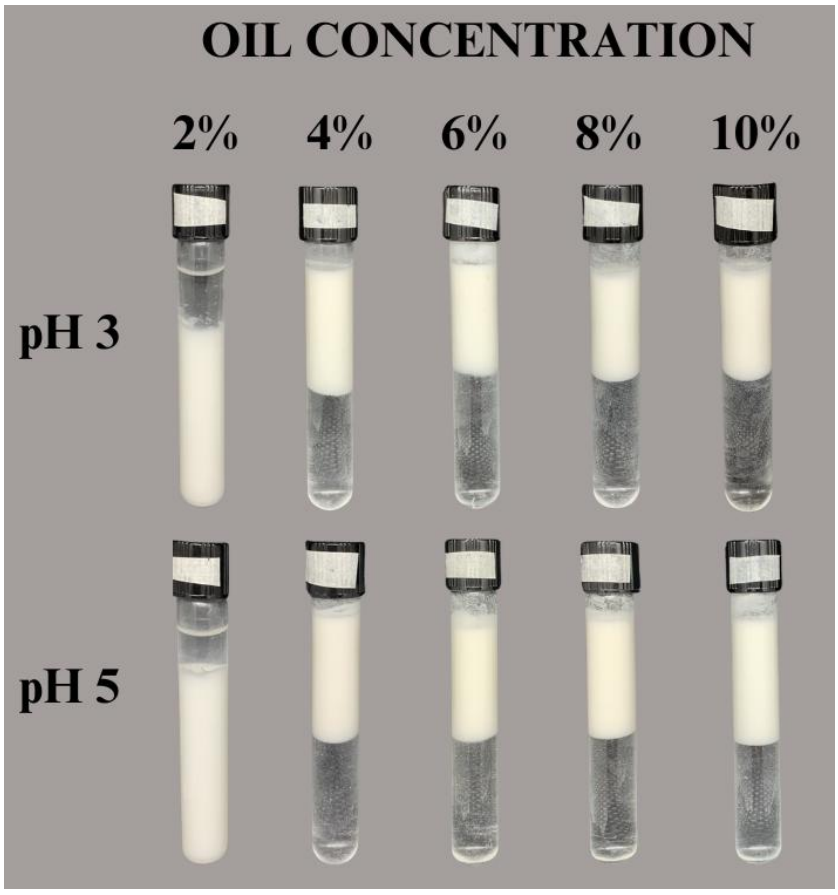
Prospects of cowpea protein as an alternative and natural emulsifier for food applications: Effect of pH and oil concentration

Maria Mariana Garcia de Oliveira[a], Ana Gabriela Baroni Wicher Fessori[a], Víctor Justiniano Huamani-Meléndez[a], Maria Aparecida Mauro[a]

[a] Department of Food Engineering and Technology, Institute of Biosciences, Humanities and Exact Sciences – São Paulo State University (UNESP), Street Cristóvão Colombo, 2265, São José do Rio Preto 15054-000, Brazil.

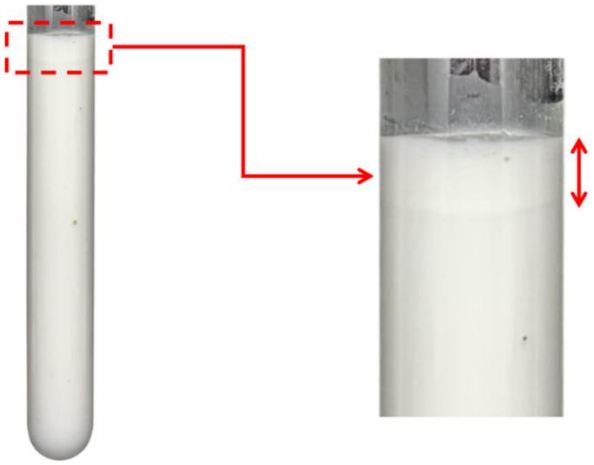
e-mail address: maria.mariana@unesp.br (corresponding author)

Figure S1. Visual aspect of emulsions at pHs 3 and 5 after 24 hours of storage (4 °C)



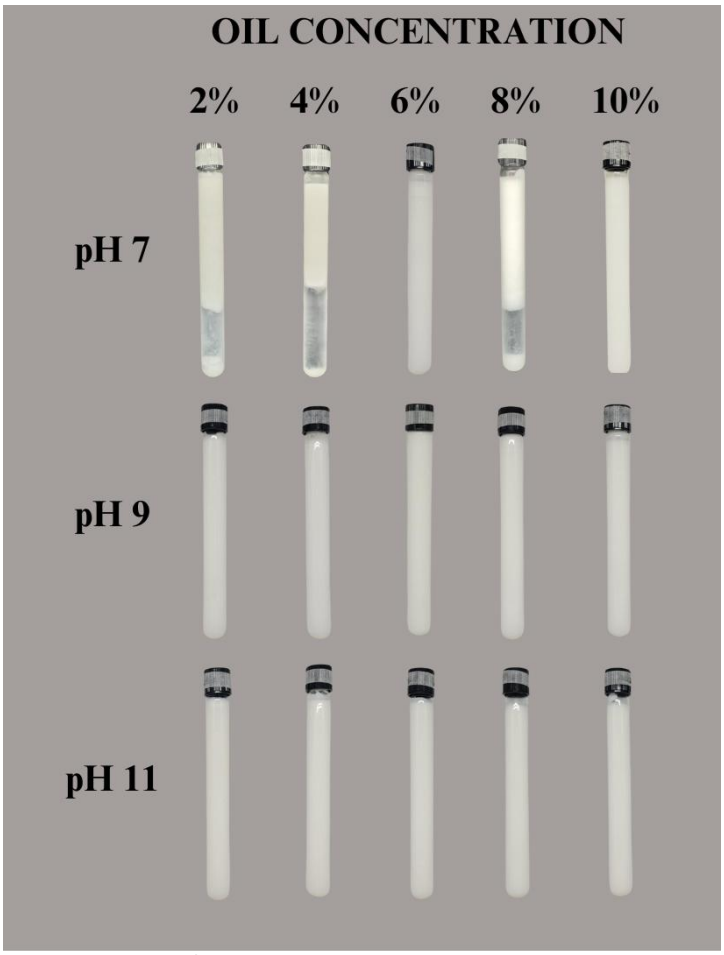
Source: elaborated by the author.

Figure S2. Cream layer formed on the top and the layer similar to the original emulsion below



Source: elaborated by the author.

Figure S3. Visual aspect of emulsions after 30 days* of storage (4 °C)



Source: elaborated by the author. *pH7: 2% - after 21 days of storage; pH7: 4% and 8% - after 28 days of storage

5 MODULATING EDIBLE FILM PROPERTIES THROUGH PH: DEVELOPMENT OF A NOVEL BIOPOLYMERIC EDIBLE FILM BASED ON COWPEA PROTEIN CONCENTRATE

Maria Mariana Garcia de Oliveira[a*], Víctor Justiniano Huamaní-Meléndez[a] and Maria Aparecida Mauro[a]

[a] Department of Food Engineering and Technology, Institute of Biosciences, Humanities and Exact Sciences – São Paulo State University (UNESP), Street Cristóvão Colombo, 2265, São José do Rio Preto 15054-000, Brazil.

e-mail address: maria.mariana@unesp.br (*corresponding author)

Abstract

Biopolymer-based edible films offer environmental benefits but face challenges in matching the water resistance and functionality of traditional plastics. Cowpeas (*Vigna unguiculata* (L.) Walp), a novel source of plant-based protein, show potential for developing edible films with desirable properties. Nevertheless, this potential remains unexplored despite evidence of this protein's favorable techno-functional properties. This study aims to assess the pH effects of the film forming solutions on the morphology, optical, mechanical, water sorption, and barrier properties of edible films made from cowpea protein concentrate (CPC). For this, films based on CPC at a concentration of 5% (m/m) were prepared at different pH values (7-11). None of the films exhibited a completely homogeneous and uniform morphological structure; however, those formed at pH 9 had fewer cracks on their surface and throughout their thickness. The pH also significantly influenced the oxygen permeability (O_2P). Specifically, at pH 9, O_2P was the lowest (9.85×10^{-16} g m^{-1} Pa^{-1} s^{-1}). Structural analysis via X-ray indicated that the films exhibit low crystallinity, with a relative crystallinity index ranging from 40.08 to 43.54%. Fourier transform infrared spectroscopy revealed similarities in the secondary structure of the proteins between the different formulations, with some particularities. Films prepared at pH 9 and 11 exhibited a more disordered structure, while at pH 7 it was more organized. The water desorption isotherms were effectively described by the GAB model and highlighted the slightly higher hygroscopicity of the films at low and intermediate aw values. Water vapor permeability, solubility, tensile strength, and deformation did not show a strict dependence on the pH of the film-forming solution. The results show how effective and adaptable CPC is regarding edible films. Furthermore, the study underscores the importance of modifying the pH of films as a strategy for tailoring their properties to optimize their suitability for a diverse array of applications.

Keywords: Plant protein, Biopolymers, Food packaging, Mechanical properties, Barrier properties

1 Introduction

Petroleum-derived polymers and plastics currently dominate the food packaging market due to their low cost and favorable properties. However, these materials are non-biodegradable and non-renewable, which increases the urgency for developing sustainable alternatives. In 2021, global plastic production reached 390.7 million tons, with 30% allocated to the food industry, according to Abiplast (2021). In Brazil, only 23.4% of consumed plastics are recycled (Abiplast, 2021), and globally, this percentage is less than 9% (Alen et al., 2024), due to technical and economic challenges. One promising solution to the excessive use of synthetic plastics is the development of edible films. These films are thin, biocompatible, and biodegradable layers, typically composed of proteins, polysaccharides, and lipids (Han, 2014). However, replacing water-resistant plastic with biopolymer-based films remains a significant challenge. The development of biopolymer food packaging must not only fulfill the basic functions of traditional packaging, such as protection, communication, convenience, and containment, but also contribute to sustainability by reducing the environmental impact of packaging waste and food loss (Vanderroost et al., 2014).

Currently, proteins are widely investigated as key components in developing biodegradable films, primarily due to their biodegradable and renewable nature, availability, sensory characteristics, and low toxicity. Films derived from proteins, whether of plant or animal origin, exhibit an ordered structure in the form of a compact network, formed by hydrogen interactions, which provides excellent mechanical and gas barrier properties (Amado et al., 2023; Oliveira et al., 2021; Silva et al., 2018). However, due to the hydrophilic nature of proteins, these films facilitate the passage of moisture, rendering them ineffective as barriers to water vapor. Despite these constraints, the properties of protein films can be modified and adjusted to meet specific needs, thereby expanding their potential for application in various contexts.

Among the numerous factors that can affect the properties of a film, the influence of the pH of the film-forming solution is particularly significant. pH plays an important role in protein denaturation, with proteins adopting an extended chain structure at values far from the isoelectric point. This alters their globular form, favoring protein-protein interactions and, consequently, the formation of an intermolecular network (Brandenburg et al., 1993; Cao et al., 2007). On the other hand, at pH values close to the isoelectric point, protein network formation is inhibited, as proteins tend to coagulate, making the formation of a homogeneous matrix unfeasible (Mauri & Añón, 2006). In this context, it is important to assess the impact of pH variation on the three-dimensional networks of films, as these intra- and intermolecular

interactions directly influence their properties. This understanding can help to offset deficiencies in protein-based films, thereby expanding their application possibilities.

Cowpeas (*Vigna unguiculata* (L.) Walp), also known as black-eyed peas, represent a novel source of plant-based protein. The protein extracted from this pulse has been subjected to research as a potential alternative source of plant-based protein (Gómez et al., 2021; Loushigam & Shanmugam, 2023; Oliveira et al., 2024), to replace animal protein and other plant proteins that are already widely utilized. Research on protein-based films derived from a variety of beans, or their combination with other biopolymers and compounds (Moghadam et al., 2020; Rojas-Lema et al., 2021, 2023), has demonstrated desirable mechanical, optical, and barrier properties.

Despite an extensive review of the scientific literature, only two studies were identified that specifically investigated the development of edible films derived from cowpea protein. The initial study, published by Hewage et al. in 2009, examined the development of cowpea protein-based films at varying pH levels (8-11) with the inclusion of diverse plasticizers (polyethylene glycol and glycerol) at distinct concentrations. While this study delves into the impact of diverse variables on the films, fundamental aspects of film characterization are still lacking, including solubility, oxygen permeability, and structural and molecular properties. A recent study (Almeida et al., 2021) evaluated the effects of incorporating cowpea protein on the properties of cassava starch films with glycerol. However, the properties of the films with only protein were not directly analyzed.

In light of these findings and the functionalities of the cowpea protein, this study aims to elucidate the impact of alterations in the pH of the film-forming solutions, a fundamental method for modifying protein properties, on the characteristics of films produced from this protein. Accordingly, the objective of this study is to assess the impact of the pH in the neutral to alkaline range on the morphology, molecular structure, and optical, mechanical, water sorption, and barrier properties of edible films based on concentrated cowpea protein.

2 Materials and methods

2.1 Materials

The edible films were prepared using cowpea protein concentrate (CPC) in powder form as the raw material, with a protein content of approximately 79%. In addition to the protein, analytical grade reagents were employed, including bi-distilled glycerol, sodium hydroxide, and hydrochloric acid (Synth, Diadema, Brazil).

2.2 Methods

2.2.1 Cowpea protein extraction

The protein extraction was conducted using the isoelectric precipitation method, as previously described by Moser, Ferreira, and Nicoletti (2019), with the incorporation of specific modifications. The cowpea grains were subjected to a 12-hour maceration process at 4 °C. Subsequently, the macerated grains were blended for a period of three minutes with distilled water at a ratio of 1:3 (w/w). The pH of the blended mixture was adjusted to 8 using a concentrated NaOH solution and stirred for 45 minutes at room temperature (25 °C) using a mechanical stirrer (MA 039, Marconi, Brazil). Subsequently, centrifugation was performed at 10,000×g for 20 minutes (Hitachi, CR22N, Japan), and the supernatant was collected. The precipitate was subjected to a second extraction under identical conditions. The supernatants from both extraction steps were combined, and the pH was adjusted to 4.5 with 0.1 M HCl. The precipitated protein was separated by centrifugation and redispersed in distilled water. The pH was then adjusted to 7, and the sample was frozen and subsequently lyophilized.

2.2.2 Preparation of edible films

Cowpea protein concentrate was dispersed in distilled water to obtain a stock solution with a concentration of 8% (m/m). The pH was adjusted to 11 using NaOH (40%), and the mixture was then heated in a thermostatic bath (Symmetrical, SI/6 Rings/18 L, Brazil) at 85 °C for 30 minutes (Moghadam et al., 2020). The solution was cooled to reach room temperature (25 °C) and then centrifuged (Hitachi, CR22N, Japan) at 4000 rpm for 10 minutes to remove any insoluble particles.

The supernatant obtained after centrifugation and glycerol were combined in calculated proportions to obtain a final film-forming solution containing 5% CPC and 2% glycerol. The pH of the solution was adjusted to values of 7, 9, and 11 using NaOH (40%) or HCl (40%), and the resulting mixtures were homogenized using an ultra-turrax (basic model T18, IKA, Brazil), operating at 15,000 rpm for 10 minutes.

The film-forming solution (approximately 100 g) was poured into Teflon molds (400 cm^2) and dried at 50 °C and 40% relative humidity for approximately 17 hours in a climate chamber (420-2TS, Ethik, Brazil). The dried films were removed from the molds and stored at room temperature and 53% relative humidity for a minimum of one week prior to analysis.

2.2.3 Characterization of edible films

2.2.3.1 Thickness measurement

The film thickness was measured using a digital micrometer (Mitutoyo, MDC-25SB, Japan) at 5 random positions on the film surface.

2.2.3.2 Moisture content

The total solid content of the films was determined in triplicate by the gravimetric method, in a vacuum oven (TE-395, Tecnal, Brazil) operating at 70 °C and 10 kPa, until a constant weight was attained.

2.2.3.3 Scanning electron microscopy (SEM)

The surface and cross-sectional microstructure of the smooth and rough surfaces of the films were examined using scanning electron microscopy (*SEM*). Following a seven-day storage period at room temperature in desiccators with silica gel, the films were affixed to aluminum stubs using carbon tape. Subsequently, the micrographs were obtained using a scanning electron microscope (Carl Zeiss, EVO LS15, Germany) operating under high vacuum and low-pressure mode. The images of the smooth surface (surface in contact with the Teflon tray) and the rough surface (surface in contact with the drying air) were captured at magnifications of 250, 1000, 5000 and 10000×.

2.2.3.4 X-ray diffraction (XRD)

A wide-angle X-ray scattering (WAXS) analysis of CPC and films was performed on a diffractometer (Rigaku, RINT 2000, Japan). The equipment operated at a voltage of 50 kV and a current of 30 mA using Cu Kα radiation and L = 1,542 Å. The diffractograms were obtained at angles (2θ) ranging from 5° to 60° at a sweep rate of 1° min^{-1}.

2.2.3.5 Fourier transform infrared spectroscopy (FTIR)

Infrared analyses were carried out using a Fourier Transform Infrared Spectrometer (*FTIR*), PerkinElmer (Spectrum Two, Waltham, MA). The measurements utilized an attenuated total reflectance (ATR) accessory featuring a diamond crystal. Spectra for individual samples were acquired within the range of 400 to 4000 cm^{-1}, with a resolution of 4 cm^{-1}. Before analysis, the films were stored at room temperature in desiccators containing silica gel for 7 days.

2.2.3.6 Water vapor permeability (WVP)

The water vapor permeability of CPC films, characterized by pH values of 7, 9, and 11 was assessed using the ASTM E96-95 gravimetric method. This involved subjecting the films to controlled environments created by anhydrous calcium chloride, maintaining a relative humidity of 2%, and distilled water, maintaining a relative humidity of 100%. Through this setup, a moisture gradient was established, allowing each side of the film to be exposed to different relative humidity conditions for analysis.

The films were hermetically sealed over diffusion cells containing calcium chloride. These cells were arranged within desiccators equipped with a miniature fan to ensure continuous air circulation, and they were filled with water. Following this, the desiccators were placed inside a BOD climate chamber (model BT 71, Biothec, Brazil) maintained at a temperature of 25 °C for 8 hours. Throughout this period, the capsules were weighed at hourly intervals.

A linear function was applied to the experimental data of water mass variation over time, with the slope of the function representing the water vapor permeability rate, *WVPR* (g water s^{-1}). The WVPR values were obtained in triplicate. Subsequently, the water vapor permeability (*WVP*) was calculated using Equation 1 based on the determined *WVPR* values.

$$WVP = \frac{WVPR \cdot \delta}{\frac{A \cdot P_S \cdot (RH_1 - RH_2)}{100}} \quad (1)$$

in which *WVP* is water vapor permeability (g m^{-1} s^{-1} Pa^{-1}), *WVPR* is the water vapor permeability rate (g water s^{-1}), δ is thickness of the films (m), A is the surface area exposed (28.14×10^{-2} m^2), P_S is the saturation pressure of water vapor at 25 °C (3.169 Pa) and $(RH_1 - RH_2)$ is the difference in the relative humidity between the interior and exterior of the capsule.

2.2.3.7 Water solubility

The solubility of the films was determined following the methodology described by Cuq et al. (1996). Film specimens (2.0 cm x 2.0 cm) were first dried in a vacuum oven (TE-395, Tecnal, Brazil) at 70 °C. Subsequently, they were immersed in 50 mL of distilled water and placed in a BOD climate chamber (BT 71/ Biothec, Brazil) at room temperature for 24 hours. Following immersion, the specimens were withdrawn from the solution and subjected to further

drying (70 °C) until reaching a constant weight. Solubility was then computed as the ratio between the final dry mass and the initial mass using Equation 2:

$$S = \frac{(W_0 - W_f)}{W_0} \cdot 100 \quad (2)$$

in which W_0 is the initial dry weight (g); W_f is the final dry weight (g), and S is the water solubility (%, m/m).

2.2.3.8 Mechanical properties

The mechanical properties, specifically tensile strength and elongation at break, of CPC (pHs 7, 9 and 11) films, were assessed utilizing the methodology recommended by ASTM D882-12 (ASTM, 2012). This analysis was conducted employing a texturometer (TA.XT Plus, Stable Micro Systems, Surrey, UK), and a minimum of 8 samples from each formulation were subjected to testing. Rectangular samples (70 mm × 25 mm) were prepared and positioned between the probes, leaving an exposed area of 50 mm × 25 mm. The initial distance between the probes was set to 40 mm, with the speed during the tensile tests of 0.8 mm s^{-1}. The tensile strength (TS) (MPa) was calculated by dividing the maximum force obtained by the original cross-sectional area of the sample (25 mm × sample average thickness). The percentage of elongation at break (EB) was calculated by the ratio between the increased length after breakage and its initial length (50 mm). Data were processed using EXPONENT software, version 5.1.1.0.

2.2.3.9 Isotherms

The sorption isotherms of the films were carried out across a range of relative humidity levels (11.3%, 32.8%, 57.6%, 75.3%, 84.3%, and 90.3%) at 25 °C. Before analysis, the samples were subjected to drying at 70 °C until reaching a constant weight to initiate the process with low moisture content and ensure the achievement of an adsorption isotherm. The films (2.0 cm x 2.0 cm) were stored in hermetically sealed jars containing the saline solution corresponding to the desired relative humidity and were placed in BOD climate chambers (BT 71, Biothec, Brazil) at 25 °C.

The samples were subjected to periodic weighing until they reached equilibrium with the surrounding environment, taking around 30 days. Once the equilibrium was reached, the total solid content was analyzed. The results were fitted with the GAB model (Guggenheim,

Anderson, and de Boer) utilizing Equation 3 (van den Berg & Bruin, 1981). The parameters were estimated using the least squares criterion based on the Levenberg-Marquardt algorithm (Marquardt, 1963).

$$X = \frac{X_m \cdot C \cdot K \cdot a_w}{(1 - K \cdot a_w) \cdot (1 - K \cdot a_w + C \cdot K \cdot a_w)} \quad (3)$$

in which C and K are constants, a_w is the water activity, X is the equilibrium moisture in dry base (kg water·kg dry sample^{-1}), and X_m is the monolayer moisture in dry base (kg water·kg dry sample^{-1}).

The fit efficiency was evaluated based on the adjusted coefficient of determination (R^2) and on the mean relative deviation modulus, P, defined by Equation 4 (Lomauro et al., 1985).

$$P(\%) = \frac{100}{N} \times \sum_{1}^{N} \left| \frac{y^{exp} - y^{calc}}{y^{exp}} \right| \quad (4)$$

in which y^{calc} represents the calculated moisture in dry basis, y^{exp} is the experimental moisture in dry basis and N is the number of observations.

2.2.3.10 Optical properties: color and transmittance

Color parameters were determined with a colorimeter (HunterLab, ColorFlex, United States). The L* parameter represents the clarity of the samples, while a* and b* represent colors ranging from red (+ a*) to green (- a*) and yellow (+ b*) to blue (-b*). In addition to the L*, a* and b* parameters, the data was also analyzed using C* (chroma, which represents the degree of color intensity) and h (hue angle, which represents the degree of tonality). Analyses were performed on four samples, each of which was subjected to readings at four distinct positions (0°, 90°, 270° and 370°). The yellowness index (YI) of samples was also calculated (Pająk et al., 2019).

$$YI = 142.86 \cdot b/L \quad (5)$$

where ‘L’ and ‘b’ are the color parameter values of the sample.

The transmittance of the films was determined using a UV-VIS spectrophotometer (GENESYS 10S UV-VIS, Thermo Scientific, USA). Film samples were cut into rectangles measuring 4.0 × 1.0 cm and placed into the spectrophotometer cuvette. Subsequently, the wavelength range of visible light, from 200 to 800 nm, was scanned for six different specimens of each formulation (Silva et al., 2018).

2.2.3.11 Oxygen permeability (O_2P)

Oxygen permeability rates (O_2PR) were determined using the coulometric method with the procedure described in F 1927 (ASTM, 2014) and MOCON model 2/21 OXTRAN equipment operating with pure oxygen as the permeant gas. The assays were performed in duplicate at 23 °C and a relative humidity of 50 ± 4%. The effective permeation area of each specimen was 50 cm^2. The results were corrected for 101325 Pa of a partial oxygen pressure gradient between the two film surfaces. This gradient corresponds to the driving force required for oxygen to permeate through the film. Once the O_2PR was determined, the oxygen permeability coefficient (O_2P) was calculated from the permeability rate using Equation 5:

$$O_2P = \frac{O_2PR \cdot \delta}{p} \quad (6)$$

in which O_2P is the oxygen permeability (g m^{-1} s^{-1} Pa^{-1}), O_2PR is the oxygen permeability rate (g s^{-1}), δ is the mean thickness of the sample (m), and *p* is the partial oxygen pressure (101 325 Pa) in the diffusion cell-permeant gas chamber, as the partial O_2 pressure in the carrier gas chamber (N_2 + H_2) is considered zero.

2.2.3 Statistical analysis

Data were statistically evaluated using an analysis of variance (ANOVA) and Tukey's test at a significance level of 5%.

3 Results and discussion

3.1 Scanning electron microscopy (SEM)

Figures 5.1 and 5.2 show the smooth (surface in contact with the Teflon, politetrafluoretileno-PTFE, plate) and rough (surface in contact with the air drying) surfaces,

respectively, of the CPC films prepared at pH 7, 9, and 11 at three different magnifications (250, 1000 and 5000×).

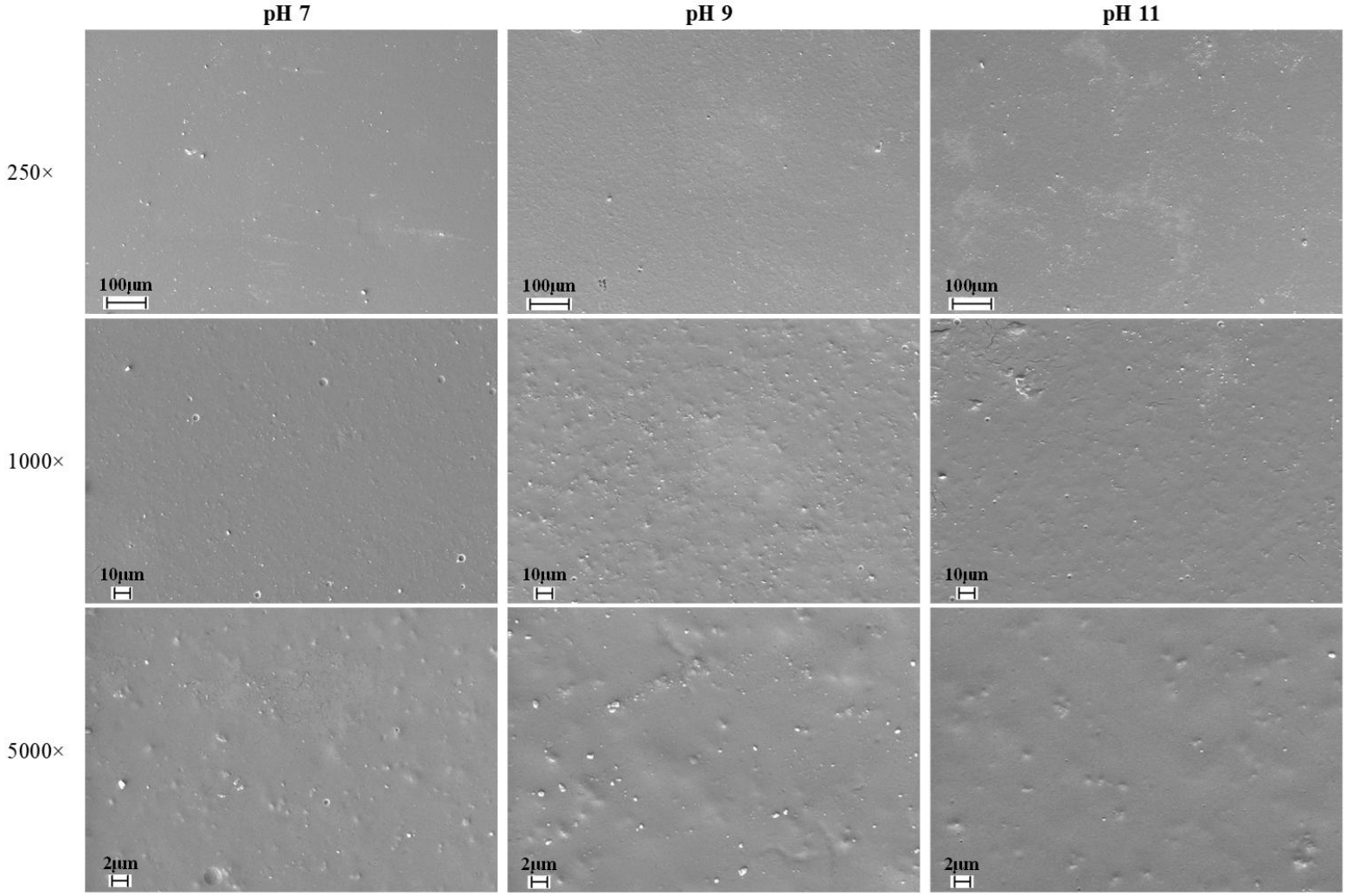
The images of the films' smooth surface (Figure 5.1) revealed uniformity concerning pH, with minimal variations observed. The presence of sedimented particles and small pores was detected in all pH conditions studied. Upon increasing the magnification to 1000 times, pH 9 appeared to exhibit a surface with a higher concentration of sedimented particles compared to the others pHs evaluated.

The rough surface of the films (Figure 5.2) revealed the presence of roughness and cracks. These may be the result of stress caused by the speed of drying. At the employed drying temperature (50 °C), the solvent in the film may evaporate more rapidly, causing uneven drying across the film surface, leading to the formation of fissures and cracks as a result of differential shrinkage and stress (Li et al., 2022; Tomar et al., 2020). Similarly to the smooth surface, pH demonstrated a limited influence on the observed characteristics. However, at pH 7, the fissures were more pronounced and deeper, particularly evident at a magnification of 5000×, while at pH 11 these fissures were less prominent. It is worth noting that the fissures can have an impact, especially on the mechanical and permeability properties of the films.

The cross-sectional images (Figure 5.3) show the presence of a discontinuous matrix at pHs 7 and 11. This peculiarity will probably facilitate the formation of channels for the diffusion of water vapor and/or gases, which will contribute to greater permeability, and also could lead to a reduction in the other properties of these films. Similar to the cracks detected on the film surface, it is assumed that the development of these channels extending throughout the film thickness occurs during the drying process.

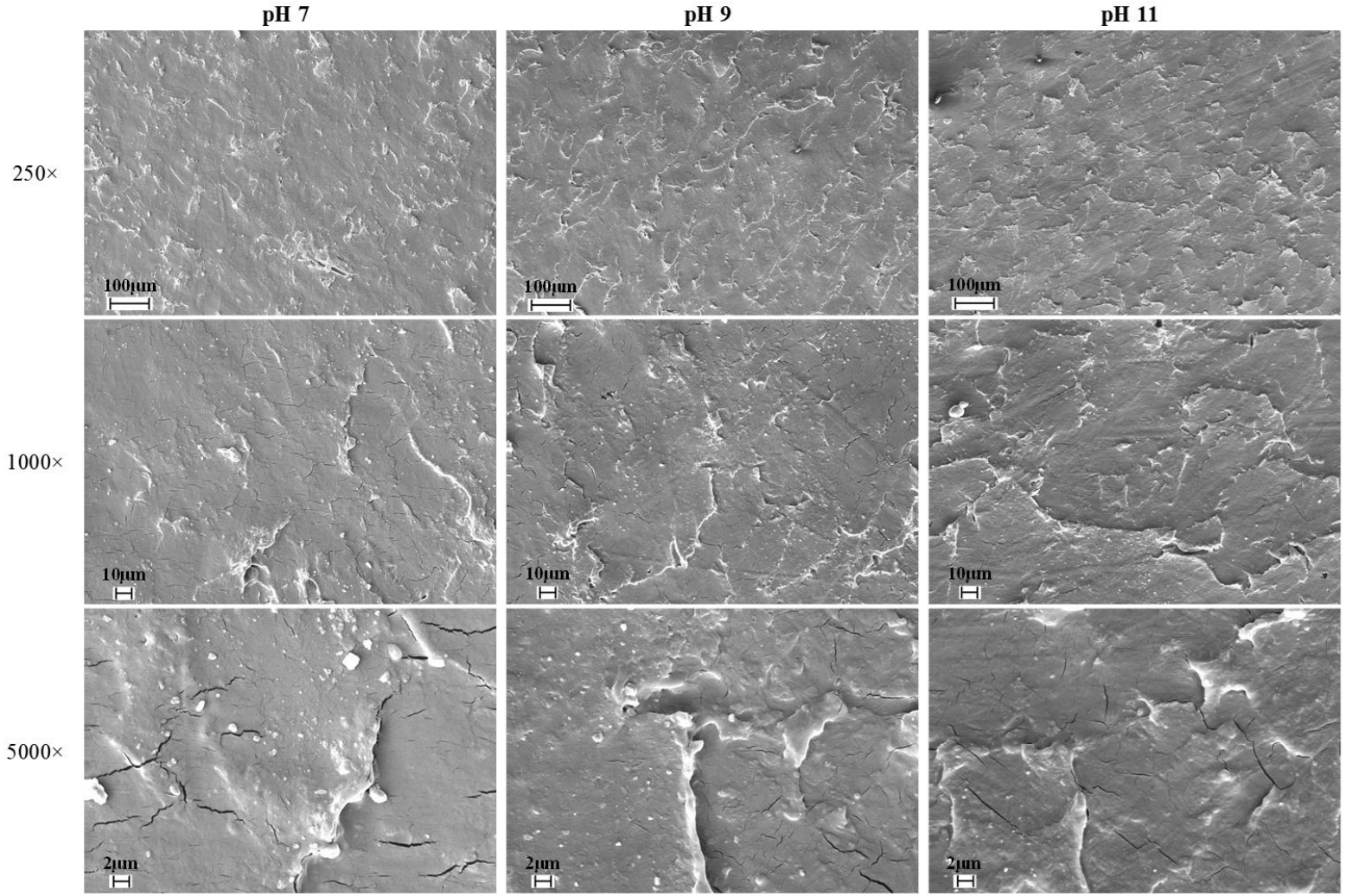
After observing both the surface and cross-sectional images, none of the films showed a completely homogeneous and uniform morphological structure, regardless of pH. However, it is relevant to emphasize the distinctive characteristics of pH 9, such as the lower incidence of fissures on the surface and their absence within its interior. These aspects may influence the characteristics to be evaluated in the following sections.

Figure Error! No text of specified style in document..**25** Micrographs of the smooth surface of CPC films at pH 7, pH 9 and pH 11 at magnifications of 250×, 1000× and 5000×



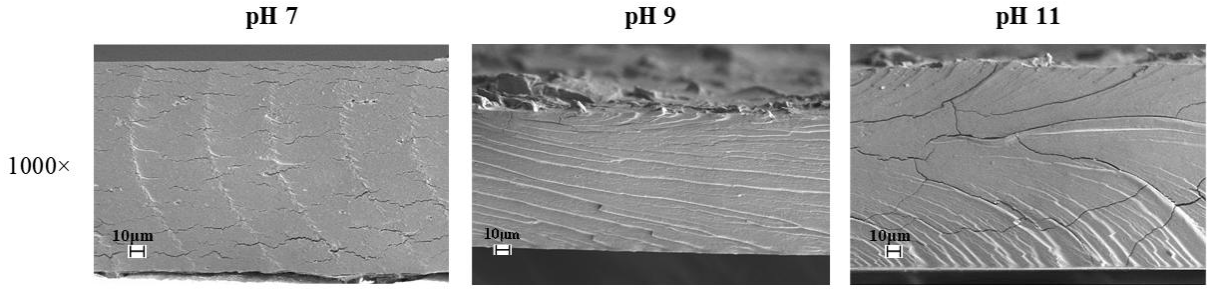
Source: elaborated by the author.

Figure Error! No text of specified style in document.**.26** Micrographs of the rough surface of CPC films at pH 7, pH 9 and pH 11 at magnifications of 250×, 1000× and 5000×



Source: elaborated by the author.

Figure Error! No text of specified style in document.**.27** Micrographs of the cross section of CPC films at pH 7, pH 9 and pH 11 at magnification of 1000×



Source: elaborated by the author.

3.2 X-ray diffraction (XRD)

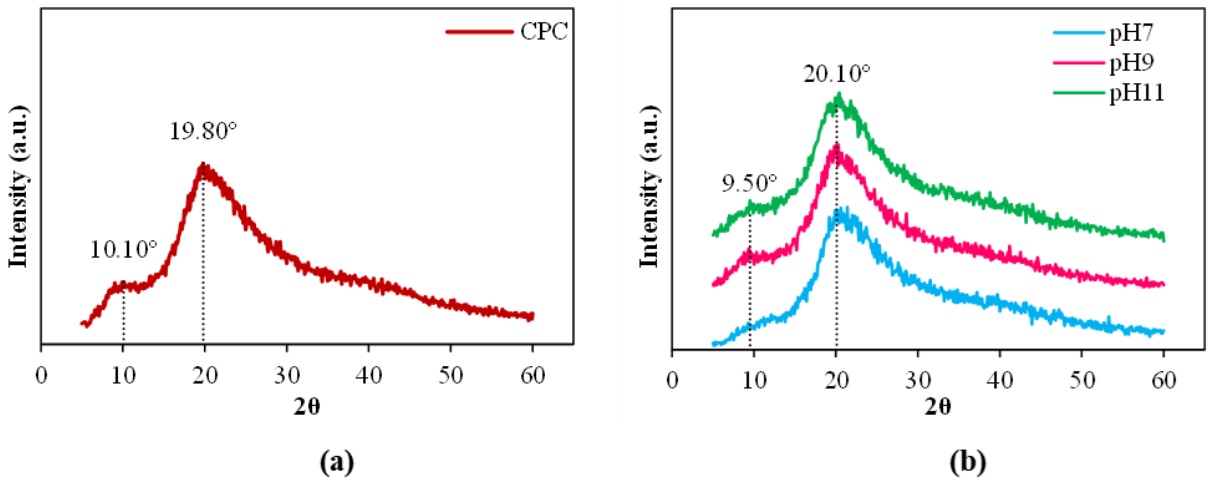
Figures 5.4a and 5.4b show the X-ray diffraction profiles of the raw material, powdered CPC, and the films at different pH levels respectively. The profile obtained for the raw material is characteristic of structures with a low degree of crystallinity. The peaks with a 2θ angle of approximately 10° and 20° in the protein X-ray reflection pattern correspond to the α-helix and β-sheet structures, in that order (Chen et al., 2013), with the second peak presenting a higher intensity than the former.

As expected, the films exhibited a diffraction pattern similar to powdered CPC, with a slight shift in the peaks and lower intensity at the shoulder (from 10.1° to 9.5°) and the main peak (from 19.8° to 20.1°). In the films (Figure 5.4b), the shoulder around 10° almost disappears at pH 7, which may indicate a lower presence of α-helix structures in films prepared at neutral conditions.

In addition to the spectra exhibiting a distinctive profile of amorphous structures, the calculation of the relative crystallinity index (RCI) corroborates this observation for both the films and the powder. The analysis revealed that the RCI was below 50% for all samples, with the CPC exhibiting a relative crystallinity of 40.83%. The films exhibited slightly different values, with 43.54%, 40.51%, and 40.08% for pHs 7, 9 and 11, respectively. The observed amorphous structure in both the concentrate and the films has the potential to impact the properties of the protein and the film itself. In crystalline structures, molecules are typically arranged in a densely packed manner, which may influence factors including solubility and water vapor permeability of films. Nevertheless, the ICRs of all films exhibited a high degree of similarity, with only minor variations. It is therefore unlikely that these differences will significantly impact their properties.

Other authors have reported that protein-based films exhibited amorphous behavior, with characteristic peaks in the same regions (Amado et al., 2023; Mir et al., 2023; Moghadam et al., 2020).

Figure Error! No text of specified style in document.**.28** XRD of (a) CPC powder and (b) CPC films at pH 7, pH 9 and pH 11



Source: elaborated by the author.

3.3 Fourier-transform infrared (FTIR) spectroscopy

Figure 5.5 shows the infrared spectrum of the CPC powder (a), the glycerol (b), the CPC-films (c) and the curve-fitting spectra of CPC-films' amide I (1700 – 1600 cm^{-1}) at pH 7 (d), pH 9 (e) and pH 11 (f).

With regard to the CPC spectrum (Figure 5.5a), the band observed at a frequency of 3273 cm^{-1} can be ascribed to the amide A band, which has been correlated with the stretching mode of the N-H bond; additionally, the band observed at and 2925 cm^{-1} may indicate the asymmetrical C-H stretching absorption from aliphatic compounds corresponding to the CH_2 group (Rozenberg & Shoham, 2007). The aforementioned peak is discernible in the films' spectra at all pH values (2928 cm^{-1}, Figure 5.5b), as well as in the glycerol spectrum (2932 cm^{-1}, Figure 5.5c). The presence of various compounds that absorb within this spectral region, makes it challenging to analyze the functional groups. Glycerol is characterized by a broad band around 3200 due to the O-H stretching, and an intense band at 1032 cm^{-1} attributed to the C-O stretching (Habuka et al., 2020).

The most characteristic bands of proteins are amide I (C=O stretching), amide II (N-H bending), and amide III bands (Garrido et al., 2016). These have been identified in the CPC in

powder form (Figure 5.5a) at frequencies of 1637 cm^{-1}, 1528 cm^{-1}, and 1236 cm^{-1}, respectively. Concerning the CPC-based films at pH 7, 9, and 11, analogous bands were observed in 1633 cm^{-1}, 1533 cm^{-1}, and 1234 cm^{-1} frequencies (Figure 5.5c). Furthermore, the presence of C-O bonds can be indicated by the band in these spectra at 1039 cm^{-1}, associated with the C-O stretching of glycerol used as a plasticizer in the films (Habuka et al., 2020; Garrido et al., 2016; Sanches et al., 2021).

The spectra of the CPC-based films (Figure 5.5b) indicate that alkalinity reduces the intensity of certain bands, including the amide I (1637 cm^{-1}), particularly at pH 11. This suggests that pH affects the secondary structures of the protein, possibly due to a greater degree of protein denaturation at this pH, which exposes functional groups that contribute to intermolecular interactions (Amado et al., 2023).

Quantitative secondary structure information was obtained by applying the second derivative and subsequent Gaussian band deconvolution (R^2>0.974) to the amide I region (1700-1600 cm^{-1}). The areas of the spectra were assigned to the different secondary structures (Figure 5.5d, 5.5e, 5.5f), including intermolecular β-sheet (1626-1610 cm^{-1} and 1700-1683 cm^{-1}), random coil (1640–1627 cm^{-1}), α-helix (1660–1641 cm^{-1}), and β-turn (1682–1661 cm^{-1}) (Zhao et al., 2021). From the relative areas of each peak, it was possible to assess variations in the composition of the secondary structures of CPC films and to make comparisons with CPC powder (Table 5.1).

As Georget and Belton (2006) have previously observed, the complete assignment of the low-frequency bands is not a straightforward process. This is because they may represent conformers with peptide groups that exhibit stronger hydrogen bonds in beta sheets or may arise from intermolecular β-sheets or even from extended hydrated structures. Ngarize et al. (2004) attributed aggregation bands in low-frequency regions present in both heated ovalbumin and β-lactoglobulin to the disruption of hydrogen bonds within some secondary structures and the formation of new stronger intermolecular hydrogen bonds associated with aggregation.

A comparison of the CPC powder with the film at pH 7 reveals an increase in the percentage of α-helix and random coil structures in the films, accompanied by a reduction in β-sheet and β-turn structures. This observation can be attributed to the steps involved in preparing and drying the films. The pH and heat treatment of the film-forming solution, the drying temperature, the film hydration, and even the type of plasticizers can affect the secondary structures of the proteins (Georget & Belton, 2006; Mangavel et al., 2001; Subirade et al., 1998).

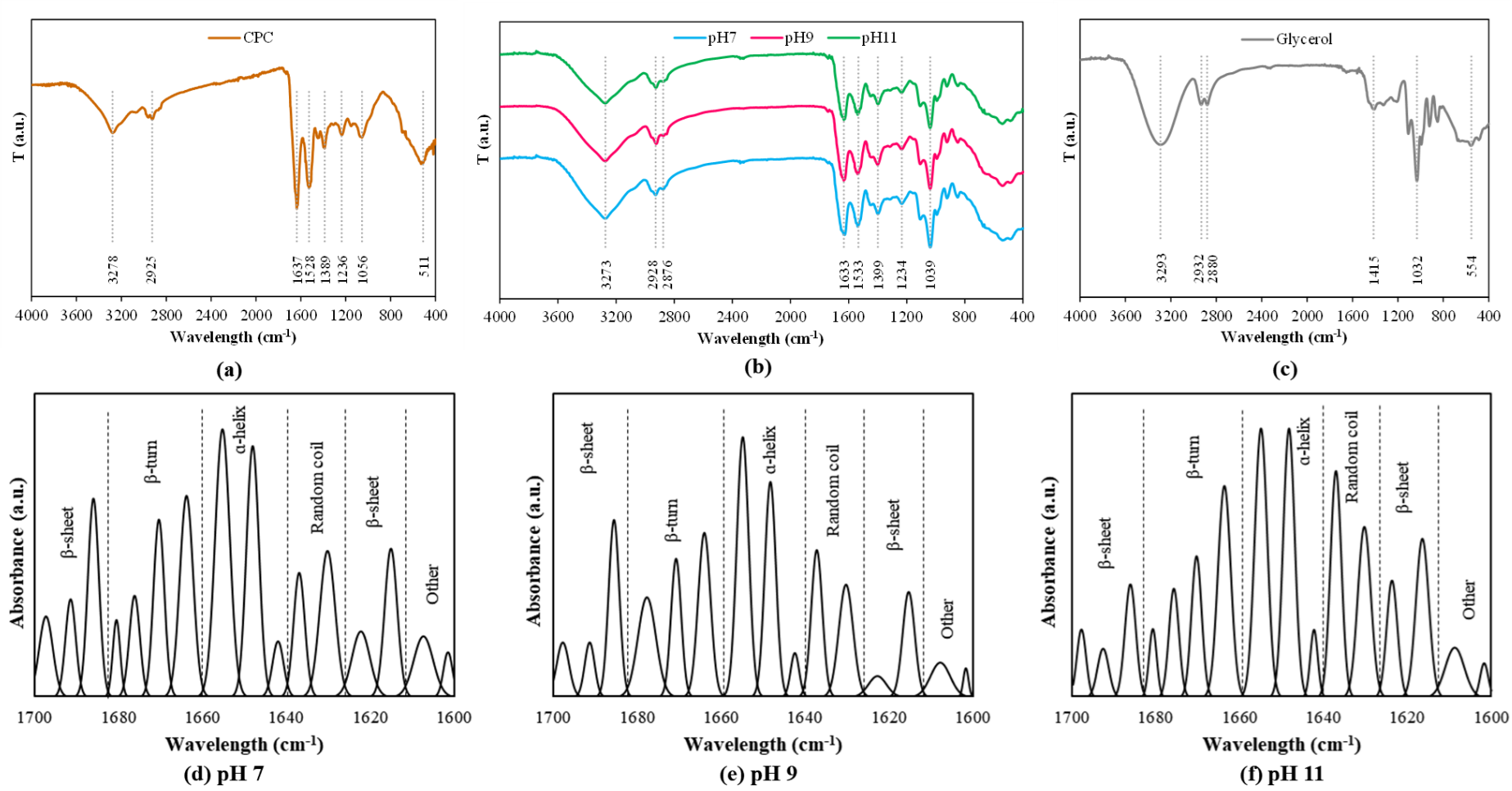
The impact of pH on protein structure was found to be minimal, with a tendency to reduce β-sheet structures in films with a neutral pH and to favor the formation of random coil structures. Nevertheless, the proportion of α-helix remained approximately constant with pH.

Table Error! No text of specified style in document.**.11** Assignments and relative areas (%) of the amide I components of the films at the different pHs and the CPC (powder)

Secondary structure	**pH**			**CPC (powder)**
	7	**9**	**11**	
α-helix	30.75%	30.69%	30.00%	16.70%
β-sheet	29.57%	24.87%	24.80%	43.29%
β-turn	25.04%	27.44%	24.89%	14.82%
Random coil	14.65%	17.00%	20.31%	25.19%

During the preparation of the film-forming solution, the electrokinetic potential of the solutions at all tested pH levels exhibited negative charge densities of approximately -30 mV (second chapter, item 3.2.2). It was thus anticipated that the impact of charged amino acid residues on the stabilization of the secondary structures of proteins forming the films under diverse pH conditions would be negligible. Both the α-helix and β-sheet structures are stabilized by hydrogen bonds. Nevertheless, the formation pattern of β-sheet bonds is distinct from that observed in α-helices. The formation of the α-helix occurs between amine groups within the same polypeptide chain (Clark et al., 2019), and the percentage of this structure did not change in all the films. In contrast, the change in pH appeared to exert a limited influence on the stability of β-sheets, which are stabilized by hydrogen bonds between adjacent polypeptide chains (Clark et al., 2019). This resulted in a slight decrease in β-sheet stability.

Figure Error! No text of specified style in document..**29** FTIR spectra of (a) CPC powder, (b) CPC-based films, (c) glycerol and the fitting spectra of amide I band for CPC films at pHs of 7 (d), 9 (e), and 11 (f)



Source: elaborated by the author.

3.4 Water vapor permeability (WVP) and water solubility (S)

The water vapor permeability (WVP) of the films is affected by factors such as the solubility and molecules migration within the film matrix. The hydrophilic nature of proteins can result in a less dense structure in the films, which in turn influences the reorganization of the network and increases the free volume and tortuosity of the structure (Amado et al., 2020). This scenario facilitates the movement of water molecules, resulting in higher WVP.

The WVP of the different CPC films was evaluated under a relative humidity gradient (ΔUR) of 100% – 2%, for which the average value was 51%. The values obtained for the films prepared at pH 7, 9 and 11 ranged from 5.65 to 8.19 10^{-10} g m^{-1} s^{-1} Pa^{-1} and are shown in Table 5.2.

Table Error! No text of specified style in document.**.12** Water content (%), WVP (g m^{-1} s^{-1} Pa^{-1}), and water solubility (%) of CPC films prepared at pH 7, 9 and 11

pH	Water content (%)	WVP × 10^{10} (g m^{-1} s^{-1} Pa^{-1})	S (%)
7	12.17 ± 0.65	6.23 ± 0.69 [a]	39.39 ± 0.59 [a]
9	13.47 ± 0.75	8.19 ± 2.06 [a]	41.43 ± 3.46[a]
11	12.77 ± 0.57	5.65 ± 0.51 [a]	41.23 ± 0.24 [a]

The WVP of CPC films did not exhibit significant differences with variations in pH. SEM results revealed that the CPC films, regardless of the preparation pH, did not exhibit a completely homogeneous morphological structure, with cracks and channels observed both on the surface and in the cross-section of the films. The lack of a uniform structure and the presence of similar features across all samples may justify the consistent WVP values observed among the different pH levels studied. The fissures and channels identified in the films, despite varying slightly in depth and distribution, as particularly observed at pH 9, may not have been sufficiently distinct to cause significant changes in permeability. The similarity in the films' morphology suggests that the mobility of water vapor through the channels formed during the drying process was relatively consistent, regardless of the pH, resulting in comparable WVP values. Therefore, the absence of significant differences in WVP values can be attributed to the structural homogeneity observed in the SEM analyses.

Also, these findings are consistent with results reported by other authors for films based on soy protein isolate (SPI). In a study conducted by Brandenburg, Weller, and Testin (1993), SPI (5%, m/m) films were investigated across a pH range from 2 to 12. The results demonstrated that there were no significant differences in barrier properties between pH levels of 6, 8, 10, and 12. Similarly, Cho et al. (2007) investigated the influence of pH (7, 8, 9, and 10) on the WVP of SPI-based films (5%, m/m) and did not observe significant differences across the alkaline pH levels evaluated. These findings support the hypothesis that elevated pH levels above 6 do not significantly affect the barrier properties of SPI films.

The WVP of plastics derived from non-renewable sources, such as low-density polyethylene (LDPE), polypropylene (PP) and polyvinylidene chloride (PVDC), typically lies around 10^{-12} g m^{-1} s^{-1} Pa^{-1} (Park, 2003; Han, 2014). When comparing the films produced in the present study with these conventional plastics, a deficiency in this property is identified due to the higher values obtained (10^{-10} g m^{-1} s^{-1} Pa^{-1}). This may restrict the applicability of these films as the unique food packaging, especially in environments with high relative humidity.

The solubility of edible films is a fundamental factor in determining their suitability for applicability in different food contexts. Films used for packaging must be water-insoluble to safeguard products that are inherently unstable and susceptible to moisture-induced deterioration. However, in cases such as edible coatings or encapsulation of food additives, the protective layer must be soluble. In the case of edible coatings, whether the coating is consumed directly or prepared in water, it must be easily soluble in the solvent used. Similarly, in the case of food additives, the capsules must dissolve easily during ingestion to release the additives. Therefore, the selection of an edible film must consider the need to strike a balance between its protective role and its dissolution capacity according to the specific requirements of the food product in question.

The water solubilities of the films ranged from 39.39 to 41.43% and were close to each other, indicating that the change in pH did not significantly alter their solubility. Despite the hydrophilic nature of protein-based films, the CPC films did not completely dissolve after 24h of immersion in water and maintained their structural integrity throughout the experiment. These changes can be attributed to alterations in pH and heat treatment, which lead to protein denaturation, favoring interactions such as intermolecular disulfide bonds. The formation of these disulfide bonds between proteins contributes to a reduction in protein interaction with water, thereby reducing the solubility of the films. The lack of a standard method for determining solubility presents a significant obstacle to comparing data from different experiments. While data obtained from different treatments within a single experiment may be

comparable, the lack of a uniform approach to solubility assessment precludes direct comparisons between different research studies. However, such comparisons can yield valuable insights into the behavior of various film types when conducted across different studies. The solubility values observed in the present study were close to those determined for soy protein films (Amado et al, 2020) but lower than those also determined for soy protein films by Jiang et al. (2023), Su et al. (2022) and Zhao et al. (2021). Conversely, our results were higher than those obtained for some films prepared from proteins of other legumes. These studies indicate solubilities ranging from 20% to 32%, specifically for films based on pea protein (Kowalczyk & Baraniak, 2011), mung bean protein (Moghadam et al., 2020), and fava bean protein (Rojas-Lema et al., 2021).

As mentioned earlier, the solubility of the films is not a limiting characteristic, as their applicability varies according to specific needs. There are numerous applications for edible films, which can be used as a standalone form of packaging, as a coating for foodstuffs, as a vehicle for active ingredients, or even for separating ingredients of heterogeneous foodstuffs into distinct compartments (Han, 2014). Therefore, considering the results indicating an intermediate solubility, it may be prudent to direct their use towards products with lower water activity (aw), such as powdered foods in general, and dried fruits and vegetables, and also to consider their use as secondary packaging. However, for this direction to be effective, further studies would be necessary to assess the feasibility of this material in food packaging.

3.5 Mechanical properties

The results of the mechanical analysis of the films formed at different pH values (7, 9, and 11) are presented in Table 5.3.

Table Error! No text of specified style in document.**.13** Tensile strength (MPa) and elongation at break (%) of CPC films prepared at pH 7, 9 and 11

pH	Tensile strength (TS) (MPa)	Elongation at break (EB) (%)
7	1.87 ± 0.30 [a]	180.16 ± 50.42 [a]
9	1.99 ± 0.37 [a]	175.90 ± 20.07 [a]
11	2.11 ± 0.26 [a]	153.06 ± 16.39 [a]

Mean ± SD are reported. Means with the same lowercase letter, in the same column, did not differ significantly at $p \leq 0.05$, according to Tukey's test.

The mechanical properties of protein-based films can be influenced by pH, as proteins unfold and may even undergo chemical denaturation at values far from the isoelectric point. This results in the exposure of their functional groups and the intensification of intermolecular interactions. However, despite the involvement of both covalent and non-covalent interactions in the formation of protein networks, the magnitude of each type of bond may vary, resulting in specific film properties (Amado et al., 2020; Mauri & Añón, 2006). As can be seen from the results in Table 5.3, the influence of the pH of the CPC film-forming solutions was minimal. Although trends of increasing stress and decreasing deformation with increasing pH were observed, these changes were not significant.

As for the WVP results, the morphology of the films has a significant impact on their mechanical properties. The presence of structural irregularities, particularly the cracks and discontinuities observed on the surfaces and cross-sections, indicates that the mechanical integrity of the films was compromised. The morphological similarities observed in the SEM results, regardless of pH, resulted in a similar impact on tensile strength and elongation at break. Consequently, the variations in pH did not cause significant changes in these mechanical properties, emphasizing the predominant influence of the films' morphological consistency.

Films derived from CPC showed comparable values of the same order of magnitude as those of SPI films in a pH range of 6 to 11 (Amado et al., 2020, 2023; Oliveira et al., 2021). SPI films prepared at pH 6 and 8 exhibited TS close to 1.9 and 1.5 MPa, respectively, with EB ranging from 97.4% to 221.4% in both cases. However, for the most alkaline pH, the trend of the CPC films did not follow that of the SPI films, i.e. increasing with increasing alkalinity. The TS and EB were close to 2.8 MPa and 132.0 – 213.2%, respectively, indicating a different behavior between these two proteins.

Mechanical properties of films produced under alkaline pH using other beans as a protein source, such as mung (Moghadam et al., 2020) and faba (Rojas-Lema et al., 2021) beans, have been previously studied by other researchers. The films by mung bean protein were formed at pH 8 and showed a higher TS, 3.3 MPa, but a considerably lower EB, 81.2%, compared to the present study (Moghadam et al., 2020). Similarly to mung bean films, films based on fava bean protein (pH 10.5) presented a higher TS (4.5 MPa) and lower EB (110%) (Rojas-Lema et al., 2021).

However, recent literature also presents discrepant results. In a comparative study, several proteins concentrate from legumes were used in the production of films at pH 9, such as lima beans, peas, lupins, lentils, and soybeans (Hopkins et al., 2019). In summary, the authors reported films with extremely low EB, ranging from 5% to 40%, and TS’s between 4 MPa and

10 MPa. This discrepancy in the results in relation to the films produced in the present study may be not only due to the protein type but also the considerable presence of other components such as starch in the composition of the concentrates used by them. The interactions between proteins and starch contribute to the mechanical reinforcement of the films, which results in greater resistance to rupture, increasing TS, and elastic modulus (Almeida et al., 2021), however, these interactions also tend to reduce the elongation capacity at break.

3.6 Sorption isotherm

Figure 5.6 shows the changes in equilibrium moisture content (X_{eq}) of CPC films prepared at pH levels 7, 9, and 11, as a function of water activity (a_w) at 25 °C.

According to the classification proposed by Brunauer et al. (1940), the curves corresponding to the films at pH 9 and 11 exhibit behavior that could be classified as Type II isotherms, as they show a slightly sigmoidal shape. At pH 7, the films resemble Type III isotherms because the inflection is not perceived (Lewicki, 1997). These materials demonstrate low water absorption at low water activities, contrasting with significantly higher absorption at higher water activities. The adsorption curves of the films revealed a sudden uptake of water in the water activity (a_w) range equal to or greater than 0.6, which is associated with the presence of protein and plasticizer (glycerol), both with available hydrophilic groups that facilitate water adsorption. This curve pattern is consistent with previous reports describing similar adsorption curves for films based on various proteins such as soy (Oliveira et al., 2021), pea (Kowalczyk & Baraniak, 2011), whey (Tavares et al., 2021), zein (Mouzakitis et al., 2022) and gelatin (Mohammadi-Nafchi et al., 2014).

Figure 5.6 also shows the proximity of the curves across all pH levels studied; however, subtle differences can be noted. In the low and intermediate a_w range, the films prepared at pH 11 exhibit a higher water adsorption capacity than those prepared at lower pH values. Conversely, in the higher a_w range, there is an inversion, with the X_{eq} values for the films at pH 11 becoming lower than those observed at pH 7 and pH 9. It can be postulated that the high alkalinity may exert a direct influence on the protein structure forming the films, propitiating exposure of more hydrophilic sites on surfaces for water adsorption in comparison to the lower pH levels. However, as the films undergo hydration, this behavior changes, rendering hydrophilic sites more available than in films formed at pH 11. This is likely related to the different molecular structures of the films formed in each pH, suggesting that these structures can also change with the relative humidity of the environment.

Table Error! No text of specified style in document**..14** GAB model parameters of the CPC films prepared at pH 7, 9 and 11

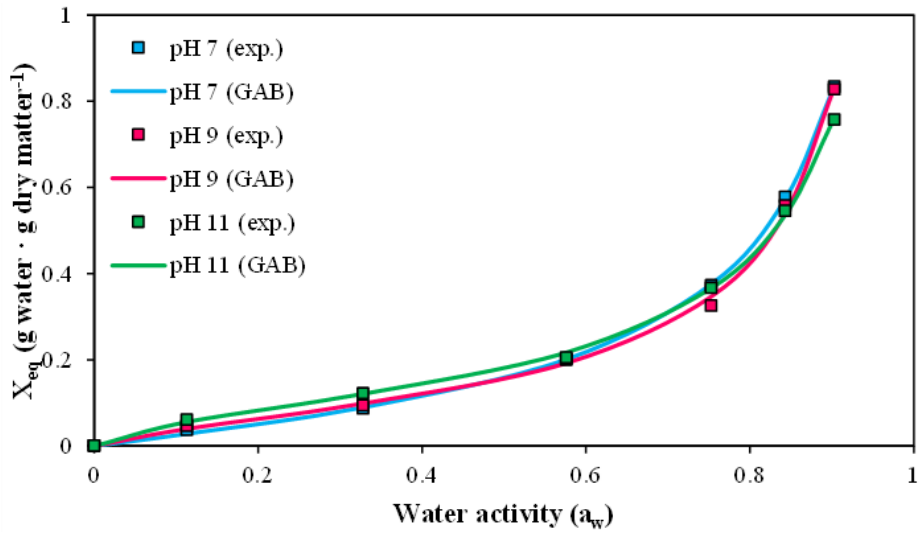
pH	Xm (d.b.)	C	K	R^2	P%
7	0.126	2.101	0.952	0.999	0.352
9	0.098	4.615	0.981	0.996	1.041
11	0.110	6.902	0.951	0.999	0.528

The GAB model was chosen to describe the water adsorption isotherms due to the advantage of having parameters with physical meaning. The model showed good fit to the experimental data, with R^2 values greater than 0.996 and P values, representing the average relative modulus, less than 10% (Table 5.4). As Lewicki (1997) asserts, at pH 11 the GAB parameters demonstrate that the model effectively describes the sigmoidal type isotherms (type II), as they are maintained within the following regions: $0.24 < K \leq 1$ and $5.67 \leq C \leq \infty$. These ranges correspond to estimates with an error lower than ± 15.5%. Conversely, the same author establishes that if C=2, the a_w value tends to be null, thereby confirming the type III curve observed in films prepared at pH 7 (Figure 5.6). The GAB model is based on the assumption that physical adsorption occurs in multiple layers, with minimal interlayer interactions. According to this theory, the water layers that form subsequently have less affinity with the material surface compared to the first layer. This first layer of water, in turn, spreads uniformly over the material surface and strongly adheres to it, forming a single layer of dense bonding (Quirijns et al., 2005). In the GAB model, the water content of the monolayer (X_m) corresponds to the amount of water strongly adsorbed at primary adsorption sites. After the monolayer formation, water molecules occupy adsorption sites to create successive multilayers, bonding relatively weakly (Kaya & Kahyaoglu, 2005; Sanches et al., 2023). X_m values as a function of pH ranged from 0.098 to 0.126.

The constant C is related to the binding strength of monolayer water to the active sites of the matrix (Quirijns et al., 2005). The increase in pH resulted in an increase in C values from 2.101 to 6.902. At the highest pH, the modified protein structure may provide adsorption sites that exhibit a stronger affinity with water, where the adsorbed water is more tightly bound (higher C) than at pH 7 and 9. Additionally, at high pH, the interactions between water and the film matrix become energetically more favorable, as the ionization of functional groups in the protein can create stronger interactions with water molecules, thereby increasing the constant C.

The values of K reflect the interactions between the adsorbent and water molecules in the multilayers. When K equals 1, the water in the multilayers has properties similar to liquid water (Quirijns et al., 2005). In this study, the values of K ranged from 0.951 to 0.981 (Table 5.4).

Figure Error! No text of specified style in document.**.30** Sorption isotherms of CPC films prepared at pH 7, 9 and 11



Source: elaborated by the author.

3.7 Optical properties

Table 5.5 presents the results of the color parameters of the films, along with visual observations from photographs.

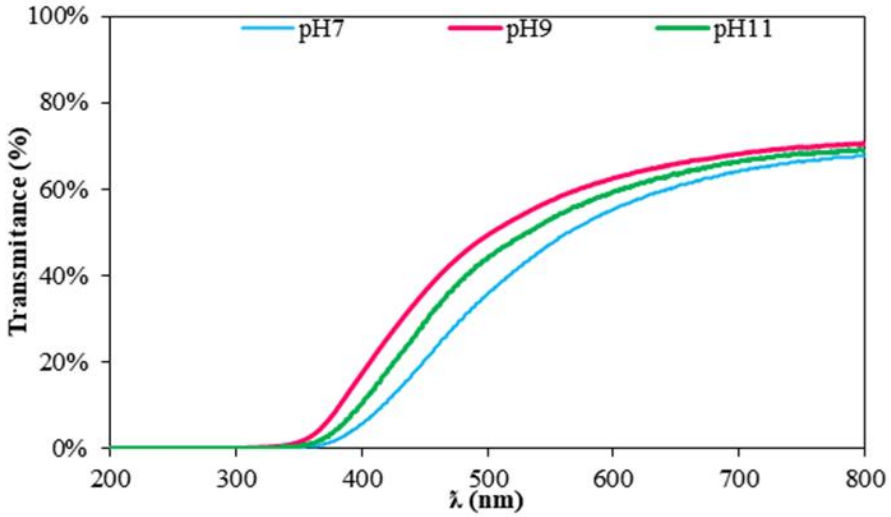
The findings indicate that pH significantly influenced the color parameters of the films. Films at pH 9 exhibited a lower L* value, indicative of a darker film compared to pHs 7 and 11 (which were statistically similar). Regarding the a* and b* parameters, representing the green (-)/red (+) and blue (-)/yellow (+) color components respectively, films at pH 9 displayed higher and positive values for both parameters, suggesting colors closer to red and yellow. Corroborating these findings, the yellowing index (YI) of CPC-based films shows significant variation across different pH levels. The highest YI value was recorded at pH 9, followed by pH 11 and pH 7, indicating a pronounced increase in yellowing at pH 9 compared to the other conditions. Moreover, films prepared at pH 9 exhibited the highest C* value, followed by pHs 7 and 11. This suggests that films at pH 9 are the most saturated in terms of color, whereas films at pH 11 are the least saturated. The h values of the films ranged between 83° and 89°, revealing significant differences among the samples. Given that the values are closer to 90°, it can be

stated that the films display a yellowish tone, with pH 9 associated with significantly lower values, exhibiting a slight orange tonality compared to the other films.

The variation in color values among different pH conditions may reflect distinct molecular and morphological structures of the films formed under each condition. Different pH levels can lead to varied molecular arrangements, influencing how light is transmitted through the film. The choice of pH for film formation significantly affects the visual characteristics of the films, which could have implications in applications where aesthetics and sensory perception are critical for consumer acceptance and product performance.

Figure 5.7 shows the transmittance of CPC films over a wavelength range of 200 to 800 nm.

Figure Error! No text of specified style in document.**.31** Transmittance of CPC-based films at different pHs



Source: elaborated by the author.

At wavelengths between 200 and approximately 350 nm, all formulations exhibited near-zero transmittance, indicating excellent UV light barrier properties. Low UV light transmission, along with other properties, is essential for food packaging (Zheng, Yu, & Pilla, 2017). Packaging that acts as UV light barriers minimizes oxidation reactions of polymer compounds and other light-sensitive materials, protecting them from degradation caused by sunlight and other sources of UV radiation (Pascal et al., 1995). The transmittance of CPC films subjected to a more alkaline treatment increased in the visible spectrum region (350–800 nm), indicating greater transparency of the films at pHs 9, followed by the films at pH 11.

Table Error! No text of specified style in document.**.15** Color parameters and visual aspect of CPC films at different pHs

pH	L*	a*	b*	C*	h	YI	Visual aspect**
7	81.35 ± 0.57^{a}	1.18 ± 0.27^{b}	33.49 ± 1.67^{c}	33.51 ± 1.67^{c}	87.89 ± 0.38^{a}	58.82 ± 3.10^{c}	
9	73.86 ± 0.61^{b}	5.54 ± 0.86^{a}	46.26±4.51^{a}	46.59 ± 4.57^{a}	83.20 ± 0.44^{b}	89.43 ±7.59^{a}	
11	81.09 ± 1.34^{a}	1.33 ± 0.49^{b}	38.48 ± 3.24^{b}	38.50 ± 3.25^{b}	88.85 ± 1.02^{a}	67.89 ± 67.89^{b}	

** Source: elaborated by the author. Means ± SD are reported. Means with the same lowercase letter in the same column did not differ significantly at $p \leq 0.05$ according to Tukey's test.

3.8 Oxygen permeability (O_2P)

The role of biopolymer-based films as effective barriers to oxygen transfer is of significant importance in maintaining the quality of oxidation-sensitive products over time. In food, oxygen is responsible for a number of processes that lead to deterioration, affecting taste, texture and nutritional value. By assessing the oxygen permeability of these biopolymer materials, it is possible to identify those that offer the best protection.

The polar nature of proteins results in their films exhibiting low permeability to nonpolar substances, such as oxygen. This fact is particularly evident under conditions of low to intermediate relative humidity, with values ranging from 10^{-15} to 10^{-17} g m (Pa s m^2)$^{-1}$ (Choi et al., 2023; Galus & Kadzińska, 2016; Oliveira et al., 2021; Porta et al., 2016). Moreover, when evaluated in comparison to conventional plastics such as low-density polyethylene (10^{-14} g m (Pa s m^2)$^{-1}$), these films may exhibit even lower oxygen permeability (Miller & Krochta, 1997).

Table 5.6 presents the oxygen permeability (O_2P) of the CPC films formed at different pH values. The O_2P values were expressed as 10^{-15} g m Pa^{-1} s^{-1} m^{-2} for the films formed at pH of 7, 9, and 11. The results indicated a non-linear relationship between permeability and film-forming pH. The O_2P of films at pH 9 was significantly lower than that observed at pH 7 and 11, which exhibited comparable values. Nevertheless, the values in Table 5.6 are relatively similar to one another, which indicates that the pH has a relatively minor influence on films based on CPC in comparison with other plant-based proteins.

Table Error! No text of specified style in document**..16** Oxygen permeability of CPC films at pHs of 7, 9 and 11

pH	**$O_2P\times10^{15}$ (g m Pa^{-1} s^{-1} m^{-2})**
7	1.21 ± 0.01[a]
9	0.98 ± 0.02[b]
11	1.24 ± 0.01[a]

Means ± SD are reported. Means with the same lowercase letter in the same column did not differ significantly at $p \leq 0.05$ according to Tukey's test.

These findings are consistent with those of Amado et al. (2020) and Soliman et al. (2007), whose observed a reduction in O_2P of SPI films as the pH of the films increased from acidic to alkaline conditions. The high solubilization of SPI at alkaline pH was identified as the underlying cause of this result. In the present study, the pH values of 7 and 11 were found to be similar. Therefore, it can be postulated that the pH 9 condition represents an optimal situation

among those studied, where the proteins are in an extended form and the ideal balance between hydrophobic and hydrophilic amino acid residue sequences is maintained, resulting in a film that is less permeable to polar substances.

The observed increase in O_2P at pH 11 can be attributed to the excessive deprotonation of functional groups, which could lead to a more unordered and permeable structure, as discussed in the FTIR section (*item 3.3*). The surface and cross-section images of the films at pH 7 and 11 (Figure 5.3) provide corroboration of this statement. They reveal the presence of cracks that extend throughout the thickness of the films, forming channels that may facilitate oxygen diffusion. In contrast, the films prepared at pH 9 exhibit a more homogeneous morphology with lower incidence of cracks on the surface and in the cross-section (Figure 5.3), indicating a denser structure with fewer favorable pathways for the passage of gases.

4 Conclusion

It is essential to note that pH 9 represented a critical point among the conditions for the formation of the edible films under study. While none of the films exhibited a completely homogeneous and uniform morphological structure, the films formed at pH 9 exhibited a lower incidence of cracks on their surface and throughout their thickness. Furthermore, this condition significantly influenced the permeability to oxygen (O_2P), resulting in a significant reduction in O_2P.

The impact of pH on the structure of the films was evidenced by X-ray and FTIR analyses. The films exhibited characteristic profiles of structures with a low degree of crystallinity. The FTIR analysis revealed that the most disordered molecular structure was observed at pH 9 and 11. Furthermore, the isotherms of the water adsorption of the films were well described by the GAB model. In low to intermediate humidity conditions the films at pH 11 demonstrated a higher water adsorption capacity than the other tested films. However, at higher water activity levels, the hydration of the films resulted in a shift in this behavior, suggesting increased exposure of polar groups from the less structured films at pH 7 and 9 to the water adsorption.

CPC films stand out for their excellent UV barrier properties, benefiting from alkaline treatment, which contributes to increasing their transparency. On the other hand, it was observed that pH variation did not have a significant impact on the permeability to vapor water (WPV), solubility, tensile strength and deformation of the films.

The findings of the study demonstrate the versatility and efficacy of CPC as a raw material for the formation of edible films, establishing the foundation for further investigation

and applications of CPC films in different food contexts. Additionally, the study demonstrates the capacity to easily modify the material properties through pH adjustments, thereby indicating the potential to tailor film functionality to specific contexts.

References

Allen, D., Spoelman, N., Linsley, C., & Johl, A. (2024). The Fraud of Plastic Recycling: How Big Oil and the plastics industry deceived the public for decades and caused the plastic waste crisis.

Almeida, F. C., de Souza, C. O., Philadelpho, B. O., Franca Lemos, P. V., Cardoso, L. G., Santana, J. S., ... & Druzian, J. I. (2021). Combined effect of cassava starch nanoparticles and protein isolate in properties of starch-based nanocomposite films. *Journal of Applied Polymer Science*, *138*(18), 50008. https://doi.org/10.1002/app.50008

Amado, L. R., de Souza Silva, K., & Mauro, M. A. (2023). Alginate and pH Improve Properties of Soy Protein-based Films. *Food Biophysics, 19*, 256–268. https://doi.org/10.1007/s11483-023-09823-5

Amado, L. R., Silva, K. de S., & Mauro, M. A. (2020). Effects of interactions between soy protein isolate and pectin on properties of soy protein-based films. *Journal of Applied Polymer Science*, *137*(21), 48732. https://doi.org/10.1002/app.48732

Associação Brasileira da Indústria do Plástico - ABIPLAST. Perfil 2022. Available at: https://www.abiplast.org.br/. Accessed: June 5, 2024.

ASTM INTERNATIONAL. ASTM D882-12, Standard Test Method for Tensile Properties of Thin Plastic Sheeting, West Conshohocken, PA, 2012.

ASTM INTERNATIONAL. ASTM E96-95: Standard test methods of water vapor transmission of materials. In: Annual Book of ASTM Standards, American Society for Testing and Materials, Philadelphia, 1995.

ASTM INTERNATIONAL. ASTM F 1927-14: Standard test method for determination of oxygen gas transmission rate, permeability and permeance at controlled relative humidity through barrier materials using a coulometric detector. Philadelphia, 2014.

Brandenburg, A. H., Weller, C. L., & Testin, R. F. (1993). Edible Films and Coatings from Soy Protein. *Journal of Food Science, 58*(5), 1085-1089.

Brunauer, S., Deming, L. S., Deming, W. E., & Teller, E. (1940). On a theory of the van der Waals adsorption of gases. *Journal of the American Chemical society*, *62*(7), 1723-1732

Cao, N., Fu, Y., & He, J. (2007). Preparation and physical properties of soy protein isolate and gelatin composite films. *Food Hydrocolloids*, *21*(7), 1153–1162. https://doi.org/10.1016/j.foodhyd.2006.09.001

Cho, S. Y.; Park, J.; Batt, H. P.; Thomas, R. L. (2007). Edible films made from membrane processed soy protein concentrates. *LWT - Food Science and Technology, 40*, p. 418-423.

Choi, J., Lee, J. S., Han, J., & Chang, Y. (2023). Development of gelatin–sodium caseinate high-oxygen-barrier film containing elderberry (*Sambucus nigra L.*) extract and its antioxidant capacity on pork. *Food Bioscience*, *53*. https://doi.org/10.1016/j.fbio.2023.102617

Clark, D. P., Pazdernik, N. J., & McGehee, M. R. (2019). Protein Structure and Function. In *Molecular Biology* (pp. 445–483). Elsevier. https://doi.org/10.1016/B978-0-12-813288-3.00014-8

Cuq, B., Gontard, N., CUQ, J. L., & Guilbert, S. (1996). Functional properties of myofibrillar protein-based biopackaging as affected by film thickness. *Journal of Food Science*, *61*(3), 580-584.

Galus, S., & Kadzińska, J. (2016). Whey protein edible films modified with almond and walnut oils. *Food Hydrocolloids*, *52*, 78–86. https://doi.org/10.1016/j.foodhyd.2015.06.013

Garrido, T., Etxabide, A., Guerrero, P., & De La Caba, K. (2016). Characterization of agar/soy protein biocomposite films: Effect of agar on the extruded pellets and compression moulded films. *Carbohydrate Polymers*, *151*, 408–416. https://doi.org/10.1016/j.carbpol.2016.05.089

Gómez, A., Gay, C., Tironi, V., & Avanza, M. V. (2021). Structural and antioxidant properties of cowpea protein hydrolysates. *Food Bioscience*, *41*. https://doi.org/10.1016/j.fbio.2021.101074

Habuka, A., Yamada, T., & Nakashima, S. (2020). Interactions of Glycerol, Diglycerol, and Water Studied Using Attenuated Total Reflection Infrared Spectroscopy. *Applied Spectroscopy*, *74*(7), 767–779. https://doi.org/10.1177/0003702820919530

Han, J. H. (2014). Edible Films and Coatings: A Review. In *Innovations in Food Packaging: Second Edition* (pp. 213–255). Elsevier Ltd. https://doi.org/10.1016/B978-0-12-394601-0.00009-6

Hewage, S., & Vithanarachchi, S. M. (2009). Biodegradable polymer films from cowpea protein isolate Preparation and characterization of biodegradable polymer films from cowpea (*Vigna unguiculata*) protein isolate. *Journal of the National Science Foundation of Sri Lanka, 37(1),* 53-57.

Hopkins, E. J., Stone, A. K., Wang, J., Korber, D. R., & Nickerson, M. T. (2019). Effect of glycerol on the physicochemical properties of films based on legume protein concentrates: A comparative study. *Journal of Texture Studies*, *50*(6), 539–546. https://doi.org/10.1111/jtxs.12460

Jiang, J., Shi, L., Ren, Z., & Weng, W. (2023). Preparation and characterization of soy protein isolate films by pretreatment with cysteine. *Food Chemistry: X*, *18*, 100735. https://doi.org/10.1016/j.fochx.2023.100735

Kaya, S., & Kahyaoglu, T. (2005). Thermodynamic properties and sorption equilibrium of pestil (grape leather). *Journal of Food Engineering*, *71*(2), 200–207. https://doi.org/10.1016/J.JFOODENG.2004.10.034

Kowalczyk, D., & Baraniak, B. (2011). Effects of plasticizers, pH and heating of film-forming solution on the properties of pea protein isolate films. *Journal of Food Engineering*, *105*(2), 295–305. https://doi.org/10.1016/j.jfoodeng.2011.02.037

Li, J., Krishna B, A., van Ewijk, G., van Dijken, D. J., de Vos, W. M., & van der Gucht, J. (2022). A comparison of complexation induced brittleness in PEI/PSS and PEI/NaPSS single-step coatings. *Colloids and Surfaces A: Physicochemical and Engineering Aspects*, *648*. https://doi.org/10.1016/j.colsurfa.2022.129143

Lomauro, C. J., Bakshi, A. S., & Labuza, T. P. (1985). Evaluation of food moisture sorption isotherm equations. Part I: Fruit, vegetable and meat products. *Lebensmittel-Wissenschaft und Technologie-LWT*, 18(2), 111-117.

Loushigam, G., & Shanmugam, A. (2023). Modifications to functional and biological properties of proteins of cowpea pulse crop by ultrasound-assisted extraction. *Ultrasonics Sonochemistry*, *97*. https://doi.org/10.1016/j.ultsonch.2023.106448

Marquardt, D. W. (1963). An algorithm for least-squares estimation of nonlinear parameters. *Journal of the society for Industrial and Applied Mathematics*, *11*(2), 431-441.

Mauri, A. N., & Añón, M. C. (2006). Effect of solution pH on solubility and some structural properties of soybean protein isolate films. *Journal of the Science of Food and Agriculture*, *86*(7), 1064–1072. https://doi.org/10.1002/jsfa.2457

Miller, K. S., & Krochta, J. M. (1997). Oxygen and aroma barrier properties of edible films: A review. *Trends in Food Science & Technology*, *81*(7), 228-237. https://doi.org/10.1016/S0924-2244(97)01051-0

Mir, N. A., Riar, C. S., & Singh, S. (2023). Effect of film forming solution pH on antibacterial, antioxidant and structural characteristics of edible films from modified quinoa protein. *Food Hydrocolloids*, *135*. https://doi.org/10.1016/j.foodhyd.2022.108190

Moghadam, M., Salami, M., Mohammadian, M., Khodadadi, M., & Emam-Djomeh, Z. (2020). Development of antioxidant edible films based on mung bean protein enriched with pomegranate peel. *Food Hydrocolloids*, *104*. https://doi.org/10.1016/j.foodhyd.2020.105735

Mohammadi Nafchi, A., Moradpour, M., Saeidi, M., & Alias, A. K. (2014). Effects of nanorod-rich ZnO on rheological, sorption isotherm, and physicochemical properties of bovine gelatin films. *LWT - Food Science and Technology*, *58*(1), 142–149. https://doi.org/10.1016/J.LWT.2014.03.007

Mouzakitis, C. K., Sereti, V., Matsakidou, A., Kotsiou, K., Biliaderis, C. G., & Lazaridou, A. (2022). Physicochemical properties of zein-based edible films and coatings for extending wheat bread shelf life. *Food Hydrocolloids*, *132*, 107856. https://doi.org/10.1016/J.FOODHYD.2022.107856

Ngarize, S., Herman, H., Adams, A., & Howell, N. (2004). Comparison of changes in the secondary structure of unheated, heated, and high-pressure-treated β-lactoglobulin and ovalbumin proteins using Fourier transform Raman spectroscopy and self-deconvolution. *Journal of agricultural and food chemistry*, *52*(21), 6470-6477. https://doi.org/10.1021/jf030649y

Oliveira, M. M. G. de, Fessori, A. G. B. W., Huamaní-Meléndez, V. J., & Mauro, M. A. (2024). Exploring the rheological and thermal behavior of cowpea protein concentrate: Impact of pH and concentration. *Colloids and Surfaces A: Physicochemical and Engineering Aspects*, *694*. https://doi.org/10.1016/j.colsurfa.2024.134106

Oliveira, M.M.G., de Souza Silva, K. & Mauro, M.A. (2021). Evaluation of Interactions Between Carboxymethylcellulose and Soy Protein Isolate and their Effects on the Preparation and Characterization of Composite Edible Films. *Food Biophysics 16*, 214–228. https://doi.org/10.1007/s11483-020-09659-3

Pająk, P., Przetaczek-Rożnowska, I., & Juszczak, L. (2019). Development and physicochemical, thermal and mechanical properties of edible films based on pumpkin, lentil and quinoa starches. *International Journal of Biological Macromolecules*, *138*, 441-449.

Park, H. J. (2003). Edible coatings HJ Park, Korea University. *Food Preservation Techniques*, 90.

Porta, R., Di Pierro, P., Sabbah, M., Regalado-Gonzales, C., Mariniello, L., Kadivar, M., & Arabestani, A. (2016). Blend films of pectin and bitter vetch (*Vicia ervilia*) proteins: Properties and effect of transglutaminase. *Innovative Food Science and Emerging Technologies*, *36*, 245–251. https://doi.org/10.1016/j.ifset.2016.07.001

Quirijns, E. J., Van Boxtel, A. J. B., Van Loon, W. K. P., & Van Straten, G. (2005). Sorption isotherms, GAB parameters and isosteric heat of sorption. *Journal of the Science of Food and Agriculture*, *85*(11), 1805–1814. https://doi.org/10.1002/jsfa.2140

Ribeiro Sanches, M. A., Camelo-Silva, C., Tussolini, L., Tussolini, M., Zambiazi, R. C., & Becker Pertuzatti, P. (2021). Development, characterization and optimization of biopolymers films based on starch and flour from jabuticaba (*Myrciaria cauliflora*) peel. *Food Chemistry*, *343*. https://doi.org/10.1016/j.foodchem.2020.128430

Rojas-Lema, S., Nilsson, K., Langton, M., Trifol, J., Gomez-Caturla, J., Balart, R., Garcia-Garcia, D., & Moriana, R. (2023). The effect of pine cone lignin on mechanical, thermal and barrier properties of faba bean protein films for packaging applications. *Journal of Food Engineering*, *339*. https://doi.org/10.1016/j.jfoodeng.2022.111282

Rojas-Lema, S., Nilsson, K., Trifol, J., Langton, M., Gomez-Caturla, J., Balart, R., Garcia-Garcia, D., & Moriana, R. (2021). "Faba bean protein films reinforced with cellulose nanocrystals as edible food packaging material." *Food Hydrocolloids*, *121*, 107019. https://doi.org/10.1016/j.foodhyd.2021.107019

Sadat, A., & Joye, I. J. (2020). Peak fitting applied to Fourier transform infrared and Raman spectroscopic analysis of proteins. *Applied Sciences (Switzerland)*, *10*(17), 5918. https://doi.org/10.3390/app10175918

Sanches, M. A. R., Augusto, P. E. D., Polachini, T. C., & Telis-Romero, J. (2023). Water sorption properties of brewer's spent grain: A study aimed at its stabilization for further conversion into value-added products. *Biomass and Bioenergy*, *170*, 106718. https://doi.org/10.1016/j.biombioe.2023.106718

Silva, K. S., Fonseca, T. M. R., Amado, L. R., & Mauro, M. A. (2018). Physicochemical and microstructural properties of whey protein isolate-based films with addition of pectin. *Food Packaging and Shelf Life*, *16*, 122–128. https://doi.org/10.1016/j.fpsl.2018.03.005

Stuart, B. H. (2012). Infrared Spectroscopy of Biological Applications: An Overview. In *Encyclopedia of Analytical Chemistry*. Wiley. https://doi.org/10.1002/9780470027318.a0208.pub2

Su, S., Xiao, Z., Wang, Y., Jiang, R., Huo, J., Li, H., ... & Duan, Y. (2023). Preparation and characterization of soy protein isolated particle film homogenized at different pressures. *International Journal of Food Science & Technology*, *58*(3), 1652-1661. https://doi.org/10.1016/j.fochx.2023.100735

Tavares, L., Souza, H. K. S., Gonçalves, M. P., & Rocha, C. M. R. (2021). Physicochemical and microstructural properties of composite edible film obtained by complex coacervation between chitosan and whey protein isolate. *Food Hydrocolloids*, *113*, 106471. https://doi.org/10.1016/j.foodhyd.2020.106471

Tomar, B. S., Shahin, A., & Tirumkudulu, M. S. (2020). Cracking in drying films of polymer solutions. *Soft Matter*, *16*(14), 3476–3484. https://doi.org/10.1039/c9sm02294e

van den Berg, C., & Bruin, S. (1981). Water activity and its estimation in food systems: theoretical aspects. *Water Activity: Influences on Food Quality*, 1–61. https://doi.org/10.1016/B978-0-12-591350-8.50007-3

Zhao, G., Zhou, C., & Fan, F. (2021). Preparation and properties of soy protein isolate/cotton-nanocrystalline cellulose films. *International Journal of Polymer Science*, *2021*(1), 5518136. https://doi.org/10.1155/2021/5518136

Zhao, J., Cui, J. K., Chen, R. X., Tang, Z. Z., Tan, Z. L., Jiang, L. Y., & Liu, F. (2021). Real-time in-situ quantification of protein secondary structures in aqueous solution based on ATR-FTIR subtraction spectrum. Biochemical Engineering Journal, 176, 108225.

6 IMPROVING PROPERTIES OF COWPEA PROTEIN CONCENTRATE FILMS WITH EMULSION INCORPORATION – A COMPARATIVE STUDY

Maria Mariana Garcia de Oliveira[a*], Lais Ravazzi Amado[a], Víctor Justiniano Huamaní-Meléndez[a] and Maria Aparecida Mauro[a]

[a] Department of Food Engineering and Technology, Institute of Biosciences, Humanities and Exact Sciences – São Paulo State University (UNESP), Street Cristóvão Colombo, 2265, São José do Rio Preto 15054-000, Brazil.

e-mail address: maria.mariana@unesp.br (*corresponding author)

Abstract

The objective of this study is to conduct a preliminary investigation into the impact of incorporating different emulsion's concentrations on the key properties of cowpea protein concentrate (CPC) films. Fatty compounds can improve the barrier properties of films and carry substances of interest. For this purpose, an oil-in-water emulsion containing 4% sunflower oil was prepared, utilizing CPC (0.6%) as the emulsifying agent. This emulsion was incorporated into CPC film-forming solution (5% protein and 2% glycerol) at different concentrations (0, 0.2, 0.4, 0.6, 0.8 and 1.0%) and dried to obtain the CPC composite film. Then, the main properties of the control and the CPC-emulsion films were evaluated. The SEM images of the films with the emulsion addition, showed emulsion droplets distributed over the surface and cross-sectional area, while the control films revealed a more uniform appearance. Relative crystallinity index of the films ranged from 32% to 41% and was significantly affected by the presence of emulsion in the films. Films' solubility and water vapor permeability did not significantly change with the addition of emulsion, while oxygen permeability (O_2P) did. The formulation containing 1% emulsion exhibited the lowest value of O_2P, which coincided with one of the highest crystallinity indices among the emulsion films, and it may be attributed to a more cohesive microstructure. Incorporating emulsion in the film-forming solutions had a minimal impact on film thickness but improved tensile strength and elongation at break. The films' isotherms displayed a typical Type II pattern, with the GAB and BET models effectively describing water adsorption, with $R^2 > 0.993$. Films above 0.2% emulsion showed higher opacity, while the control film was significantly more transparent. The study demonstrates the efficacy of incorporating emulsions into CPC-based films, with encouraging preliminary outcomes. This opens the possibility of complementing the studied formulations, aiming at the development of films and coatings for specific applications.

Keywords: Plant protein, Emulsion-based films, Biopolymers, Mechanical properties, Barrier properties

1 Introduction

The dominance of petroleum-derived polymers food packaging is largely attributable to their low cost and favorable properties; however these materials are non-biodegradable and non-renewable, causing environmental impact. Edible films, made from proteins, polysaccharides, and lipids, offer a sustainable alternative for packaging and a range of other application possibilities. These thin, biocompatible, and biodegradable films can reduce environmental impact. However, replacing water-resistant plastics with biopolymer-based films is challenging. Biopolymer packaging must meet traditional packaging functions—protection, communication, convenience, and containment—while enhancing sustainability by reducing packaging waste and food loss (Han, 2014; Vanderroost et al., 2014).

Films derived from proteins in general exhibit an ordered structure in the form of a compact network, formed by hydrogen interactions, which provides excellent mechanical and gas barrier properties (Amado et al., 2023; Oliveira et al., 2021; Silva et al., 2018). However, due to the hydrophilic nature of proteins, these films facilitate the passage of moisture, rendering them ineffective as barriers to water vapor. One strategy for modifying and adjusting the water vapor barrier to meet specific needs is to incorporate a lipid into a hydrocolloid matrix to obtain hydrocolloid–lipid composite films with reduced water vapor permeability (Amjadi et al., 2021; Galus, 2018; Valenzuela et al., 2013). The incorporation of lipids into a hydrocolloid matrix has been achieved through two principal methodologies. The first method involves the formation of bilayer films, while the second entails the dispersion of lipids in a hydrocolloid aqueous solution. The formation of multi-layer packaging, in general, is susceptible to delamination over time and has deficiencies relating to cohesion and compatibility between the materials, in addition to having the major disadvantage of needing to be subjected to at least two drying stages (Garrido-López & Tena, 2010; La Fuente Arias et al., 2023; Zhang et al., 2021). In the second method, the direct dispersion of oil into a colloidal solution hinders the formation of emulsion films with uniformly dispersed oil droplets, resulting in inferior properties (Paglione et al., 2019).

In contrast, previous studies (Zhao et al., 2023ab) have demonstrated that the incorporation of a hydrophobic component into films can be achieved with greater efficacy through the formation of a "pre-emulsion". Subsequently, the pre-emulsion is incorporated into the original film-forming solution, enabling the successful preparation of emulsified films. The uniform distribution of oil droplets, resulting from the pre-emulsification process, has been confirmed to enhance the barrier to water vapor (Zhao et al., 2023ab).

Cowpeas (*Vigna unguiculata (L.)* Walp), also known as black-eyed peas, has been subjected to research as a potential alternative source of plant-based protein (Gómez et al., 2021; Loushigam & Shanmugam, 2023; Oliveira et al., 2024). Despite an extensive literature review, only two studies specifically focused on edible films from cowpea protein. Hewage & Vithanarachchi (2009) examined films with varying pH levels (8-11) and different plasticizers (polyethylene glycol and glycerol). The second study analyzed the incorporation of cowpea protein into cassava starch films (Almeida et al., 2021) yet did not assess the properties of films composed solely of cowpea protein.

Nevertheless, despite the existing literature indicating that cowpea protein has the potential to form satisfactory films, the development of films using this relatively unexplored raw material, in conjunction with the modification of its characteristics through the incorporation of an emulsion, still represents a significant challenge.

The incorporation of the emulsion into the film matrix may result in alterations in the microstructure, thereby mitigating the expected impact on the reduction of water vapor permeability and influencing other essential properties for food packaging. Therefore, it becomes essential to conduct a fundamental study on the effect of the presence of a lipid component in these cowpea protein-based films. Therefore, in this study, an emulsion (O/W) was prepared dispersing sunflower oil and cowpea protein as the emulsifying agent. Subsequently, this emulsion was incorporated, in different proportions, into the film-forming solutions containing cowpea protein concentrate (CPC) to produce the emulsified films.

The objective of this study was to investigate the behavior of CPC-based films with the addition of different concentrations of an emulsion, also based on CPC, and to evaluate how the emulsions influence the structure and main properties of the films.

2 Materials and methods

2.1 Materials

CPC with a protein content of 79% was utilized as the principal raw material for both preparing emulsions and films. Type 1 sunflower oil (Liza, Brazil) was also used to prepare the emulsions. Additionally, analytical grade reagents including bi-distilled glycerol, sodium hydroxide, and hydrochloric acid (Synth, Brazil) were employed in the experimental procedures.

2.2 Methods

2.2.1 Cowpea protein extraction

Protein extraction was performed using an isoelectric precipitation method, following an adapted protocol from Moser, Ferreira, and Nicoletti (2019). Initially, cowpea grains were washed and macerated at 4 °C for 12 hours. The macerated grains were then blended with distilled water at a 1:3 (m/m) ratio for 3 minutes. The pH of the resulting mixture was adjusted to 8 using a concentrated NaOH solution. The suspension was stirred for 45 minutes at room temperature (25 °C) with a mechanical stirrer (MA 039, Marconi, Brazil). Following this, the mixture was centrifuged at 10,000×g for 20 minutes (Hitachi, CR22N, Japan), and the supernatant was collected. The precipitate underwent a secondary extraction under identical conditions. The supernatants from both extraction steps were combined, and the pH was adjusted to 4.5 with 0.1 M HCl. To separate the protein precipitated, an additional centrifugation was performed, and the supernatant was discarded. The precipitated protein was redispersed in distilled water, the pH was adjusted to 7, and the sample was subsequently frozen and lyophilized.

2.2.2 Preparation of oil-in-water emulsion stabilized by cowpea protein concentrate

Oil-in-water emulsion was formulated at pH 9, with a constant concentration of 0.6% of CPC (m/m emulsion) and 4% of sunflower oil (m/m emulsion). The concentration of the oil phase and the continuous phase, as well as the pH level, were determined based on preliminary experimentation aimed at identifying conditions for achieving greater stability to the emulsion. The emulsions were homogenized using an ultra-turrax (basic model T18, IKA, Brazil) operating at 15,000 rpm for 10 minutes.

2.2.3 Protein stock solution

CPC was dispersed in distilled water to obtain a stock solution with a concentration of 8% (m/m). The pH was adjusted to 11 using NaOH (40%), after which the mixture was heated in a thermostatic bath (Symmetrical, SI/6 Rings/18 L, Brazil) at 85 °C for 30 minutes (Moghadam et al., 2020). The solution was cooled to reach room temperature (25 °C) and then subjected to centrifugation (Hitachi, CR22N, Japan) at 4,000 rpm for 10 minutes to remove any insoluble particles.

2.2.4 Preparation of films incorporating emulsion

For the preparation of films with emulsion incorporation, the supernatant resulting from the centrifugation of the stock solution was collected. Subsequently, glycerol was added, and the pH was adjusted to 9. Later, the emulsion was mixed with the film-forming solution in calculated proportions. Thus, the resulting film-forming solution was composed of fixed concentrations of 5% CPC, 2% glycerol, and different emulsion concentrations (0; 0.2; 0.4; 0.6; 0.8; and 1.0%, m/m). The mixtures were homogenized using an ultra-turrax (basic model T18, IKA, Brazil), operating at 15,000 rpm for 10 minutes.

The film forming solution (approximately 100-120 g) was poured into Polytetrafluoroethylene-PTFE (Teflon®) molds (400 cm^2) and dried at 50 °C and 40% relative humidity for about 17 hours in a climate chamber (420-2TS, Ethik, Brazil). The formed films were removed from the molds and stored for at least one week before analysis, at room temperature and a relative humidity of 53%.

2.2.5 Characterization of edible films

2.2.5.1 Thickness measurement

The film thickness was measured using a digital micrometer (Mitutoyo, MDC-25SB, Japan) at 5 random positions on the film surface.

2.2.5.2 Moisture content

The total solid content of the films was assessed in triplicate employing a gravimetric approach at 70 °C within a vacuum oven (TE-395, Tecnal, Brazil) at 10 kPa until a constant weight was reached.

2.2.5.3 Scanning electron microscopy (SEM)

Scanning electron microscopy (SEM) was employed to evaluate the morphology of the lower and upper surfaces of the films, which were identified as exhibiting smooth and rough surfaces, respectively. Carbon tape was used to attach films to aluminum stubs after they had been kept for seven days in desiccators containing silica gel (25 °C). Then, using a scanning electron microscope (Carl Zeiss, EVO LS15, Germany) in low-pressure and high vacuum mode, the micrographs were captured at magnifications from 250 to 10000 ×.

2.2.5.4 X-ray diffraction

CPC and films were subjected to a wide-angle X-ray scattering (WAXS) investigation using a diffractometer (Rigaku, RINT 2000, Japan). The device used Cu Kα radiation with L = 1,542 Å and ran at a voltage of 50 kV and a current of 30 mA. At a sweep rate of 1° min^{-1}, diffractograms were generated at angles (2θ) ranging from 5° to 60°.

2.2.5.5 Fourier transform infrared spectroscopy (FTIR)

Fourier Transform Infrared Spectrometer (PerkinElmer - Spectrum Two, Waltham, MA), were employed for the infrared analyses. The measurements were conducted using an attenuated total reflectance (ATR) accessory with a diamond crystal, with a resolution of 4 cm^{-1}. The spectra of individual samples were obtained in the 400–4000 cm^{-1} range (Amado et al., 2023). The films were kept for seven days in desiccators with silica gel before analysis (25 °C).

2.2.5.6 Water vapor permeability (WVP)

The ASTM E96-95 gravimetric technique was used to evaluate the water vapor permeability of CPC films. This involved subjecting the films to controlled environments created by anhydrous calcium chloride, maintaining a relative humidity of 2%, and distilled water, maintaining a relative humidity of 100%. Through this setup, a moisture gradient was established, allowing each side of the film to be exposed to different relative humidity conditions. The apparatus was placed inside a BOD climate chamber (model BT 71, Biothec, Brazil) at a temperature of 25 °C for 8 hours. Throughout this period, the capsules were weighed at hourly intervals.

A linear function was applied to the experimental data of water mass variation over time, with the slope of the function representing the water vapor permeability rate, WVPR (g water s^{-1}). The WVPR values were obtained in triplicate. Subsequently, the water vapor permeability (WVP) was calculated using Equation 1 based on the determined WVPR values.

$$WVP = \frac{WVPR \cdot \delta}{\frac{A \cdot P_S \cdot (RH_1 - RH_2)}{100}} \quad (1)$$

in which WVP is water vapor permeability (g m^{-1} s^{-1} Pa^{-1}), WVPR is the water vapor permeability rate (g water s^{-1}), δ is the thickness of the films (m), *A* is the surface area exposed

(28.14×10^{-2} m^2), P_S is the saturation pressure of water vapor at 25 °C (3.169 Pa) and (RH_1-RH_2) is the difference in the relative humidity between the interior and exterior of the capsule.

2.2.5.7 Water solubility

Water solubility was determined according to the methodology described by Cuq et al. (1996). The films (2.0 cm x 2.0 cm) were dried in a vacuum oven (TE-395, Tecnal, Brazil) at 70 °C for 48 hours. Afterward, the samples were immersed in 50 mL of distilled water and placed in a BOD climate chamber (BT 71/ Biothec, Brazil) at room temperature (25 °C) for 24 hours. The specimens were withdrawn from the solution and subjected to further drying (70 °C) until reaching a constant weight. Solubility was then calculated as the ratio between the final dry mass and the initial mass using Equation 2:

$$S = \frac{(W_0 - W_f)}{W_0} \cdot 100 \quad (2)$$

in which W_0 is the initial dry weight (g); W_f is the final dry weight (g) and S is the water solubility (%, m/m).

2.2.5.8 Mechanical properties

Tensile strength and elongation at break of CPC films were measured as described by the ASTM D882-12 standard (ASTM, 2012). This analysis was conducted in a texturometer (TA.XT Plus, Stable Micro Systems, Surrey, UK), and a minimum of 8 samples from each formulation were subjected to testing. Rectangular samples (70 mm × 25 mm) were prepared and positioned between the probes, leaving an exposed area of 50 mm × 25 mm. The initial distance between the probes was set to 40 mm, with the speed during the tensile tests of 0.8 mm s^{-1}. The tensile strength (TS) (MPa) was determined by dividing the maximum force obtained by the original cross-sectional area of the sample (25 mm × sample average thickness). The percentage of elongation at break (EB) was calculated by the ratio between the increased length after breakage and its initial length (50 mm). Version 5.1.1.0 of the EXPONENT software was used to process the data.

2.2.5.9 Isotherms

The films (2.0 cm x 2.0 cm) were subjected to vacuum drying at 70 °C until reaching a constant weight to initiate the process with low moisture content and ensure the achievement

of an adsorption isotherm. The dried samples were stored in hermetically sealed jars containing the saline solution corresponding to the desired relative humidity (11.3%, 32.8%, 57.6%, 75.3%, 84.3%, and 90.3%) and were placed in BOD climate chambers (BT 71, Biothec, Brazil) at 25 °C.

The samples were subjected to periodic weighing until they reached equilibrium with the surrounding environment, which took approximately 30 days. Once equilibrium was reached, the total solid contents were analyzed. The results were fitted with the GAB model (Guggenheim, Anderson, and de Boer) utilizing Equation 3 (van den Berg & Bruin, 1981). The parameters of the model were estimated employing the least squares criterion, by the Levenberg-Marquardt algorithm (Marquardt, 1963).

$$X = \frac{X_m \cdot C \cdot K \cdot a_w}{(1 - K \cdot a_w) \cdot (1 - K \cdot a_w + C \cdot K \cdot a_w)} \tag{3}$$

in which C and K are constants, a_w is the water activity, X is the equilibrium moisture in dry base (kg water·kg dry sample^{-1}), and X_m is the monolayer moisture in dry base (kg water·kg dry sample^{-1}).

The fit efficiency was evaluated based on the adjusted coefficient of determination (R^2) and on the mean relative modulus, P, defined by Equation 4 (Lomauro et al., 1985).

$$P(\%) = \frac{100}{N} \sum_{1}^{N} \left| \frac{y^{exp} - y^{calc}}{y^{exp}} \right| \tag{4}$$

in which y^{calc} represents the calculated moisture in dry basis, y^{exp} is the experimental moisture in dry basis and N is the number of observations.

2.2.5.10 Optical properties: color, opacity and transmittance

Color (L*, a*, b*, C* and h) and opacity measurements were performed in a colorimeter (HunterLab, ColorFlex, United States) on four samples, each of which was subjected to readings at four different positions (0°, 90°, 270° and 370°). The total color difference (ΔE*) and yellowness index (YI) of samples were also calculated (Bodart et al., 2008; Pająk et al., 2019).

$$\Delta E^{*} = \sqrt{(L^{*} - L)^{2} + (a^{*} - a)^{2} + (b^{*} - b)^{2}} \quad (5)$$

$$YI = 142.86 \cdot b/L \quad (6)$$

where L*, a*, and b* are the standard color parameter values and 'L', 'a' and 'b' are the color parameter values of the sample.

Using a UV-VIS spectrophotometer (GENESYS 10S UV-VIS, Thermo Scientific, USA), the transmittance of the films was measured. Film samples (4.0 × 1.0 cm) were placed into the spectrophotometer cuvette and the spectra of individual samples were obtained in the wavelength range of visible light, from 200 to 800 nm (Silva et al., 2018).

2.2.5.11 Oxygen permeability (O_2P)

Oxygen permeability rates (O_2PR) were determined using the coulometric method with the procedure described in F 1927 (ASTM, 2014) and MOCON model 2/21 OXTRAN equipment operating with pure oxygen as the permeant gas. The assays were performed in duplicate at 23 °C and a relative humidity of 50 ± 4%. The effective permeation area of each specimen was 50 cm^2. The results were corrected for 101325 Pa of a partial oxygen pressure gradient between the two film surfaces. This gradient corresponds to the driving force required for oxygen to permeate through the film. Once the O_2PR was determined, the oxygen permeability coefficient (O_2P) was calculated from the permeability rate using Equation 7:

$$O_2P = \frac{O_2PR \cdot \delta}{p} \quad (7)$$

in which O_2P is the oxygen permeability (g m^{-1} s^{-1} Pa^{-1}), O_2PR is the oxygen permeability rate (g s^{-1}), δ is the mean thickness of the sample (m), and *p* is the partial oxygen pressure (101 325 Pa) in the diffusion cell-permeant gas chamber, as the partial O_2 pressure in the carrier gas chamber (N_2 + H_2) is considered zero.

2.2.6 Statistical analysis

An analysis of variance (ANOVA) and Tukey's test at a significance level of 5% were used to statistically analyze the data.

3 Results and discussion

3.1 Scanning electron microscopy (MEV)

Figure 6.1 (a-f) shows the smooth and rough surface of control and CPC-emulsion films. The smooth surface is the surface in contact with the Polytetrafluoroethylene - PTFE (Teflon®) mold, corresponding to the lower surface, and the rough surface is exposed to the drying air, corresponding to the upper surface.

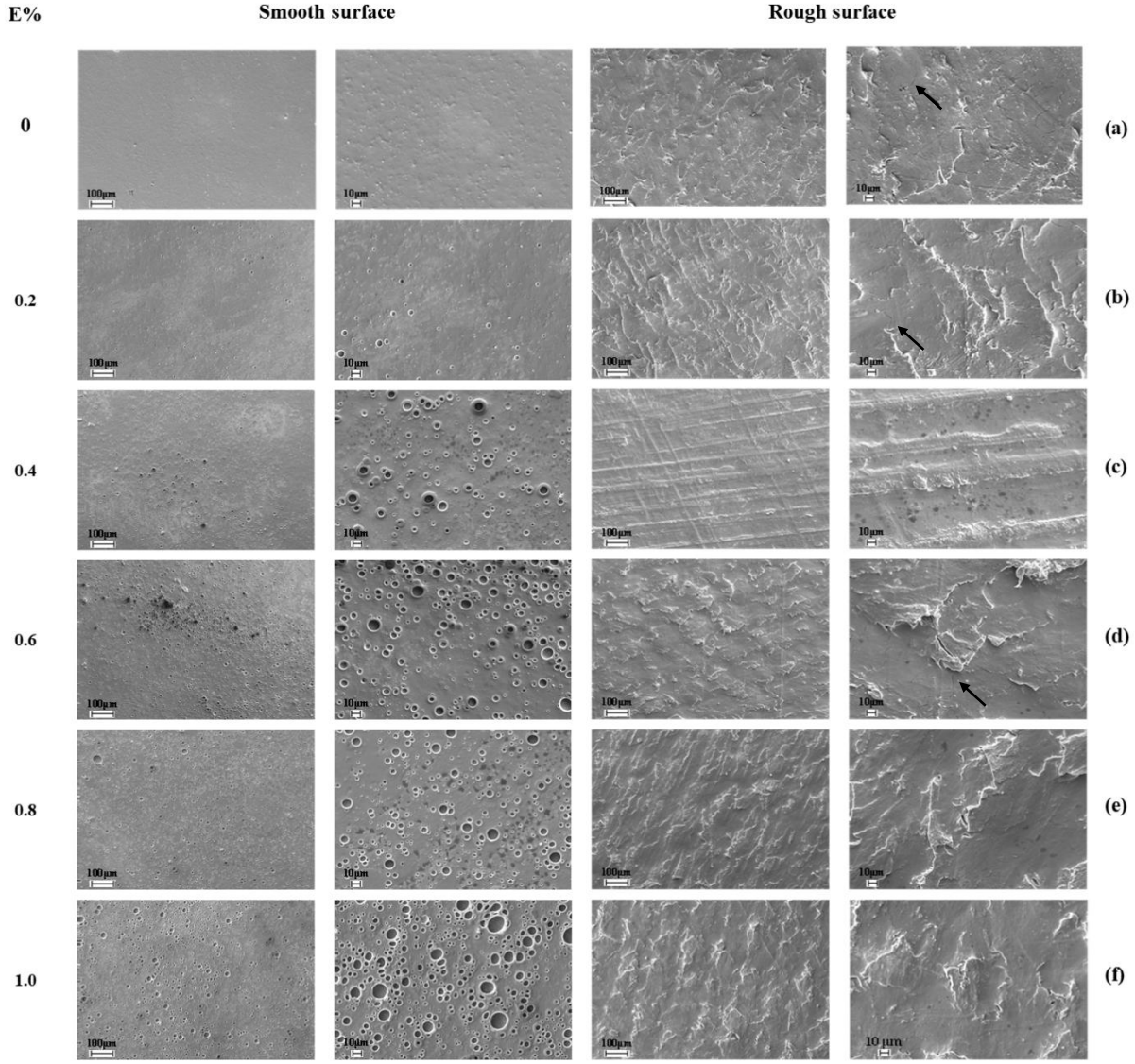
The images of the control film's smooth surface (Figure 6.1a) revealed a uniform appearance, though with the presence of sedimented particles and small pores, which became more noticeable upon increasing the magnification to 1000×. The upper surface of the control films revealed the presence of roughness and small cracks (1000×), as indicated by the arrow. The application of a drying air temperature of 50 °C, which exceeds the room temperature, as employed in the present study, results in a more rapid solvent evaporation, which may result in uneven drying across the film surface that can lead to the formation of fissures and cracks due to differential shrinkage and stress (Li et al., 2022; Tomar et al., 2020).

The addition of an emulsified component to the films induced meaningful changes in their microstructure, as evidenced in Figure 6.1, mainly in the smooth surface. Films formed with emulsion concentrations of 0.2% to 1% exhibit the presence of emulsion droplets distributed on the smooth surface. The droplets displayed a lack of uniformity in size and distribution; however, they demonstrated a tendency to increase in number and size with increasing emulsion concentration. In particular, in film formulations containing emulsion concentrations of 0.4% and 0.8% (magnification of 1000×), the small, darker areas, may indicate the presence of oil below the surface.

Unlike the images of the smooth side, the micrographs of the rough surface did not show the presence of the emulsion, since the spherical areas visible on the opposite side were not present. The structure shown was similar to the control film, with a rough surface, but more heterogeneous. Despite the absence of emulsion droplets, the darker areas observed on the smooth side remained on the rough surface. Moreover, cracks (arrows) were evident on nearly all films. In summary, the microstructure of the protein single film surface is smoother and seems more homogeneous compared to the CPC-emulsion films. Generally, the incorporation of hydrophobic components into edible films can lead to a coarser microstructure, resulting in

a less compact and more porous structure (Agudelo-Cuartas et al., 2020; Dammak & do Amaral Sobral, 2017; Dammak & Sobral, 2019). However, the absence of cracks in some emulsion films, particularly those formulated with an emulsion concentration of 1%, suggests that the emulsion may have contributed to an improvement in the cohesivity and flexibility of these films.

Figure Error! No text of specified style in document.**.32** Micrographs of the smooth and rough surface of control and CPC-emulsion films prepared at different emulsion concentrations at magnifications of 250× and 1000×

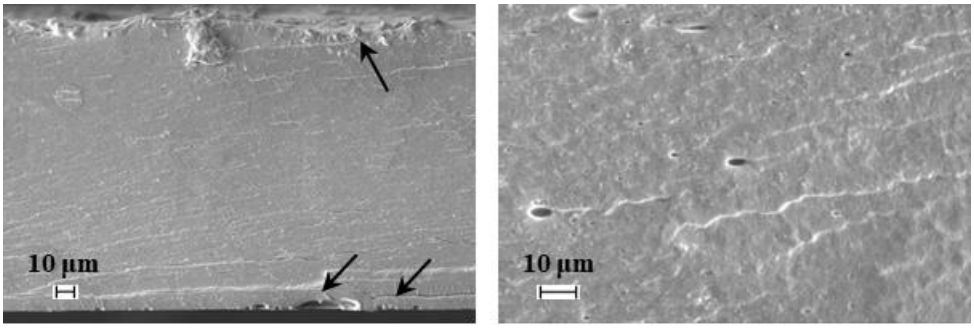


Source: elaborated by the author.

Figure 6.2a (magnification of 1000×) illustrates the upper (rough) and the lower (smooth) surfaces of the cross-sectional film obtained through the formulation with 1% emulsion. The arrows indicate an irregular upper surface in contact with the drying air and a

flat aspect of the lower surface in contact with the mold. Figure 6.2b (magnification of 10000×) depicts a limited number of oil droplets, which are smaller than those observed in Figure 6.1. The latter reached diameters exceeding 10 μm, indicating that the oil did not accumulate on the upper surface. This is contrary to expectations when phase separation occurs (Zhao et al., 2023a). Moreover, the visible and voluminous droplets at the lower surface appear to be the result of a localized coalescence of individual droplets due to the hydrophobic nature of the PTFE surface. It can be reasonable to suggest that the accumulation of oil droplets at the smooth surface is a consequence of the affinity of the oil phase with the solid surface of the mold.

Figure Error! No text of specified style in document.**.33** Micrographs of the cross section of the film formed with 1% emulsion concentration at magnifications of 1000× (a) and 10000× (b)



Source: elaborated by the author.

3.2 X-ray diffraction (XRD)

Figure 6.3 (a,b,c) shows the X-ray diffraction profiles of the raw material (CPC powder), and the CPC films prepared at different emulsion concentrations.

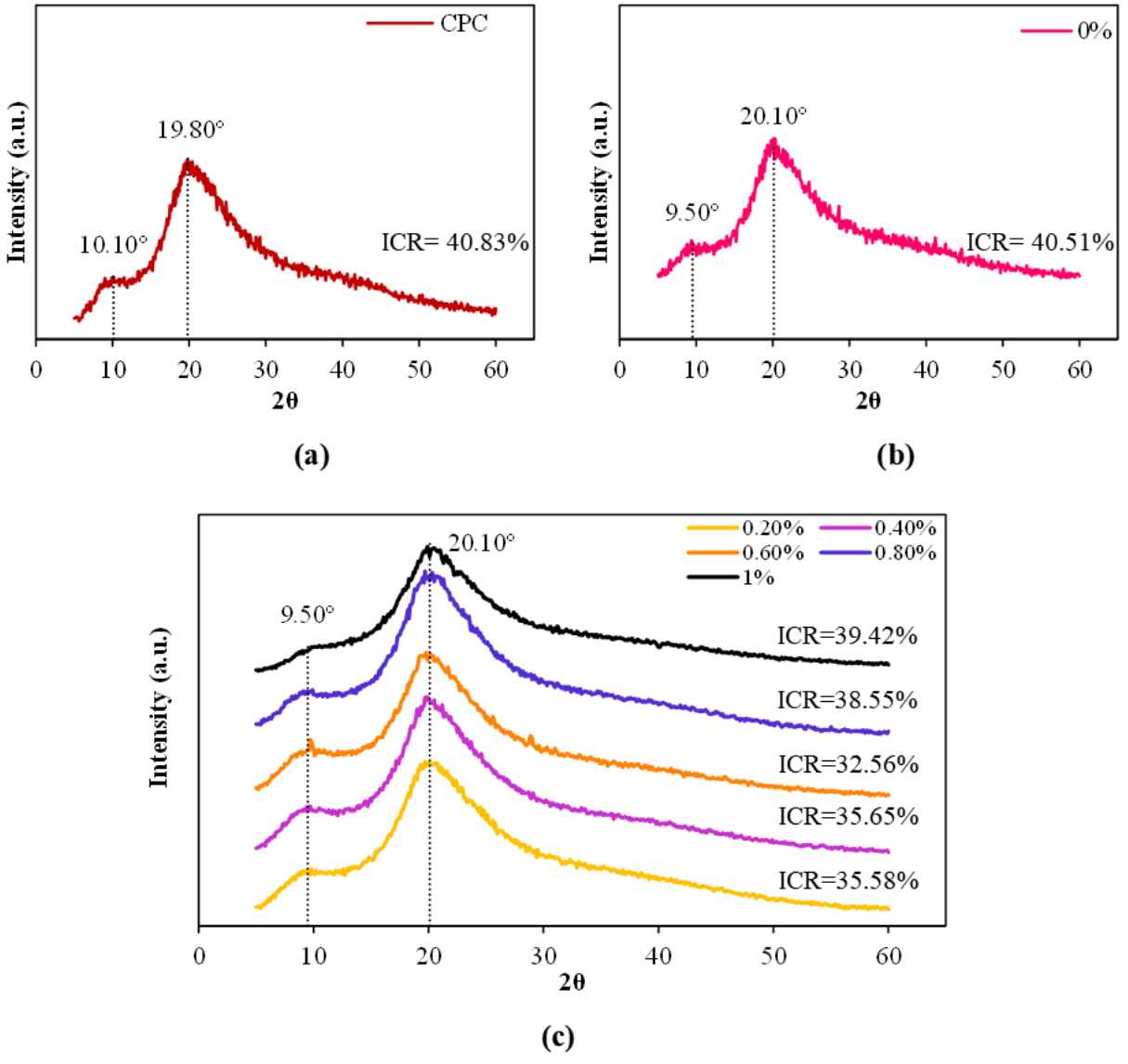
The X-ray spectrum obtained for both the raw material and the films exhibits characteristics of amorphous structures. The peaks observed at an angle of approximately 10° and 20° in the X-ray reflection pattern correspond, respectively, to the α-helix and β-sheet secondary structures of the protein (Oliveira et al., 2021; Chen et al., 2013). As anticipated, the films showed a diffraction pattern analogous to CPC powder, with a slight displacement of the principal peaks. In films prepared with the addition of 1% emulsion, it is observed that the shoulder around 10° almost disappears.

The relative crystallinity index (ICR) reveals that the films exhibit low crystallinity, with values ranging from 32.56% to 40.51%. The incorporation of emulsion at concentrations up to 0.6% significantly reduced the crystallinity of the film compared to the control sample,

evidenced by a decrease in ICR values from 40.51% to 32.56%. However, beyond this critical concentration, the crystallinity progressively increased, reaching an ICR of approximately 40% (1%), which ICR is statistically equivalent to the control film.

The combination of protein and the different emulsions amounts exhibits good compatibility, once the observed XRD pattern is analogous to the control films (Dammak et al., 2017b), exhibiting only slight variations in crystallinity. In the event of low compatibility, each component of the film would exhibit its own distinct crystalline region. Other authors have also reported great compatibility when incorporating a hydrophobic component into a biopolymeric matrix (Alexandre et al., 2016; Dammak et al., 2017a; Shen et al., 2021).

Figure Error! No text of specified style in document.**.34** XRD of (a) CPC powder, (b) control CPC films and (c) CPC-emulsion films prepared at different emulsion concentrations



Source: elaborated by the author.

3.3 Fourier-transform infrared (FTIR) spectroscopy

Figure 6.4 displays the infrared spectra of the films main components, including CPC (a), glycerol (b), and the emulsion (c) and the spectra of the films (d) prepared with varying concentrations of emulsion (0 – 1%).

The amide A region's band, located at 3279 cm^{-3} in the CPC spectrum (Figure 6.6a), may be related to the N-H bond's stretching mode (Stuart, 1997; Rozenberg & Shoham, 2007). The band at 2931 cm^{-1} indicates the asymmetrical C-H stretching absorption from aliphatic compounds corresponding to the CH_2 group (Stuart, 1997). The bands at 1637 and 1529 cm^{-1}, in conjunction with the band at 1244 cm^{-1}, are attributed to the amide I (C=O stretching), amide II (N-H bending) and amide III (C-N stretching vibration/N-H folding) bands, respectively (Garrido et al., 2016). Furthermore, bands at 1062 cm^{-1} indicate C-O bonds (Garrido et al., 2016; Sanches et al., 2021).

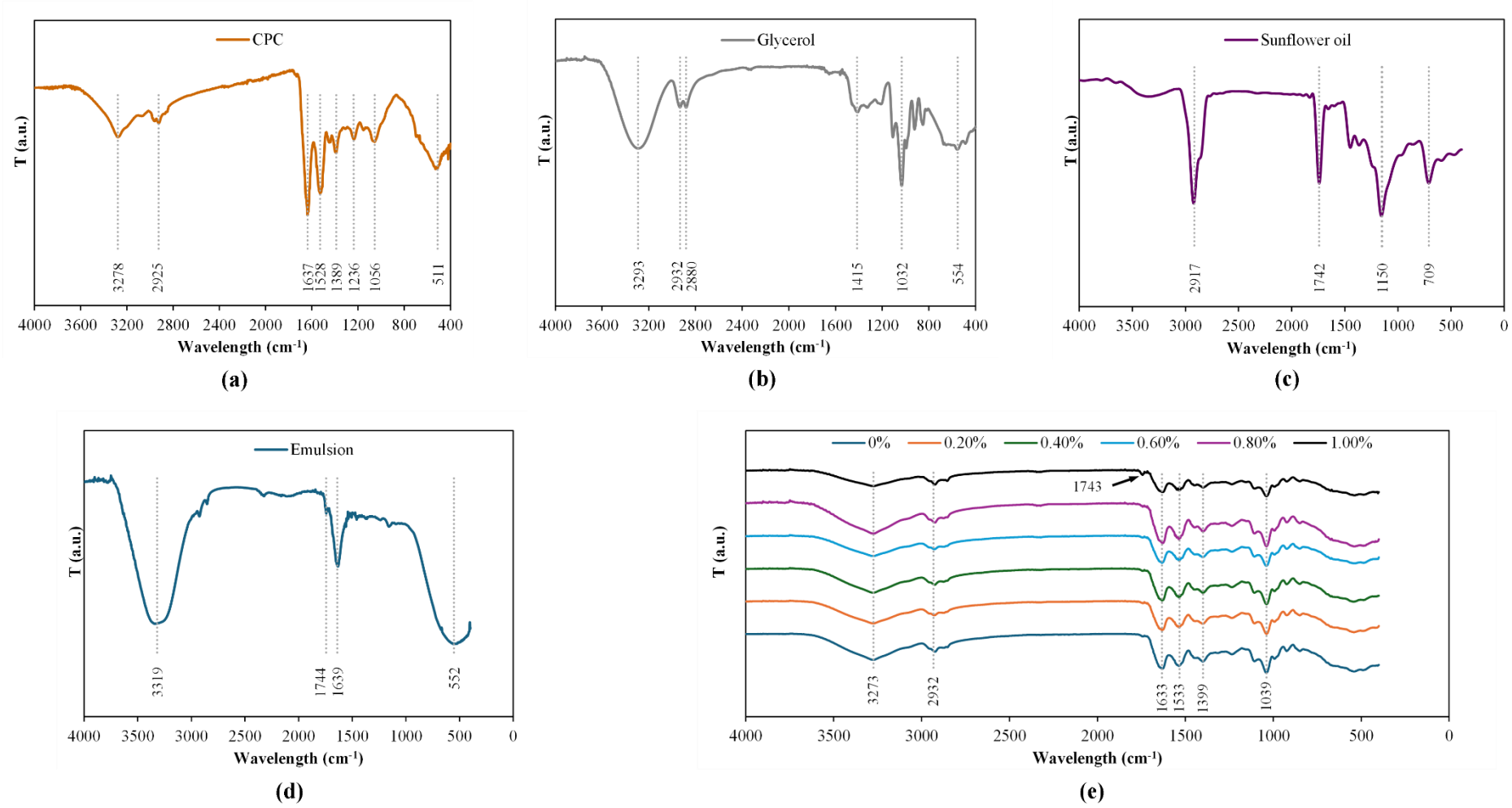
Glycerol (Figure 6.4b), employed as a plasticizer in the films, exhibited the main bands at 3293 cm^{-1}, 2932 cm^{-1}, and 1032 cm^{-1}, in addition to a potentially overlapping set in the range of approximately 1420 to 1220 cm^{-1}. The bands located between 3000 and 3700 cm^{-1}, are associated with OH stretching (Amado et al., 2023). The region at 1032 cm^{-1} and 1415 cm^{-1} were attributed to the stretching of the CO group in CH_2OH and, the range from 2880 to 2932 cm^{-1} can be attributed to the presence of symmetric and asymmetric stretching vibrations of CH_2 (Habuka et al., 2020).

The spectra of the control films and those with the emulsion addition (Figure 6.4e) show the presence of the main protein bands (Figure 6.4a) practically similar, with slight peak shifts and a reduced intensity. A peak corresponding to aldehyde (Stuart 1997) in the spectrum of sunflower oil (1743 cm^{-1}, Figure 6.4c), appears as a small peak in the spectrum of the emulsion (Figure 6.4d). A particularity observed in the films with and without emulsion incorporation is the presence of a band at 1039 cm^{-1}. This band is likely indicative of the effects of glycerol, given that this compound exhibits a particularly pronounced band at 1032 cm^{-1} (Figure 6.4b).

However, no novel bands or substantial alterations in existing bands were identified when the CPC-emulsion films were compared to the control samples, except by a very small band at 1743 cm^{-1} in the spectrum of the film with 1% emulsion (indicated with an arrow, Figure 6.4e). The findings suggest that the emulsion did not interact considerably with cowpea protein or subtle changes were not detectable due to the low oil concentrations (0.11% to 0.57%, g of oil per 100 g of dry matter). Furthermore, one potential explanation for the absence of

identifiable interactions is the presence of glycerol, which can result in spectral overlap, thereby masking potential interactions between the emulsion and the protein (Amado et al., 2023).

Figure Error! No text of specified style in document..**35** FTIR spectra of (a) CPC powder; (b) Glycerol; (c) emulsion (0.6% protein + 4% oil) and (d) CPC films prepared at different emulsion concentrations



Source: elaborated by the author.

3.4 Water vapor permeability (WVP) and water solubility (S)

The solubility and diffusion of molecules in the film matrix influence its permeability to water vapor (Oliveira et al., 2021). The hydrophilic nature of proteins can lead to the formation of films with less dense structures, leading to an increase in the free volume of the structure (Amado et al., 2020). This increase in free volume facilitates the movement of water molecules, resulting in greater permeability to water vapor. To address this limitation, incorporating a hydrophobic component into the films may reduce their WVP, primarily due to their enhanced hydrophobicity (Abdalla et al., 2023).

The WVP of the different CPC films was evaluated under a relative humidity gradient (ΔUR) of 100% – 2% (average UR=51%) and the results are shown in Table 6.1.

Table Error! No text of specified style in document.**.17** Water content (%), WVP (g m^{-1} s^{-1} Pa^{-1}), and water solubility (%) of CPC films prepared at different emulsion concentrations

% Emulsion	Water content (%)	WVP × 10^{10} (g m^{-1} s^{-1} Pa^{-1})	S (%)
0	13.47 ± 0.75 [a]	8.18 ± 2.06 [a]	41.43 ± 3.46 [a]
0.2	13.60 ± 0.67 [a]	8.96 ± 0.55 [a]	41.97 ± 3.96 [a]
0.4	13.86 ± 0.76 [a]	7.48 ± 0.91 [a]	39.25 ± 1.63 [a]
0.6	13.30 ± 0.62 [a]	8.48 ± 1.33 [a]	41.62 ± 2.26 [a]
0.8	13.20 ± 1.40 [a]	7.79 ± 0.74 [a]	43.60 ± 2.74 [a]
1	13.43 ± 0.82 [a]	7.54 ± 0.41 [a]	39.63 ± 1.46 [a]

Means ± SD are reported. Means with the same lowercase letter in the same column did not differ significantly at $p \leq 0.05$ according to Tukey's test.

The WVP of the films ranged from 7.54 to 8.96× 10^{-10} (g m^{-1} s^{-1} Pa^{-1}), however, the values are not statistically significant, as shown in Table 6.1.

Since water migration occurs through the hydrophilic fraction of a film and the continuous phase is predominantly composed of protein, with only minimal occupation by emulsion droplets, the lower emulsion concentrations could not significantly reduce the transfer rate (Alexandre et al., 2016). Consequently, under these conditions, permeability could not be increased or decreased as a result of incorporating a small number of hydrophobic particles.

A slight decreasing tendency could suggest that the emulsion would reduce the WVP at the highest emulsion proportions. This may be attributed to the fact that a certain lipid quantity would be sufficient to be distributed homogeneously within the protein network of the dried film matrix, thereby exerting a hindering effect on water transfer. According to Ma et al. (2021), this increases the tortuosity factor of the water diffusion path through the films, thereby decreasing the WVP. Although higher emulsion concentrations may have more significant

effects, it was observed during the film production process that concentrations greater than 1% resulted in an excess of emulsion, evidenced by the release of fat from the surface of the films following the drying process.

Previous studies have analyzed the impact of incorporating hydrophobic components on the water barrier properties of edible films and conflicting results have been presented. The addition of a lipid compound to films composed of soy protein (Galus, 2018), quinoa protein (Valenzuela et al., 2013), and whey protein (Amjadi et al., 2021) demonstrated a decrease in the WVP of these films. In contrast, no improvement in the water vapor barrier was observed in pea protein and gelatin films incorporated with essential oils (Cheng et al., 2024; Alexandre et al., 2016). Accordingly, the differences in water vapor transmission through films comprising hydrophobic constituents can be attributed to the lipid nature, concentration, and distribution of the lipid phase within the film (Kowalczyk et al., 2016; Galus, 2018).

Highly water-soluble edible films disintegrate easily in natural environments and are easily digested by humans. Conversely, films with low water solubility prevent moisture loss in foods. For products needing stability and resistance to moisture, like those with high water activity (a_w), water-insoluble films are essential. However, in applications like food additive encapsulation, films must dissolve readily for additive release during ingestion. Therefore, choosing an edible film balances moisture resistance and dissolution capacity, meeting specific food product requirements.

The integrity of the films analyzed was maintained for a minimum of 24 hours in water, indicating a highly stable protein network. The water solubility of the films (Table 6.1) exhibited a range of values between 39.25% and 43.60% (Table 6.1), with no statistically significant effect on solubility observed with the addition of the emulsified component. The increased replacement of water by oil droplets may result in a reduction of the hydrophilicity of protein films, which may lead to a decrease in soluble matter in the films (Dammak et al., 2017b). However, the extent of this reduction depends on the amount of hydrophobic compounds present.

In light of the observed intermediate solubility, there is a potential for these materials to be utilized in specific contexts. For instance, they could be employed as secondary packaging for items with a lower a_w, such as dried fruits and vegetables and powdered meals in general. Alternatively, they could be used as an edible coating to be dissolved in the mouth or in water, depending on the food preparation. Furthermore, they could also be utilized as a capsule wall material for substances of interest that need to dissolve during ingestion to release the

substances. However, it is essential to conduct further research to assess their potential applications.

3.5 Mechanical properties

The results of the mechanical analysis of the films formed at different emulsion concentrations are presented in Table 6.2. The CPC-control films showed values of tensile strength (TS) and elongation at break (EB) to be within the same order of magnitude of those reported for other plant protein sources, including soy protein isolate (SPI) films (Amado et al., 2020, 2023; Oliveira et al., 2021), mung beans (Moghadam et al., 2020), and faba beans (Rojas-Lema et al., 2021). As demonstrated in Table 6.2, the incorporation of the emulsion into the film-forming solutions resulted in a negligible influence on the film thickness, however, it did exert a discernible effect on the TS and EB parameters.

Table Error! No text of specified style in document.**.18** Tensile strength (MPa) and elongation at break (%) of CPC films prepared at different emulsion concentrations

Emulsion (%)	Thickness (mm)	Tensile strength (MPa)	Elongation at break (%)
0	0.16 ± 0.03 ^{a}	1.99 ± 0.37 ^{d}	175.90 ± 20.07 ^{b}
0.2	0.15 ± 0.01 ^{a}	2.96 ± 0.48 ^{ab}	331.28 ± 36.19 ^{a}
0.4	0.14 ± 0.02 ^{a}	2.53 ± 0.32 ^{bc}	276.22 ± 60.78 ^{a}
0.6	0.15 ± 0.02 ^{a}	3.16 ± 0.40 ^{a}	293.98 ± 58.03 ^{a}
0.8	0.14 ± 0.02 ^{a}	2.15 ± 0.25 ^{cd}	268.37 ± 54.09 ^{a}
1.0	0.14 ± 0.01 ^{a}	2.48 ± 0.20 ^{bc}	286.85 ± 29.95 ^{a}

Means ± SD are reported. Means with the same lowercase letter, in the same column, did not differ significantly at $p \leq 0.05$, according to Tukey's test.

The addition of emulsion at different concentrations generally increased the TS of the films compared to the control, with the highest TS of 3.16 MPa observed in the formulation containing 0.6% emulsion. However, apart from this formulation, samples with concentrations above 0.2% did not show significant changes in TS, except those with 0.8% that showed TS values comparable to the control. The presence of emulsion had a marked effect on EB in comparison to the control. However, the emulsion concentrations did not demonstrate any additional impact. The enhanced film flexibility upon emulsion incorporation suggests that this component exerts a plasticizing effect. The improvement in the mechanical properties of the films with the addition of emulsion, in comparison to the control (0% emulsion), can be attributed to the alterations observed in the SEM results (Figure 6.1). The SEM images revealed

that the incorporation of emulsion appeared to enhance the overall cohesion of the film matrix, as evidenced by the absence of cracks in films with higher emulsion concentrations.

It is anticipated that an increase in the concentration of the hydrophobic component will result in a greater disruption of the structural order within the film, leading to an increase in EB and a decrease in TS. This phenomenon has been observed with frequency in studies on protein-based films with the incorporation of lipid components (Cheng et al., 2024; Galus et al., 2020; Galus & Kadzińska, 2016a; Jusoh et al., 2022; Tao et al., 2022; Zhao et al., 2024). Although unexpected, the observed increase in TS and EB parameters in this study aligns with findings from previous research on protein-based films combined with hydrophobic components (Hopkins et al., 2015; Li et al., 2020; Ma et al., 2012). The low emulsion concentrations into the films in the present study may be within a safe and optimal range, where the benefits, such as the plasticizing effect, surpass the potential negative effects, such as the disruption of the material's structural order. In this context, the emulsion may have served as a "filler", filling the spaces between the protein chains and functioning as a reinforcing agent. Consequently, a more robust protein network may have been formed in the composite films, with the oily component uniformly entangled by the protein molecules (Wang et al., 2009).

The cited studies demonstrated that TS and EB are affected differently, which may be attributed to a number of factors. These factors primarily encompass the type and structure of the material, the concentration of the lipid phase, the size and distribution of the droplets, as well as the interaction and compatibility between the film components.

3.6 Sorption isotherm

Figure 6.5 shows the changes in equilibrium moisture content (X_{eq}) of CPC films prepared at different emulsion concentrations, as a function of water activity (a_w) at 25 °C.

According to the classification proposed by Brunauer et al. (1940), the curves corresponding to the films exhibit a behavior similar to Type II isotherms. This indicates that the material in question demonstrates low water absorption at low water activities, contrasting with higher absorption at higher water activities. This isotherm profile is characteristic of most protein-based materials, such as soy (Oliveira et al., 2021), pea (Kowalczyk & Baraniak, 2011), whey (Tavares et al., 2021), zein (Mouzakitis et al., 2022) and gelatin (Mohammadi Nafchi et al., 2014).

Figure 6.5 illustrates the proximity of X_{eq} values analyzed under low a_w conditions (0.11 – 0.32). At higher a_w (0.58 – 0.90), the greater the amount of emulsion, X_{eq} tends to reduce indicating that CPC-emulsion films exhibit a decreased water adsorption capacity under

intermediate to high humidity conditions. This is due to the more hydrophobic nature of emulsions due to the presence of sunflower oil, in contrast to the naturally hydrophilic nature of protein-based films. The addition of lipidic components occupies part of the film matrix that would normally absorb water, reducing the overall moisture retention capacity of the film (Galus & Kadzińska, 2016). Consequently, changes in the matrix's hydrophobicity due to lipid presence and potential interactions among film components can affect the overall water adsorption capacity (Soazo et al., 2011).

The GAB (Guggenheim-Anderson-de Boer) model was considered the most appropriate for describing the film's water adsorption isotherms given its advantage of having parameters with physical meaning. The model showed a good fit to the experimental data, with R^2 values greater than 0.993 and P values, representing the average relative modulus, of less than 10% (Table 6.3).

Table Error! No text of specified style in document.**.19** GAB model parameters of the CPC films prepared at different emulsion concentrations

Emulsion (%)	Xm (d.b.)	C	K	R^2	P%
0	0.098	4.615	0.981	0.996	1.06
0.2	0.096	4.731	0.978	0.996	1.04
0.4	0.094	5.712	0.984	0.993	1.31
0.6	0.101	4.638	0.964	0.994	1.02
0.8	0.080	13.000	0.996	0.999	0.55
1	0.071	11.875	1.019	0.998	0.80

The GAB model elucidates the mechanism of physical adsorption of water molecules in multiple layers on the sorbent surfaces of a material. According to this theory, the initial layer of water molecules exhibits a strong adherence to the material's surface, spreading uniformly and forming a densely bound monolayer. Subsequent layers of water molecules display a comparatively lower affinity for the material surface and are characterized by minimal interactions between them. Thus, the primary layer is the most robustly bound to the material, whereas the subsequent layers are less tightly and directly associated with the surface (Quirijns et al., 2005).

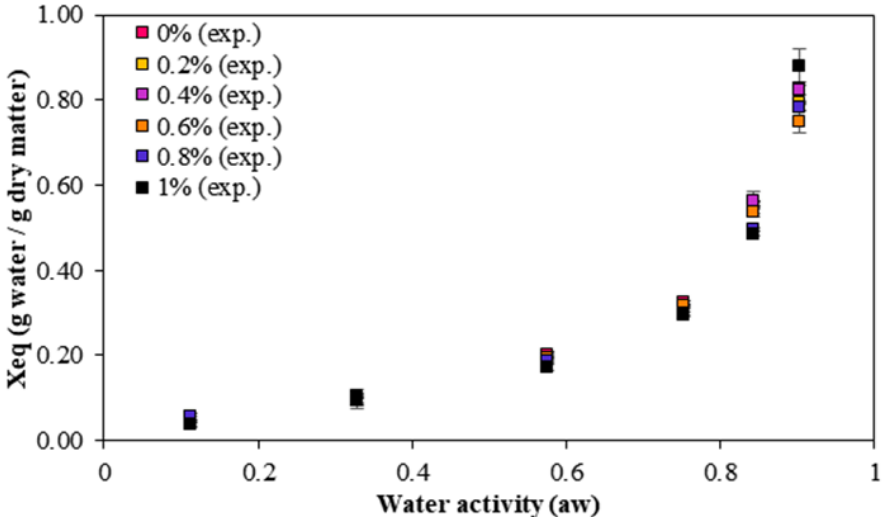
The parameters obtained for the GAB model used to describe the sorption isotherms are shown in Table 6.3. The water content of the monolayer (X_m) corresponds to the amount of water strongly adsorbed at primary adsorption sites (Kaya & Kahyaoglu, 2005; Sanches et al.,

2023). X_m values as a function of emulsion content ranged from 0.071 to 0.101, showing a more pronounced reduction at concentrations of 0.8% and 1%.

The constant C is related to the binding strength of monolayer water to the active sites of the matrix (Quirijns et al., 2005). The most expressive variations in the C values were observed in the formulations containing the highest emulsion concentrations (0.8 and 1.0%).

At lower emulsion concentrations (0–0.6%), the values of X_m and C appear to be independent of the concentration of the emulsion. Conversely, at higher concentrations (0.8 and 1.0%), although the monolayer adsorbs less water (lower X_m), the adsorbed water appears to be more strongly bound (higher C). CPC-emulsion films tend to exhibit greater hydrophobicity than the control or those with lower emulsion concentrations. This characteristic may result in a natural repulsion of water, leads to the water adsorbed in the film matrix being more strongly bound to resist this repulsion. Consequently, the energy required to maintain the water adsorbed in the film matrix will increase, which will be reflected in an increase in the C parameter.

Figure Error! No text of specified style in document.**.36** Sorption isotherms of CPC films prepared different emulsion concentrations



Source: elaborated by the author.

According to the GAB model, the values of K reflect the interactions between the adsorbent and water molecules in the multilayers. When K equals 1.0, the water molecules beyond the monolayer are not structured in multilayers and have properties similar to liquid water (Quirijns et al., 2005). In this study, the values of K were approximately 1.0 for all samples, particularly at formulations with 0.8% and 1% emulsion concentrations. This indicates that these isotherms tend to be reduced to the BET model. In the specific case of 1%

concentrations, K>1, which signifies that this constant lacks a physical meaning in the GAB equation (Lewicki, 1997). Indeed, the BET model was well fitted to this condition, with R2= 0.994, P% = 1.79%, Xm= 0.085, and C=4.065.

3.7 Optical properties

Table 6.4 presents the results of color and opacity analyses of the films.

In general, the clarity of the films decreased with the addition of the emulsion, with the film with the highest concentration being the darkest among the formulations. On the other hand, the parameter a*, representing the green (-) and red (+) components, increased significantly from the 0.6% emulsion concentration. With regard to the b* parameter, which indicates the blue (-) and yellow (+) components, the observed changes were more subtle, resulting in a color closer to yellow. This was particularly evident in the formulations containing 0.6% and 1.0% emulsion, which exhibited the highest b* values. Consequently, the outcomes of the a* and b* parameters indicate that the color of the films is approximate to red and yellow.

The data indicated that there was no clear pattern in the chroma values as the emulsion concentration increased. However, formulations containing 0.6% and 1.0% emulsion exhibited a significant increase in the C* value, indicating a higher degree of saturation. The remaining formulations exhibited C* values similar to those of the control.

The h values of the films varied between 79° and 84°, with an evident decrease at concentrations greater than 0.6% that remained unaffected up to 1%. The color of the samples is located in the yellow-red region, exhibiting a greater tendency towards yellow than red. In practical terms, the samples are predominantly yellow with a slight orange tone.

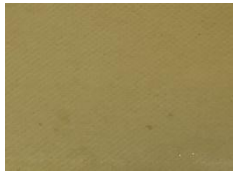
The yellowness index (YI) of the control films (YI ≈ 80.31) is classified as one of the lowest values among all the groups analyzed. A general trend of increasing yellowness is observed with the rise in emulsion concentration, which can be attributed to chemical reactions or interactions between the emulsion and other film components, resulting in intensified yellow coloration. The formulations containing 0.6% and 1.0% emulsion showed the highest YI values, indicating a significant increase in the yellowing of the films compared to the control.

The perception of color difference ΔE* varies according to the observed color and the sensitivity of the human eye, which can only distinguish color differences when ΔE* exceeds 1–3 (Bodart et al., 2008). Taking the control film (0% emulsion) as a reference, the formulations containing 0.2%, 0.4%, and 0.8% emulsion exhibit color changes that are barely perceptible to the human eye, as the ΔE* values do not exceed 1.77. In contrast, with ΔE* greater than 3, the

formulations with 0.6% and 1.0% emulsion indicate a noticeable and significant color difference, with the highest concentration showing a change easily detectable to the naked eye.

A higher opacity was identified in films with concentrations above 0.2% emulsion. In contrast, the control film exhibited significantly lower opacity values, suggesting greater transparency compared to those formed with the addition of a lipid component. These characteristics are complemented by the data derived from the transmittance analysis of CPC films across the wavelength spectrum of 200 to 800 nm (Figure 6.6), illustrating an inverse relationship between opacity and transmittance. The control film demonstrated higher transparency, indicating greater light transmission compared to the films with added emulsion. As the concentration of the lipid component increased, these films exhibited reduced light transmission through the film. On the other hand, at wavelengths between 200 and approximately 350 nm, all formulations exhibited near-zero transmittance, indicating excellent UV light barrier properties.

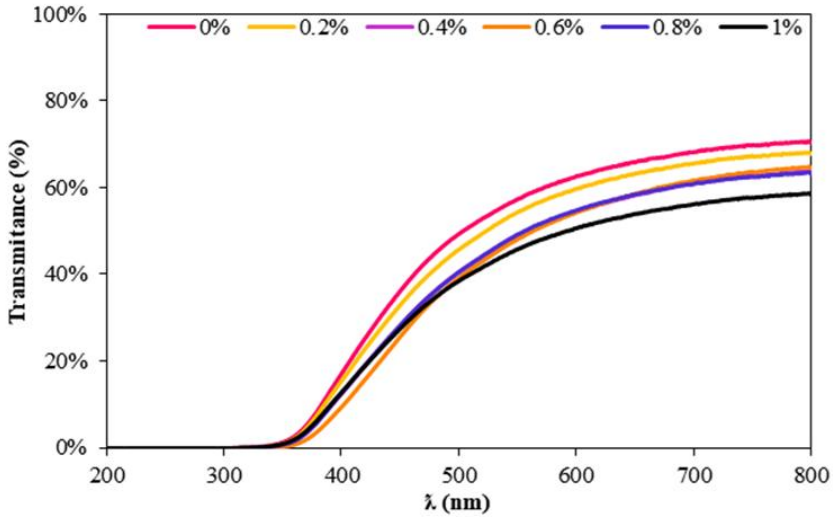
Table Error! No text of specified style in document..**20** Color parameters and opacity of CPC films prepared at different emulsion concentrations

E (%)	L*	a*	b*	C*	h	Opacity (%)	YI	ΔE	Visual aspect**
0	73.50 ± 1.33^{a}	4.76 ± 0.44^{c}	41.29 ± 1.27^{bc}	41.56 ± 1.31^{bc}	83.43 ± 0.44^{a}	8.78 ± 0.92^{b}	80.31 ± 3.87^{c,d}	-	
0.2	72.64 ± 1.15^{ab}	4.99 ± 0.43^{c}	42.61 ± 1.24^{b}	42.91 ± 1.25^{ab}	83.32 ± 0.53^{a}	8.77 ± 0.77^{b}	83.86 ± 3.48^{b,c}	1.60	
0.4	74.12 ± 2.82^{a}	4.36 ± 1.35^{c}	39.68 ± 4.13^{c}	39.93 ± 4.24^{c}	83.86 ± 1.43^{a}	9.76 ± 0.49^{a}	76.86 ± 10.52^{d}	1.77	
0.6	71.71 ± 2.52^{b}	6.33 ± 0.81^{b}	44.70 ± 2.01^{a}	45.15 ± 2.08^{a}	81.96 ± 0.78^{b}	10.11 ± 0.58^{a}	89.27 ± 6.79^{a,b}	4.16	
0.8	73.31 ± 2.24^{a}	6.02 ± 1.37^{b}	41.72 ± 3.22^{bc}	43.16 ± 3.37^{b}	81.87 ±1.23^{b}	9.79 ± 0.49^{a}	81.55 ± 8.70^{c,d}	1.35	
1.0	69.80 ± 1.25^{c}	8.64 ± 1.11^{a}	46.20 ± 2.40^{a}	47.00 ± 2.55^{a}	79.45 ± 0.88^{c}	10.27 ± 0.33^{a}	94.66 ± 6.37^{a}	7.27	

** Source: elaborated by the author. Mean ± SD are reported. Means with the same lowercase letter, in the same column, did not differ significantly at $p \leq 0.05$, according to Tukey's test.

The properties of color, opacity, and transmittance reflect structural changes induced by varying emulsion concentrations. Emulsion addition prompts protein chains to rearrange around droplets, affecting color and light transmission. These alterations are crucial for consumer acceptance and product performance, particularly in applications emphasizing aesthetics and sensory perception. Moreover, effective UV light blocking in food packaging is essential, as it prevents oxidation of polymers and light-sensitive materials, shielding them from degradation caused by sunlight and UV radiation (Zheng, Yu, & Pilla, 2017; Pascal et al., 1995).

Figure Error! No text of specified style in document.**.37** Transmittance of CPC-based films prepared at different emulsion concentrations



Source: elaborated by the author.

3.8 Oxygen permeability (O_2P)

Films can be employed as effective barriers to prevent the flow and exchange of oxygen in foods, thus preventing the negative effects caused by the surrounding environment, such as spoilage, changes in flavor, texture, and nutritional value. This functionality ensures the quality of food and underscores the significance of its application in the food industry.

Table 6.5 presents the oxygen permeability (O_2P) of the CPC films prepared at different emulsion concentrations. The control films exhibited an O_2P de 0.98×10^{-15} g m Pa^{-1} s^{-1} m^{-2}, a value consistent with that observed in protein-based films. This is due to the polar nature of these films, which results in low permeability to nonpolar substances, such as oxygen. The O_2P of films composed of other plant and animal protein sources has been found to range from 10^{-15} to 10^{-17} g m Pa^{-1} s^{-1} m^{-2} (Choi et al., 2023; Galus & Kadzińska, 2016; Oliveira et al., 2021; Porta et al., 2016).

Table Error! No text of specified style in document.**.21** Oxygen permeability of CPC films prepared at different emulsion concentrations

Emulsion (%)	$O_2P \times 10^{15}$ (g m Pa^{-1} s^{-1} m^{-2})
0	0.98 ± 0.02^{a}
0.2	0.96 ± 0.03^{a}
0.4	1.00 ± 0.01^{a}
0.6	0.95 ± 0.04^{a}
0.8	1.03 ± 0.01^{a}
1.0	0.62 ± 0.02^{b}

Means ± SD are reported. Means with the same lowercase letter in the same column did not differ significantly at $p \leq 0.05$ according to Tukey's test.

The incorporation of the emulsion into the films at concentrations up to 0.8% did not result in alterations in O_2P relative to the control films. However, a significant impact was observed in the films formulated with the highest emulsion concentration (1%), which exhibited a reduction in permeability greater than 36%. Crystallinity is commonly correlated with oxygen permeability, demonstrating an inverse relationship where an increase in crystallinity is associated with a reduction in O_2P (Miller and Krochta, 1997). In the present study, this relationship was observed as the amorphous characteristics of the films were altered by incorporating emulsion. Films containing 1% emulsion exhibited one of the highest crystallinities, likely contributing to a decrease in O_2P.

On the other hand, over the years, some studies have reported that the addition of a hydrophobic component to protein and/or polysaccharide-based films caused an increase in O_2P (Bertan et al., 2005; Galus & Kadzińska, 2016, 2019; Kowalczyk et al., 2016; Valenzuela et al., 2013). Hydrophobic compounds exhibit greater permeability to nonpolar substances such as oxygen due to their higher chemical affinity and solubility with nonpolar substances (Miller & Krochta, 1997). Consequently, the addition of lipids to hydrocolloid films can result in an increased oxygen permeability. Furthermore, authors observed that the incorporation of oil resulted in the formation of a heterogeneous film structure, which may have contributed to the formation of a less densely packed network (Bertan et al., 2005; Galus & Kadzińska, 2019). In this configuration, oxygen molecules permeate more easily, which results in greater oxygen permeability in films containing lipids (Galus & Kadzińska, 2019).

Therefore, it is possible to infer that the oxygen permeability through films with the addition of hydrophobic components is influenced by the incorporation form, type of lipid,

biopolymer and the interactions between the film components. Furthermore, the efficient incorporation of these components into a polymer matrix depends on the size and distribution of the oil phase particles; the smaller and more uniformly distributed they are, the greater the homogeneity and cohesion of the structure, potentially resulting in superior barrier properties (Li et al., 2023).

4 Conclusion

The CPC protein-based films revealed substantial transformations in their properties in response to the addition of varying emulsion concentrations.

The control films exhibited a more uniform surface microstructure, with sedimented particles and small pores visible under higher magnification. On the other hand, the incorporation of the emulsion resulted in an uneven distribution of emulsion droplets on the lower surface of the films that were in contact with the hydrophobic surface of the mold. A homogeneous aspect was observed throughout the films, and no oil accumulation was evident on the upper surface. Optically, CPC films had a predominantly yellow tone, and the incorporation of the emulsion led to a reduction in overall transparency and an increase in opacity, especially at concentrations above 0.2%.

The emulsion addition may have acted as a "filler", occupying the spaces between protein chains and serving as a reinforcing agent. Thereby, an increase in tensile strength (TS) and elongation at break (EB) was observed in the CPC-emulsion films, particularly for the formulation with 0.6% emulsion, which exhibited the highest resistance.

The barrier properties and solubility were not compromised by the incorporation of the hydrophobic component. On the contrary, there was a trend of decreasing these properties as the emulsion concentration increased in the film composition, reaching a significant decrease in oxygen permeability at the highest emulsion concentration (1%). This is compatible with a morphological aspect that is relatively cohesive, as well as a higher crystallinity index, as observed in this emulsion film condition. Considering that CPC is a relatively unexplored raw material in film production, this study successfully developed CPC films and demonstrated that the controlled emulsion addition can enhance their key properties. Emulsion incorporation improved flexibility for future modifications, considering allowing the addition of different lipids and bioactive compounds to impart antimicrobial and antioxidant properties and extending product shelf life. CPC-emulsion films meet diverse food packaging needs, promoting innovation and sustainability.

References

Abdalla, G., Mussagy, C. U., Sant'Ana Pegorin Brasil, G., Scontri, M., da Silva Sasaki, J. C., Su, Y., Bebber, C., Rocha, R. R., de Sousa Abreu, A. P., Goncalves, R. P., Burd, B. S., Pacheco, M. F., Romeira, K. M., Picheli, F. P., Guerra, N. B., Farhadi, N., Floriano, J. F., Forster, S., He, S., Herculano, R. D. (2023). Eco-sustainable coatings based on chitosan, pectin, and lemon essential oil nanoemulsion and their effect on strawberry preservation. *International Journal of Biological Macromolecules*, *249*. https://doi.org/10.1016/j.ijbiomac.2023.126016

Agudelo-Cuartas, C., Granda-Restrepo, D., Sobral, P. J. A., Hernandez, H., & Castro, W. (2020). Characterization of whey protein-based films incorporated with natamycin and nanoemulsion of α-tocopherol. *Heliyon*, *6*(4). https://doi.org/10.1016/j.heliyon.2020.e03809

Alexandre, E. M. C., Lourenço, R. V., Bittante, A. M. Q. B., Moraes, I. C. F., & Sobral, P. J. do A. (2016). Gelatin-based films reinforced with montmorillonite and activated with nanoemulsion of ginger essential oil for food packaging applications. *Food Packaging and Shelf Life*, *10*, 87–96. https://doi.org/10.1016/j.fpsl.2016.10.004

Almeida, F. C., de Souza, C. O., Philadelpho, B. O., França Lemos, P. V., Cardoso, L. G., Santana, J. S., Alves da Silva, J. B., Cruz Correia, P. R., Camilloto, G. P., de Souza Ferreira, E., & Druzian, J. I. (2021). Combined effect of cassava starch nanoparticles and protein isolate in properties of starch-based nanocomposite films. *Journal of Applied Polymer Science*, *138*(18). https://doi.org/10.1002/app.50008

Amado, L. R., de Souza Silva, K., & Mauro, M. A. (2023). Alginate and pH Improve Properties of Soy Protein-based Films. *Food Biophysics*. https://doi.org/10.1007/s11483-023-09823-5

Amado, L. R., Silva, K. de S., & Mauro, M. A. (2020). Effects of interactions between soy protein isolate and pectin on properties of soy protein-based films. *Journal of Applied Polymer Science*, *137*(21). https://doi.org/10.1002/app.48732

Amjadi, S., Almasi, H., Ghadertaj, A., & Mehryar, L. (2021). Whey protein isolate-based films incorporated with nanoemulsions of orange peel (*Citrus sinensis*) essential oil: Preparation and characterization. *Journal of Food Processing and Preservation*, *45*(2). https://doi.org/10.1111/jfpp.15196

ASTM INTERNATIONAL. ASTM D882-12, Standard Test Method for Tensile Properties of Thin Plastic Sheeting, West Conshohocken, PA, 2012.

ASTM INTERNATIONAL. ASTM E96-95: Standard test methods of water vapor transmission of materials. In: Annual Book of ASTM Standards, American Society for Testing and Materials, Philadelphia, 1995.

ASTM INTERNATIONAL. ASTM F 1927-14: Standard test method for determination of oxygen gas transmission rate, permeability and permeance at controlled relative humidity through barrier materials using a coulometric detector. Philadelphia, 2014.

Bertan, L. C., Tanada-Palmu, P. S., Siani, A. C., & Grosso, C. R. F. (2005). Effect of fatty acids and "Brazilian elemi" on composite films based on gelatin. *Food Hydrocolloids*, *19*(1), 73–82. https://doi.org/10.1016/j.foodhyd.2004.04.017

Bodart, M., de Peñaranda, R., Deneyer, A., & Flamant, G. (2008). Photometry and colorimetry characterisation of materials in daylighting evaluation tools. *Building and Environment*, *43*(12), 2046-2058. https://doi.org/10.1016/j.buildenv.2007.12.006

Brunauer, S., Deming, L. S., Deming, W. E., & Teller, E. (1940). On a theory of the van der Waals adsorption of gases. *Journal of the American Chemical society*, *62*(7), 1723-1732

Chen, J., Chen, X., Zhu, Q., Chen, F., Zhao, X., & Ao, Q. (2013). Determination of the domain structure of the 7S and 11S globulins from soy proteins by XRD and FTIR. *Journal of the Science of Food and Agriculture*, *93*(7), 1687-1691.

Cheng, J., Velez, F. J., Singh, P., & Cui, L. (2024). Fabrication, characterization, and application of pea protein-based edible film enhanced by oregano essential oil (OEO) micro- or nano-emulsion. *Current Research in Food Science*, *8*. https://doi.org/10.1016/j.crfs.2024.100705

Choi, J., Lee, J. S., Han, J., & Chang, Y. (2023). Development of gelatin–sodium caseinate high-oxygen-barrier film containing elderberry (*Sambucus nigra L.*) extract and its antioxidant capacity on pork. *Food Bioscience*, *53*. https://doi.org/10.1016/j.fbio.2023.102617

Cuq, B., Gontard, N., CUQ, J. L., & Guilbert, S. (1996). Functional properties of myofibrillar protein-based biopackaging as affected by film thickness. *Journal of Food Science*, *61*(3), 580-584.

Dammak, I., & do Amaral Sobral, P. J. (2017). Formulation and Stability Characterization of Rutin-Loaded Oil-in-Water Emulsions. *Food and Bioprocess Technology*, *10*(5), 926–939. https://doi.org/10.1007/s11947-017-1876-5

Dammak, I., & Sobral, P. J. do A. (2019). Active gelatin films incorporated with eugenol nanoemulsions: effect of emulsifier type on films properties. *International Journal of Food Science and Technology*, *54*(9), 2725–2735. https://doi.org/10.1111/ijfs.14183

Dammak, I., Bittante, A. M. Q. B., Lourenço, R. V., & do Amaral Sobral, P. J. (2017a). Properties of gelatin-based films incorporated with chitosan-coated microparticles charged with rutin. *International Journal of Biological Macromolecules*, *101*, 643–652. https://doi.org/10.1016/j.ijbiomac.2017.03.163

Dammak, I., de Carvalho, R. A., Trindade, C. S. F., Lourenço, R. V., & do Amaral Sobral, P. J. (2017b). Properties of active gelatin films incorporated with rutin-loaded nanoemulsions. *International Journal of Biological Macromolecules*, *98*, 39–49. https://doi.org/10.1016/j.ijbiomac.2017.01.094

Galus, S. (2018). Functional properties of soy protein isolate edible films as affected by rapeseed oil concentration. *Food Hydrocolloids*, *85*, 233–241. https://doi.org/10.1016/j.foodhyd.2018.07.026

Galus, S., & Kadzińska, J. (2016). Whey protein edible films modified with almond and walnut oils. *Food Hydrocolloids*, *52*, 78–86. https://doi.org/10.1016/j.foodhyd.2015.06.013

Galus, S., & Kadzińska, J. (2019). Gas barrier and wetting properties of whey protein isolate-based emulsion films. *Polymer Engineering and Science*, *59*, E375–E383. https://doi.org/10.1002/pen.24992

Galus, S., Gaouditz, M., Kowalska, H., & Debeaufort, F. (2020). Effects of candelilla and carnauba wax incorporation on the functional properties of edible sodium caseinate films. *International Journal of Molecular Sciences*, *21*(24), 1–19. https://doi.org/10.3390/ijms21249349

Garrido, T., Etxabide, A., Guerrero, P., & De La Caba, K. (2016). Characterization of agar/soy protein biocomposite films: Effect of agar on the extruded pellets and compression moulded films. *Carbohydrate Polymers*, *151*, 408–416. https://doi.org/10.1016/j.carbpol.2016.05.089

Garrido-López, Á., & Tena, M. T. (2010). Study of multilayer packaging delamination mechanisms using different surface analysis techniques. *Applied Surface Science*, *256*(12), 3799–3805. https://doi.org/10.1016/J.APSUSC.2010.01.029

Gómez, A., Gay, C., Tironi, V., & Avanza, M. V. (2021). Structural and antioxidant properties of cowpea protein hydrolysates. *Food Bioscience*, *41*. https://doi.org/10.1016/j.fbio.2021.101074

Habuka, A., Yamada, T., & Nakashima, S. (2020). Interactions of glycerol, diglycerol, and water studied using attenuated total reflection infrared spectroscopy. *Applied Spectroscopy*, *74*(7), 767-779.

Han, J. H. (2014). Edible Films and Coatings: A Review. *Innovations in Food Packaging: Second Edition*, 213–255. https://doi.org/10.1016/B978-0-12-394601-0.00009-6

Hewage, S., & Vithanarachchi, S. M. (2009). Biodegradable polymer films from cowpea protein isolate Preparation and characterization of biodegradable polymer films from cowpea (*Vigna unguiculata*) protein isolate. *Journal of the National Science Foundation of Sri Lanka, 37(1)*, 53-57.

Hopkins, E. J., Chang, C., Lam, R. S. H., & Nickerson, M. T. (2015). Effects of flaxseed oil concentration on the performance of a soy protein isolate-based emulsion-type film. *Food Research International*, *67*, 418–425. https://doi.org/10.1016/j.foodres.2014.11.040

Jusoh, N. A. M., Isa, M. I. N., & Sarbon, N. M. (2022). Physical, mechanical and antioxidant properties of chicken skin gelatin films incorporated with virgin coconut oil. *Biocatalysis and Agricultural Biotechnology*, *45*. https://doi.org/10.1016/j.bcab.2022.102525

Kaya, S., & Kahyaoglu, T. (2005). Thermodynamic properties and sorption equilibrium of pestil (grape leather). *Journal of Food Engineering*, *71*(2), 200–207. https://doi.org/10.1016/J.JFOODENG.2004.10.034

Kowalczyk, D., & Baraniak, B. (2011). Effects of plasticizers, pH and heating of film-forming solution on the properties of pea protein isolate films. *Journal of Food Engineering*, *105*(2), 295–305. https://doi.org/10.1016/j.jfoodeng.2011.02.037

Kowalczyk, D., Gustaw, W., Zieba, E., Lisiecki, S., Stadnik, J., & Baraniak, B. (2016). Microstructure and functional properties of sorbitol-plasticized pea protein isolate emulsion

films: Effect of lipid type and concentration. *Food Hydrocolloids*, *60*, 353–363. https://doi.org/10.1016/j.foodhyd.2016.04.006

La Fuente Arias, C. I., Kubo, M. T. K. neiwa, Tadini, C. C., & Augusto, P. E. D. (2023). Bio-based multilayer films: A review of the principal methods of production and challenges. In *Critical Reviews in Food Science and Nutrition* (Vol. 63, Issue 14, pp. 2260–2276). Taylor and Francis Ltd. https://doi.org/10.1080/10408398.2021.1973955

Li, C., Pei, J., Xiong, X., & Xue, F. (2020). Encapsulation of grapefruit essential oil in emulsion-based edible film prepared by plum (Pruni domesticae semen) seed protein isolate and gum acacia conjugates. *Coatings*, *10*(8). https://doi.org/10.3390/COATINGS10080784

Li, J., Krishna B, A., van Ewijk, G., van Dijken, D. J., de Vos, W. M., & van der Gucht, J. (2022). A comparison of complexation induced brittleness in PEI/PSS and PEI/NaPSS single-step coatings. *Colloids and Surfaces A: Physicochemical and Engineering Aspects*, *648*. https://doi.org/10.1016/j.colsurfa.2022.129143

Li, X. L., Shen, Y., Hu, F., Zhang, X. X., Thakur, K., Rengasamy, K. R., ... & Wei, Z. J. (2023). Fortification of polysaccharide-based packaging films and coatings with essential oils: A review of their preparation and use in meat preservation. *International Journal of Biological Macromolecules*, *242*, 124767.

Lomauro, C. J., Bakshi, A. S., & Labuza, T. P. (1985). Evaluation of food moisture sorption isotherm equations. Part I: Fruit, vegetable and meat products. *Lebensmittel-Wissenschaft und Technologie-LWT*, 18(2), 111-117.

Loushigam, G., & Shanmugam, A. (2023). Modifications to functional and biological properties of proteins of cowpea pulse crop by ultrasound-assisted extraction. *Ultrasonics Sonochemistry*, *97*. https://doi.org/10.1016/j.ultsonch.2023.106448

Ma, W., Tang, C. H., Yin, S. W., Yang, X. Q., Wang, Q., Liu, F., & Wei, Z. H. (2012). Characterization of gelatin-based edible films incorporated with olive oil. *Food Research International*, *49*(1), 572–579. https://doi.org/10.1016/j.foodres.2012.07.037

Ma, W., Tang, C. H., Yin, S. W., Yang, X. Q., Wang, Q., Liu, F., & Wei, Z. H. (2012). Characterization of gelatin-based edible films incorporated with olive oil. *Food Research International*, *49*(1), 572-579.

Marquardt, D. W. (1963). An algorithm for least-squares estimation of nonlinear parameters. *Journal of the society for Industrial and Applied Mathematics*, *11*(2), 431-441.

Moghadam, M., Salami, M., Mohammadian, M., Khodadadi, M., & Emam-Djomeh, Z. (2020). Development of antioxidant edible films based on mung bean protein enriched with pomegranate peel. *Food Hydrocolloids*, *104*. https://doi.org/10.1016/j.foodhyd.2020.105735

Mohammadi Nafchi, A., Moradpour, M., Saeidi, M., & Alias, A. K. (2014). Effects of nanorod-rich ZnO on rheological, sorption isotherm, and physicochemical properties of bovine gelatin films. *LWT - Food Science and Technology*, *58*(1), 142–149. https://doi.org/10.1016/J.LWT.2014.03.007

Mouzakitis, C. K., Sereti, V., Matsakidou, A., Kotsiou, K., Biliaderis, C. G., & Lazaridou, A. (2022). Physicochemical properties of zein-based edible films and coatings for extending wheat

bread shelf life. *Food Hydrocolloids*, *132*, 107856. https://doi.org/10.1016/J.FOODHYD.2022.107856

Oliveira, M. M. G., Fessori, A. G. B. W., Huamaní-Meléndez, V. J., & Mauro, M. A. (2024). Exploring the rheological and thermal behavior of cowpea protein concentrate: Impact of pH and concentration. *Colloids and Surfaces A: Physicochemical and Engineering Aspects*, *694*. https://doi.org/10.1016/j.colsurfa.2024.134106

Oliveira, M. M. G., Silva, S. K., & Mauro, M. A. (2021). Evaluation of interactions between carboxymethylcellulose and soy protein isolate and their effects on the preparation and characterization of composite edible films. *Food Biophysics*, *16*(2), 214-228. https://doi.org/10.1007/s11483-020-09659-3

Paglione, I. S., Galindo, M. V., de Medeiros, J. A. S., Yamashita, F., Alvim, I. D., Grosso, C. R. F., ... & Shirai, M. A. (2019). Comparative study of the properties of soy protein concentrate films containing free and encapsulated oregano essential oil. *Food Packaging and Shelf Life*, *22*, 100419.

Pająk, P., Przetaczek-Rożnowska, I., & Juszczak, L. (2019). Development and physicochemical, thermal and mechanical properties of edible films based on pumpkin, lentil and quinoa starches. *International Journal of Biological Macromolecules*, *138*, 441-449.

Porta, R., Di Pierro, P., Sabbah, M., Regalado-Gonzales, C., Mariniello, L., Kadivar, M., & Arabestani, A. (2016). Blend films of pectin and bitter vetch (Vicia ervilia) proteins: Properties and effect of transglutaminase. *Innovative Food Science and Emerging Technologies*, *36*, 245–251. https://doi.org/10.1016/j.ifset.2016.07.001

Quirijns, E. J., Van Boxtel, A. J. B., Van Loon, W. K. P., & Van Straten, G. (2005). Sorption isotherms, GAB parameters and isosteric heat of sorption. *Journal of the Science of Food and Agriculture*, *85*(11), 1805–1814. https://doi.org/10.1002/jsfa.2140

Ribeiro Sanches, M. A., Camelo-Silva, C., Tussolini, L., Tussolini, M., Zambiazi, R. C., & Becker Pertuzatti, P. (2021). Development, characterization and optimization of biopolymers films based on starch and flour from jabuticaba (Myrciaria cauliflora) peel. *Food Chemistry*, *343*. https://doi.org/10.1016/j.foodchem.2020.128430

Rojas-Lema, S., Nilsson, K., Trifol, J., Langton, M., Gomez-Caturla, J., Balart, R., Garcia-Garcia, D., & Moriana, R. (2021). "Faba bean protein films reinforced with cellulose nanocrystals as edible food packaging material." *Food Hydrocolloids*, *121*. https://doi.org/10.1016/j.foodhyd.2021.107019

Rozenberg, M., Shoham, G. (2007). FTIR spectra of solid poly-L-lysine in the stretching NH mode range. *Biophysical Chemistry*, *125*, 166–171. https://doi.org/10.1016/j.bpc.2006.07.008

Sanches, M. A. R., Augusto, P. E. D., Polachini, T. C., & Telis-Romero, J. (2023). Water sorption properties of brewer's spent grain: A study aimed at its stabilization for further conversion into value-added products. *Biomass and Bioenergy*, *170*. https://doi.org/10.1016/j.biombioe.2023.106718

Shen, Y., Ni, Z. J., Thakur, K., Zhang, J. G., Hu, F., & Wei, Z. J. (2021). Preparation and characterization of clove essential oil loaded nanoemulsion and pickering emulsion activated

pullulan-gelatin based edible film. *International Journal of Biological Macromolecules*, *181*, 528–539. https://doi.org/10.1016/j.ijbiomac.2021.03.133

Silva, K. S., Fonseca, T. M. R., Amado, L. R., & Mauro, M. A. (2018). Physicochemical and microstructural properties of whey protein isolate-based films with addition of pectin. *Food Packaging and Shelf Life*, *16*, 122–128. https://doi.org/10.1016/j.fpsl.2018.03.005

Soazo, M., Rubiolo, A. C., & Verdini, R. A. (2011). Effect of drying temperature and beeswax content on moisture isotherms of whey protein emulsion film. *Procedia Food Science*, *1*, 210–215. https://doi.org/10.1016/j.profoo.2011.09.033

Stuart, B. H. (1997). *Biological applications of infrared spectroscopy*. John Wiley & Sons.

Tao, R., Sedman, J., & Ismail, A. (2022). Characterization and in vitro antimicrobial study of soy protein isolate films incorporating carvacrol. *Food Hydrocolloids*, *122*. https://doi.org/10.1016/j.foodhyd.2021.107091

Tavares, L., Souza, H. K. S., Gonçalves, M. P., & Rocha, C. M. R. (2021). Physicochemical and microstructural properties of composite edible film obtained by complex coacervation between chitosan and whey protein isolate. *Food Hydrocolloids*, *113*, 106471. https://doi.org/10.1016/J.FOODHYD.2020.106471

Tomar, B. S., Shahin, A., & Tirumkudulu, M. S. (2020). Cracking in drying films of polymer solutions. *Soft Matter*, *16*(14), 3476–3484. https://doi.org/10.1039/c9sm02294e

Valenzuela, C., Abugoch, L., & Tapia, C. (2013). Quinoa protein-chitosan-sunflower oil edible film: Mechanical, barrier and structural properties. *LWT*, *50*(2), 531–537. https://doi.org/10.1016/j.lwt.2012.08.010

van den Berg, C., & Bruin, S. (1981). WATER ACTIVITY AND ITS ESTIMATION IN FOOD SYSTEMS: THEORETICAL ASPECTS. *Water Activity: Influences on Food Quality*, 1–61. https://doi.org/10.1016/B978-0-12-591350-8.50007-3

Vanderroost, M., Ragaert, P., Devlieghere, F., & De Meulenaer, B. (2014). Intelligent food packaging: The next generation. In *Trends in Food Science and Technology* (Vol. 39, Issue 1, pp. 47–62). Elsevier Ltd. https://doi.org/10.1016/j.tifs.2014.06.009

Wang, L., Auty, M. A. E., Rau, A., Kerry, J. F., & Kerry, J. P. (2009). Effect of pH and addition of corn oil on the properties of gelatin-based biopolymer films. *Journal of Food Engineering*, *90*(1), 11–19. https://doi.org/10.1016/j.jfoodeng.2008.04.030

Zhang, X., Liu, D., Jin, T. Z., Chen, W., He, Q., Zou, Z., Zhao, H., Ye, X., & Guo, M. (2021). Preparation and characterization of gellan gum-chitosan polyelectrolyte complex films with the incorporation of thyme essential oil nanoemulsion. *Food Hydrocolloids*, *114*. https://doi.org/10.1016/j.foodhyd.2020.106570

Zhao, Y., Ren, Z., Shi, L., & Weng, W. (2023a). Effect of W/O pre-emulsion prepared with different emulsifiers on the physicochemical properties of soy protein isolate-based emulsion films. *Food Hydrocolloids*, *139*. https://doi.org/10.1016/j.foodhyd.2022.108440

Zhao, Y., Ren, Z., Shi, L., Zhang, Y., & Weng, W. (2023b). Effects of pre-emulsion prepared using sucrose esters with different hydrophile-lipophile balances on characteristics of soy

protein isolate emulsion films. *Food Research International*, *165*. https://doi.org/10.1016/j.foodres.2023.112542

Zhao, Y., Shi, L., Ren, Z., Liu, Q., Zhang, Y., & Weng, W. (2024). Physicochemical and antimicrobial properties of soy protein isolate films incorporating high internal phase emulsion loaded with thymol. *Food Chemistry: X*, *22*. https://doi.org/10.1016/j.fochx.2024.101251

GENERAL CONCLUSIONS

The primary objective of this thesis was to extract, characterize, and apply cowpea protein concentrate (CPC), to establish its potential as a versatile biopolymer with a wide range of possible applications.

The SDS-PAGE analysis of the CPC revealed a spectrum of protein sizes, with pronounced bands around 50 kDa, indicative of 7S globulins (vicilins). From a nutritional perspective, the extraction of CPC resulted in a reduction in trypsin inhibitor levels. Furthermore, the conversion of raw cowpea into CPC resulted in proportions of both essential and non-essential amino acid levels that meet the recommendations set forth by the FAO. Its high concentration of lysine, an essential amino acid often limiting in most cereals, endows CPC with significant nutritional value, rendering it a highly suitable option for dietary supplementation. In terms of functionality, protein concentrate solutions under alkaline pH conditions demonstrated enhanced solubility, as well as superior emulsifying and foaming capabilities, in comparison to protein concentrates under acidic pH conditions. These functional characteristics are essential for the optimal application of plant proteins in food processing.

Further elucidation was made regarding the rheological and thermal aspects of aqueous CPC solutions under different concentration and pH conditions. The rheological analysis demonstrated a high degree of sensitivity to protein concentration and shear rate, particularly at elevated concentrations. The apparent viscosity at low shear rates for concentrations up to 10% indicated a shear thinning behavior, becoming similar to Newtonian fluids at higher shear rates. At a 20% concentration, shear thinning behavior was observed across all shear rates. The pH had a significant impact on the observed behavior: acidic conditions near the isoelectric point affected shear stress, viscosity, and elastic behavior, while neutral and alkaline pH levels maintained consistent behavior. During the thermal cycle, changes in molecular interactions and protein structure led to progressive changes in viscosity. The pH also influenced viscosity and elastic properties, with alkaline pH causing significant structural changes and a reduction in denaturation and gelation temperatures. The reduced viscosity of cowpea protein suspensions, particularly at concentrations up to 5%, offers substantial benefits in process engineering. Their lower resistance to flow enhances efficiency in industrial operations like mixing, homogenization, and pumping, leading to energy savings and easier handling. This study also extends the rheological analysis of cowpea solutions to higher pH ranges, a relatively unexplored area in the literature. The findings could be valuable for food science, particularly

in developing new systems and materials, such as emulsions (Chapter 4) and films (Chapters 5 and 6).

Based on the previous results, CPC demonstrated promising potential for emulsion stabilization, especially at neutral to alkaline pH levels, where proteins exhibit greater solubility and repulsion, reducing aggregation and flocculation, resulting in improved stability. Furthermore, its low viscosity, particularly at low concentrations, enhances its suitability for emulsions without significantly affecting system viscosity. Considering this evidence, the third part of this thesis investigated the behavior of CPC-stabilized emulsions under different pH conditions and oil concentrations. The results indicated a broader droplet size distribution, with enhanced homogeneity observed in the emulsions at pH 9, in comparison to pH 7 and 11. Emulsions with higher oil concentrations demonstrated a more pronounced shear thickening behavior, while pH variations exerted a significant influence on the consistency index and flow behavior index, underscoring the emulsions' responses to shear forces. Heating and cooling led to changes in viscosity, which were attributed to modifications in the emulsion's microstructure and intermolecular interactions. Emulsions prepared at pH 11 exhibited enhanced stability and resistance to thermal fluctuations. The physical stability analysis indicated that emulsions prepared at pH 9 and 11 exhibited enhanced stability of the cream layer, with a comparable stability profile.

The final two chapters were built on the previous one to establish guidelines for film formulation. An optimal pH range of 7 to 11 was identified, ensuring high solubility and stable charge density. The rheological analysis showed that low viscosities in protein solutions and emulsions are favorable for film production. Therefore, in the fourth and fifth parts of this study, the CPC was evaluated for its film-forming capacity under different pH conditions and subsequently with the incorporation of varying emulsion concentrations into its composition. The results demonstrated that pH 9 emerged as a critical point for the formation of the edible films studied, exhibiting a notable reduction in the incidence of cracks on the surface and within the thickness of the films. This condition also had a significant impact on oxygen permeability (O_2P) of the material. The films formed at the different pH levels under study exhibited structures with a low degree of crystallinity. This was accompanied by a reduction in the prevalence of disordered structures when the pH was decreased from 11 to 7. The CPC films demonstrated excellent UV barrier properties. However, the variation in pH did not significantly affect the water vapor permeability, solubility, tensile strength, or elongation at break of the films. In response to the addition of emulsions at varying concentrations, the film microstructure exhibited an uneven distribution of emulsion droplets on the lower surface in

contact with a mold. Nevertheless, the films presented a cohesive structure, particularly at 1%, without apparent cracks. The emulsion may have acted as a filler, which resulted in an increase in the films' tensile strength and elongation at break. The addition of the hydrophobic component did not compromise the barrier and solubility properties. Furthermore, there was a significant reduction in oxygen permeability in films with the highest emulsion concentration (1%). These findings demonstrate the efficacy of the methodology for incorporating lipidic substances into CPC films and their potential for future modifications, including the incorporation of lipophilic compounds such as bioactive substances.

The central argument of this thesis is that CPC is a significant and multifaceted material with a wide range of applications. The thesis demonstrates how the findings of each chapter are interconnected, providing a comprehensive understanding of CPC. The study indicates that CPC is a highly versatile biopolymer, with the potential for enhanced effectiveness through adjustments in pH and concentration conditions. The integration of the findings provides a comprehensive understanding of the nutritional and functional properties of CPC, as well as its applications in emulsions and edible films. This work generates a significant dataset that reveals the advantages and limitations of different compositions and pH levels tested, thereby providing a solid foundation for future research. These findings contribute to our understanding of CPC and provide valuable preliminary evidence for its potential applications in both technological and food-related fields.

FUTURE PERSPECTIVES

Future perspectives for the work conducted in this thesis include investigating:

- *Evaluation of the impact of seed pretreatments:* Investigate how seed pretreatments, including soaking and boiling, affect the composition and nutritional quality of the resulting flour. This study should also explore the impact of these pretreatments on the structure and functionality of the proteins, providing a more comprehensive understanding of how preparation techniques influence the nutritional and functional properties of the CPC;
- *Optimization of the extraction process*: Refine the CPC extraction process by exploring and adjusting extraction conditions, as well as investigating the combination of different pretreatments;
- *Evaluation of new variables:* Study the impact of additional variables, such as concentration and temperature, beyond pH, on the techno-functional properties of the protein, to maximize CPC functionality and applicability;
- *Development of high-concentration emulsions:* Develop emulsions with higher concentrations of oil and protein, and to assess the impact of these conditions on the stability and functionality of the emulsions;
- *Development of new film formulations:* Develop new film formulations by combining CPC with polysaccharides, aiming to significantly enhancing the key properties of the films;
- *Development of active films:* Investigate the incorporation of specific functional agents (such as antioxidants and antimicrobial substances) into films for targeted applications, such as packaging for sensitive foods or high demand products;
- *Application as a food packaging material:* Select from a variety of perishable foods (fruits, vegetables, meats) to assess the suitability of CPC films as packaging. Monitor the preservation properties of the foods over time and compare these results with those of products packaged with conventional materials;
- *Scalability and commercialization study:* Assess the scalability of the CPC extraction and utilization process, identifying technical and economic barriers to large-scale .

REFERENCES

AHMED, N., ALI, A., RIAZ, S., AHMAD, A., & AQIB, M. (2022). Vegetable Proteins: Nutritional Value, Sustainability, and Future Perspectives. In *Vegetable Crops - Health Benefits and Cultivation*. IntechOpen. https://doi.org/10.5772/intechopen.100236

AIKING, H. Future protein supply. **Trends in Food Science & Technology**, v. 22, n. 2-3, p. 112-120, 2011.

ALENCAR, J. (S.D.). Frase atribuída. Não há fonte específica publicada.

ALEXANDER, P., BROWN, C., DIAS, C., MORAN, D., & ROUNSEVELL, M. D. A. Sustainable Proteins Production. In *Proteins: Sustainable Source, Processing and Applications* (pp. 1–39). Elsevier. (2019). https://doi.org/10.1016/B978-0-12-816695-6.00001-5

ALMEIDA, F. C., DE SOUZA, C. O., PHILADELPHO, B. O., FRANÇA LEMOS, P. V., CARDOSO, L. G., SANTANA, J. S., ALVES DA SILVA, J. B., CRUZ CORREIA, P. R., CAMILLOTO, G. P., DE SOUZA FERREIRA, E., & DRUZIAN, J. I. Combined effect of cassava starch nanoparticles and protein isolate in properties of starch-based nanocomposite films. **Journal of Applied Polymer Science**, v. 138, n. 18, p. 50008, (2021). https://doi.org/10.1002/app.50008

BESSADA, S. M., BARREIRA, J. C., & OLIVEIRA, M. B. P. Pulses and food security: Dietary protein, digestibility, bioactive and functional properties. **Trends in Food Science & Technology**, v. 93, p. 53-68, 2019.

CAMPBELL, L., EUSTON, S. R., & AHMED, M. A. Effect of addition of thermally modified cowpea protein on sensory acceptability and textural properties of wheat bread and sponge cake. **Food Chemistry**, v. 194, p. 1230-1237, 2016.

CARVALHO, M., LINO-NETO, T., ROSA, E., & CARNIDE, V. Cowpea: a legume crop for a challenging environment. **Journal of the Science of Food and Agriculture**, v. 97, n. 13, p. 4273-4284, 2017.

DE BOER, J., SCHÖSLER, H., & AIKING, H.. "Meatless days" or "less but better"? Exploring strategies to adapt Western meat consumption to health and sustainability challenges. **Appetite**, v. 76, p. 120-128, 2014. https://doi.org/10.1016/j.appet.2014.02.002

DICKINSON, E., GOLDING, M., & POVEY, M. J. Creaming and flocculation of oil-in-water emulsions containing sodium caseinate. **Journal of colloid and interface science**, v. 185, n. 2, p. 515-529, 1997.

EHLERS, J. D.; HALL, A. E. Cowpea (*Vigna unguiculata L.* walp.). **Field crops research**, v. 53, n. 1-3, p. 187-204, 1997.

FAO. *Production Quantities of Cow Peas Dry by Country*. Accessed July 21, 2024. http://faostat.fao.org/

FREIRE FILHO, F. R., RIBEIRO, V. Q., FREIRE FILHO, F. R., & RIBEIRO, V. Q. Feijão-Caupi na Embrapa Meio-Norte: melhoramento, cultivares lançadas, genealogias e base genética. Embrapa, 2023.

FREIRE, F. F. R., RIBEIRO, V. Q., & ROCHA, M. D. M. Production, breeding and potential of cowpea crop in Brazil. Embrapa, 2012.

GE, J., SUN, C. X., MATA, A., CORKE, H., GAN, R. Y., & FANG, Y. Physicochemical and pH-dependent functional properties of proteins isolated from eight traditional Chinese beans. **Food Hydrocolloids**, v. 112, p. 106288, 2021.

HEWAGE, S., & VITHANARACHCHI, S. M. Preparation and characterization of biodegradable polymer films from cowpea (*Vigna unguiculata*) protein isolate. **Journal of the National Science Foundation of Sri Lanka**, v. 37, n. 1, 2009.

OLIVEIRA, M. M. G., FESSORI, A. G. B. W., HUAMANÍ-MELÉNDEZ, V. J., & MAURO, M. A. (2024). Exploring the rheological and thermal behavior of cowpea protein concentrate: Impact of pH and concentration. **Colloids and Surfaces A: Physicochemical and Engineering Aspects**, v. 694, p. 134106, 2024. https://doi.org/10.1016/j.colsurfa.2024.134106

PEREIRA, H. V. R., SARAIVA, K. P., CARVALHO, L. M. J., ANDRADE, L. R., PEDROSA, C., & PIERUCCI, A. P. T. R. (2009). Legumes seeds protein isolates in the production of ascorbic acid microparticles. **Food Research International**, v. 42, n. 1, p. 115-121, 2009. https://doi.org/10.1016/j.foodres.2008.10.008

RAGAB, D. D. M., BABIKER, E. E., & ELTINAY, A. H. (2004). Fractionation, solubility and functional properties of cowpea (Vigna unguiculata) proteins as affected by pH and/or salt concentration. **Food chemistry**, v. 84, n. 2, p. 207-212, 2004. https://doi.org/10.1016/S0308-8146(03)00203-6

SCHLANGEN, M., TAGHIAN DINANI, S., SCHUTYSER, M. A. I., & VAN DER GOOT, A. J. (2022). Dry fractionation to produce functional fractions from mung bean, yellow pea and cowpea flour. **Innovative Food Science & Emerging Technologies**, v. 78, p. 103018, 2022. https://doi.org/10.1016/j.ifset.2022.103018

SINGH, P., KUMAR, R., SABAPATHY, S. N., & BAWA, A. S. (2008). Functional and edible uses of soy protein products. **Comprehensive reviews in food science and food safety**, v. 7, n. 1, p. 14-28, 2008.

STONE, A. K., WANG, Y., TULBEK, M., & NICKERSON, M. T. (2018). Plant protein ingredients. In *Encyclopedia of Food Chemistry* (pp. 229–234). Elsevier. https://doi.org/10.1016/B978-0-08-100596-5.21601-6

TANG, X., SHEN, Y., ZHANG, Y., SCHILLING, M. W., & LI, Y. (2021). Parallel comparison of functional and physicochemical properties of common pulse proteins. **Lwt**, v. 146, p. 111594, 2021.

THOMPSON, C. M. B., ACEVEDO, B. A., AÑÓN, M. C., & AVANZA, M. V. (2023). Emulsifying Capacity of Cowpea Protein Isolates. Effect of Thermal and Hydrolytic Treatment. **Plant Foods for Human Nutrition**, v. 78, n. 2, p. 366-374, 2023.

UNITED NATIONS, Population Division. *World Population Prospects*. Accessed July 21, 2024. https://population.un.org/wpp/

VASCONCELOS, I. M., MAIA, F. M. M., FARIAS, D. F., CAMPELLO, C. C., CARVALHO, A. F. U., De AZEVEDO MOREIRA, R., & De OLIVEIRA, J. T. A. (2010). Protein fractions,

amino acid composition and antinutritional constituents of high-yielding cowpea cultivars. **Journal of food composition and analysis**, v. 23, n. 1, p. 54-60, 2010. https://doi.org/10.1016/j.jfca.2009.05.008